UNIVERSITÄT SIEGEN

Mitteilungen des Forschungsinstituts Wasser und Umwelt der Universität Siegen

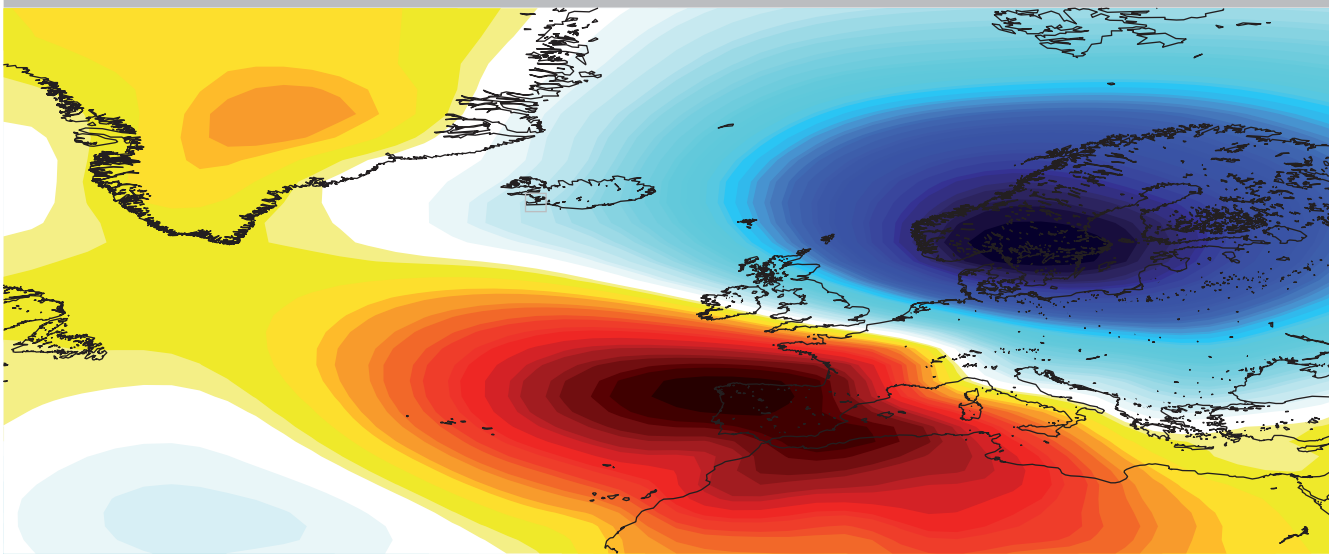

Sönke Dangendorf

Sea level variability and its role for coastal flood risk in the southeastern North Sea

Insights into past, present and future sea level changes

Heft 8

2015

ISSN 1868-6613

Sönke Dangendorf

Sea level variability and its role for coastal flood risk in the southeastern North Sea

Insights into past, present and future sea level changes

Erscheinungsort: Siegen
Erscheinungsjahr: 2015
D 467

Mitteilungen des Forschungsinstituts Wasser und Umwelt der Universität Siegen
Heft 8 | 2015

Herausgeber:
Forschungsinstitut Wasser und Umwelt (fwu)
der Universität Siegen
Paul-Bonatz-Str. 9-11
57076 Siegen

Druck:
UniPrint, Universität Siegen

ISSN 1868-6613

Vorwort

Mit der ersten Promotion am Forschungsinstitut Wasser und Umwelt (fwu), die nach der Integration des Departments Bauingenieurwesen am fwu durchgeführt werden konnte, wurde eine eigene fwu-Schriftenreihe etabliert. Neben den Promotionen am fwu werden in dieser Schriftenreihe die Ergebnisse von Institutsveranstaltungen, Konferenzen und Workshops sowie andere Forschungsergebnisse, die im Kontext des fwu erarbeitet werden, veröffentlicht. Bis dahin wurden die Forschungsergebnisse in verschiedenen internen und externen Schriftenreihen publiziert.

Eine Übersicht der bisher veröffentlichten Schriftenreihen kann der letzten Seite entnommen werden. In dem vorliegenden Heft 8 (2015) wird die Promotion von Sönke Dangendorf mit dem Titel „Sea level variability and its role for coastal flood risk in the southeastern North Sea - Insights into past, present and future sea level changes" in Papierform veröffentlicht; die digitale Veröffentlichung erfolgte im August über die Universitätsbibliothek Siegen. Herr Sönke Dangendorf hat eine kumulative Dissertation auf Grundlage von fünf begutachteten Beiträgen (peer-reviewte Journal Paper) in internationalen Journalen vorgelegt.

Küstenschutzbauwerke werden in der Regel für eine Lebensdauer von mehreren Dekaden bemessen. Potentielle Langzeitänderungen in den maßgebenden Einwirkungsgrößen, wie z.B. die Sturmflutwasserstände, verursacht durch natürliche und klimatische Änderungen infolge erhöhter Treibhausgasemissionen sind bei der Entwicklung von Küstenschutzkonzepten zu beachten. Aus diesem Grund sind sowohl für politische Entscheidungsträger als auch für die Ingenieure Erkenntnisse über die Entwicklung des globalen Klimas und insbesondere den daraus resultierenden Veränderungen im regionalen Meeresspiegel von größter Bedeutung, um nachhaltige Anpassungsstrategien realisieren zu können. Dabei ist zu untersuchen, welchen Langzeitentwicklungen der regionale Meeresspiegel aktuell folgt und zukünftig folgen wird. Neben dem deterministischen Langzeittrend weist der Meeresspiegel auch eine signifikante intra-annuelle bis mehrdekadische Variabilität auf, die aus klimainternen natürlichen Prozessen resultiert.

In der von Herrn Sönke Dangendorf vorgelegten Dissertation werden die Variabilitätsmuster (auf unterschiedlichen Zeitskalen) in den zwei für den Küstenschutz wichtigsten Einwirkungsgrößen, dem mittleren Meeresspiegel (englisch: Mean Sea Level, MSL) und dem Windstau (bzw. Sturmfluten), untersucht. Der Fokus liegt dabei auf dem Gebiet der Nordsee bzw. der Deutschen Bucht. Nach der Identifizierung der maßgebenden Einflussparameter auf die regionale Wasserstandsvariabilität wird die Langzeitentwicklung über die vergangenen 140 Jahre rekonstruiert und der Einfluss einzelner Wirkungsprozesse für das 21. Jahrhundert bis zum Bezugshorizont 2100 projiziert.

Abschließend möchte ich mich für die Mitbetreuung der Promotion bei meinen Kollegen Prof. Hans von Storch vom Helmholtz Zentrum Geesthacht (HZG) und für die Mitwirkung im Prüfungsausschuss bei Herrn Prof. Dr. rer.-nat. Athanasios Vafeidis von der Christian-Albrechts-Universität zu Kiel (CAU) sowie bei Herrn Prof. Dr. Alfred Müller vom Department Mathematik der Universität Siegen herzlich bedanken.

Siegen im August 2015

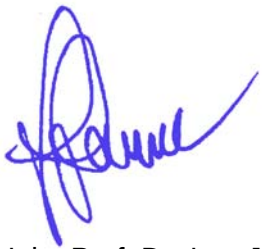

Univ.-Prof. Dr.-Ing. Jürgen Jensen

Sea level variability and its role for coastal flood risk in the southeastern North Sea

Insights into past, present and future sea level changes

Vom Department für Bauingenieurwesen der Naturwissenschaftlich-Technischen Fakultät der Universität Siegen angenommene

Dissertation

zur Erlangung des akademischen Grades

Doktor der Ingenieurwissenschaften (Dr.-Ing.)

von

Dipl.-Ing. Sönke Dangendorf

Referent:	**Univ-Prof. Dr.-Ing. Jürgen Jensen** Universität Siegen
Koreferent:	**Prof. Dr. Hans von Storch** Helmholtz-Zentrum Geesthacht

Tag der Einreichung: 05.06.2014

Tag der mündlichen Prüfung: 05.09.2014

The cover:

The cover shows parts of a figure from chapter 6 of this thesis. The figure illustrates the spatial correlation between daily surges in Cuxhaven and each grid point time series of daily sea level pressure from the 20th century reanalysis data set in the larger North Atlantic region over the period 1950-2012. The cover has been selected, since it demonstrates the linkage between the local storm surges and large-scale climate patterns, which determine a considerable part of the inter-annual to decadal variability of surges. For us, as coastal engineers, knowledge about the physics driving sea level variations is indespensible, since it contributes significantly to the flood risk in coastal areas.

Contact: Sönke Dangendorf | email: soenke.dangendorf@uni-siegen.de

Acknowledgements

The investigations presented in this thesis were conducted during my time at the Research Institute for Water and Environment (fwu) where I started working as a research assistant after receiving my diploma in 2010 (most of the work presented in this thesis was done between 2011 and 2014). In the following, I would like to acknowledge numerous friends and colleagues, who supported me during the time.

First, I want to acknowledge my supervisor Prof. Dr.-Ing. Jürgen Jensen for his guidance, patience and continous support of my research. During my study he was the first person encouraging me to get into science. I am grateful that he gave me the opportunity to conduct such an interdisciplinary work by allowing me to develop my own ideas. Whenever necessary, he had an open ear for scientific or non-sicientific discussions. Furthermore, he enabled me to participate at numerous conferences and workshops where I could build my own scientific network. Not at least these meetings were an unpayable input for my PhD. Thank you for that! I would like to express my sincere gratitude to Prof. Dr. Hans von Storch for being my co-supervisor and finding time for meetings in Hamburg. Prof. Dr. Nassos Vafeidis and Prof. Dr. Alfred Müller are greatly acknowledged for being examiner and head of the board of examiners, respectively.

Such a work is not possible without a great team of colleagues and friends. I am very grateful that I could work in such a friendly and cooperative atmosphere. Thanks go out to: Sandra Sziburis, Andre Stettner-Davis, Jörg Wieland, Jens Bender (one of the proof readers), Torsten Frank, Sebastian Niehüser, Jessica Schmidt, Vitalij Kelln, and Ugur Öztürk. I owe particular thanks to my colleagues Thomas Wahl, who guided much of my work and gave valuable comments on an earlier draft of this thesis, Arne Arns and Christoph Mudersbach for hundreds of technical discussions and supporting my ideas.

Most of my research was conducted within the KLIWAS project in cooperation with the Federal German Maritime and Hydrographic Agency and the German Weather Service. I am very thankful to a great team discussing the research continuously in meetings. In particular, I would like to acknowledge Birgit Klein, Hartmut Heinrich, Anette Ganske, Sylvin Müller-Navarra, Jens Möller, Birger Tinz, Nils Schade, Gudrun Rosenhagen, Katharina Bülow, Elisabeth Rudolph, Hartmut Hein, and Enno Nilson for the fruitful discussions, numerous telephone calls, and sharing data.

There are also a number of colleagues and friends who supported my research by sharing data and in many discussions: My sincere thanks go to: Ivan Haigh, Kristin Richter, Jan Even Oie Nilsen, Marta Marcos, Thomas Pohlmann, Xinping Chen, Ralf Weisse, Frederik Schenk, and Aimee Slangen. During my first stay at the AGU in San Francisco I met Francisco “Kiko” Calafat. During the last year we had a lot of scientific discussions. Kiko provided me many data sets, participated in my last paper as a co-author and opened my eyes for physical oceanography. Thank you very much; I learned a lot throughout this year!

I would like to acknowledge my parents, family, and friends for their moral support and patience during my thesis and my entire education. Finally, I express my sincere and deepest gratitude to my partner Katha. Without your patience, support, and love this work and all the associated travels would not have been possible.

Siegen, in May 2014

Sönke Dangendorf

List of Papers

The main sections (section 2 to 6) are primarily based on five peer-reviewed papers, which have been published in different international journals:

Section 2: Dangendorf, S., Wahl, T., Hein, H., Jensen, J., Mai, S., and Mudersbach, C. (2012): Mean sea level variability and influence of the North Atlantic Oscillation on long-term trends in the German Bight, *Water*, 4(1), 170-195, doi:10.3390/w4010170.

Section 3: Dangendorf, S., Mudersbach, C., Wahl, T., and Jensen, J. (2013): Characteristics of intra-, interannual and decadal sea level variability and the role of meteorological forcing: the long record of Cuxhaven, *Ocean Dynamics*, 63, 209-224, doi: 10.1007/s10236-013-0598-0.

Section 4: Dangendorf, S., Calafat, F.M., Arns, A., Wahl, T., Haigh, I.D., and Jensen, J. (2014): Mean sea level variability in the North Sea: processes and implications, *Journal of Geophysical Research*, 119, 6820-6841, doi: 10.1002/2014JC009901.

Section 5: Dangendorf, S., Wahl, T., Nilson, E., Klein, B., Jensen, J. (2013): A new atmopheric proxy for sea level variability in the southeastern North Sea: observations and future ensemble projections, *Climate Dynamics*, online first, doi:10.1007/s00382-013-1932-4.

Section 6: Dangendorf, S., Müller-Navarra, S., Jensen, J., Schenk, F., Wahl, T., and Weisse, R. (2014): North Sea storminess from a novel storm surge record since AD 1843, *Journal of Climate*, 27, 3582-3595, doi:10.1175/JCLI-D-13-00427.1.

Although the papers have four to six authors, the main work was done by the first author. The co-authors were involved in the research projects where most of the presented methods and results were developed. They participated in helpful technical discussions and gave valuable advices and comments while preparing the manuscripts for the journal articles. Due to the cumulative character of the thesis, minor repetitions may occur in the individual sections. Please note that minor (but no contentual) differences between the chapters in the thesis and the finally printed papers may occur, due to: (i) editorial changes by the journals, (ii) editorial changes by the author regarding the transfer from active (we/I do…) into passive language, and (iii) adjustments of some figures with respect to the overall layout of the thesis. The only substantial adjustment is related to the standard error of a linear trend. While in the first two publications (the printed versions) no serial correlation was considered for the estimation of the standard errors, in the last three publications it was accounted for by reducing the number of degrees of freedom (Santer et al., 2000). To be consistent thoughout the thesis, the standard errors in chapter 2 and 3 have been handled in a similar way as in the last three publications. This, however, has no influence on the final conclusions drawn in each chapter.

Kurzfassung

In dieser Arbeit wird ein Beitrag zur Berücksichtigung intra-anueller bis mehrdekadischer Variabilität in Küstenschutzkonzepten geliefert. Küstenschutzbauwerke werden in der Regel für eine Lebensdauer von mehreren Dekaden bemessen. Aufgrund des zu erwartenden Klimawandels infolge erhöhter Treibhausgasemissionen im 21. Jahrhundert ist es notwendig, dass potentielle Langzeitänderungen in den maßgebenden Einwirkungsgrößen (z.B. Sturmflutwasserständen) bei der Entwicklung von Küstenschutzkonzepten berücksichtigt werden.

Um nachhaltige Anpassungsstrategien zeitnah realisieren zu können, müssen sowohl politische Entscheidungsträger als auch Ingenieure so früh wie möglich über den Entwicklungspfad des globalen Klimas und den daraus resultierenden Veränderungen im regionalen Meeresspiegel Kenntnis erlangen. Dabei stellt die Frage, welcher Langzeitentwicklung der regionale Meeresspiegel aktuell folgt und zukünftig folgen wird, eine erhebliche Herausforderung dar. Neben dem deterministischen Langzeittrend weist der Meeresspiegel auch eine signifikante intra-annuelle bis mehrdekadische Variabilität auf, die aus klimainternen natürlichen Prozessen resultiert. Solche Variabilitätsmuster können eine Amplitude derselben Größenordnung wie der säkulare Meeresspiegelanstiegs über das gesamte 20. Jahrhundert erreichen. Darüber hinaus können diese über mehr als eine Dekade andauern. Das hat zum einen zur Folge, dass anthropogen verursachte Trends und Beschleunigungen im Meeresspiegelanstieg schwerer zu detektieren sind. Zum anderen führen Perioden mit anhaltend erhöhten Wasserständen zu einem Anstieg des Überflutungsrisikos in Küstenregionen.

In dieser Dissertation werden die Variabilitätsmuster in den zwei für den Küstenschutz wichtigsten Einwirkungsgrößen, dem mittleren Meeresspiegel und dem Windstau (bzw. Sturmfluten), untersucht. Hierfür wird die Variabilität der Wasserstände in der Nordsee zunächst unter Verwendung unterschiedlicher Filtermethoden, statistischer Regressionsmodelle und physikalischer Theorien auf unterschiedlichen Zeitskalen charakterisiert. In einem zweiten Schritt erfolgt dann die Verknüpfung einzelner Variabilitätsmuster mit verschiedenen ozeanografischen und meteorologischen Prozessen. Nach der Beschreibung der wichtigsten Wirkungsprozesse auf die regionale Wasserstandsvariabilität der Nordsee wird die Langzeitentwicklung unter Berücksichtigung der identifizierten Prozesse über die vergangenen 140 Jahre reevaluiert und der Einfluss atmosphärisch induzierter Variabilität für das 21. Jahrhundert bis zum Bezugshorizont 2100 projiziert. Die Ergebnisse verdeutlichen, dass ein vertieftes Verständnis der Prozesse sowie die anschließende Berücksichtigung intra-annueller bis mehrdekadischer klimainterner Variabilität die Unsicherheiten bei der Schätzung von Langzeittrends reduziert und potentielle Beschleunigungen im Meeresspiegelanstieg deutlich früher detektiert werden können (je nach Standort und Szenario bis zu 60 Jahre). Gleichzeitig wird die statistische Sicherheit von Langzeitprognosen erhöht, ein Informationsgewinn, der direkt in den Entscheidungsprozess über mögliche Anpassungsstrategien mit einfließen kann.

Abstract

This thesis provides a contribution to the consideration of intra-annual to multi-decadal sea level variability in coastal enginnering concepts. Coastal structures are usually designed for a lifetime of several decades. Nowadays a sustainable design requires the consideration of long-term changes in the loading factors due to enhanced greenhouse gas emissions throughout the 21st century.

Hence, policy makers and managers need to know as early as possible which climate change pathway the Earth's climate is following and by how far regional sea levels are changing to support adequate and timely adaption. This, however, is challenging since superimposed on any deterministic long-term trend in sea level there is a considerable fraction of intra-annual to decadal variability linked to climate internal processes. Such variability patterns may be as large as the secular change observed through the 20th century and persist over at least one decade, (i) hampering an early detection of long-term changes or accelerations and (ii) increasing/decreasing the risk of coastal flooding during these periods.

This thesis therefore investigates variability patterns in two of the most important loading factors for coastal infrastructure: mean sea level and storm surges. Different filtering techniques in combination with statistical regression models and physical theory are used to characterize the sea level variability in the North Sea (German Bight) over various time scales and to discover the contribution of different oceanographic and atmospheric forcing factors. After identifying the main contributors to the sea level variability, the long-term changes are reassessed over the past 140 years and the atmospherically induced variability patterns are projected over the ongoing century up to the target year of 2100. It is demonstrated that an improved understanding and the subsequent removal of interannual to decadal variability reduces the uncertainties when estimating long-term trends and allows for earlier detection of accelerations (up to 60 years depending on the considered location scenario). This in turn increases the statistical certainty about possible future states, which can be considered in the process of decision making for possible adaption strategies.

Content

Figures

Tables

Abbreviations and symbols

Abbreviation	Notation
AMJ	Spring season from April to June
AMSeL	Research project at the University of Siegen
AO	Arctic Oscillation
AOGCM	Atmosphere Ocean Global Circulation Model
AR1	First order Autoregressive Process
AR4	Fourth Assessment Report of the IPCC
AR5	Fifth Assessment Report of the IPCC
BCM2	Climate model of the Bjerkness Centre in Bergen, Norway
CGPS	Continuous Global Positions Systems
CNCM3	Climate model of the CNRM in Toulouse, France
COA	Centres of Action
DMIEH5	Climate model of the DMI in Copenhagen, Denmark
EGMAM	Climate model of the FU Berlin, Berlin
ENSO	El-Ninó-Southern Oscillation
EOF	Empirical Orthogonal Function
GMSL	Global Mean Sea Level
GIA	Glacial Isostatic Adjustment
GRACE	Gravity Recovery and Climate Experiment
HADGEM	Climate model of the Hadley Centre in Exeter, UK
HADCM3	Climate model of the Hadley Centre in Exeter, UK
HAMSOM	Hamburg Shelf Ocean Model
IBE	Inverse Barometer Effect
IOD	Indian Ocean Dipole
IPCC	Intergovernmental Panel of Climate Change
IPCM4	Climate model of the IPSL in Paris, France
JFM	Winter season from January to March
JAS	Summer season from July to September
LOWESS	Locally Weighted Scatterplot Smoother
LRM	Linear Regression Model
MCAP	Monte-Carlo Autoregressive Padding
MJJASO	Hydrological summer half year from May to October
MSL	Mean Sea Level
MHW	Mean Tidal High Water

Abbreviation	Notation
MLW	Mean Tidal Low Water
MPEH5	Climate model of the Max-Planck Institute, Hamburg
MTR	Mean Tidal Range
NAO	North Atlantic Oscillation
NDJFMA	Hydrological winter half year from November to April
NPO	North Pacific Oscillation
NCEP	National Centre for Environmental Prediction
NCAR	National Centre for Atmospheric Research
NSCI	Northern Scandinavia Iberian Peninsula Index
OND	Autumn season from October to December
ONDJFM	Winter half year from October to March
P	Precipitation
PC	Principal Component
PCT	Percentile
PDO	Pacific Decadal Oscillation
R	Resistence
RMSE	Root Mean Squared Error
S	Stress
Sa	Annual Tide (seasonal cycle)
SAM	Southern Annular Mode
SE	Standard Error
SLP	Sea Level Pressure
SLR	Sea Level Rise
SRES	Special Report on Emission Scenarios
Ssa	Semiannual Tide (seasonal cycle)
SSH	Sea Surface Height
SST	Sea Surface Temperature
TSM	Tide+Surge Model
20CRv2	Twentieth Century Reanalysis Project v2
VLM	Vertical Land Motion
Wsu	Zonal wind stress
Wsv	Meridional wind stress
WSV	Wasser und Schifffahrtsverwaltung

Symbol	Dimension	Notation
D_{KS}	[]	Distance between two empirical distributions
$Fx(x)$, $Fy(x)$	[-]	Samples
N	[-]	Number of degrees of freedom
N_E	[-]	Effective number of degrees of freedom
R^2	[-]	Coefficient of determination
SLP_{SC}	[hPa]	Sea level pressure over Scandinavia
SLP_{IB}	[hPa]	Sea level pressure over Iberian Peninsula
H	[m]	Ocean depths
a, b, c	[-]	Regression coefficients
f	[m/s]	Wind speed
r	[-]	Correlation coefficient
g_n	[-]	Functions of wind surge formulas
z	[m]	Reference depths for steric sea level
β	[°]	Wind direction
ε	[cm]	Error term of a regression model
ξ	[cm]	Sea level
ξ_{Atm}	[cm]	Atmospheric component of sea level
ξ_{Geo}	[cm]	Geocentric sea level
ξ_{P}	[cm]	Sea level in response to changes in precipitation
ξ_{SLP}	[cm]	Sea level in response to SLP forcing
ξ_{Steric}	[cm]	Steric component of sea level
ξ_{Wsu}	[cm]	Sea level in response to zonal wind stress
ξ_{Wsv}	[cm]	Sea level in response to meridional wind stress
ρ	[kg/m³]	Density

1 Introduction

Sea level rise (SLR) currently represents one of the more certain and one of the most dangerous societal challenges. According to the Fifth Assessment Report (AR5) of the Intergovernmental Panel on Climate Change (IPCC), it is very likely that global mean sea level (GMSL) has risen by a rate of roughly 1.7 mm/yr between 1901 and 2010 with higher values of 3.2 mm/yr between 1993 and 2010 and comparable high values between 1930 and 1950 (Church et al., 2013). Furthermore, it is very likely that the rate of GMSL rise will exceed the 1971-2010 values during the 21st century for all considered greenhouse gas emission scenarios due to a growth in ocean heat content and an icreasing freshwater contribution due to mass loss from glaciers and ice sheets (Church et al., 2013). Since coastal regions are by far the most densily populated areas in the world, with an average population density exceeding the global mean by approximately three times (Small and Nicholls, 2003), the human society needs to adapt against hazards linked to these changing oceanographic boundary conditions.

Unconstrained by the growing human influence on climate change (Meehl et al., 2007) coastal flooding already constitutes one of the most dangerous hazards for coastal regions. This has been demonstrated by a long list of disastrous events throughout the past century. For instance, in the North Sea, the area of interest of the present thesis, the most disastrous events happened in 1953 in the UK and Netherlands and 1962 in the German Bight with its centre of devastation in Hamburg-Wilhelmsburg. The big North Sea flood from 1953 occurred in the night of January 31st as a result of a high spring tide and a severe storm over northern Europe. Thousands of people lost their life in an event, which surpassed the mean sea level in some areas by up to 5.6 m. 1962 the storm Vincinette hit the German North Sea coastline during the night from February 16th to 17th. With wind speeds exceeding 200 km/h the storm pushed water masses from the North Sea against the coastline of the German Bight. Many of the coastal defence structures failed leading to severe flooding with over 300 fatalities. These two examples demonstrate the disastrous power of severe storms and highlight the urgent need for coastal safety and management plans as a protection for the hinterland.

The adaption and protection of coastal areas, their population and economic merits are the superior tasks for coastal engineers. As in other engineering fields, coastal structures are generally dimensioned in a way that the resistence *R* of the structure is larger than the operating force or stress *S* (e.g. Mudersbach and Jensen, 2010, Figure 1-1). The main loading factors are storm surge water levels acting on the exterior of a coastal structure

(e.g., dikes, walls, etc.). An improved knowledge about the loading mechanisms is indespensible for an anticipatory and economical coastal safety management. As also demonstrated by the two aforementioned flood events, storm surge water levels result from a combination of severe weather situations creating atmospheric conditions which cause water levels to rise along the coast (including wind waves), and high tides, forced by periodic variations in the astronomical cycles. Additional contributing factors are river flooding triggered by strong rainfall events in the upland watershed or other large scale or regional oceanic variations, for instance, related to the seasonal heating and cooling of the ocean and/or ocean dynamics. The large number of different processes envolved in the generation of storm surge water levels makes their assessment to an interdisciplinary challenge, which requires inputs from different disciplines such as oceanography, meteorology and engineering.

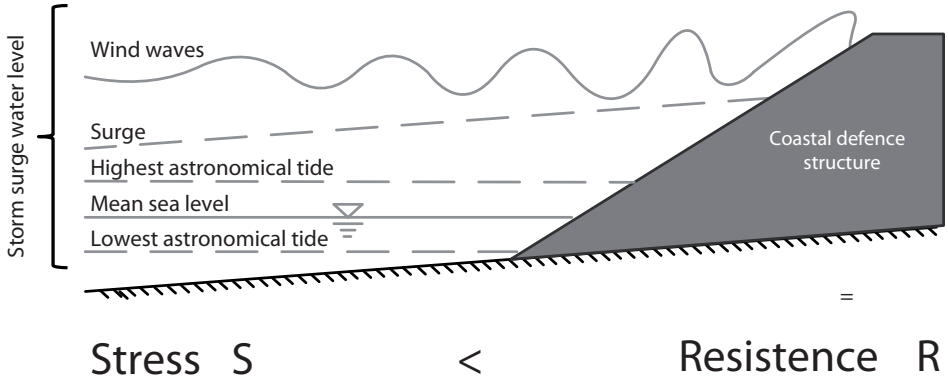

Figure 1-1: Coastal engineering concept for the design of coastal defence structures.

It is expected that storm surge water levels will become more severe in a warming climate either due to the above mentioned rise in global and/or regional mean sea level (MSL) (e.g. Slangen et al., 2012) and/or changes in regional wind fields (Woth et al., 2006). Any long-term change in the statistics of storm surge water levels will require an adjustment of present day design water levels. Therefore, much effort has been made to project potential changes in both contributing factors. This has typically been done in two different ways: (i) estimating trends over the entire projection period of a specified time horizon or (ii) the comparison of future statistics in time slices of for example 30 years relative to a historical reference period. Both methods have in common that they are sensitive to decadal or multidecadal fluctuations related to climate internal processes. Such fluctuations have been observed in many parts of the global ocean (e.g. Wenzel and Schröter, 2010; Chambers et al., 2012; Calafat et al., 2012, 2013a) and they are known to be often larger in magnitude than the frequently discussed 20th century long-term trend itself. Hence, they may mask or amplify any expected long-term change. This implies that coastal sea level may exceed a certain critical threshold much earlier than the global mean sea level. Given the already huge vulnerability of coastal zones against elevated sea levels, variations on all time scales upon any long-term trend therefore represent a non-neglegible contribution to the flood risk. Additionally, persistent variability patterns provide at least to some degree the potential of predictability of decadal scale changes. Since coastal safety and management plans are typically constructed proactive for several decades, improved

knowledge of the mechanisms driving those variations will ultimately help to include the information in political decisions and design processes.

This thesis assesses long-term changes in North Sea MSL and storm surge statistics in the light of intra-annual to decadal scale variability (wind waves and tides are not considered, since wind waves are not measured by tide gauges (the main data source used in the present thesis) and changes in tides are comparably small). The thesis builts on recent assessments of Wahl et al. (2010), Wahl et al. (2011) and Wahl (2012), who reconstructed MSL data sets for 13 tide gauge locations in the German Bight and determined the linear and non-linear long-term changes. In particular, the temporal and spatial variations around the long-term trend as determined by Wahl (2012) as well as their connection with large- and small-scale atmospheric and oceanographic forcing are explored.

This first chapter provides a general introduction into the state of sea level research. It will be discussed (i) how sea level is measured, (ii) which processes are included, (iii) how these processes can be separated, and (iv) what is up to date known about sea level variations. This will be done on a global scale first, while the state of science for the North Sea region and in particular for the German Bight will be given with respect to each specific topic in the different following sub-chapters. Additionally, a brief introduction into the main oceanographic North Sea physics is given. This chapter finishes with an outline of the main research questions as asked in the present thesis.

1.1 Regional and global sea level: how it is measured and determined

Observations of sea level around the globe represent by far the longest oceanographic measurement system and it has been continuously evolved over time (Church et al., 2013). First measurements have been provided by tide gauges since the 1700's, with the longest ones recorded by tide gauges in Amsterdam, Liverpool, Stockholm and Kronstadt (Woodworth et al., 2011). The earliest tide gauges were simply rocks or wooden rods in the ocean (Slangen, 2012) while later they were further advanced to stilling wells with floats eliminating the effects of wind waves. Nowadays, electronic sensors measure sea level and send the data directly to computers. Tide gauges are most often located in harbours where they were originally installed to provide information on sea levels to support shipping. This is important to notice, since the records are also used as in the present thesis for scientific studies with special requirements often not fulfilled by the simple equiqiment utilized in the earlier years (von Storch, 2013).

Tide gauge measurements have different advantages and disadvantages, which must be considered in scientific analyses. First, tide gauges measure sea level relative to the Earth's surface, which includes ocean volume and mass changes, but also vertical land motion (VLM, see also Schütte, 1908; Rietschel, 1933; Lüders, 1936). As already mentioned for example by Wahl et al. (2011, 2013) these relative sea levels are the major concern for coastal engineering aspects, but for detecting climatic signals VLM's have to be removed from the data set. VLM's can generally be separated into different groups of components. The worldwide dominating effect is related to the viscoelastic response of

the earth's surface to changes in land ice mass since the last glacial maximum (Peltier, 2004), also known as glacial isostatic adjustment (GIA). In some regions, however, VLM's are also related to local effects resulting from tectonic activities, ground water mining, or hydrocarbon extraction (e.g. Wöppelmann et al., 2009). The combined effects have serious consequences for the sampling of globally representative means and also point to differences between the northern and southern hemisphere over the past 100 years (Wöppelmann et al., 2014). Assessing the uncertainties in VLM estimates is challenging because of differences in the results from a range of GIA models (Jevrejeva et al., 2014) and the shortness of direct measurements of VLM rates by continuous global positions systems (CGPS); this may also result in large uncertainties in estimates of long-term MSL change (Wahl et al., 2013). Another problem of tide gauge measurements is the temporal and spatial uneven distribution of records around the globe. While some tide gauge measurements give unique insights into sea level changes over several centuries, the majority of the nowadays available network has been installed since the mid-20th century (Holgate et al., 2013). Furthermore, the longest and most reliable measurements are predominantly available from locations in the northern hemisphere. For the reconstruction of global means this implies that the estimates become increasingly biased back in time, when the majority of tide gauge measurements are accumulated in some specific regions such as Northern Europe. As it will also be demonstrated in the next chapter such regional averages may differ substantially from the "true" global signal.

These shortcomings can be partly compensated by satellite altimetry providing a near global coverage of sea level measurements since 1993 with a precision of rougly one centimeter (Nerem and Cazenave, 2004). First, satellites measure sea level with respect to the earth's center of mass and therefore give a measure of absolute or geocentric MSL change. Second, the near global coverage (from 66°S to 66°N) is by far better than the local information given by tide gauges. However, (i) arctic regions are still not well covered, (ii) the data set is with 20 available years still rather short especially in light of the large decadal to centennial variations present in sea level (e.g. Chambers et al., 2012), and (iii) several corrections have to be applied to make the data comparable to tide gauge measurements. In addition to these direct mearurements of sea level, the observational system of the oceans also comprises several other measurement techniques such as temperature and salinity profiles from ARGO and earth gravity recordings from Gravity Recovery and Climate Experiment (GRACE), which are important to distinguish between the different sources of SLR.

One of the major challenges of sea level research is the sampling of the different measurements to a representative GMSL series extending back in time as long as possible. Since remote sensing is only available after 1993, tide gauges still represent the main sea level archive over the past 300 years. There are, however, only a handful century-long tide gauge records available. Several attempts have been undertaken to overcome the sampling problem: some authors tried to built sea level curves for specific coherent regions before calculating the global mean (e.g. Jevrejeva et al., 2006; Merrifield et al., 2009; Jevrejeva et al. 2014); others collected only the longest, most continuous and less VLM affected records (Douglas, 2001; Holgate, 2007) or applied neuronal network tech-

niques (Wenzel and Schröter, 2010). Most modern global sea level reconstructions combine the different measurement techniques, i.e. in situ observations as given by tide gauges and remote sensing as for example given by satellites, to overcome the individual shortcomings. A common approach is to use the spatial information determined by empirical orthogonal functions (EOF) of satellite altimetry data, which are then combined with historical tide gauge measurements. The most popular reconstructions are those by Church et al. (2004) and their updates given in Church and White (2006) and Church and White (2011).

Three different GMSL reconstructions are shown in Figure 1-2 as derived by Jevrejeva et al. (2006; 2008) and Church and White (2011). The Jevrejeva et al. (2006; 2008) reconstructions are based on the so called virtual station technique. In this technique two neighbouring stations are combined recursively into a virtual station and later iteratively averaged to the global mean as shown in Figure 1-2. The two reconstructions mostly differ in the time before 1850. While Jevrejeva et al. (2006) used all available tide gauges information from 1807 Jevrejeva et al. (2008) processed only the three longest stations worldwide before 1850, namely Amsterdam, Liverpool and Stockholm, to derive a global curve. This example shows the first problem of GMSL reconstructions which are simply based on tide gauge sampling: the period before 1850 consists only of a few records mostly located in the North Sea/Baltic Sea region. Hence, they represent the variability and trend of regional sea level and not the “true” global mean. Due to the limited information during that time the uncertainties are much larger, compared to the later periods. The second difficulty as already mentioned above is related to known differences between coastal and open ocean variability. The two Jevrejeva curves sample coastal sea level variability, which is not necessarily coupled to the open/deep ocean due to the influences of winds and tides (Rahmstorf et al., 2012; Calafat et al., 2014). Church and White (2011) therefore combined the spatial information given by satellite altimetry measurements after 1993, assumed that the major modes are well sampled by this short period and projected sea level globally back to 1880. The method is generally more sophisticated and better suited to resamble global variability, at least if the assumption holds that the twenty years of available satellite altimetry data adequately describe the major modes of variability. This is critical (Cristiansen et al., 2010; Calafat et al, 2014) and represents the third problem, since several authors have pointed to significant decadal to multi-decadal scale variability in sea level (e.g. Calafat et al., 2012; Calafat et al., 2013a,b; Chambers et al., 2012) which is likely not captured by the 20 years of measurements.

Comparing the reconstructions in Figure 1-2 demonstrates their statistical agreement in terms of the long term trend; the estimates for the two Jevrejeva curves over the period 1880 to 2002 are 1.7 ± 0.2 mm/yr and 1.7 ± 0.3 mm/yr, while the linear trend for the Church and White (2011) dataset is 1.5 ± 0.1 mm/yr. However, one major difference becomes obvious when comparing the standard errors (SE) of the trends. The variability within the Church and White (2011) reconstruction is considerably smaller compared to the Jevrejeva curves. This demonstrates that a major fraction of the variability within the different reconstructions (this is also true for further reconstructions which are availablenut not discussed here; see Rahmstorf et al. 2012 for an overview) is not related to the varia-

tion of the true global mean but rather reflects the sampling issues discussed above (Rahmstorf et al. 2012). This clarifies the urgent need of a better understanding of regional as well as global sea level variability. To get confidence in past reconstructions it is therefore important to analyze characteristics and processes of regional sea level change, particularly for the longest records. If patterns of variability are better understood on a regional scale, the knowledge can be transferred into the reconstruction techniques for the global mean.

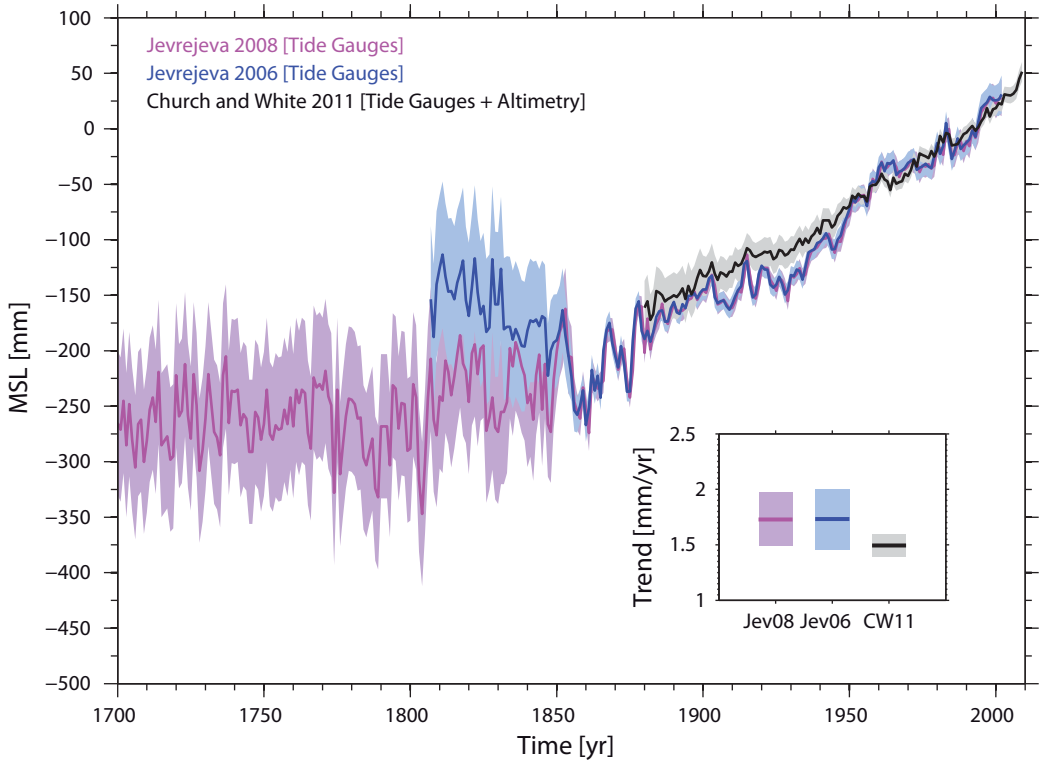

Figure 1-2: Comparison of three different global reconstructions (Jevrejeva et al., 2006; Jevrejeva et al., 2008; Church and White, 2011) (colored lines) and their related uncertainties (shaded areas). In the small subplot linear trends over their common period from 1880 to 2002 are shown with 2σ SEs (accounting for serial correlation).

1.2 Processes behind sea level variations

Sea level changes observed at a certain location reflect the combination of global and regional scale processes. In a geodetic jargon it can either be expressed as (i) the mean height of the ocean surface with respect to the earth's center of mass (geocentric sea level), or (ii) the ocean surface relative to the surrounding land or ocean floor (relative sea level) (Stammer et al., 2013). The difference between both is, therefore, the reference frame to which sea level is measured, or in other words: VLMs, which are included into all measurements to a specified position at the earth's surface (as tide gauge measurements). An illustration of all components affecting sea level on different time scales is given in Figure 1-3.

Since the various contributors act on different time scales, it makes sense to first discuss processes contributing to long-term MSL changes and then debate their temporal variability. Essentially, MSL around the globe can be affected in two different ways: mass can be

added or removed from the basins or the ocean density (and in turn the ocean volume) can change. The mass component is controlled by the exchange between land, atmosphere and the ocean. The transfer is carried out either by evaporation/precipitation processes or water from land ice, glaciers and other terrestrial reservoirs such as rivers, lakes and aquifers. The largest source of freshwater is stored in land-locked ice, currently retaining mass. A complete melting could lead to approximately 65 m of sea level change (~57 m are stored in Antarctica, while from the remaining 8 m ~7.4 m and 0.6 m are stored in Greenland and in glaciers and ice caps, respectively). While the contribution of glaciers is limited for the far future compared to the contribution currently stored in Antarctica and Greenland, their contribution has dominated the mass component over the past century (e.g. Church et al., 2011; Church et al., 2013). According to the recently published AR5 of the IPCC the contribution of terrestrial water storage (rivers, lakes, aquifers) to GMSL rise was negative from 1901 to 1990, but stabilized afterwards (Church et al., 2013). A major source coming from terrestrial water storage is human induced, for example impoundment in reservoirs or groundwater withdrawal. Chao et al. (2008) estimated a sea level fall of ~23 mm mostly related to increased (manmade) reservoir capacity since 1940. The largest contributor to present day SLR is, however, thermal expansion associated with net uptake/release of heat by the ocean. Since 1971 0.96 mm/yr of sea level change can be explained by thermal expansion alone (Church et al., 2013). The contribution of the halosteric component has been estimated to be small on a global scale (for both present day and future SLR), but may contribute a more important fraction in marginal seas such as the Arctic Ocean, the Mediterranean, or the Baltic Sea (Jorda and Gomis, 2013).

One major challenge – especially at regional scales – is that the contributions do not only change temporally (on different time scales), but also spatially. For instance, dynamic sea level changes are linked to the redistribution of heat, mass or freshwater input, which are in turn marked by substantial temporal variability. Density changes are related to variations in ocean temperature (thermosteric changes) or salinity (halosteric changes). The main driver behind regional density variations are changing surface winds, affecting the ocean dynamics through coupled processes such as Ekman pumping, coastal up-/downwelling, or Rossby waves. A prominent example for suchlike changes in surface winds and related regional changes in sea level is the Pacific Ocean. From satellite altimetry (i.e. the period 1993 to 2011) it is well known that there is a substantial east-west gradient in sea level with larger trends (up to three times the global mean) in the western Pacific Ocean and lower sea level (two times lower the global mean) in the eastern margin (Figure 1-4a). The pattern has been intensifely studied by numerous authors (e.g. Merrfield, 2011; Merrifield et al., 2012; Bromirski et al., 2011; Meyssignac et al., 2012) and it has been found that these decadal trends are caused by an intensification of the Pacific trade winds (e.g. Timmermann et al., 2010), which are closely linked to climate internal variability modes (e.g. El Nino Southern Oscillation: hereafter ENSO; Pacific Decadal Oscialltion; hereafter PDO). Further examples for such climate internal variability modes in other regions are – without being complete - the North Atlantic Oscillation (NAO), the Arctic Oscillation (AO), the Indian Ocean Dipole (IOD), or the Southern Annular Mode (SAM).

It is important to notice that steric changes are generally larger in the open ocean than over a shallow continental shelf (Bingham and Hughes, 2012), which may result in mass exchange between both. As it will be discussed later, this is also of importance in the North Sea.

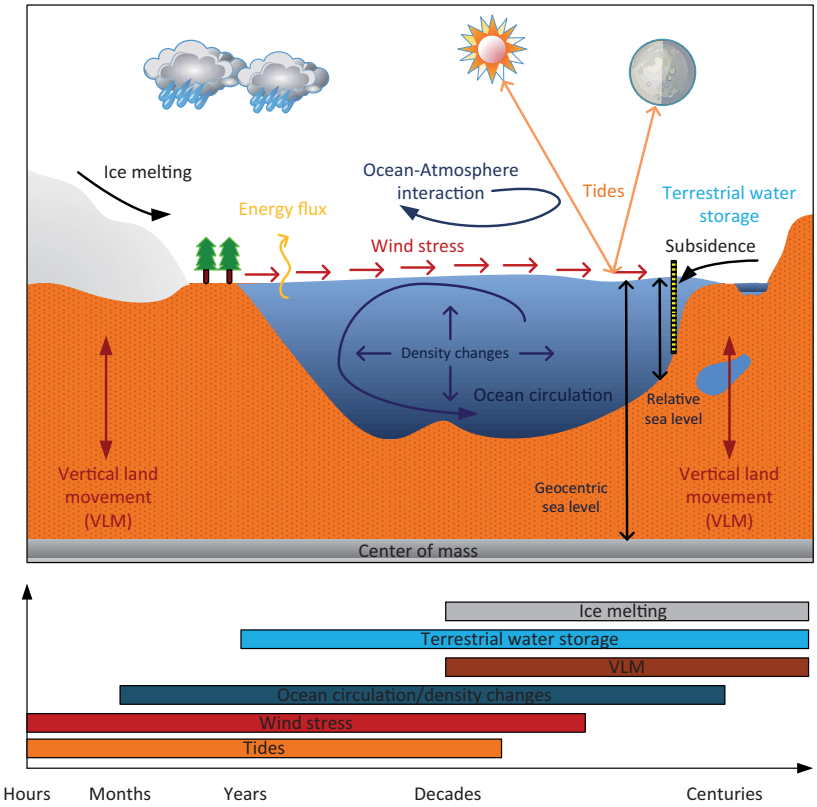

Figure 1-3: Processes that affect sea level (top) on varying time scales (bottom). Each component – except that of VLM - shown, has its own effect on sea level changes (reproduced and extended from Stammer et al. (2013)).

The role of heat or freshwater fluxes is not fully understood yet, but it is suggested that they will play an increasingly important role in the future, e.g. due to freshwater fluxes from melting glaciers or polar ice sheets (Stammer et al., 2013). There are two global adjustments following a freshwater addition: a barotropic, i.e. a quick response of the ocean in form of waves or basin modes (e.g. Lorbacher et al., 2012), and a baroclinic, that is a much slower long-term steric adjustment (e.g. Stammer, 2008). In addition, sea level also reacts in an isostatic manner on fluctuations of local sea level pressure (SLP). This effect is commonly referred to as inverse barometer effect (IBE), and has large impacts on the regional distribution of sea level (Ponte, 2006) as well as longer-term changes (Stammer and Hüttemann, 2008). In the case of full adjustment, a variation of one hPa in SLP leads to one cm change in sea surface height (SSH). Finally, there are also gravitational feedbacks of the ocean to all sources of mass exchange between land and the ocean, producing regionally varying fingerprints in sea level (e.g. Mitrovica et al., 2001; Riva et al., 2010; Slangen et al., 2012). According to Newton's law of universal gravitation, mass attracts mass. If mass is added for example from an ice sheet to the ocean, the gravitational pull of the ice decreases, leading to a non-uniform redistribution of water around the globe with sinking sea levels near the melt source and increasing sea levels in the far field. This

in turn also results in viscoelastic solid earth changes and changes in earth rotation, additionally producing a regional varying pattern (Tamisiea et al., 2010). This response is true for all components of mass exchange, i.e. ice metling as well as changes in terrestrial water storage. Recent studies further showed that terrestrial water storage is also a key driver of inter-annual variability in GMSL. While GMSL has been highly positively correlated with the ENSO indices (e.g., Nerem et al., 2010; Calafat et al., 2014), an inverse feedback to ENSO driven changes in terrestrial water storage was found. This is suggested to be related to varying ocean and land precipitation. Cazenave et al. (2012), for instance, showed decreasing land and increasing ocean precipitation in the tropics during El-Nino events, while Boening et al. (2012) and Fasullo et al. (2013) recently pointed to the unique role of Australian rainfall patterns during La-Nina events.

The combination of all the aforementioned factors results in regionally varying patterns of SLR. This is illustrated for the altimetry period from 1993 to 2011 in Figure 1-4. The figure demonstrates different important issues, which will be adopted in the present thesis. Figure 1-4a visualizes linear trends of regional sea level change relative to the global mean (i.e. the GMSL rate has been removed from each grid point time series; note that the mean seasonal cycle has also been removed before estimating trends). The most striking patterns are (i) the already discussed PDO/ENSO imprint in the Pacific Ocean and (ii) the distinct trend deviations near the Kurisho current in the western Pacific and the Gulf Stream along the US eastcoast. The latter suggests dynamic factors following changes in ocean circulation. It is thus clear that at least over that short period of approximately two decades regional sea level has strongly varied from the global mean with deviations ranging from -12 mm/yr to +12 mm/yr. For the North Sea the area of interest in the present thesis it becomes obvious that the trends followed the trend of GMSL at least during the altimetry era (see also Figure 1-4c). But is this also true for the variability?

Figure 1-4b shows linear correlations between monthly detrended and deseasonalized MSL grid point time series and similarly processed GMSL. Interestingly, the patterns visible in that map show some similarities to the trend patterns in Figure 1-4a, which are confirmed by a pattern correlation in the order of -0.44 (statistically significant on the 95% confidence level). This significant pattern correlation is mainly determined by similarities in the tropical Pacific, along the US westcoast and the large currents such as Kurisho and Gulf Stream. The correlations itself are also significant in these regions with values of ±0.6, but are less distinctive in other areas. This leads to the following conclusions: first, it clearly demonstrates the influence of internal climate modes such as ENSO/PDO on GMSL variations as already discussed by various authors before (e.g. Nerem et al., 2010; Cazenave et al., 2012; Boening et al., 2012; Fasullo et al., 2013) and second, it exhibits significant differences between regional and GMSL variability. The latter is also demonstrated for the North Sea area by the comparison of the GMSL time series with the mean North Sea time series in Figure 1-4d. While the trend is similar during that period, the regional North Sea MSL variability exceeds that of the GMSL significantly (the standard deviations of the two time series are 4.8 mm for the North Sea and 1.5 mm for the GMSL time series). The coefficient of determination is insignificant with a value of approximately 0.01, suggesting that the GMSL can only account for approximately 1 % of the totally ob-

served variability in the North Sea. In other words: the North Sea MSL variations are mostly decoupled from the global mean. Therefore, GMSL represents a poor measure for MSL variations in the North Sea. The example clearly points out that improved understanding of regional MSL variability over long time scales is indespensible for regional planning and mitigation purposes, since the regional variability shifts the base level for storm surges by several tens of centimeters along the North Sea coastline. This in turn requires a profound knowledge of the hydrographic principles of the region, a topic that will briefly be explored in the following subchapter.

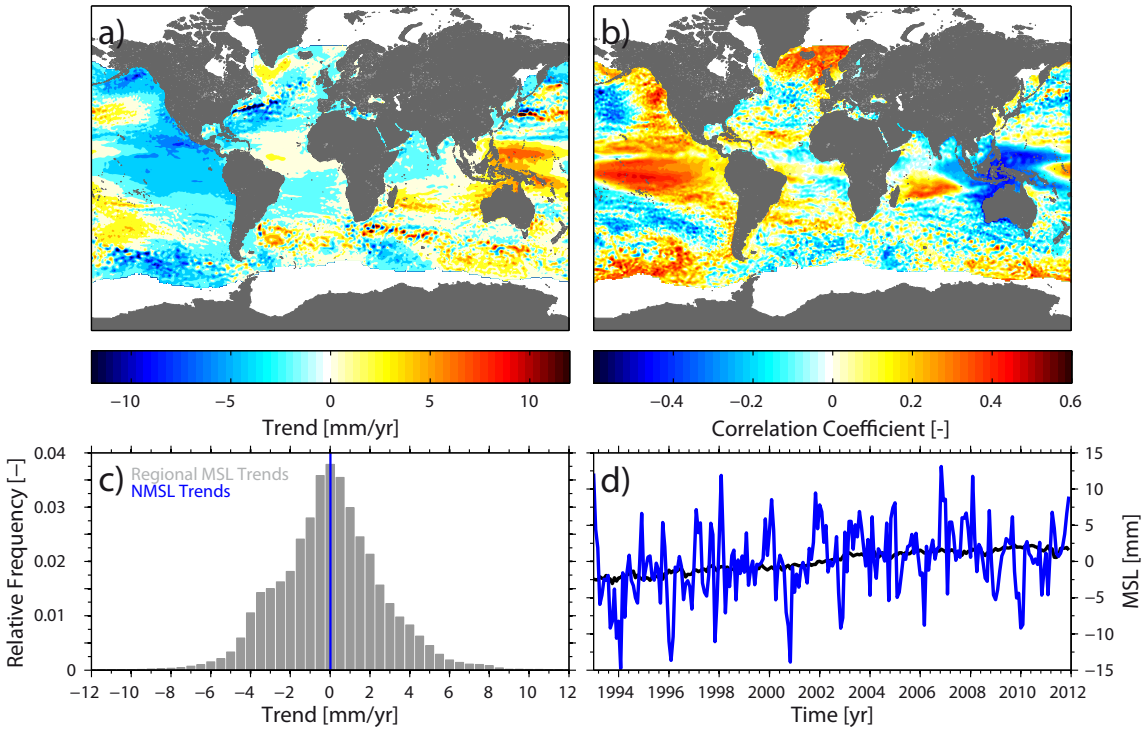

Figure 1-4: Evaluation of monthly AVISO MSL time series over the period from 1993 to 2011. a) Linear trends as determined for each grid point time series with monthly MSL anomalies (i.e. the seasonal MSL cycle has been removed) corrected for the GMSL rate. b) Correlation coefficients between detrended GMSL and each detrended grid point time series. c) Histogram of the trends calculated in a). The blue line marks the corresponding trend for the North Sea basin. d) Comparison of the mean North Sea MSL time series and the simoultaneus GMSL time series.

1.3 Geographic and hydrographic properties of the North Sea

The North Sea is a marginal sea at the eastern boundary of the North Atlantic opening in the southwest through the English Channel and in the North through the Norwegian Sea. In the east it is connected via the Skagerrak and Kattegat to the Baltic Sea (Figure 1-5). The North Sea is one of the best explored ocean basins in the world and there are several excellent reviews discussing the hydrographic properties (e.g. Otto et al., 1990; Rodhe, 1998; OSPAR, 2000). The North Sea is located on a shallow continental shelf with water depths mostly below 100 m. Deep parts can only be found near the Norwegian coastline in the so called Norwegian Trench with a maximum depth of approximately 700 m. The lowest water depths are found in the near coastal areas, for instance, along the southern coastlines, where the water depths are partly below 10 m.

The decrease of water depths from approximately 200 m at the northern entrance to less than 10 m in the southern bight leads to a prominent influence of bottom topography on the resonance to tidal forcing and the water level rise during storm surge conditions (Sündermann and Pohlmann, 2011). Tides enter the North Sea northeast of Scotland or through the English Channel in the southeast and travel counterclockwise through the basin. The tidal conditions can be trisected with amphidromic points near the Norwegian coast, in the central North Sea and near the English Channel.

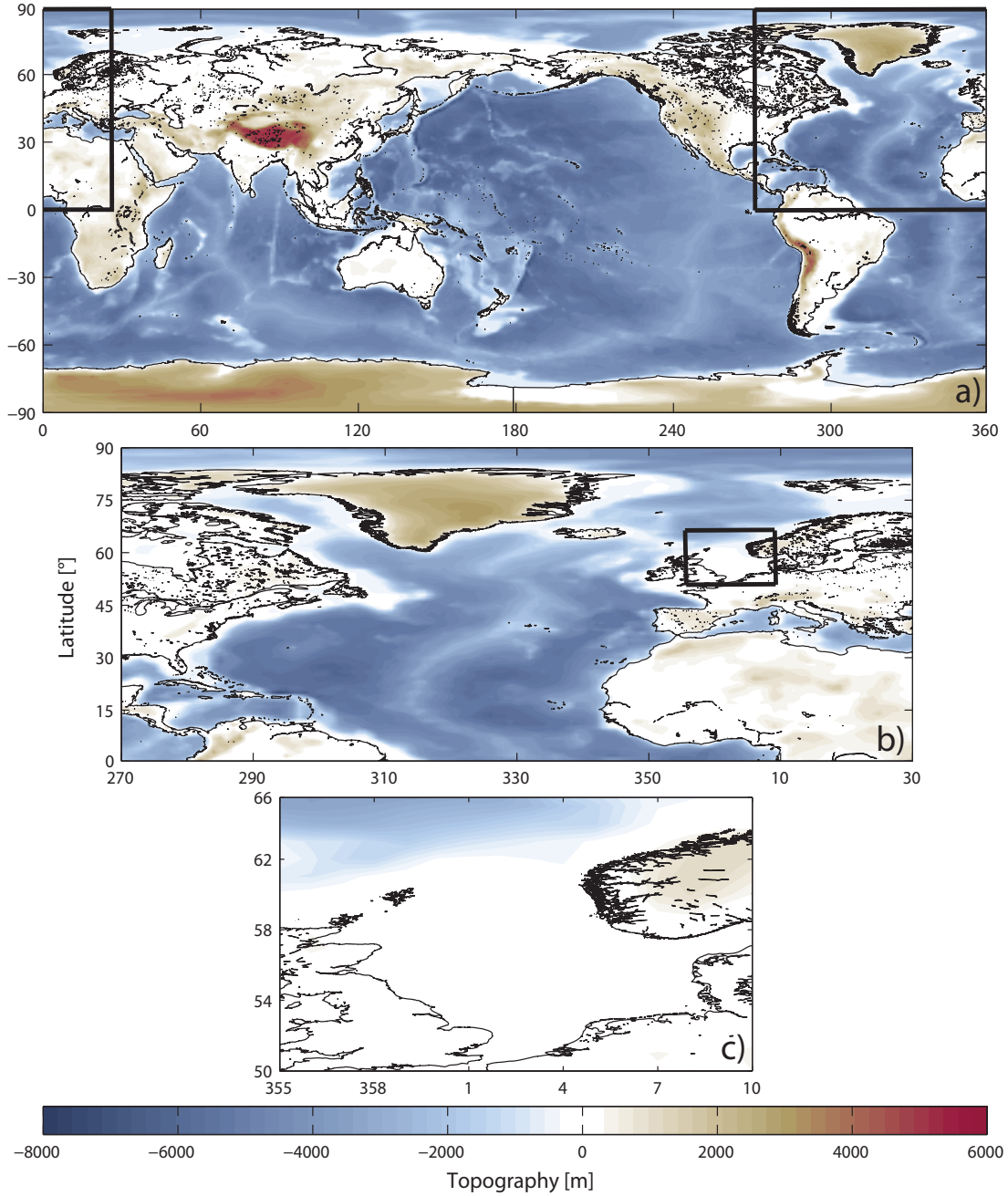

Figure 1-5: Earth's topography and study area. From top to bottom: a) Global ocean, b) North Atlantic Ocean, and c) North Sea.

Within the basin, the main flows are concentrated in areas of steep slopes with currents following the depths contours (OSPAR, 2000). The mean circulation is cyclonic (e.g. Sündermann and Pohlmann, 2006), and the major inflows are coming through the Norwegian

Trench, around the Shetland Islands and the English Channel (Turrel et al., 1992). Largest inflows are observed in the Norwegian Trench with water masses of 0.7-1.1 Sv (1 SV = 10^6 m^3s^{-1}), followed by 0.6 Sv east of the Shetland Islands and 0.3 Sv through the Orkney-Shetland section. The inflow through the English Channel is less important with 0.1-0.17 Sv (Chen, 2014). The outflow is confined to the Norwegian Trench.

While in the northwest the broad connection to the North Atlantic leads to strong exchange processes with the open ocean (tides, NAO, etc.), in the eastern parts considerable continental impacts (freshwater discharge, heatflow, etc.) on the North Sea physics prevail (Sündermann and Pohlmann, 2011). This interplay leaves a unique footprint in the characteristics of North Sea physics. Through the vertical transfer of momentum flux, the atmosphere plays a major role for the residual circulation. Prevailing westerlies enhance the cyclonic circulation, while during conditions of enhanced easterlies the situation turns opposite. Strong winds further lead to regularly occurring storm surges, which represent the major hazard for the adjacent coastal regions and have formed the shape of the coastline for many centuries.

During winter, when the sea level variability in the basin is largest (see also chapter 2), the North Sea is vertically mostly well mixed; i.e there is no clear stratification in the water body. During spring when the solar energy and surface heat increase a thermocline forms over large parts of the basin (OSPAR, 2000). The thermocline seperates the water body into two layers: a warmer and less dense surface layer and a colder and denser deep layer. The strength of the thermocline is strongly governed by tidal and atmospheric influences and is deepest during late summer (Becker et al., 1996). In the autumn months, when the atmosphere tends to be more variable and the number of storms increases, the thermocline forms back until the two layers are mixed. In the German Bight, however, this seasonal dependence is limited to the deeper areas around Helgoland, because in the shallow coastal zones the strong tidal currents hinder a clear stratification (Otto et al., 1990). These properties are important to notice when analyzing sea level variability along the North Sea coasts, since they directly impact the interplay between atmospheric and oceanographic forces. The location on the shallow continental shelf further provides indication for the dominant role of the atmosphere on the characteristics of sea level variability.

1.4 Objectives and outline of the thesis

As outlined in the previous sections, this thesis aims at investigating the characteristics of SLR and variability on different timescales, its forcing and underlying processes. The complex oceanographic situation with varying forces on different timescales requires an analysis in different frequency bands. Hence, the variations will be assessed for the components of MSL and storm surges, seperately. This will be achieved by first investigating the average conditions over timescales ranging from months to several decades and then incorporating the synoptic scale variations due to storm surges into the study. The five major objectives are:

- **To describe the characteristics of intra-annual to decadal scale variability of MSL time series**

  Monthly MSL time series from a novel data set recently reconstructed in the AMSeL ("MSL and Tidal Analysis at the German North Sea coastline") research project (Jensen et al., 2011) are explored for underlying variability patterns. Different filtering techniques are applied to analyse the variability on different time scales and quantify its magnitude.

- **To explore various components of regional MSL variability on different time scales and derive statistical-empirical relationships describing their forcing**

  A detailed investigation of the characteristics of MSL variability in different frequency bands with respect to different forcing factors is carried out. This is done in a multiple regression framework, where (i) spatial correlation maps in combination with plausible physical mechanisms are used to identify major forcing factors, and (ii) multiple stepwise regression models are applied to determine their contribution to MSL variability. This is achieved by incorporating the ouputs of long historical atmospheric and oceanographic reanalysis into the study. The developed models are calibrated with state of the art numerical models, which are, however, limited to the second half of the 20th century.

- **To investigate the influence of different forcing factors on the estimation of long-term trends and acceleration/deceleration patterns in sea level time series**

  After distinguishing between different forcing factors of regional MSL variability on different time scales the information is used to remove known parts of variability from MSL time series and to estimate whether long-term trends and acceleration/deceleration patterns are affected. This is tested with a statistical Monte-Carlo experiment with artificial time series simulated on the basis of past observations as well as observational data itself.

- **To utilize statistical-empirical relationships for a downscaling of future SLR and variability projections**

  The statistical-empirical relationships between the major modes of MSL variability and physical mechanisms controlling them are adapted to downscale future MSL rise and variability projections from state of the art atmosphere ocean global climate models (AOGCM). This is done under the consideration of different uncertainties related to different climate change pathways and internal climate variability.

- **To use historical tide gauge information for the reconstruction of a long storm surge record and investgate its relationship to North Sea storminess**

  The historical tide gauge record of Cuxhaven is used to reconstruct the contemporary longest storm surge record in the world. The record is analysed for linear and non-linear long-term changes over the past 170 years, its relationship to large-

scale atmospheric circulation patterns and regional storminess as derived from the newest generation of global atmospheric reanalyses.

The thesis is structured as follows. In section 2, the seasonal cycle – the most prominent feature of monthly MSL variability – is explored for the first time at 13 tide gauge locations in the German Bight. This comprises the analyses of its mean state as well as inter-annual and long-term changes as measured along the coast. Regional variations along the German North Sea coastline are also assessed. The variations are discussed in the light of their influence on the flood risk and the timing of strong storm surge water levels. As a first proxy for the forcing of interannual changes in the seasonal cycle, the influence of the NAO index is determined at each tide gauge.

In section 3, the physical mechanisms driving MSL variability and different NAO related meteorological forcing factors are studied in more detail. This is initially conducted on seasonal time scales by applying a combination of spatial correlation and multiple regression analyses. Multiple linear stepwise regression models (LRM) are developed, in which the meteorological forcing factors are used as independent predictors and MSL as the dependend variable. The role of meteorological forcing with respect to low frequency variations and long-term trend is also explored. The investigation is exemplarily applied to the long tide gauge record of Cuxhaven.

In section 4, the presented methods are applied to a larger data set covering the entire North Sea basin. While in section 3 the main focus is on seasonal influences, in this section special attention is given to inter-annual to decadal scale processes and the role of large-scale atmospheric and oceanographic forcing. The variability is described and distinguished into barotropic and baroclinic adjustment processes of the ocean. After explaining major sources of North Sea MSL variability, the impact of such fluctuations on the estimation long-term trends and acceleration/deceleration patterns is explored in a statistical Monte-Carlo framework under the consideration of plausible future SLR projections with relatistic noise.

Section 5 contains a practical application of the presented methods for deriving future MSL projections in the German Bight. Atmospherically induced MSL variations are described on the basis of large-scale SLP fields. A simple proxy is introduced and validated with respect to its ability in simulating future states of MSL rise and variability. The proxy is further used to downscale future changes in SLP onto MSL variations along the German North Sea coastline with a particular focus on inter-annual changes.

In section 6, historical storm surges are analysed. A novel storm surge record is reconstructed back to 1843 just on the basis of observed tidal high and low water levels. This record is investigated for long-term trends in the occurrence and intenstity of strong storms. The connection between storm surges and large-scale atmospheric forcing is also assessed. After demonstrating the similarity between the novel storm surge record and conventional storminess proxies in the region, the 20th century reanalysis (20CRv2) data sets, which are also applied in the present thesis to analyse MSL variability, are investigated for their homogeneity and their skill to derive long-term trends in storminess.

A summary of key findings is given in section 7. Final conclusions are drawn on the basis of the resuls presented in section 2 to 6. Recommendations for further research and practical applications for coastal planning and management tasks are also given.

2 MSL variability and influence of the NAO on long-term trends in the German Bight

2.1 Abstract

Changes in the seasonal cycle of MSL may affect the heights of storm surges and thereby flood risk in coastal areas. This chapter investigates the intra- and inter-annual variability of monthly MSL and its link to the NAO using records from 13 tide gauges located in the German Bight. The amplitudes of the seasonal MSL cycle are not regionally uniform and vary between 20 and 29 cm. Generally, the amplitudes are smaller at the southwestern stations, increasing as one travels to the northeastern part. The amplitudes, as well as the phase of the seasonal cycle, are characterized by a large inter-annual and inter-decadal variability, but no long-term trend could be detected. Nevertheless, in the last two decades annual maximum peaks more frequently occurred in January and February, whereas beforehand an accumulation was detected for the November and December period. These changes in phase in the various sea level time series are consistent with a shift in the annual cycle, which is, however, not significant. The changes are associated with strongly increasing trends in monthly MSL of the winter season (January–March), which are considerably higher compared to the remaining seasons. For the same season, the MSL and NAO indices show strong similarities, resulting in statistically significant correlations (r = ~0.7). Hence, these changes are linked with changing pressure conditions over the North Atlantic, which lead to a strong phase of positive values in the NAO index between the 1960's and 1990's.

2.2 Introduction

During the last century, coastal regions have been strongly governed by a rapid growth in populations and economic assets with increasing urbanization affecting the vulnerability. At the same time, global sea levels have risen as a result of a warming climate. Over the 20th century a significant rise in GMSL has been detected by different authors using various techniques (Church et al., 2010). The results of these studies show a strong variability in the rates of rise that is far from linear with inter-annual fluctuations linked to regional climate patterns (Church et al., 2008). Furthermore, the rates of observed MSL vary across the globe with regions of increase and regions of decrease (Bindoff et al., 2007). An extensive study addressing regional sea level development in the German Bight was conducted by Führböter and Jensen (1985). They analyzed mean tidal high water levels

(MHW) and mean tidal low water levels (MLW) over a time span of about 140 years and found significant increasing trends for the MHW of about 2.5 mm/yr on average but no significant change in the MLW. Jensen and Mudersbach (2007) updated and extended the study (in terms of the considered time period) and affirmed the key findings. They reported an increase in the mean tidal range (MTR) of about 10 % since 1955 along the German North Sea coastline. MSL changes in the German Bight have recently been investigated by Wahl et al. (2010, 2011), based on MSL time series from 13 tide gauges covering the entire German Bight. The focus was on analyzing long-term changes, making use of different statistical techniques. They found two periods of accelerated SLR, one at the end of the 19th century and another covering recent decades with some differences along the coastline.

For coastal planning it is not only important to understand long-term changes in MSL but also short-term variability, e.g., on annual time scales. First studies on the intra-annual (seasonal) behavior of MLW and MHW in the German Bight were conducted by Jensen et al. (1992). The key findings can be summarized as follows: The minima for MHW usually occur between February and April, while the maxima occur between July and August. From the corresponding seasonal cycle for the MLW minima were detected in April or May and maxima in October or November. Anyway, until now no studies have been undertaken aimed at analyzing the seasonal cycle of the MSL in the German Bight in detail.

For a better understanding of sea level changes, high quality sea level observations are needed. Different external factors, such as atmospheric pressure variations or meteorological forces, may affect observed water levels. These factors have to be analyzed in detail to quantify their influence on different time scales. One common method of addressing external effects is the observation of major atmospheric modes of variability that can have significant effects on the variability of sea level on inter-annual and inter-decadal time scales (Woolf and Tsimplis, 2002). The NAO, the El Nino-Southern Oscillation (ENSO) and the Northern Pacific Oscillation (NPO) are part of the global oscillation system. This global oscillation system has significant influences on weather and climate, including sea levels. For the investigation area considered for the present study (*i.e.*, the German Bight), the NAO is the main oscillation of interest. Commonly, the different oscillations are addressed by a normalized index.

Many authors studied the influence of the NAO using different atmospheric factors, such as rainfall and temperature (Hurrel, 1995; Hurrel et al., 2003), wind and other meteorological parameters (Thompson and Wallace, 1998; Ambaum et al., 2001; Martin et al., 2011). Further investigations on the link between NAO and Arctic ice export have been performed by Hilmer and Jung (2000), while Petrow et al. (2009) analyzed the relationship between changes in circulation patterns and flood hazard in Germany. Other publications indicate the influence of circulation patterns such as the NAO on sea level. Wakelin et al. (2003) examined sea level dependence over the Northwestern European Shelf and found varying correlations, which are positive in the northern region and strongly negative in the south. They measured sensitivity by looking at the seasonal (December to March) sea level changes (in mm) per unit NAO over the whole region by considering results from a

tide and surge model. Highest sensitivities with values up to 96 mm per unit NAO have been detected for the German Bight. Woodwort et al. (2007) investigated the dependence of sea level percentiles on the NAO in the North Sea and found a homogeneous distribution throughout the tidal range for the UK, but a larger dependence for extreme high waters compared to the median sea levels for the eastern parts of the North Sea (e.g., the German Bight). Yan et al. (2004) and Jevrejeva et al. (2005) noted that the relationship between NAO and sea level in the northern European parts is unsteady over time, with highest correlation values between the two parameters at the end of the 20th century. Tsimplis et al. (2005) summarized findings of a large number of earlier studies (which were published in the framework of a Tyndall Centre research project) on the NAO influence on sea level data and wave heights across northern Europe (using Cuxhaven as a proxy for the entire German Bight) and especially along the UK coastline. They identified the NAO as a major forcing for sea level variability using different statistical methods, such as correlation and regression analysis, wavelet analysis and trend estimations. Tsimplis and Shaw (2008) reconstructed regional MSL indices using EOF analysis of tide gauge records and investigated the correlation between sea level reconstructions and different climate indices. They found a dominant NAO influence on sea level, especially throughout the winter, which causes regional MSL anticorrelation between sea level observed by tide gauges located along northwestern European coasts and tide gauges located in the Mediterranean.

The present paper has three main objectives. The first is to analyze the observed changes in the seasonal cycle of the MSL along the German North Sea coastline. Changes in the seasonal cycle may affect the heights of storm surges, which often occur during the winter months. In the end, this has significant implications in terms of flood risk for the affected coastal areas. Furthermore, it is important to know how changes in MSL are distributed over the whole year. Therefore, the second objective is to investigate inter-annual changes based on seasonal MSL time series. The third objective consists of estimating the connection between inter-annual MSL variability in the German Bight and the NAO index. The influence of the NAO on observed long-term MSL changes is also analyzed. This allows for a better understanding of observed MSL changes, which is a crucial step, by means of deriving reliable regional MSL scenarios to be considered for regional and local coastal management strategies. The paper is structured as follows: In Section 2.3 the considered data sets are described, while the applied methods are described in detail in Section 2.4. The results are summarized in Section 2.5 and discussed in Section 2.6. Section 2.7 contains the final conclusions.

2.3 Data

In the present paper two different types of data are used:

1. Monthly MSL data from tide gauges located in the southwestern North Sea (German Bight)
2. Monthly data of the station based NAO index.

2.3.1 Sea level data

This section makes use of the monthly MSL data sets of 13 tide gauges in the German Bight. The tide gauges are operated by the German Federal Waterways and Shipping Administration. From the raw data (high frequency data and high and low waters), time series of MSL were reconstructed within the AMSeL project Wahl et al., 2010, 2011) . While Wahl et al. (2010, 2011) focused on analyzing the observed long-term changes based on annual MSL time series, in this chapter extended monthly MSL series are used for the first time. Figure 2-1 shows the investigation area of the German Bight with the location of the considered tide gauges (Figure 2-1a) and the monthly MSL time series of individual stations (Figure 2-1b). Each tide gauge provides at least 50 years of data. Although three gauges provide much longer records (Cuxhaven, Norderney and LT Alte Weser), only data from 1937 onwards are considered here to assure comparability of the results, especially from linear trend analyses.

The MSL data sets described above are considered in different ways with respect to the main objectives outlined in Section 1. Some of the investigations are undertaken, based on the monthly MSL time series of individual stations as presented in Figure 2-1; e.g., partial investigations in the seasonal cycle, the inter-annual changes of monthly MSL and sensitivities of MSL per unit NAO. At different stages of the chapter, so-called index time series (or 'virtual stations') covering larger areas in the German Bight are also considered. Virtual stations are computed from a specified number of single gauges by following the approach described by Wahl et al. (2011). In this approach, the first differences of monthly MSL time series are averaged. The resulting time series are integrated backwards by adding the previously calculated averaged first differences. Three virtual stations are used in the present chapter. The virtual station for Schleswig-Holstein represents the northeastern part of the German Bight. It comprises the available data from the tide gauges of List, Hörnum, Wyk, Dagebüll, Wittdün and Husum. Virtual station for Lower Saxony is constructed from the time series of the tide gauges of Cuxhaven, Bremerhaven, Wilhelmshaven, LT Alte Weser, Norderney and Emden, which are all located in the southwestern part of the German Bight. A third virtual station is constructed for the entire German Bight, including all tide gauges mentioned above (the tide gauge of Helgoland is additionally used to cover the offshore region).

2.3.2 NAO data

The NAO can be described as a varying strength of two atmospheric pressure fields over the subpolar and subtropical regions of the North Atlantic. The variability of the NAO is commonly described through the NAO index. This index is derived by computing the differences between anomalies of both pressure fields. The index becomes positive if both pressure systems over the Azores and Iceland are well formed, which means the combination of a low pressure field over Iceland and a high pressure field over the Azores. Periods of positive NAO generally induce low-pressure fields over Iceland resulting in high precipitation, mild temperatures and increasing westerly winds over northern Europe

(Hilmer and Jung, 2000). A negative index means a low gradient, i.e., the deviation from the mean pressure is rather small. There are two different types of NAO indices.

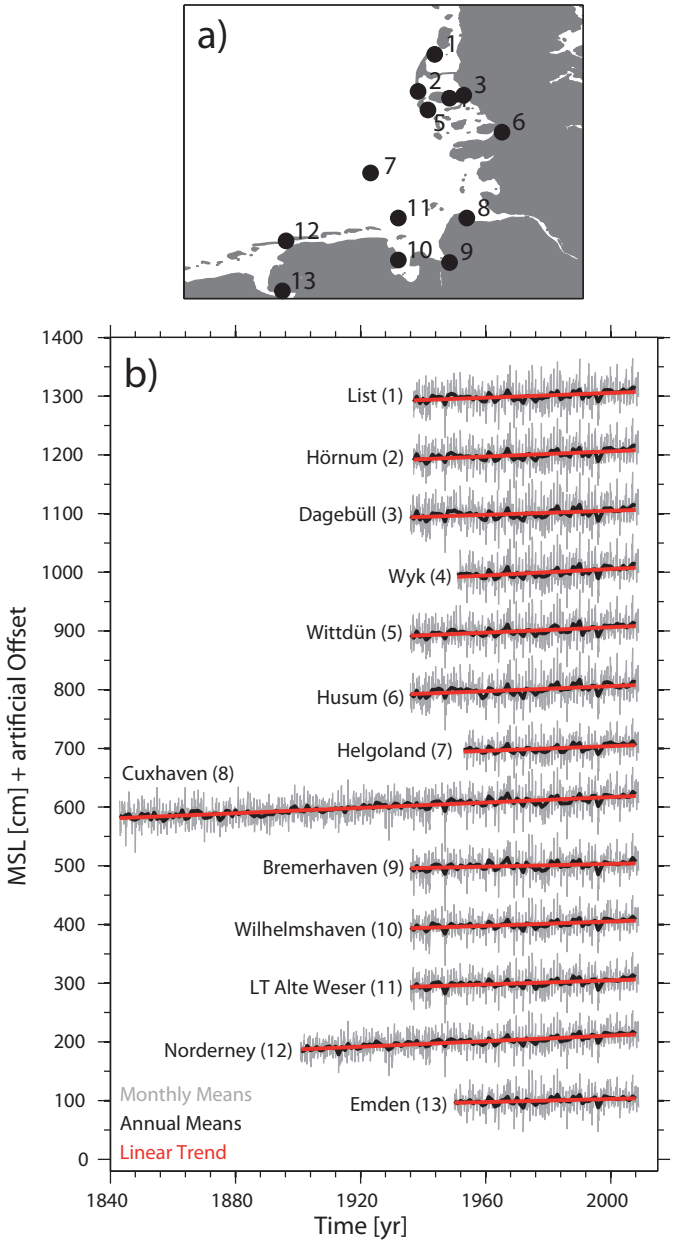

Figure 2-1: a) Investigation area and tide gauge locations. b) Monthly (grey) and annual (black) MSL time series of each tide gauge location shown in a). The linear trend is also shown in red.

One well established index is the so-called station based index, computed on the data basis of two different stations between north and south. Jones et al. (1995) computed an index using the difference between SLP anomalies at Gibraltar and Reykjavik. One typical uncertainty of this index is that the stations are fixed in space, while the NAO centers (centers of the pressure fields—centers of action; COA) underlie movements resulting from annual cycles or other processes. Therefore, the use of principle component analysis of atmospheric pressure constitutes is the more sophisticated approach. However, detailed comparison of the two different indices (not shown here) pointed out that the differences between the two indices are small and do not have influences on the results of this study (i.e., regression and trend analyses). Hence, the NAO index, established by Jones

et al. (1995), is used. The data set was downloaded from the website of the Climatic Research Unit, University of East Anglia for the time period from 1937 to 2008.

2.4 Methods

2.4.1 Calculating the seasonal cycle

At this stage, the seasonal cycle of the time span from 1951 to 2008 (all tide gauges provide data for this period) is analyzed. As a long-period tide, the seasonal cycle is formed by the solar annual (Sa) and solar semiannual (Ssa) tidal constituents with periods of 12 months and 6 months driven by solar heating (Pugh, 2004). There are different ways of how to compute the seasonal MSL cycle from tidal observations. An empirical method is described by Pezzulli et al. (2005), in which the seasonal cycle is represented by averaging each calendar month over a defined time span. Another option is to use harmonic analysis, in which the annual cycle can be described by its amplitude and phase (Plag and Tsimplis, 1999). For the present chapter, the empirical description of the seasonal cycle is considered.

In a first step, the monthly MSL records are detrended by using linear regression analysis. The removal of the linear trend enables the consideration of the annual cycle separately from its annual long-term development. In a second step the detrended monthly MSL series are transferred into twelve time series for each calendar month (i.e., one time series for January, one for February, and so on). The annual series of each month are averaged over the time span from 1951 to 2008. These averages represent the mean seasonal cycle. The seasonal cycle is then plotted in a similar manner as presented in (Barbosa et al., 2008).

Furthermore, the year-to-year variability of the maximum and minimum values of the seasonal cycle is analyzed. It is calculated how often each month the maximum or minimum monthly intra-annual sea level (absolute frequency) occurs within a decade. Seven different decades, starting with 1939 to 1948 and ending with the decade 1999 to 2008, are evaluated.

2.4.2 Amplitudes of the seasonal cycle

When using the empirical description of the seasonal cycle, the amplitude is defined as the difference between the maximum and minimum monthly values for the analyzed period. In this chapter, the inter-annual development of the amplitude of the seasonal cycle is of special interest. It is analyzed whether changes in the amplitudes of the seasonal cycle are evident from the available observations, as such changes may enhance flood risk for the investigation area. The amplitude is computed for each single year of the analyzed detrended time series, introduced in Section 3.1. These investigations are solely done for the two virtual stations of Schleswig-Holstein and Lower Saxony.

2.4.3 Inter-annual changes in monthly MSL

As described above, Wahl et al. (2011) analyzed the long-term development of MSL, based on annual data sets. Here, the inter-annual changes in monthly MSL series of each of the 13 tide gauges along the German North Sea coastline are analyzed. One major interest for flood risk management is whether or not the MSL changes are homogeneous over the whole year or different seasons, respectively. Inhomogeneous changes in different seasons (e.g., winter and summer) may affect the phase of the seasonal cycle. Hence, the inter-annual development of winter and summer season is analyzed for each site and for different time spans. The winter half year are defined as the first half of the so-called “hydrological year”, which includes 6 months between November and April (hereafter: NDJFMA MSL). Consequently, the hydrological summer half year comprises the months from May to October of each year (hereafter: MJJASO MSL). The time spans under consideration are the same as used by Wahl et al. (2011) to ensure comparability of the results of both studies. Because of the length of the different data sets three different time spans are used. The first one and the longest one considered for the present chapter starts in 1937 and ends in 2008. In this period three gauges (Emden, Helgoland, Wyk) cannot be taken into account because of missing data. The second time span covers the years between 1951 and 2008. For this time span all gauges can be analyzed, even if the Helgoland tide gauge starts in 1953 (more than 93 % of the data of all records are available). The third time period consists of 38 years of data from 1971 to 2008. The inter-annual changes are solely analyzed with respect to their long-term linear development.

2.4.4 The influence of the NAO on MSL

To evaluate the relationship between inter-annual MSL variability and regional climate patterns, the monthly MSL time series of the virtual stations of Schleswig-Holstein, Lower Saxony and the entire German Bight are compared to the NAO index. In a first step, the MSL time series for each month are correlated with the analogical NAO time series. The significance of the correlation coefficients r_{xy} is tested with a t-test as described by von Storch and Zwiers (1999).

The total sea level, which is recorded by tide gauges, is composed of three main components: the astronomical tides, the MSL and the surge component (Pugh, 2004). The surge component is generally larger in the storm surge season during the winter. Hence, the NAO index as a proxy for westerly winds over the North Atlantic is mostly useful in the colder season of the winter months. From correlation and trend analyses (see Section 4.4) it was found that the NAO influence on MSL is largest between January and March. Hence, these months are considered for most of the analyses where the connection between NAO and MSL is investigated. The MSL values of the three months are averaged for each year to yield a time series, which is denoted here as winter season MSL (hereafter referred to JFM MSL and JFM NAO for short winter NAO). The interaction of JFM MSL and JFM NAO is analyzed with LRMs between JFM MSL time series and corresponding JFM NAO time series following the approach proposed by Wakelin et al. (2003). In a first step, both short winter time series (i.e., JFM MSL and JFM NAO) are detrended. After-

wards, the detrended JFM MSL values are regressed with the detrended JFM NAO values. Thus, the sensitivity of the JFM MSL to the JFM NAO index can be estimated, suggesting that the JFM MSL is a linear function of the JFM NAO index. Furthermore, the NAO effects are subtracted from the JFM MSL to estimate the influence of the JFM NAO on long-term changes of JFM MSL in the German Bight. For comparison, linear trends are computed for the original JFM MSL time series and the JFM NAO corrected JFM MSL time series (i.e., difference between JFM MSL and regression residuals).

For the detection of non-linear changes in both parameters (JFM MSL and JFM NAO), the time series are smoothed. Smoothing techniques (or low pass filters) are often applied when analyzing climatic time series, as such time series cannot be exactly described mathematically (Hänggi et al., 2011). The different techniques available from literature are controversially discussed by the scientific community, because of their mathematical background and especially with respect to different techniques of computing values for the smoothed time series near the sample boundaries (see e.g., Wahl et al., 2011; Mann, 2004; Mann, 2008). Here, a locally-weighted-scatterplot-smoother (LOWESS, Cleveland, 1979; Cleveland and Devlin, 1988) in combination with Monte-Carlo autoregressive padding (MCAP) as described in Wahl et al. (2010, 2011) is used. The MCAP method is applied to assess uncertainties when continuing smoothed time series to the end of the original time series. The LOWESS filter considers individual polynomial functions and the weighted least squares method and represents a robust low pass filter assigning lower weight to outliers. The method is applied here to detect different periods of SLR and fall (or non-linear changes in the NAO index) that cannot be detected through linear trend analyses. Furthermore, the smoothed time series are used to derive the rates of rise (for both MSL and NAO) by calculating the first differences.

2.5 Results

2.5.1 The seasonal MSL cycle

In this section the results from analyzing the seasonal component of the detrended monthly MSL are presented. The variability of the seasonal cycle is figured by the means of month plots that are shown in Figure 2-2. The blue lines represent the time series for every single month over the period 1951 to 2008 (i.e., for example, all January values from 1951 to 2008). The horizontal black lines represent the average values for the particular month. The bold red lines show the months with minimum and maximum values of the seasonal cycle. For all tide gauges in the German Bight the maximum is found in November, while the minimum is in April for List, Wilhelmshaven, LT Alte Weser, Helgoland and Norderney and in May for Hörnum, Wyk, Dagebüll, Wittdün, Husum, Cuxhaven, Bremerhaven and Emden. The amplitude of the seasonal cycle is higher along the northeastern coastline (i.e., the state of Schleswig-Holstein) with values from 27–29 cm compared to the southwestern part of the German Bight (i.e., the state of Lower Saxony) with values for the amplitudes of about 20–23 cm. These amplitudes are higher than those computed for the

North Atlantic region (e.g. Barbosa et al., 2008), but comparable to those for the Baltic Sea reported in Hünicke et al. (2008).

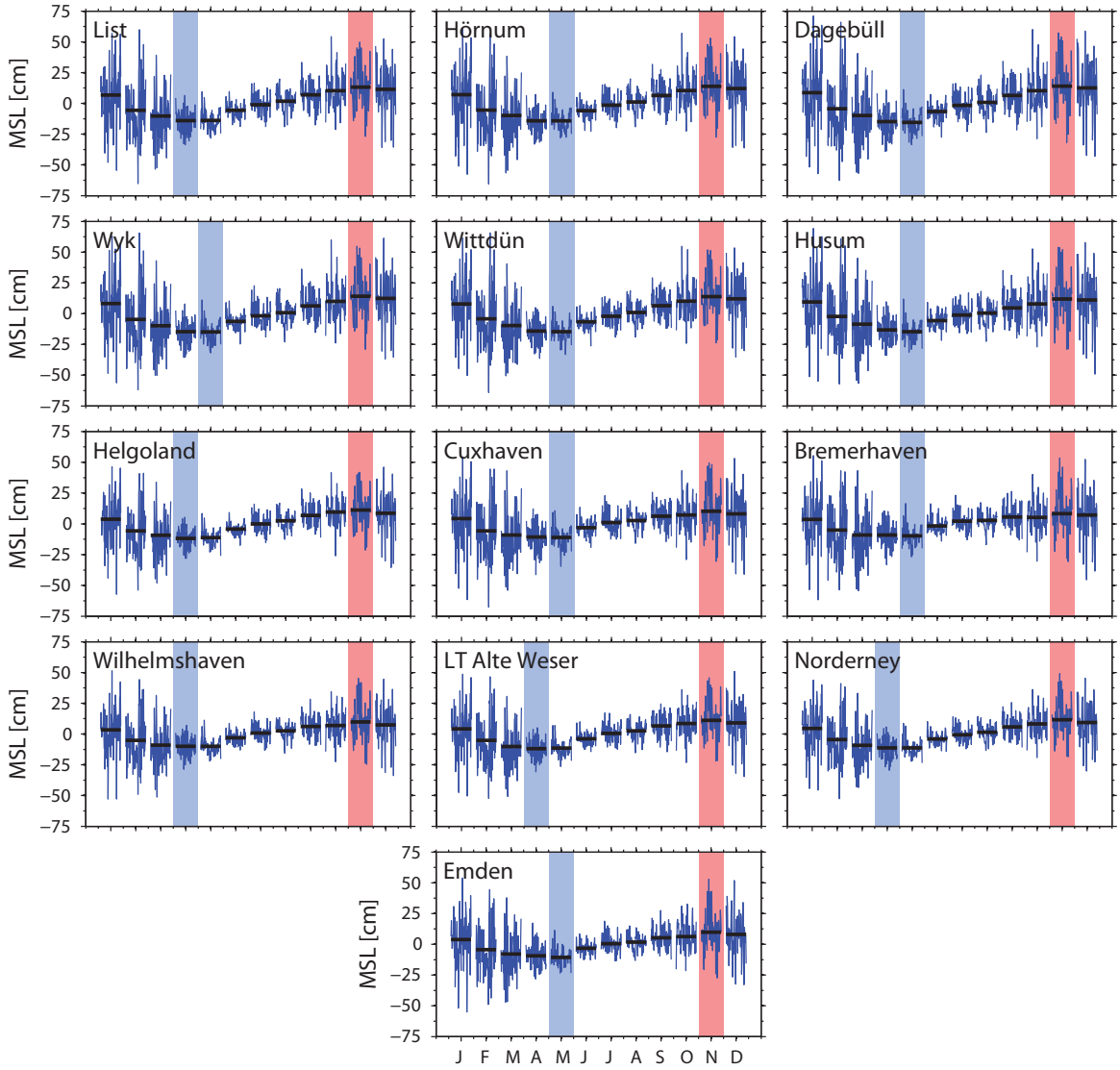

Figure 2-2: Plot of the annual component for each tide gauge and the period from 1951 to 2011. The blue lines represent the individual monthly time series, while the black horizontal lines show the long-term MSL cycle. The blue shaded area marks the month in which the mean seasonal cycle has its minimum at each gauge, while the red shaded area represents the maximum.

The plots of the seasonal cycle in Figure 2-2 further show higher variability in the MSL for the winter months compared to the summer months. The seasonal cycle becomes visible at each tide gauge, but is overlapped by a large inter-annual variability. Sea levels in the North Sea are generally driven by atmospheric effects: On the one hand, atmospheric pressure fluctuations affect sea levels through the inverse barometer effect. On the other hand, cross-shore winds as well as alongshore winds together with the Coriolis effect can cause a sea level increase (or decrease) near the coastline. Generally these effects are stronger during the winter seasons when storm surges are stronger and more frequent (Wakelin et al., 2003). Similar to the gradient in the seasonal amplitudes, the overall inter-annual variability is higher in the northeastern part of the German Bight (i.e., the state of Schleswig-Holstein) compared to the region of Lower Saxony in the southwestern part.

The year-to-year variability of maximum and minimum values of the seasonal cycle in the German Bight is analyzed for all of the 13 tide gauges during the last 7 decades from 1939 on (results are summarized in Figure 2-3). For every single decade the occurrence time of maximum and minimum values is evaluated. As it is to be expected from Figure 2-2 the maximum and minimum values are widely distributed over the year. Maximum values occurred between August and March with an accumulation during November and February, while minimum values are distributed over several months between October and June with an accumulation between February and May. The occurrence time of both maximum and minimum values was found to be homogeneous between the different tide gauges.

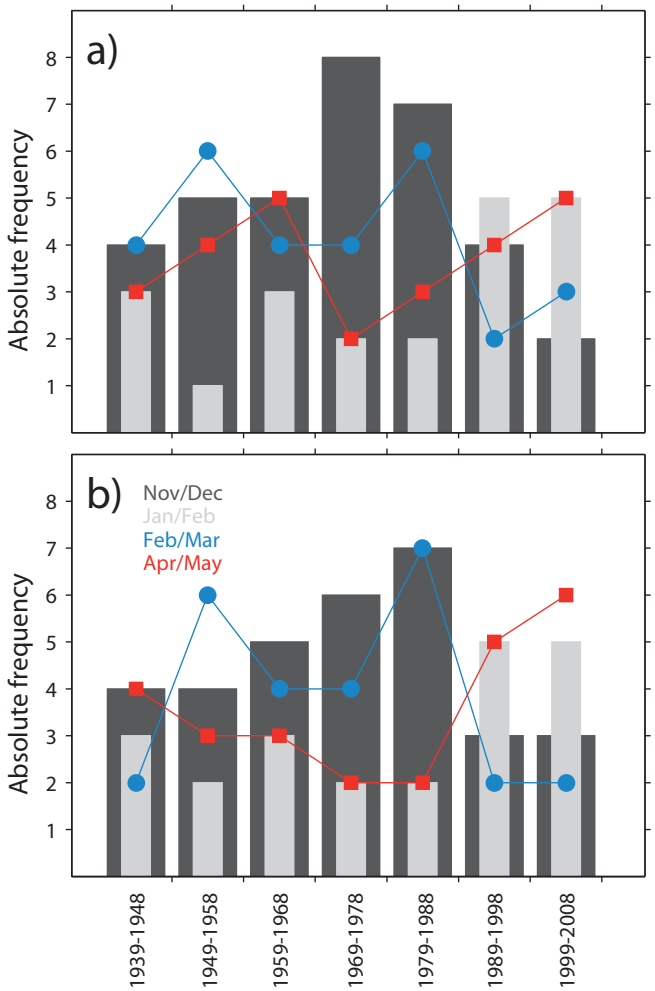

Figure 2-3: Development of the occurrence times of maximum (November to February, bars) and minimum (February to March, lines with dots and squares) values of the seasonal cycle over the past seven decades between 1939 and 2008 for the two virtual stations Schleswig-Holstein (a)) and Lower Saxony (b)).

Furthermore, the evaluation of the occurrence time shows regional homogeneous change in the last two decades (i.e., 1989 to 2008) compared to the first five analyzed decades (i.e., 1939 to 1988). While in the first five decades maximum values of the seasonal cycle predominantly occurred during November and December, after 1988 the months of January and February show an increasing number of maximum values. Simultaneously, the occurrence time of minimum values shifted from February and March into April and May. This is ideally represented by the two virtual stations of Schleswig Holstein and Lower Saxony in Figure 2-3. The figure shows histograms of absolute frequency of maximum and minimum values for the months of accumulation (i.e., November/December and Jan-

uary/February for maximum values; February /March and April/May for minimum values) over the seven decades. Before 1988 in approximately 55 % of all years' maximum values occurred during November and December, while afterwards the percentage decreased to 30 %. The amount of maximum values in January and February in turn increased from approximately 23 % before 1988 to 50 % afterwards. For the minimum values, a similar development is found. While in the first five decades the dominant months of accumulation are February and March (approximately 49 %; April and May approximately 26 %), in the last decades the minimum of the seasonal cycle predominantly peaks in April and May (approximately 53 %; February and March approximately 25 %).

2.5.2 Annual amplitudes of the seasonal cycle

Annual amplitudes of the seasonal cycle are computed as differences between maximum and minimum values for each year. Figure 4 shows the temporal development of the amplitude of the two virtual stations for Schleswig-Holstein and Lower Saxony and for the time period from 1937 to 2008. Both time series show similar temporal behaviors. The correlation coefficient of the amplitudes of both areas is found to be $r = 0.93$, whereas the amplitude of the annual cycle for Schleswig-Holstein is characterized by a slightly higher variability (and a higher mean value as already mentioned in Section 4.1) compared to Lower Saxony. Note that the annual amplitudes computed by this method are considerably higher than those mentioned in Section 4.1, where average values were considered to calculate mean amplitudes (in the order of 20 to 25 cm). Here, annual amplitudes are determined and found to be of the order of 50 to 60 cm. This is caused by the high temporal variability in the German Bight, which is described in section 4.1. However, as can be seen from Figure 4, the annual amplitudes for both virtual station time series do not show significant linear trends during the investigation period from 1937-2008, but considerable decadal variability with a clear amplification between the 1960s and mid-1990s.

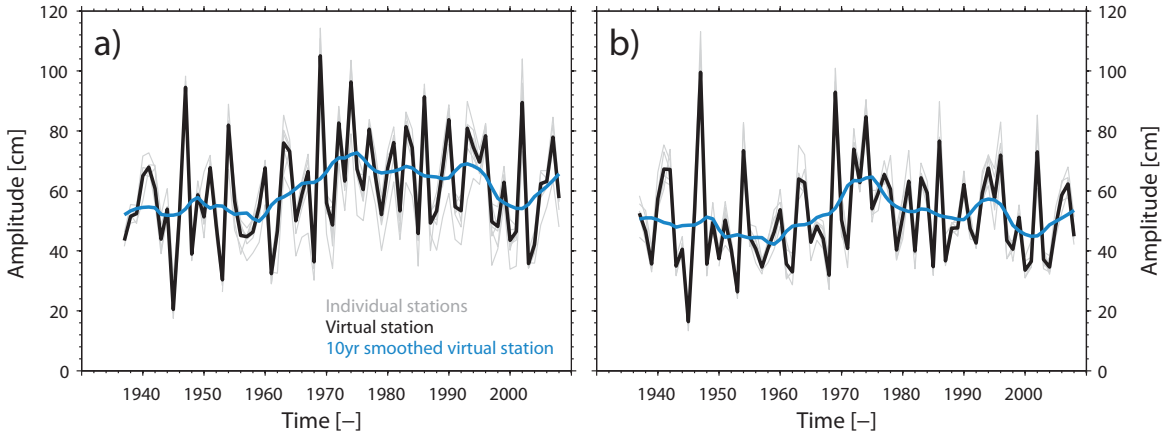

Figure 2-4: Time series of annual amplitudes for the virtual stations of Schleswig-Holstein (a)) and Lower Saxony (b)) for the period from 1937 to 2008. Individual stations are also shown (grey). The thick blue lines represent the 10yr smoothed amplitudes using a LOWESS filter. The annual amplitudes are computed as differences of monthly maximum and minimum values for each year.

2.5.3 Inter-annual MSL changes

In this section, inter-annual MSL changes are analyzed for each tide gauge site. The time series are divided into winter (November to April, NDJFMA MSL) and summer (May to October, MJJASO MSL) half years (see Section 3.3). Table 1 shows the linear trends (with 1σ SEs accounting for serial correlation as recommended by Santer et al. (2000), see also chapter 5) for different time periods. Values are marked bold if the trends of the two seasons under consideration differ significantly, i.e., the difference between both trends is larger than the maximum SE. The estimated trends are different in both seasons for all of the time periods and tide gauges under consideration, but statistically significant differences are only found for the two time periods from 1937 to 2008 and 1951 to 2008. Even if they also show different seasonal tendencies, the tide gauges of Husum and Emden are striking here, as their seasonal trends are not statistically significant. While in the first two time spans the winter season trends rise by a factor of up to 2.5 (on average), compared to the trends in the summer season (differences are in the order of 1.0 to 1.5 mm/yr), they are only 1.1 times (on average) higher (differences in the order of 0.5 mm/yr) for the shorter time period from 1971 to 2008.

Table 2-1: Linear trends for different periods differentiated in winter (November to April) and summer (Mai to October) half year. The values are marked bold if the linear trends of the two seasons differ significantly (95 % confidence level t-test statistics). Cases where less than 75 % of data were available during a specific period are not considered and marked by NaNs.

Tide Gauge	Linear trends					
	1937-2008		1951-2008		1971-2008	
	Winter	Summer	Winter	Summer	Winter	Summer
List	**2.51 ± 0.62**	**1.42 ± 0.39**	**3.49 ± 0.93**	**1.46 ± 0.67**	4.80 ± 1.93	3.78 ± 1.02
Hörnum	**2.83 ± 0.62**	**1.60 ± 0.39**	**3.81 ± 0.91**	**1.69 ± 0.65**	4.70 ± 1.90	3.82 ± 1.15
Dagebüll	**2.30 ± 0.68**	**1.08 ± 0.39**	**3.36 ± 0.97**	**1.20 ± 0.68**	3.99 ± 1.98	3.42 ± 1.15
Wyk	NaN ± NaN	NaN ± NaN	**3.96 ± 0.96**	**1.67 ± 0.60**	5.01 ± 1.99	4.24 ± 0.78
Wittdün	**2.90 ± 0.60**	**1.78 ± 0.36**	**3.50 ± 0.91**	**1.82 ± 0.61**	4.28 ± 1.89	3.77 ± 1.02
Husum	2.29 ± 0.67	1.98 ± 0.37	3.04 ± 0.96	2.06 ± 0.61	3.58 ± 1.95	3.68 ± 1.13
Helgoland	NaN ± NaN	NaN ± NaN	**2.99 ± 0.79**	**1.23 ± 0.60**	4.18 ± 1.58	3.47 ± 0.76
Cuxhaven	**2.67 ± 0.64**	**1.51 ± 0.37**	**2.84 ± 0.90**	**1.19 ± 0.58**	4.10 ± 1.78	3.53 ± 0.76
Bremerhaven	**1.69 ± 0.62**	**0.65 ± 0.36**	**1.84 ± 0.86**	**0.21 ± 0.54**	3.24 ± 1.69	1.91 ± 0.87
Wilhelmshaven	2.32 ± 0.55	1.39 ± 0.30	**2.81 ± 0.75**	**1.29 ± 0.45**	3.93 ± 1.54	3.21 ± 0.66
LT Alte Weser	2.05 ± 0.53	1.37 ± 0.34	**2.27 ± 0.75**	**1.17 ± 0.49**	3.48 ± 1.53	2.87 ± 0.89
Norderney	**2.84 ± 0.51**	**1.91 ± 0.30**	**3.57 ± 0.67**	**2.20 ± 0.48**	4.55 ± 1.35	4.33 ± 0.57
Emden	NaN ± NaN	NaN ± NaN	1.91 ± 0.81	0.91 ± 0.43	2.31 ± 1.58	2.10 ± 0.83

Similar to the findings reported by Wahl et al. (2011), highest trends are detected for the shortest period from 1971 to 2008. While the trends for the NDJFMA MSL and MJJASO MSL of the first period from 1937 to 2008 are about 2.4 mm/yr and 1.6 mm/yr respectively (averaged over all sites), the trends for the last period (i.e., 1971 to 2008) are about 3.9 mm/yr and 3.4 mm/yr for the two seasons. SEs increase inversely to the length of the time period under consideration. Thus, smallest SEs (in the order of 0.5 mm/yr and 0.3 mm/yr for the NDJFMA MSL and MJJASO MSL, respectively) are found for the first period (i.e., 1937 to 2008). The highest SEs, in the order of about 1.31 mm/yr and 0.64 mm/yr, are derived for the final period (i.e., 1971 to 2008). Furthermore, averaged SEs (over all gauges) show significant differences between NDJFMA MSL and MJJASO MSL. As outlined by Wahl et al. (2011), from analyzing annual MSL time series, higher trends are

found for tide gauges along the coastline of Schleswig-Holstein compared to Lower Saxony.

2.5.4 Relationship between the NAO and MSL

The relationship between the detrended MSL, represented by the two virtual stations for Schleswig-Holstein and Lower Saxony, and the detrended NAO is shown in Figure 5. The blue line represents the correlation coefficients for the individual months and the period from 1937 to 2008. The red lines indicate the 95 % and 99 %-confidence levels (based on t-test statistics (e.g von Storch and Zwiers, 1999)). There is a strong annual cycle in the correlation, with significant correlations in the winter season and weak or no correlations in the summer months. For the whole year, correlation coefficients for time series from Schleswig-Holstein and the NAO are slightly higher than the coefficients for MSL time series from Lower Saxony and the NAO. This gradient between Schleswig-Holstein and Lower Saxony has also been found in the variability of the seasonal cycle in Sections 4.1 and 4.2. The highest correlations are found from January to March. This leads to the assumption that the highest influence of NAO on long-term development of MSL should also be found in these three months. While for the correlation analysis only detrended time series are investigated, it is of particular importance in which manner the NAO may influence linear trends of MSL. To consider this, linear trends of MSL time series for each month are compared with those found from corresponding monthly NAO time series. The linear trends of monthly time series for both parameters are pictured in Figure 6. At the top of the figure the different dots indicate the trends of monthly MSL time series for the individual sites and the period from 1951 to 2008. Figure 6 (bottom) shows the monthly trends of the NAO. Both parameters show similar behavior for the winter months, indicating significantly higher trends from January to March compared to the remaining months (i.e., significantly different on the 1σ-confidence level). Although correlation over the whole year is not constant between the two parameters and partially weak (especially in the summer months), a similar trend pattern is notable from Figure 6. This behavior was also found for the other two time periods (i.e., 1937–2008 and 1971–2008), which are not pictured here.

The similar trend pattern, with higher values for the three months from January to March, leads to the assumption that the high NAO trends in the three winter months strongly influence the MSL changes for the same months. Hence, the interaction between JFM MSL and JFM NAO is described by the sensitivity of JFM MSL (unit is mm) per unit JFM NAO. As described in Section 3.4, sensitivity is estimated by applying LRMs between both parameters. Figure 7 shows the derived sensitivities for the three different time periods that have been used in Section 4.3 for the linear trend analyses. The largest sensitivities of the JFM MSL are found at the northeastern coastline in the area of Schleswig-Holstein with values up to 130 mm per unit JFM NAO index for the last period (i.e., 1971 to 2008), while the sensitivities for the area of Lower Saxony are considerably smaller (up to 45 mm per unit JFM NAO). The sensitivities change over time. While the sensitivity is almost the same for the first two periods (1937 to 2008 and 1951 to 2008), it is considerably higher for the last period (1971 to 2008). Jevrejeva et al. (2005) also reported a remarkable tem-

poral change of the NAO influence on sea levels in Northern Europe, with highest correlation values between both parameters found for the last three decades. These results indicate that the NAO influences the inter-annual variability of winter MSL at least to some degree. In agreement to the results presented by Jevrejeva et al. (2005), the contribution of the NAO is 30–35 % of winter MSL variability in the German Bight. Generally, MSL is higher in winters with positive NAO indices than in winters with negative NAO indices.

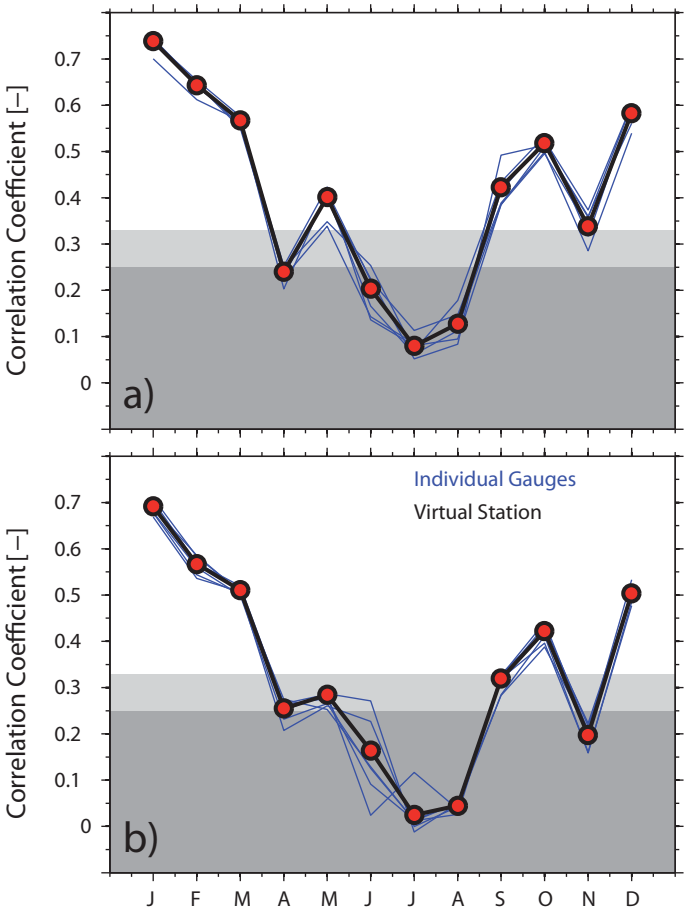

Figure 2-5: Correlation coefficient between the monthly NAO index and monthly MSL as measured by the individual tide gauges (blue) and the two virtual stations (black line with red filled dots) for Schlewig-Holstein (a)) and Lower Saxony (b)). The grey shades represent the 95 % and 99 % confidence level as given by t-test statistics (von Storch and Zwiers, 1999), respectively.

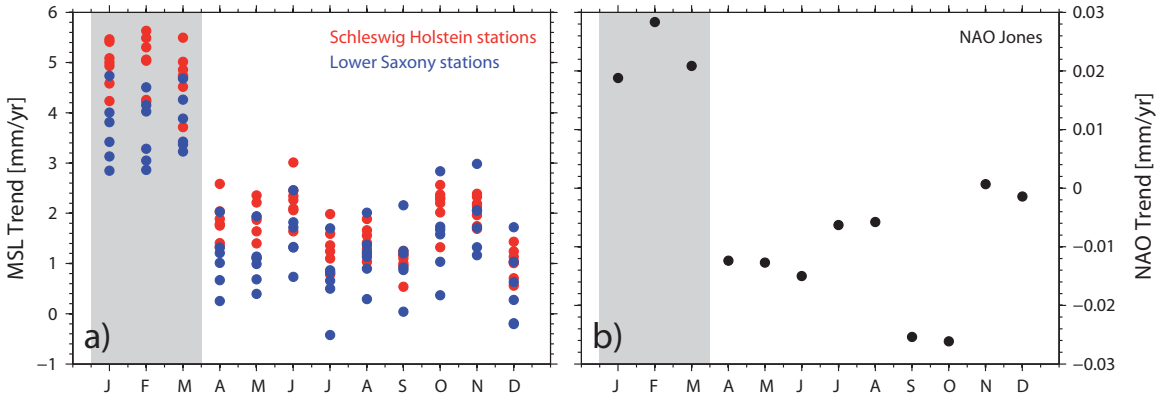

Figure 2-6: Inter-annual trends of monthly MSL (a)) and NAO (b)) over the period from 1951 to 2011. Blue dots correspond to stations located along the Schleswig-Holstein coastline, blue dots to stations located along the Lower Saxony coastline and back dots to the NAO. The grey shaded area marks the three months which differ significantly from the remaining year.

If the JFM NAO influences the JFM MSL variability in the German Bight over a specified time period and shows a significant trend at the same time, the question arises whether the JFM NAO also influences the JFM MSL long-term trends as well. Tsimplis et al. (2005) analyzed the NAO influence on long-term winter (December to March) MSL trends for different gauges in Northern Europe and found that in most cases the MSL trends are smaller if the NAO influence is considered (of course only for those gauges where a positive correlation exists between NAO and MSL). To investigate the JFM NAO influence on long-term JFM MSL trends in the German Bight, Table 2 shows trends calculated directly from the JFM MSL time series (January to March) and for comparison, the trends, which are found after the JFM MSL time series, are corrected for the JFM NAO influence. The latter is estimated by applying the same LRMs that have been used to study the sensitivities as shown in Figure 7. Beside the two virtual station time series for Schleswig-Holstein and Lower Saxony, a virtual station for the entire German Bight is also considered at this stage. The results clearly point out that the JFM NAO influences the long-term winter MSL trends. Again, however, this influence changes over time. Considering the first two time spans from 1937 to 2008 and 1951 to 2008 the winter MSL trends are about 3.3 mm/yr and 4.3 mm/yr, respectively (for the entire German Bight). After removing the JFM NAO influence the residuals show smaller trends of 2.2 mm/yr and 2.3mm/yr. The trends for the two virtual stations Schleswig-Holstein and Lower Saxony show small differences with a higher JFM NAO influence in Schleswig-Holstein than in Lower Saxony as was expected from the results presented in Figure 5. As reported in Section 4.3, the NDJFMA MSL trends increase for the shorter time period from 1971 to 2008. For the virtual station of the entire German Bight, the JFM MSL trend is found to be 7.6 mm/yr, whereas it decreases to 6.2 mm/yr after removing the JFM NAO influence (equals a trend reduction of 18 %). Due to the reduction of the variability by considering the JFM NAO influence, the SEs of the estimated trends also decrease (from 2.4 mm/yr to 1.4 mm/yr).

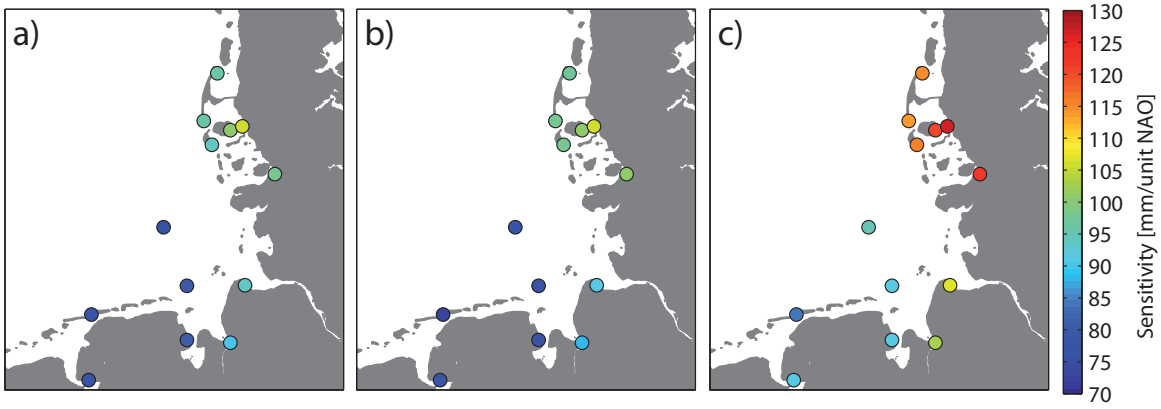

Figure 2-7: Sensitivity (sea level changes in mm/unit NAO change) of JFM MSL (January to March) at different tide gauge locations (dots) to JFM NAO over the periods a) 1937-2008, b) 1951-2008 and c) 1971-2008.

To analyze more in detail in which way the JFM NAO influences decadal JFM MSL trends, 19-year running linear trends of JFM MSL (for the entire German Bight) and the JFM NAO are shown in Figure 8. According to their different scaling, the 19-year running JFM NAO trends (red line) are scaled to be comparable to the 19-year running JFM MSL trends. The latter are represented by the blue line and corresponding 1σ SEs (grey-filled areas) are

also shown. Both time series of the running 19-year linear trends show a similar temporal behavior with only two phases (1971 to 1989 and 1972 to 1990, 1989 to 2007 and 1990 to 2008), where the JFM NAO trends proceed outside the 1σ confidence intervals calculated for the JFM MSL trends. More than 93 % of all estimated JFM NAO trends proceed inside the 1σ confidence intervals of the JFM MSL trends.

Table 2-2: Linear trends of JFM MSL for the three virtual station time series over diferent periods and before and after correcting for the influence of JFM NAO. If the trends differ significantly (95 % confidence level t-test statistics) after correcting for the NAO influence values are marked in bold. The values in the brackets provide the linear correlation between JFM MSL and the JFM NAO.

Tide Gauge	Linear trends					
	1937-2008		1951-2008		1971-2008	
	with NAO	NAO corrected	with NAO	NAO corrected	with NAO	NAO corrected
German Bight	**3.31 ± 0.92**	**2.14 ± 0.59**	**4.30 ± 1.19**	**2.07 ± 0.84**	7.58 ± 2.60	6.27 ± 1.87
	[0.75]		**[0.72]**		[0.82]	
Schleswig-Holstein	**3.59 ± 1.01**	**2.33 ± 0.62**	**5.01 ± 1.32**	**2.59 ± 0.89**	8.36 ± 2.79	6.94 ± 1.99
	[0.76]		**[0.74]**		[0.84]	
Lower Saxony	**3.24 ± 0.85**	**2.15 ± 0.58**	**3.70 ± 1.13**	**1.63 ± 0.80**	6.90 ± 2.47	5.68 ± 1.80
	[0.73]		**[0.70]**		[0.80]	

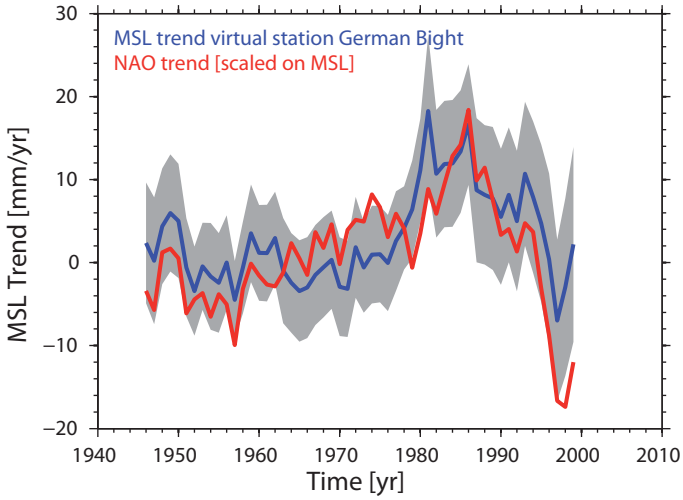

Figure 2-8: 19 year moving trend for JFM MSL (blue line) at the virtual station German Bight ± 1σ SE (grey area). The scaled JFM NAO trends (red line) are also shown.

Figure 9 shows the time series of the JFM MSL for the entire German Bight (top, left, black line) and the JFM NAO index (top, right, black line) for the period from 1937 to 2008 and the smoothed time series (blue lines in the upper subplots). The rates of rise calculated as the first differences from the smoothed time series are shown in the lower subplots of Figure 9. The window length for smoothing the time series was chosen to be 30 years and the values near the sample boundaries result from applying the MCAP method briefly described in the Section 3 and in Wahl et al. (2010). The uncertainties resulting from smoothing the time series to the boundaries are represented by the grey-shaded areas. The time series of the JFM NAO and JFM MSL are highly correlated (r = 0.74). Both of the original time series show similar peak values in many years: e.g., 1938, 1941, 1947, 1967,

1983, 1990, 1996 and 2002. In some years the values are also different, suggesting that the NAO is not the only driver of MSL variability. However, the smoothed time series show a similar temporal behavior (especially between the mid 1970's and mid 1990's) with some differences near the sample boundaries. By considering the rates of rise (Figure 8, bottom) both time series show similar tendencies near the sample boundaries as well, even if the estimates for the boundaries are uncertain. Although the rates of rise indicate negative values for the JFM NAO index and positive values for the JFM MSL at the end of the 1990s, they are marked by a comparable shape. Hence, significant influences of the JFM NAO on JFM MSL can be detected. These influences changed over time, suggesting the non-stationary behavior of the COAs of the NAO as is described by Kolker and Hameed (2007). In some phases it seems that other external forcing factors are getting stronger from time to time. The phases in the beginning of the 1960's and the last ten years are striking here.

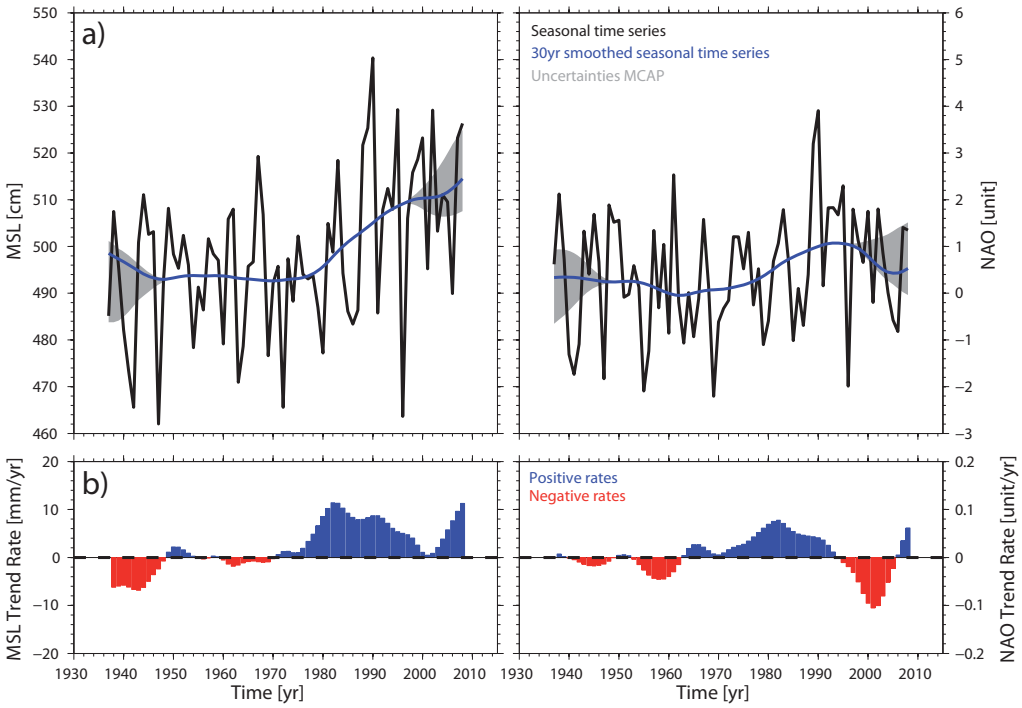

Figure 2-9: a) Time series of JFM MSL (left, black) and JFM NAO (right, black) and their low-pass filtered version (blue, cut-off period: 30 years). The grey areas represent the uncertainties as calculated with the MCAP method at the ends of the time series. b) Annual positive (blue) and negative (red) trend rates series shown in a) calculated by the first differences of the low-pass filtered time.

2.6 Discussion

Recent assessments of MSL changes in the German Bight have mostly focused on inter-annual changes and hence considered annual time series. Especially for aspects of coastal safety management, inter-annual MSL assessment is particularly important as it considerably affects storm surge heights and frequencies. As pointed out in Mai and Zimmermann (2005) and Schuchardt et al. (2005), accelerating MSL diminishes the present safety level along the German North Sea coastline, even if the vulnerability is relatively moderate. However, increasing sea levels involve a higher water inflow in the event of the failure of coastal protection structures. Storm surges are the main events affecting coastal

areas, especially when they are combined with high astronomical tides (e.g., spring tides). Changes in the seasonal cycle may influence water levels occurring during a storm surge season and until now seasonal investigations of MSL in the German Bight have not received much attention.

The results from analyzing the intra-annual variability in MSL along the German North Sea coastline (Section 4.1) show that there are considerable seasonal effects. As a shallow shelf sea, the North Sea is strongly influenced by wind forces. This implies higher variability of MSL in the storm surge or winter season respectively, compared to the summer season. In summer months the wind stress is considerably lower, which results in lower variability. Therefore, tidal forces have a stronger relative influence on the MSL. Furthermore, the results point to some differences along the coastline with higher variability in the northeastern than in the southwestern part of the German Bight. These differences result from the fact that westerly winds are predominant in the North Sea with a stronger influence on the coastline of Schleswig-Holstein with its north-south expansion.

The mean amplitude of the seasonal cycle in the German Bight, computed by the empirical approach, is found to be about 27 to 29 cm for the area of Schleswig-Holstein and about 20 to 23 cm for tide gauges located in Lower Saxony. The amplitude is considerably higher than in other parts of the world. Generally, in mid latitudes the mean amplitude of the seasonal cycle is about approximately 4 to 7 cm (Pugh, 2004). In the German Bight the seasonal cycle is overlapped by strong variability, resulting from wind forces, effects from river run-off, salinity and thermal effects. The averages of the MSL values for the particular months and over the period from 1937 to 2008 illustrate that the seasonal cycle reaches its maximum in November, while the minimum occurs in April or May. The strong variability leads to a strong year-to-year variation of maximum and minimum values. Maximum values scatter over 8 months (from August to March) and minimum values have been found between October and June, even if there are considerable accumulations. The decadal analysis of the maximum and minimum values points to a shift of these accumulations. The maximum values have been moved over the last two decades from November/December to January/February and the minimum values have been shifted from February/March to April/May. As described above, there is a large amount of inter-annual variability in the phase of the seasonal cycle. Changes in the phase of the seasonal cycle have been repeatedly observed in different climatic parameters (e.g. Johansson et al., 2001; Lehmann et al., 2011), but the causes are poorly understood (Stine et al., 2009). The changes in phase are consistent between stations but, probably due to the large natural variability, are statistically insignificant. However, similar studies support such changes. First of all, similar findings for the maximum values of the seasonal sea level cycle in the Baltic Sea were presented by Johansson et al. (2001). The relationship between the seasonal cycles of NAO and MSL were analyzed by Yan et al. (2004). They compared anomalous strong (and weak) signals in both parameters. In their Figure 7 they computed the seasonal cycles before and after 1989. This figure shows that the seasonal NAO cycle after 1989 peaks in the months of January/February, while before it rather peaks in autumn. If — as expected here — the NAO or NAO-related processes drive changes in the phase of the seasonal MSL cycle, the observed changes are a result of an anomalous

strong NAO cycle after 1988. Apart from this, Marcos and Tsimplis (2007) also found higher trends in MSL for the winter season (December to March) and the period from 1960 to 2000 for tide gauges located in the German Bight, by analyzing the output of a two-dimensional hydrodynamic model of the NW European shelf. The authors argue that approximately 4 mm/yr (i.e., about 50 %) of the estimated trend is due to meteorological forces. Furthermore, Lehmann et al. (2011) studied the variability of different climate related parameters, such as wind speed or precipitation in comparison to the NAO for the greater Baltic Sea area (including the southeastern parts of the German Bight) over a period from 1958 to 2009. They report a seasonal shift of strong winds from autumn to winter and early spring in line with an eastward shift of the atmospheric COA. Since wind in particular is the major factor in local sea level variability in the North Sea (Wakelin et al., 2003), the observed phase shift in sea level can be explained (at least to some degree).

Another challenge regarding the high variability in the German Bight is that the computation of the year-to-year amplitude of the seasonal cycle becomes non-stationary with respect to its phase (see Section 4.2). Hence, using maximum and minimum values to calculate annual amplitudes results in a comparison of values derived from different monthly values in particular years. This means that the computation of amplitude is strongly biased by other effects, such as variability caused by local meteorological influences, river run-off or thermal effects. Different methods to separate the annual cycle from the overlapping variability can be found in the literature. On the one hand, variability can be filtered out by investigating seasonal averages. Hünicke et al. (2008) computed the year-to-year amplitude by using seasonally-averaged maximum and minimum values (winter: November to January; spring: March to May). This leads to a better approximation of the intra-annual amplitude. On the other hand, moving monthly averages of several years or moving Fourier analysis may be used, as described by Plag and Tsimplis (1999) and Ekman (1999). Furthermore, one of the reviewers proposed inter-quartile ranges for the computation of annual amplitudes. This method is more robust.against outliers. For the present chapter, all of these approaches have been tested in addition to the min/max-approach described in Section 3.1 in order to analyze whether there are any long-term changes evident in the amplitudes of the seasonal cycle. Amplitudes, computed by the min/max-approach, lead to values of approximatly 50–60 cm on average, compared with much smaller values derived using the other approaches. However, the aim was to calculate any long-term changes in the annual amplitudes. From all the different methods, no significant trends in the amplitude of the seasonal cycle could be found in the German Bight.

The detailed analysis of long-term changes in seasonal MSL components (Section 4.3) indicates that the long-term trends in the NDJFMA MSL are higher than in the MJJASO MSL for all time periods under consideration (i.e., 1937 to 2008, 1951 to 2008 and 1971 to 2008), but only statistically significant for the first two periods. It has been noticed that the differences in the long-term changes of the two seasons are unsteady over time. While in the first two time spans (i.e., 1937 to 2008 and 1951 to 2008) the winter trends are more than two times stronger (on average) than the summer trends, they are more equal for the short time period from 1971–2008. From analyzing the trends for each single month of a year (see Section 4.4), considerably stronger MSL trends are found for the months from

January to March. The estimated trends are in agreement with those presented for the North Sea area in Ekman (1999) and potentially caused the shift in the maximum values of the seasonal cycle described in Section 4.1. This raises the question of which parameters are the main factors causing such changes.

Due to its location on the northwestern continental shelf, the German Bight is strongly affected by meteorological forces. Therefore it is assumed that changes in the NAO are linked to changes in the seasonal cycle of the MSL. The MSL shows significant correlations with the NAO in the winter months, especially from January to March, whereby the influence is not stationary in time as described by Yan et al. (2004) and Jevrejeva et al. (2005). However, the higher trends between January and March are also imaged in the monthly NAO values. This indicates that the JFM NAO is one major driving factor for changes in JFM MSL, which results in the increasing gradient between winter and summer season and the shift in the phase of the seasonal cycle. The smaller gradient between the MSL in the summer and winter half year after 1971 compared to the two longer time periods is most likely due to lower trends in the JFM NAO for this time period. From separate trend analyses (not discussed in detail here) it was depicted that the JFM NAO shows similar tendencies for all of the three considered time periods, but the smallest trend is calculated for the 1971–2008 period. Hence, the acceleration in JFM MSL after 1971 cannot be explained solely by higher trends in the JFM NAO index over the same time period, particularly with regard to the strongly increasing trends in summer season observed in section 4.3.

The interaction between JFM NAO and JFM MSL is considered by computing sensitivities of JFM MSL (in mm) per unit JFM NAO (see Sections 3.4 and 4.4). The identified sensitivities are comparable to those found in other studies for the same area. Wakelin et al. (2003) and Tsimplis et al. (2005) reported sensitivities of up to 96 mm/unit NAO (December to March) in the German Bight using a two dimensional tide + surge model for the time period from 1955 to 2000. Tsimplis et al. (2005) pointed out that the sensitivity of model data was found to be lower compared to the sensitivity computed with tide gauge data. They suggested an additional sea level influence of the NAO through thermosteric effects or model inaccuracies. Tsimplis et al. (2006) confirmed sensitivities in the order of 10 mm/unit NAO via thermosteric effects. Nevertheless, the sensitivities computed in this chapter show that the results from the above-mentioned studies are still valid for time periods covering nearly three more decades than the model data. The spatial distribution of the sensitivity in the German Bight is not homogeneous with stronger sensitivity (up to 130 mm/unit JFM NAO) in the northeastern part compared to the southwestern part (up to 110 mm/unit JFM NAO). This gradient becomes logical, comparing the computed sensitivities with the results of the two dimensional tide + surge model presented in Wakelin et al. (2003), Woodworth et al. (2007) and Tsimplis et al. (2005). This is confirmed by the correlation analyses and supports the assumption that westerly winds are responsible for higher variability along the coastline of Schleswig-Holstein.

The influence of JFM NAO on long-term JFM MSL changes is also analyzed. The results, given in Table 2, indicate that the JFM NAO influences JFM MSL, in two different ways.

On the one hand, the JFM NAO influence explains 30–35 % of the inter-annual JFM MSL variability in the German Bight. These findings are in agreement with the results presented by Jevrejeva et al. (2005) for the North and Baltic Sea, even if the IBE has not been considered for the present chapter. On the other hand, the JFM NAO also influences the long-term JFM MSL trends in the German Bight. For all of the three time periods under consideration, the NAO influence leads to higher trends from January to March. For the first two time spans (i.e., 1937 to 2008 and 1951 to 2008) the JFM NAO explains up to 47 % (2.3 mm/yr) of the estimated JFM MSL trends. For the period from 1971 to 2008, the JFM NAO influence is considerably smaller and explains about 18 % (1.3 mm/yr) of the estimated JFM MSL trend. This is caused by a smaller trend in the JFM NAO for the latter time period compared to the longer periods considered in the present chapter. This highlights that the influence of the JFM NAO on long-term JFM MSL trends depends on the time period under consideration. This is also confirmed from analyzing 19-year running linear trends and the non-linear behavior for the time period from 1937 to 2008. The main influences of the JFM NAO on JFM MSL in the German Bight are summarized in Figure 10. The JFM MSL estimations for Schleswig-Holstein (Figure 10a) and Lower Saxony (Figure 10b) are shown before (blue line) and after, removing the JFM NAO influence (red line) (only the long time period from 1937–2008 is considered). The standard deviations are represented by the dotted lines and the long-term trends are highlighted as bold lines. For both virtual stations it can be stated that a correction of the JFM MSL estimations for the JFM NAO influence causes a reduction of variability and trends.

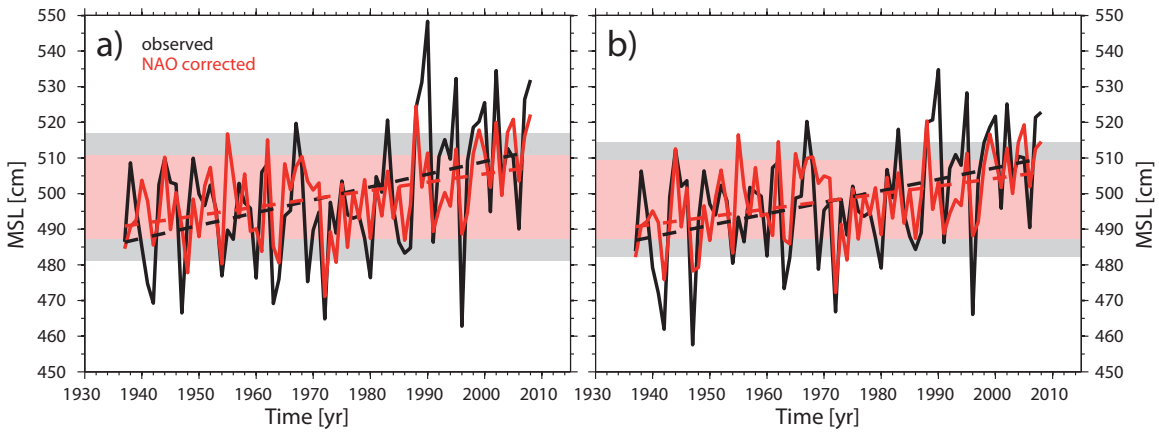

Figure 2-10: Influence of the JFM NAO on JFM MSL in the German Bight over the period 1937 to 2011 for the virtual station of a) Schleswig-Holstein and b) Lower Saxony. The thin lines with thick dots (black = observed; red = NAO corrected) represent the JFM MSL data. The shaded areas show the corresponding standard deviations, while the dotted lines represent the linear trends over the entire period.

The results presented here aim to clarify the role of meteorological forces on JFM MSL in the German Bight. The different behavior of MSL during the months from January to March (compared to the remaining months) led to a redistribution of annual maximum peaks in the last two decades. Assuming that this shift consolidates, the future flood risk may be affected more intensively than previously expected. As described by Pugh (2004), highest storm surges can be observed when they are accompanies by high astronomical tides and high MSL values. Hence, higher NDJFM MSL/JFM MSL may affect coastal structures in two different ways. First, higher NDJFM MSL/JFM MSL causes higher con-

stant loads due to extended duration times of high water levels. Second, the maximum water level heights during storm surge events may be also affected. Since the NAO is one of several important driving factors for NDJFMA MSL/JFM MSL, it will be crucial in which direction the NAO will develop in future. It is well known that a significant trend to more positive values in the NAO index has been observed over the last decades of the 20th century (especially between the 1960's and 1990's). This has caused a warmer and more humid climate over Northern Europe (Hilmer and Jung, 2000), but it is rather uncertain how the NAO will change in future. Different global climate models have been used to simulate the NAO variability. The IPCC (2007) exposed that many climate model simulations show a decrease of the arctic SLP for the 21st century, which would result in more positive values of the NAO index (Osborn, 2004; Kuzmina et al., 2005).

2.7 Conclusions

MSL records from 13 tide gauges in the German Bight have been analyzed to determine the seasonal and inter-annual development of monthly MSL in the 20th and the beginning of the 21st century. The results of this study show that the seasonal cycle has mean amplitude of approximately 20–29 cm along the German North Sea coastline with minimum values in April and May and maximum values in November. The seasonal cycle is overlapped by a strong year-to-year variability, which is significantly higher during the storm surge season (October to March) than in the remaining months. The analysis of the development of the seasonal cycle in the German Bight indicates no long-term changes in the amplitude and phase but a large inter-annual variability. While between 1939 and 1988 the seasonal MSL cycle mostly peaked in November and December, in the last two decades tendencies to a stronger incidence in January and February have been observed.

The more frequent maximum values in January and February coincide with an inhomogeneous seasonal trend development in the German Bight. Considerable differences have been found between winter and summer seasons (i.e., NDJFMA MSL and MJJASO MSL). For two of three analyzed periods (1937 to 2008, 1951 to 2008) NDJFMA MSL is significantly higher compared to the MJJASO MSL. This gradient between summer and winter months is also found for the period from 1971 to 2008 whereas the gradient is considerably smaller and not statistically significant. The investigation of the monthly components reveals the months between January and March, which are represented in the JFM MSL, as the main driver of this gradient. The stronger trend in the last three decades reported by Wahl et al. (2011) is confirmed in this chapter for both seasons. An explanation for the increasing MJJASO MSL cannot be given in this study, but will be part of future studies.

It is well known that atmospheric circulation has a considerable influence on climate variability over Northern Europe (Hurrel, 1995; Hurrel et al., 2003; Lehmann et al., 2011). Since sea level responds to different climatic forces, such as wind, pressure or precipitation, the NAO becomes a reasonable proxy for such influences. Confirming earlier studies from (Tsimplis and Shaw, 2008; Kolker and Hameed 2007; Johansson et al., 2001; Tsimplis et al. 2005), the statistical comparison of MSL and NAO shows positive correlations at

tide gauges located in the German Bight. These correlations are significant in winter and autumn and weaken or get insignificant throughout the summer months. Therefore, the comparison of MSL and the NAO is only straightforward for the winter and autumn months (e.g. Tsimplis and Shaw, 2008). From the regression analysis between JFM MSL and JFM NAO it has been found that the JFM NAO influences JFM MSL in two different ways. On the one hand the JFM NAO explains 30–35 % of the year-to-year variability of JFM MSL, which confirms earlier findings from Wakelin et al. (2003) and Jevrejeva et al. (2005) for the larger North and Baltic Sea area. On the other hand similarities are found in the trend patterns of both parameters. The comparison of 19-year running trends and the rates of rise shows strong coherency between JFM MSL and JFM NAO. This suggests that meteorological forces are the main driving factors of JFM MSL changes and therefore also of changes in the seasonal cycle in the past 70 years. The results confirm the importance of seasonal sea level analysis for the matters of coastal defense strategies highlighted by previous studies for the North Sea (Wakelin et al., 2003; Tsimplis et al., 2005). In particular, in the German Bight there is a huge amount of non-tidal variability which considerably influences flood risk. Furthermore, this high degree of variability complicates reliable estimations of trends and possible future sea level developments. It can be concluded that the trend of the MSL in the German Bright is overestimated if the influences of the atmosphere are not excluded from the MSL time-series. This is important: one way to find numbers for regional future states (e.g., for the year 2100) of MSL is the comparison of the regional with the global MSL, for which projections already exist. Higher MSLs contain higher levels upon which storm surges built (Barbosa and Silva, 2009). Hence, especially higher trends during the storm surge season are very important as they may affect the effects of storm surges along the coastline. For the future it will be important to assess the contribution of local or remote meteorological factors affecting residual fluctuations (especially on trends) which cannot be explained with the NAO index, especially for the remaining seasons (i.e., spring and summer), which have not been considered in this or related studies.

3 Characteristics of intra-, inter-annual and decadal sea level variability and the role of atmospheric forcing: the long record of Cuxhaven

3.1 Abstract

This paper addresses the role of meteorological forcing on MSL variability at the tide gauge of Cuxhaven over a period from 1871 to 2008. It is found that seasonal sea level differs significantly from annual means in both, variability and trends. The causes for the observed differences are investigated by comparing to changes in wind stress, SLP and precipitation. Stepwise regression is used to estimate the contribution of the different forcing factors to sea level variability. The model validation and sensitivity analyses show that a robust and timely independent estimation of regression coefficients becomes possible if at least 60 to 80 years of data are available. Depending on the season, the models are able to explain between 54 % (spring, April to June) and 90 % (winter, January to March) of the observed variability. Most parts of the observed variability are attributed to changes in zonal wind stress, whereby the contribution of SLP, precipitation and meridional wind stress is rather small but still significant. On decadal timescales the explanatory power of local meteorological forcing is considerable weaker, suggesting that the remaining variability is attributed to remote forcing over the North Atlantic. Although meteorological forcing contributes to linear trends in some sub-periods of seasonal time series, the annual long-term trend is less affected. However, the uncertainties of trend estimation can be considerably reduced, when removing the meteorological influences. A SE smaller than 0.5 mm/yr requires 55 years of data when using observed MSL at Cuxhaven tide gauge. In contrast, a similar SE in the meteorologically corrected residuals is reached after 32 years.

3.2 Introduction

In the last few decades there has been a great effort to understand the characteristics of long-term global SLR (Douglas, 1991; Woodworth, 1990; Church et al., 2006, 2011). The importance of such studies is rooted in the high impacts, which are related to possible future SLR. The Fourth Assessment Report (AR4) of the IPCC (IPCC, 2007) suggested a GMSL rise of up to 60 cm by 2100 as a result of global ocean warming, glacier melting

and the balance between melting, snowfall and the regular outflow from glaciers from ice sheets (potential accelerated ice-sheet melting, which could add another 20 cm of SLR, is not included in these projections). Such an increase would have considerable consequences for the flood risk in coastal areas, as the MSL is the reference frame for storm surges. However, studies dealing with future SLR base on the knowledge of the physics behind past sea level changes. Hence, a detailed understanding of observed sea level in the past is a fundamental step before doing studies focusing on future SLR.

Sea level has been observed since the 18th century with the longest records based on tide gauge measurements at coastlines. Since 1992, there has been a quasi-global coverage of sea level observations with the introduction of satellite measurements. Both measurement methods have different advantages and disadvantages. Tide gauge measurements, for example, are available since the 18th century and consequently provide a good insight into the history of sea level. The disadvantage of tide gauges is that they give a measure of relative sea level change, i.e. the observations include both, sea level changes and VLM. These relative measurements are important for coastal planners, as for coastal zone management the relative sea level change is the proper magnitude, but disregarding the VLM can compromise estimates of global SLR. Furthermore, the heterogeneous distribution of tide gauges around the world biases the estimation of global SLR (Merriefield et al., 2009). Satellite altimetry, however, allows the observation of absolute sea level in a precise reference frame with quasi-global coverage, but as satellite altimetry observations are only available since 1992, the data sets are not yet usable for the estimation of long-term trends. Additionally, satellite measurements are not reliable for coastal areas. Hence, for understanding past sea level changes, both data types have to be combined. While tide gauge observations point to a significant increase in global MSL (GMSL) of ~17 cm throughout the 20th century, a closer look on the development shows that this rise is far from linear with considerable inter-annual and decadal fluctuations, which are linked to climate patterns (Bindoff et al., 2007). Additionally, satellite altimetry reveals a high spatial heterogeneity of sea level changes around the world with regions of increase and regions of decrease (Milne et al., 2008). This fact clarifies the particular importance of understanding past sea level changes and variability. The large deviations in regional SLR show that regional MSL variability, rather than the global mean, is the main concern for risk assessments.

Generally, fluctuations in the SSH are caused by changes in the steric components, i.e. changes due to variations in water temperature or salinity. Likewise, meteorological forces drive regional sea level through the effects of wind and SLP. While wind pushes sea level towards or away from the coastline, SLP influences the SSH through the IBE, i.e. hydrostatic de-/compression. In some areas river runoff or climatic effects are other prominent forcing factors of SSH variability (Tsimplis and Woodworth, 1994). Apart from these direct forcing factors it should be noted that sea level is affected by long-period tides such as the nodal cycle (e.g. Jensen, 1985; Haigh et al., 2011). These cycles have to be taken into account, especially if the trend development or acceleration/deceleration characteristics are investigated (Baart et al., 2012).

Many studies have tried to identify the climatic factors that drive sea level variability (Tsimplis and Josey, 2001; Wakelin et al., 2003; Woolf et al., 2003; Yan et al., 2004; Tsimplis et al., 2005; Jevrejeva et al., 2005; Woodworth et al., 2010; Dangendorf et al., 2012, capter 2 of this thesis). In the North Atlantic region the leading atmospheric mode is the NAO during wintertime. The NAO index is defined as the standardized difference of the two leading atmospheric pressure fields, the Azores High and the Icelandic Low. Since the NAO dominates the winter climate over Northern Europe (Hurrel, 1995), there is a clear link between sea level and the NAO index. Especially during the last decades, MSL along the European coasts correlates well with the NAO (Yan et al., 2004; Jevrejeva et al., 2006). The problem with the NAO is that it is just presented as an index. Therefore, it does not affect sea level directly. It rather represents a proxy affecting different related parameters, such as wind, SLP or precipitation (Suursaar and Soosäär, 2007).

The main objective of this chapter is to examine the effects of such NAO related processes on MSL variability in the Cuxhaven record. The tide gauge of Cuxhaven is located in the mouth of the Elbe estuary in the southeastern part of the shallow North Sea. The record is of particular interest for sea level studies, as it is one of the longest records available worldwide. Starting in 1843, the tide gauge has recorded over 160 years of sea level changes up to date. In the last decades the tide gauge has been the subject of several sea level studies (Jensen et al., 1993; Tsimplis et al., 2005; Jevrejeva et al., 2006; Mudersbach and Jensen, 2008; Wahl et al., 2010, 2011; Albrecht et al., 2011, 2012; Dangendorf et al., 2012, capter 2 of this thesis). While earlier studies (Jensen et al., 1993; Mudersbach and Jensen, 2008) deal with the mean high (MHW) and mean low water levels (MLW), Wahl et al. (2010, 2011) reconstructed monthly MSL time series using the k-factor approach, a method which allows the combination of low and high frequency data for the reconstruction of MSL time series.

It is well known that the major forcing factor of MSL variability in the German Bight is wind (Wakelin et al., 2003), but its full contribution is only known by the output of hydrodynamical models providing data only for the past 50 years. Since the NOAA provides long-term gridded climatic reanalysis datasets back to the 19th century (Compo et al., 2011), the comparison of different related parameters with regional sea level over longer timescales becomes possible. In this chapter the contribution of wind stress, SLP and precipitation on sea level variability in the German Bight is estimated, exemplary shown for the tide gauge of Cuxhaven. These investigations have several implications for the aspects of coastal planning and management. First, an improved knowledge about past sea level changes allows for a better look into the near future. Here, the near future refers to time spans of 30 to 50 years, which are interesting for coastal planning purposes. Second, the large variability, which is regionally present in a lot of sea level time series, complicates a reliable estimation of long-term trends. Under the assumption that one can consistently estimate the amount of non-tidal variability in sea level data, the estimation of long-term trends should become more precise. Several authors (Douglas, 1991; Tsimplis and Spencer, 1997; Woodworth, 1990; Woodworth et al., 1999; Haigh et al., 2009) pointed out that periods of 30 or 50 years are necessary, to get a stable trend estimate with an adequate SE. Locally or regionally the available data often does not fulfill these require-

ments. A good example in this context is the area of the Halligen, which are located northeastwards from Cuxhaven. The Halligen are small islands with high cultural importance (UNESCO World Cultural Heritage Site), but they are highly impacted by climatic change (Arns et al., 2011). Therefore, local MSL studies are required for an integrated risk assessment. The available data in this area is sparse and does not provide such long periods; however an improved understanding of the driving mechanisms could help for local coastal planning. Finally, since decades sea level scientists and coastal planners attempt to answer the questions whether or not acceleration in SLR can be detected. In a recent paper, Haigh et al. (2014) demonstrated that the large amount of non-tidal variability hampers an early detection of accelerating SLR. For global reconstructions, in which the variability is smaller through the applied methods (Church and White, 2004, 2006, 2011), the acceleration can be detected earlier than in the different local records. Especially on regional scales, the variability therefore needs to be minimized to get more information about the shape of the long-term trend. MSL time series in the German Bight, such as the Cuxhaven record, are characterized by a large intra-, inter-annual and decadal variability (Wahl et al., 2013). Hence, the explanation of this variability is an important step for the above mentioned issues.

The paper is structured as follows. In section 3.3 the data and methods used for the different investigations are described. The corresponding results are presented and discussed in section 3.4, while Section 3.5 contains the conclusion.

3.3 Data and methods

Monthly MSL data from the tide gauge of Cuxhaven is used in this chapter (Figure 3-1). The raw data has been provided by the Federal German Waterways and Shipping Administration (WSV). Observations at the tide gauge are available since 1843. These observations are restricted to the tidal high and low water levels handwritten in log books. In 1899, the measurement technique has changed making it possible to observe the full tidal curve on tidal charts. Extensive digitization works provided hourly sea level data from 1918 to the present. Since the mid 1990's tide gauge observations are directly and digitally archived with a one minute resolution. While monthly or annual MSL back to 1918 can be calculated from high resolution data (at lest hourly resolution), before that time Wahl et al. (2010, 2011) applied a technique to reconstruct MSL values on the basis of LW and HW back to 1843. Here the reconstruction is used for a deeper analysis of observed changes during a period from 1871 to 2008 (a time span for which climate reanalysis data exists). The data set has been checked for errors and corrected for local datum shifts, as reported in IKÜS (2008).

The main aim of this chapter exists in investigating climatic and meteorological induced variations of MSL, which are related to the large scale atmospheric circulation pattern (NAO). Monthly data sets were extracted from the 20CRv2 data set on a 2*2 grid for the larger European and North Atlantic area, provided by the NOAA-CIRES Climate Diagnostics Center, Boulder, Colorado, USA (http://www.esrl.noaa.gov). Here, investigation SLP, zonal (WSu) and meridional (WSv) wind stress and precipitation (P) data covering a peri-

od from 1871 to 2008 were extracted. The data is based on ensemble model simulation with data assimilation. SLP and sea surface temperature observations are used as boundary conditions. Since especially for earlier periods the observations are sparse and spatially uneven distributed, the uncertainties of the data are larger before 1950 than afterwards. Krüger et al. (2012) pointed to some discrepancies between the long-term trends of storminess proxies from 20CRv2 reanalysis data and observations. However, since our main focus is on investigating variability patterns, our results should be independent from these discussions. Furthermore, the correlations have been tested to be stationary high during the whole investigated period.

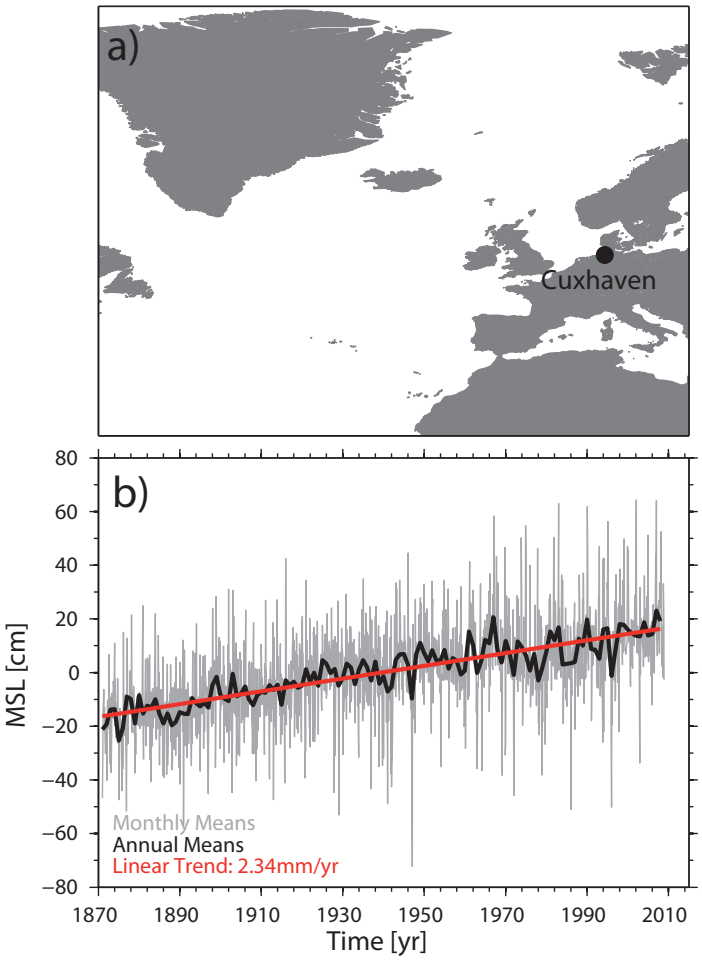

Figure 3-1: a) Investigation area and location of the Cuxhaven tide gauge. b) Monthly (grey) and annual (black) MSL record as observed at the tide gauge of Cuxhaven. The linear trend estimated with the annual record is also shown (red).

Before investigating the various time series, the seasonal cycle has been removed by subtracting the long-term monthly average from every monthly subseries. If not stated otherwise, the time series were further corrected for their observed linear long-term trend, as the main motivation is an investigation of intra- and inter-annual variability. To analyze the relationship between the different forcing factors and sea level, in a first step correlation coefficients between MSL in Cuxhaven and gridded meteorological time series covering the larger Northern European and the North Sea area are computed. The correlation between two different time series can be computed with

$$r = \frac{\sum xy}{\sqrt{x^2 \sum y^2}} \tag{3-1}$$

The significance of the correlation can be estimated using

$$T = |r| \sqrt{\frac{n-2}{1-r^2}} \tag{3-2}$$

and comparing *T* with critical values from the *t* distribution with *n-2* degrees of freedom (von Storch and Zwiers, 1999). The resulting correlations between the different time series are presented as contour lines of similar correlations on geographic maps. This allows us to find the coherencies over the larger continental area.

If there is a significant relationship between two or more parameters, the contribution can be estimated within multiple LRMs. Since the different MSL contributors vary considerably throughout the whole year, the LRMs are built up on seasonal time scales. For that purpose the following definitions are used: The winter season is defined as the seasonal mean from January to March (JFM), spring season means the average from April to June (AMJ), summer indicates the months between July and September (JAS), while October to December (OND) are summarized as the autumn season. The above mentioned meteorological parameters are used to explain the MSL variability in Cuxhaven. The following model has been fitted to the time series, to estimate the effects of meteorological forcing. The multiple LRM for observed MSL ξ is given by the following equation

$$\xi = \alpha_0 + \alpha_1 Wsu + \alpha_2 Wsv + \alpha_3 SLP + \alpha_4 P + \varepsilon \tag{3-3}$$

where the variables *Wsu*, *Wsv*, *SLP* and *P* are the zonal and meridional wind stress, SLP and precipitation, respectively. The coefficient a_0 is constant and ε represents the random error. The explained variance of the multiple LRMs (i.e. they include all meteorological parameters) can then be estimated by

$$VAR_{exp} = \left[1 - \frac{var\left(\xi - \left(\xi_{Wsu} + \xi_{Wsv} + \xi_{SLP} + \xi_P\right)\right)}{var(\xi)}\right] \tag{3-4}$$

while the variances explained by each contributing factor are

$$VAR_{exp,i} = \left[1 - \frac{\left(var(\xi - \xi_i)\right)}{var(\xi)}\right] \tag{3-5}$$

The range of VAR_{exp} lies between 0 and 100 % and describes how much of the observed variability can be explained by the prediction. A value of zero means no correlation between both curves, whereas a value of 100 % means that the observed variability is equal to the predicted one. It should be noted that all the different predictors are driven by the NAO, which means, that they should not be independent from each other. Hence, the sum of the explained variances of the linear regressions will not be the same as the explained variances by the multiple regression models:

$$VAR_{exp} \neq VAR_{exp,i} \tag{3-6}$$

For the identification of the different predictors stepwise regression with forward selection is applied. A stepwise regression means that different meteorological contributing factors are included step by step into the regression model, if their relation is statistically significant and if they explain a significant part of the observed variances. This approach allows for finding a model consisting of preferably few predictors and explaining as much variability as possible. The procedure can be summarized as follows:

1. Including the predictor with the largest bivariate correlation.
2. Including the predictor that explains the most significant part of the variability after removing the influence of the first predictor.
3. Including the predictor that explains the most significant part of the variability after removing the influence of the first and second predictor.
4. Including the predictor that explains the most significant part of the variability after removing the influence of the first to nth predictor
5. The LRM is finished if no more predictors are able to give a significant contribution to the explained variability.

The significance of the LRMs can be tested with *t*-statistics or *f*-statistics which can be found in standard mathematical literature. As a further quality control for the accuracy of the LRMs, the Root Mean Squared Error (RMSE) is computed:

$$RMSE = \sqrt{\frac{\sum_{i=1}^{n}\left(\xi_i - \left(\xi_{Wsu,i} + \xi_{Wsv,i} + \xi_{SLP,i} + \xi_{P,i}\right)\right)^2}{n}} \tag{3-7}$$

where n is the sample size. The RMSE is a measure for the resulting differences between observed and predicted MSL. In contrast to the explained variability the RMSE gives a direct measure of the resulting size of the residuals.

It should be noted that these LRMs are restricted to the detrended data, which means that no discussion of seasonal trends is possible. To allow the estimation of the contribution of the different climatic forcing factors to seasonal trend development, the estimated regression coefficients are applied to the non-detrended meteorological time series (Hünicke et al., 2008). Linear trends are estimated by using the ordinary least squares (OLS) fit. The confidence intervals are described by the SE of the regression residuals. It is assumed that the regression residuals are serially correlated following a first-order autoregressive process (AR1-process). Hence, when estimating the SE the degrees of freedom are reduced as recommended by Santer et al. (1999).

3.4 Results

3.4.1 Observed seasonal MSL variations

The findings of Dangendorf et al. (2012, chapter 2 of this thesis) indicate significant dissimilarities between seasonal and annual MSL trends in the southeastern North Sea during the second part of the 20th century. This heterogeneous development can be confirmed by the present investigations. To compare seasonal with annual MSL trends over the whole period from 1871 to 2008, moving trends are computed using a 30-year moving window (Figure 3-2). For each window the linear trend together with its SE is calculated for the annual MSL values as well as for seasonal means.

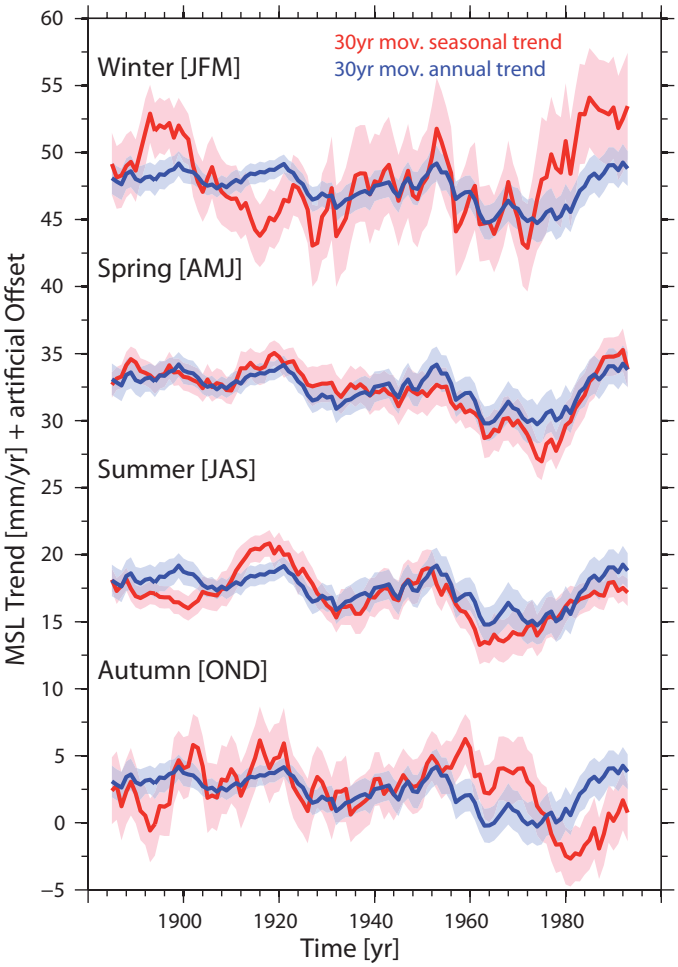

Figure 3-2: 30yr moving trend of seasonal (red) and annual (blue) MSL and their related 1σSE estimated for observations over the period from 1871 to 2011.

At times, especially during the winter and autumn season, the seasonal trends differ significantly from the annual means. For example before 1900, seasonal deviations from the annual mean of up to ~5 mm/yr can be found during winter seasons. Until 1900 especially the winter trends exceed the trends of annual means considerably, whereby afterwards annual trends exceed winter trends over a period of ~20 years. From ~1920 on, the winter trends scatter around the annual MSL trends until the 1970s. Afterwards, considerably larger trends in the winter season have been detected. The differences as well as the inter-annual variability are in the spring and summer seasons considerably smaller, which is

due to the fact that the atmospheric induced variability is largest in the winter and autumn months (Tsimplis et al., 2005; Dangendorf et al., 2012, chapter 2 of this thesis). However, the larger trends during the winter season in the second half of the 20th century are also striking. Largest trend rates with values up to ~10 mm/yr are observed in the winter season of the mid 1980s, a phase in which the atmospheric variability represented by the NAO index reached a local maximum (Hurrel, 1995; Tsimplis and Josey, 2001). The high variability during that time expresses itself in larger than normal SEs. Therefore, it can be suggested that a combination of different physical processes, which are related to the NAO, are responsible for the anomalous large variations between the different seasons.

3.4.2 Meteorological forcing of seasonal MSL

3.4.2.1Correlation analysis

To examine these processes more precisely, meteorological time series of different related parameters are evaluated. Figure 3-3 shows correlation maps between monthly MSL in Cuxhaven and gridded climate data. The MSL time series is correlated to every gridpoint time series of SLP, wind stress and precipitation. First, the results of the correlation analysis between SLP and MSL (Figure 3-3a) show that the relationship at the nearest grid point to the tide gauge is rather weak with values around ~-0.3, meaning that the MSL variability in Cuxhaven is not directly linked with the SLP variability over the southeastern German Bight. Therefore, the IBE by the classical approach is not the main forcing factor influencing MSL in Cuxhaven. In theory, for an infinite ocean, the response of sea level to SLP changes can be well described by a linear relationship. A hydrostatic reduction of ~ 1 mb in atmospheric pressure causes a stationary rise of 1 cm in sea level (Pugh, 2004). The North Sea basin, however, has open boundary conditions, which complicates a clear description of that process. Interestingly, a linear relationship can be observed between MSL in Cuxhaven and the SLP field over Scandinavia with correlations over -0.8. A smaller but still significant correlation is further found with the SLP field over the Iberian Peninsula. This relationship between MSL and both pressure fields shows similarities to the NAO, but it is even stronger. The spatial SLP pattern describes large parts of the observed variability in the German Bight (~70-80 % of the observed variance; not shown). The physical process behind that strong connection can be explained by the typical tracks of low pressure systems in the North Sea (Ullmann, 2010). Usually, the low pressure systems move from southern Greenland over the North Sea to Scandinavia. Largest winds, which push the water masses into the German Bight, are observed at the rear of those low pressure systems over Scandinavia. Thus, a large gradient between both SLP fields can be associated with strong westerly winds influencing the MSL variability in the German Bight.

This assumption can be confirmed by the correlation between MSL in Cuxhaven and zonal/meridional wind stress over the North Sea area (Figure 3-3c, d). Strongest correlations are found with zonal wind stress reaching values up to ~0.9. For meridional wind stress the relationship is considerably weaker but still significant on the 95 % confidence level (t-

test statistics). A further important correlation has been found between MSL variability and precipitation. Figure 3-3b shows a significant coherence between both parameters at the nearest grid points to the tide gauge of Cuxhaven. Precipitation can be connected with sea level through a couple of different processes. The salinity (and therefore the halosteric height) in near coastal areas is correlated with the difference between evaporation and precipitation. Large variations in the salinity content can lead to volume changes associated with variations in the SSH (Schott, 1966; Barbosa et al., 2004; Hünicke et al., 2008).

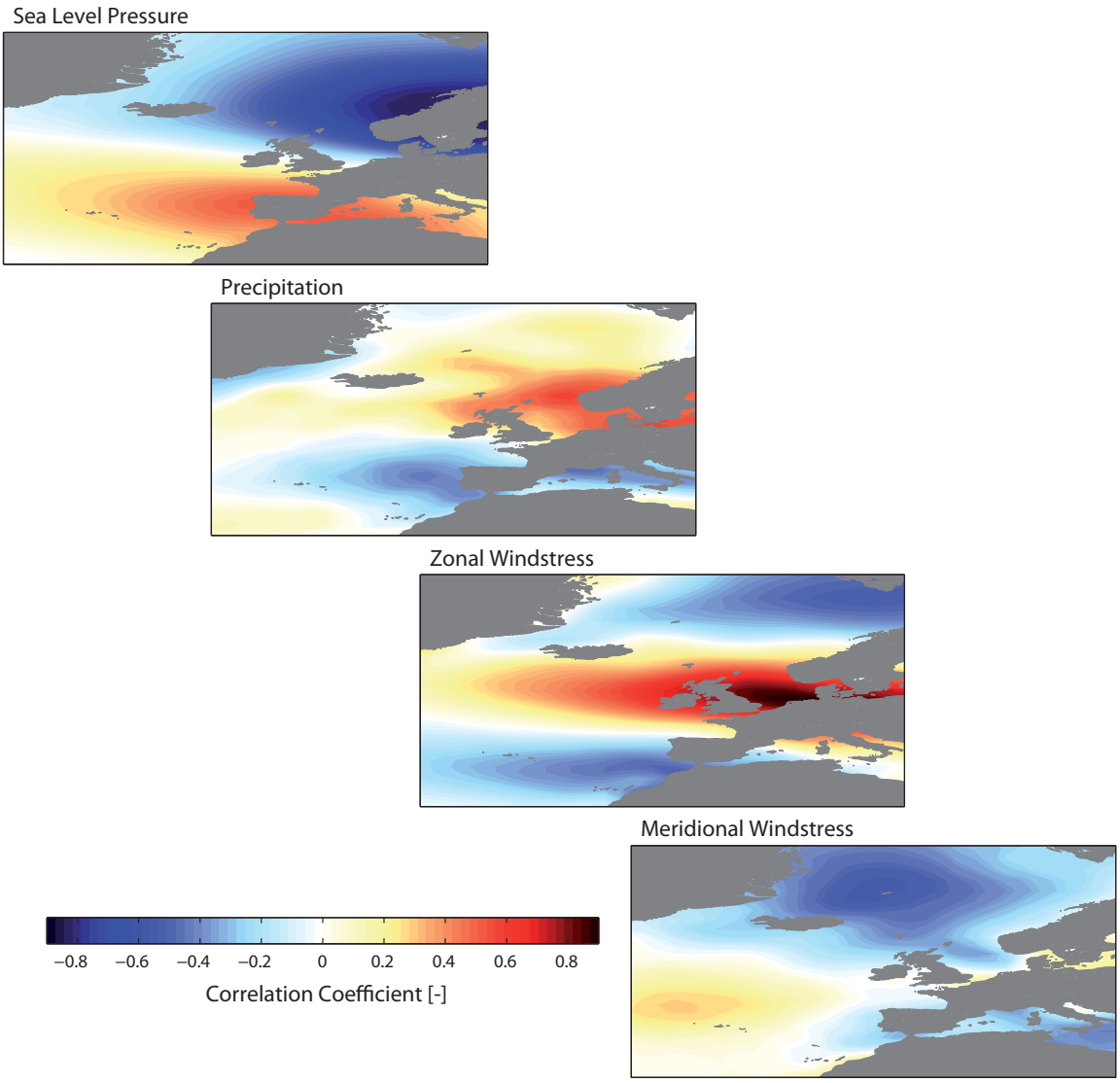

Figure 3-3: Correlation maps between MSL anomalies measured at the Cuxhaven tide gauge and gridded meteorological data over the period from 1871 to 2011 for SLP, precipitation, zonal wind stress and, meridional wind stress.

The correlation between the different forcing factors further shows considerable seasonal differences in all parameters Table 3-1). The largest similarities are found between zonal wind stress and MSL through all the different seasons with largest values in winter of up to 0.93 and smallest values in spring (0.71). The second strongest relationship is observed between MSL and precipitation, followed by SLP and the meridional wind stress. While the seasonal correlation of zonal wind stress and precipitation peaks with a maximum in winter, largest correlation coefficients for SLP and meridional wind stress are found

through the summer season. However, the correlation analysis points to a common influence of all selected parameters on MSL measured in Cuxhaven. Since all these parameters are directly linked to the NAO, co-variability between the different parameters can be suggested. This is confirmed by the cross-correlations between the different forcing factors (Table 3-1). Therefore, in the following a stepwise regression is applied to the datasets. For the regression models meteorological time series from the nearest grid point to Cuxhaven with the coordinates 7.5000°E and 54.2846°N are used

Table 3-1: Pearson correlation coefficients between seasonal MSL as measured in Cuxhaven and different meteorological forcing factors from the next grid point over the period from 1871 to 2011. Correlations which are statistically significant on the 95 % confidence level are marked in bold.

Season	Winter [JFM]					Spring [AMJ]				
Variables	MSL	WSU	WSV	SLP	P	MSL	WSU	WSV	SLP	P
MSL	**1**	**0.92**	**0.29**	-0.1	**0.59**	**1**	**0.67**	0.18	-0.22	**0.4**
WSU	-	**1**	**0.37**	0.07	**0.51**	-	**1**	**0.22**	-0.02	**0.31**
WSV	-	-	**1**	-0.02	**0.3**	-	-	**1**	**-0.2**	**0.41**
SLP	-	-	-	**1**	**-0.6**	-	-	-	**1**	-0.59
P	-	-	-	-	**1**	-	-	-	-	**1**
Season	**Summer [JAS]**					**Autumn [OND]**				
Variables	MSL	WSU	WSV	SLP	P	MSL	WSU	WSV	SLP	P
MSL	**1**	**0.73**	**0.45**	**-0.5**	**0.5**	**1**	**0.85**	-0.06	**-0.2**	**0.5**
WSU	-	**1**	**0.54**	**-0.4**	**0.42**	-	**1**	0.12	-0.08	**0.41**
WSV	-	-	**1**	**-0.4**	**0.46**	-	-	**1**	-0.11	0.12
SLP	-	-	-	**1**	**-0.8**	-	-	-	**1**	**-0.7**
P	-	-	-	-	**1**	-	-	-	-	**1**

3.4.2.2Regression analysis

The results of the multiple LRMs are presented in Figure 3-4 and Figure 3-5a, b. While Figure 3-4 displays the relationship between observed and predicted MSL, Figure 3-5a, b represents the regression results as explained variances and the RMSE. The black lines in Figure 3-4 indicate the detrended seasonal MSL, whereby the meteorologically reconstructed MSL is shown by the colored lines. From that figure it can be seen that the largest variability in seasonal MSL is observed during autumn and winter with standard deviations of 10 and 13 cm, respectively. Throughout the spring and summer seasons the standard deviations are considerably lower with values around 5 cm. Hence, the amount of non-tidal variability, which can be explained through these seasons, is much higher than in winter and autumn. This is also reflected in the explained variances for the different seasons (Figure 3-5a). During autumn and winter ~83 and ~90 % of the observed variability can be explained, while through the spring and summer seasons the contribution of meteorological forcing on MSL variability weakens considerably to values of ~54 and ~57 %. For the autumn and winter seasons the predicted MSL is able to explain most of the observed peaks. Even the largest peaks such as the maximum and minimum values in the winter seasons of 1990 and 1996 are well reproduced by the model. During spring and summer seasons the performance of the model is weaker and several peaks are not well reproduced. For example there is a remarkable minimum value observed in the spring season of 1978. The predictors used in the model cannot fully explain that peak.

The RMSE between observed and reconstructed MSL is, however, largest in winter and smallest in summer season, but the seasonal differences are considerably smaller than the observed standard deviations, indicating that the model is able to reproduce a major part of meteorological induced variability.

The contributors to MSL variability vary considerably through the different seasons. The largest amount is given by zonal wind stress across all seasons. In the winter, seasonal zonal wind stress alone is able to explain ~87 % percent of the observed variability. This value weakens through spring and summer seasons with values of ~50 % and ~54 % and then rises up again to a value of ~78 % in autumn. A further significant contribution to MSL variability in winter is given by SLP. Adding SLP to the sea level equation increases the performance of the LRM to an explained variance of ~90 %, whereby the contribution of SLP explains 2.8 % of the non-tidal variability. Precipitation is a significant forcing factor in summer and autumn. Throughout the summer and autumn seasons Precipitation is able to explain another 3.8 and 1.9 % of variations in MSL. In autumn, nevertheless, meridional wind stress gets also significant for the explanation of seasonal MSL variability with a value of 2.7 %.

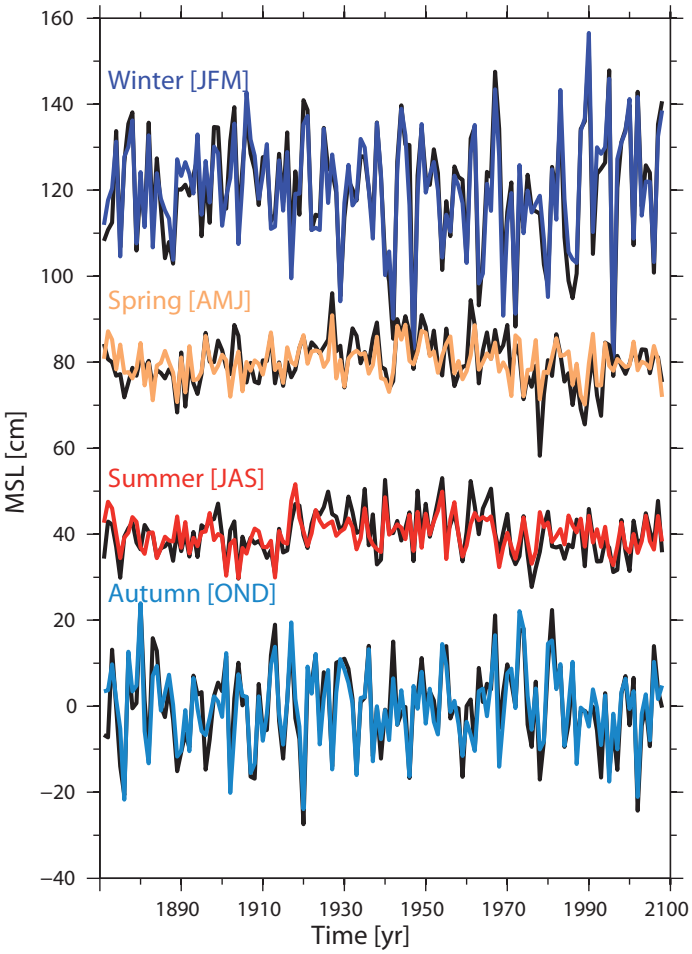

Figure 3-4: Observed (black) and reconstructed (colored) seasonal MSL at the tide gauge of Cuxhaven from 1871 to 2011.

As stated above, considerable differences between seasonal and annual trend development have been detected throughout the 19th and 20th century. Hence, the impacts of meteorological forcing on seasonal MSL trends are analyzed. Since the second half of the

20th century is a period of anomalous large atmospheric variability, a sub-period from 1951 to 2008 is also investigated. The trends for every seasonal subseries are estimated first for the observed time series and second for the residuals after correcting the time series for meteorological forcing. Note that trends are assumed to be significantly different from each other if their 1σ SEs do not intersect, i.e. the minimum confidence bound of the larger trend is larger than the maximum confidence bound of the smaller trend. The results are shown in Figure 3-5c for the whole period from 1871 to 2008 and in Figure 3-5d for the shorter period from 1951 to 2008. The linear trend estimates of the observed seasonal subseries are shown as blue dots with their related 1σ SEs as blue lines, while the trend estimates after the meteorological correction are presented in a similar manner in red color.

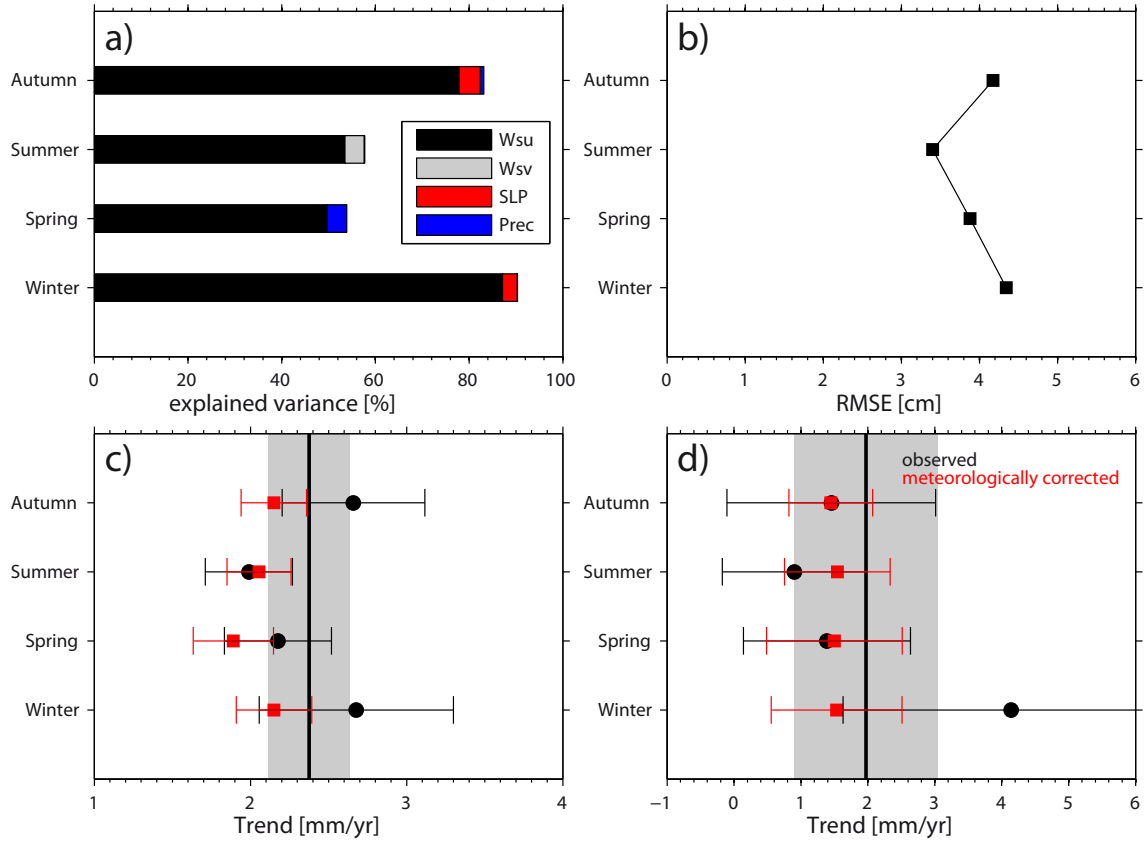

Figure 3-5: Results of the seasonal stepwise regression; a) explained variances by the LRMs for the period from 1871 to 2008. The different contributors are shown in differently colored bars. The sum of of all bars represents the explained variances of the full model. b) RMSE between observed and reconstructed MSL. c) Observed and meteorologically corrected MSL trends ±2σ SE for the period 1871 to 2011. d) same as c), but for the period 1951-2011. The black line with the grey shading represents the linear trend of the annual mean.

For the longer period from 1871 to 2008 the trends are as follows: For the winter season a trend of 2.7 ± 0.3 mm/yr has been observed. During spring and summer seasons the trends are significantly smaller with values of 2.2 ± 0.1 mm/yr and 2.0 ± 0.1 mm/yr. In autumn the seasonal MSL trend is approximately the same as in winter season (2.7 ± 0.2 mm/yr). The differences between autumn/winter and spring/summer trends can be explained by meteorological forcing to some extent. After removing meteorological forcing from the observed data the seasonal trends are reduced to values of 2.1 ± 0.1 mm/yr (winter), 2.0 ± 0.1 mm/yr (spring), 2.0 ± 0.1 mm/yr (summer) and 2.2 ± 0.1 mm/yr (au-

tumn). Hence, the seasonal trend distribution becomes more homogeneous. Furthermore, the seasonal differences in the SE are mostly removed. For the shorter period from 1951 to 2008 a similar but considerable larger phenomenon has been found. While the trends in spring, summer and autumn are approximately the same (1.4 ± 0.5 mm/yr, 0.9 ± 0.4 mm/yr, 1.5 ± 0.8 mm/yr), the winter trend exceeds the remaining trends significantly with a value of 4.1 ± 1.3 mm/yr. The SEs show considerable dissimilarities as well. After removing the meteorological influences from the seasonal MSL time series, the trend distribution as well as the SEs get more homogeneous with values of 1.5 ± 0.3 mm/yr (winter), 1.5 ± 0.4 mm/yr (spring), 1.4 ± 0.3 mm/yr (summer) and 1.3 ± 0.3 mm/yr (autumn). Hence, meteorological forcing is identified to be the main driving factor for the large derivations in seasonal trends in the second part of the 20th century.

3.4.2.3Model validation

If one variable in the climate system should be described through one or more other variables within a LRM, the quality of the model depends on different factors. Climate is a highly variable system showing large changes on different time scales. Observed relationships between different climatic or non-climatic variables need not to be stationary in time. Since observations, such as tide gauge records or meteorological measurements, have a heuristic character, i.e. they only extract a narrow window from a more complex system, it is rather uncertain whether or not the observed relationship will hold in the future. Hence, there are two major questions that need to be addressed here within the process of model validation. (i) Are the observed seasonal relationships between MSL and the different meteorological parameters constant over time? (ii) How many years of data are required to explain most of the observed MSL variability?

To investigate these questions in detail, the following procedure has been applied. First a window consisting of 20 observations is built. The data within that window is used to estimate a seasonal LRM. This model is then applied to predict the whole observation period from 1871 to 2008. To measure the quality of the prediction, the regression coefficients as well as the explained variances between prediction and observation are extracted. The window is moved over the whole period to prove whether or not the used window size plays an important role for the model quality. That means that the first prediction is based on the first 20 years of the observation from 1871 to 1890, the second on the 20 years from 1872 to 1891 and so on, until the last prediction is based on the last 20 observations. This procedure has been repeated for 101 different window sizes varying between 20 and 120 years. Finally, for every window size different numbers of predictions exist, whereas the number of predictions decreases as the window size increases. Therefore, the number of predictions varies for the 101 window sizes. To measure whether the models estimated within the different time windows are comparable to the models for the whole investigation period, the related 95 % confidence bounds are computed and the following definition is applied: With a window size *x* a trustworthy regression model can be estimated, if the related regression coefficients are within the confidence bounds of the whole investigation period.

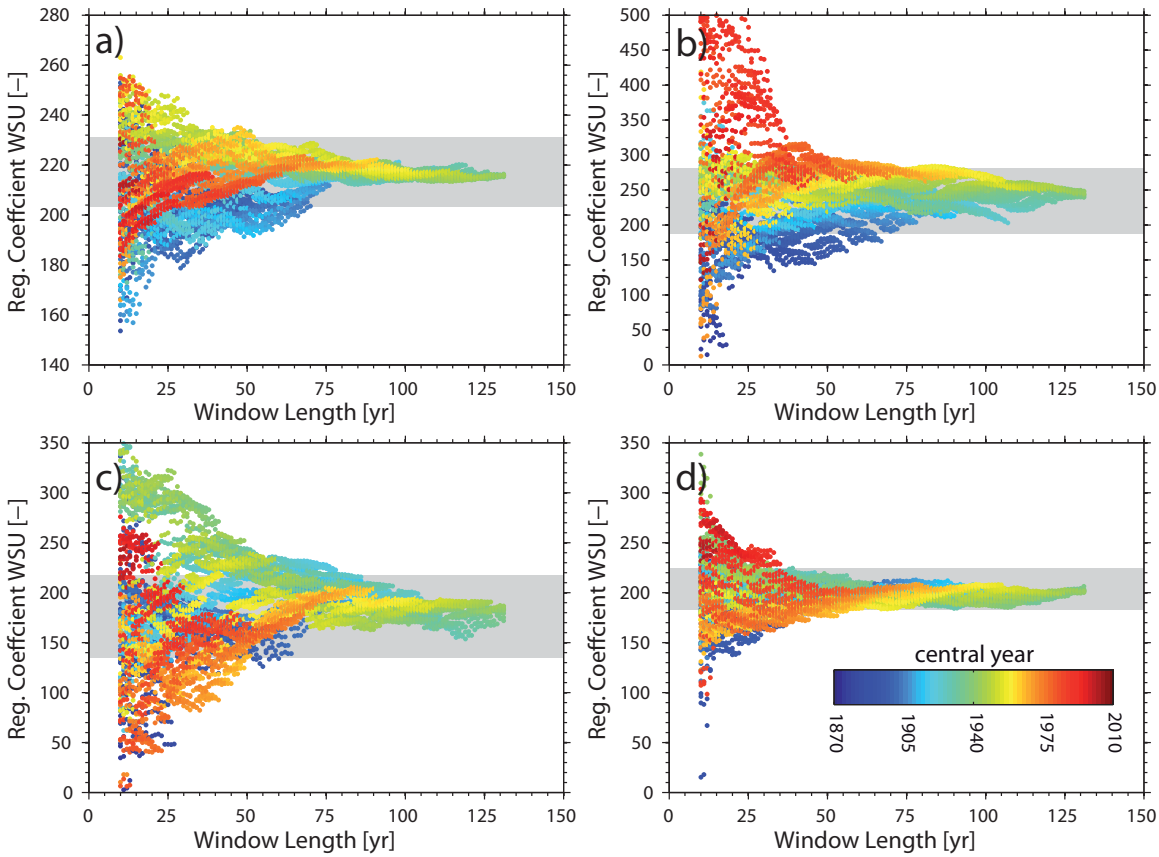

Figure 3-6: Results of model validation. The colored dots indicate the regression coefficients of zonal wind stress (in N/m²) by the different time dependent simulations. The different color shades represent the central year of the period for which the regression coefficients have been determined. The grey shaded area shows the 95% confidence bounds of the regression coefficient estimated for the whole observation period (1871-2008). The model validation is shown for a) winter (JFM), b) spring (AMJ), c) summer (JAS) and d) autumn (OND).

The results of the cross validation are shown for in Figure 3-6. Since zonal wind stress is the main forcing factor influencing sea level variability across all seasons, the validation is only shown and discussed for the regression coefficients of zonal wind stress. The validation results of the regression coefficients of the remaining contributors have been found to be similar to those of zonal wind stress. The regression coefficients for the whole period vary from season to season between 189.7 during summer season and 265.3 during spring season (for wind stress in N/m²). The regression coefficients estimated within the different time dependent windows also vary considerably, but for the four seasons the time and window size dependent regression coefficients generally show a similar shape. For small window sizes the estimates of the regression coefficients show substantial deviations from the mean with a large number of models estimating regression coefficients outside the confidence bounds. With an increasing window size these deviations decrease. For all selected seasons the regression coefficients are getting stable (i.e. they are within the confidence bounds) after approximately 60 to 80 years.

The explained variances were analyzed in a similar manner as the regression coefficients and similar results were obtained, i.e. the explained variances estimated within the process of model validation are getting comparable to the variances explained within the whole investigation period after approximately 60 to 80 years. These results reflect the

dependence of the LRMs from the used window length and time period. The band of regression coefficients and the explained variances are both getting stable for similar window sizes of 60 to 80 years. Therefore, it is suggested that models estimated with window sizes larger than approximately 60 to 80 years provide a trustworthy estimate for the relationship between meteorological forcing and sea level variability measured at the Cuxhaven tide gauge.

3.4.2.4Meteorologically corrected MSL variations

To prove the general influence of meteorological forcing on seasonal MSL trends, seasonal and annual 30-year moving trends are computed for the residuals after correcting seasonal MSL for meteorological influences and reconstructing the annual means. The results are presented in Figure 3-7. In comparison to Figure 3-2 (same results without corrections) the dissimilarities between seasonal and annual moving MSL trends are reduced considerably. Especially for the seasons of spring, summer and autumn, the differences are rather negligible. The large deviations of winter MSL in the second half of the 20th century are removed completely. Sensitivity analysis (not shown) suggests zonal wind stress as the main forcing factor for the large gradient in seasonal trends, which has been detected by Dangendorf et al (2012, chapter 2 of this thesis). Before that time for the winter season some differences remain, especially between the 1910s and the end of the 1950s. On the one hand these differences may indicate other forcing factors influencing seasonal MSL during that time, otherwise uncertainties and inaccuracies of the statistical model or the used data sets may be possible explanations. However, the general shape of annual moving MSL trends is better described by meteorologically corrected seasonal MSL than before, which implies that meteorological forcing is able to explain large parts of the intra- and inter-annual variability and significant parts of seasonal trends in some subperiods.

3.4.3 Meteorological forcing on inter-annual and decadal time scales

The seasonal MSL time series used here can be averaged to annual means to investigate the inter-annual long-term development. The observed annual MSL time series and the annual residuals after removing the meteorologically predicted MSL are presented in Figure 3-8a. The observed annual MSL time series (blue) has a linear long-term trend of 2.4 ± 0.1 mm/yr over the period from 1871 to 2008 and it is characterized by a large inter-annual and decadal variability. This variability as well as the linear long-term trend are reduced in the meteorologically corrected MSL time series (black line with red dots) showing a long term trend of 2.1 ± 0.1 mm/yr.

In the last decades, one of the most discussed questions in sea level science is whether or not acceleration due to anthropogenic climate change has been taken place in the recent past (Woodworth et al. 2009, 2011). Generally, there are two approaches which have been used to analyze the evidence of increase in the rate SLR. Some authors try to fit quadratic trends to the MSL observations and prove the evidence of acceleration with the quadratic coefficient, while others use moving linear trends.

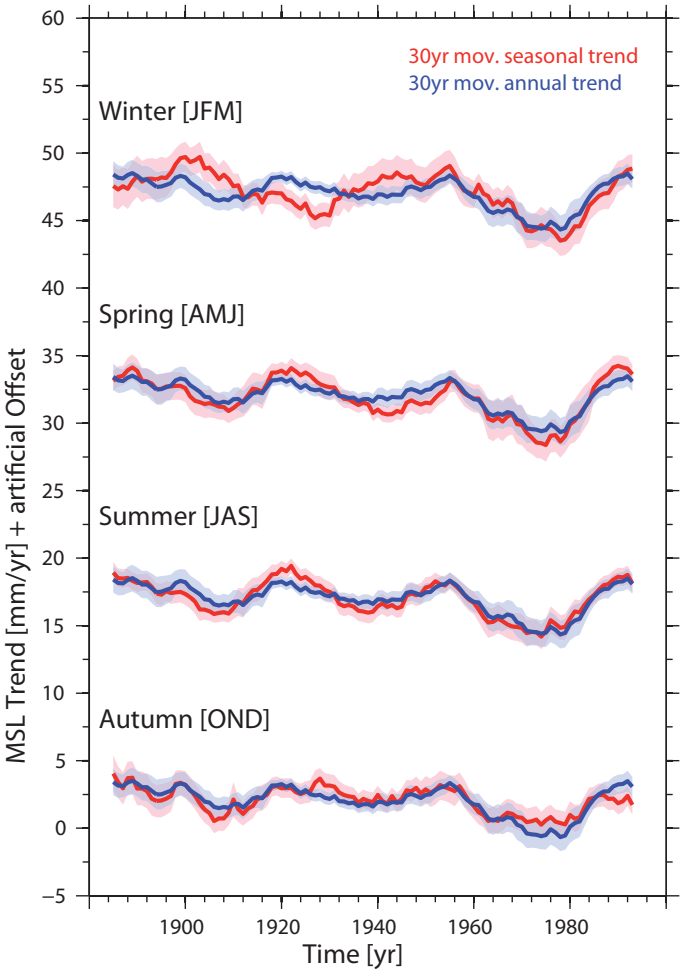

Figure 3-7: 30yr moving trend of seasonal (red) and annual (blue) MSL and their related 1σSE estimated for meteorologically corrected obser-vations over the period from 1871 to 2011.

Haigh et al (2014) have tested the applicability of both methods and suggest 30 to 40-year moving trends to be the most stable method for the detection of acceleration in SLR. Hence, this method is applied to the annual MSL values before and after removing meteorological forcing from the annual data. The rates of observed MSL rise vary considerably between ~0 and ~4 mm/yr (Figure 3-8). There are four noticeable periods during that time span: The high rates at the end of the 19th and the middle of the 20th century, the low rates during the 1960's and 1970's and the high rates afterwards. In agreement with the finding of Wahl et al. (2011), the largest rates of rise have been observed during the last three decades. Starting from the low point in the 1970's the rates increase to an absolute maximum of over 4 mm/yr in the last overlapping periods. Even if it is the highest rate measured during the observation period, comparable values have been observed at the end of the 19th and the middle of the 20th century. The meteorologically corrected residuals show in general a similar decadal variability in the rates of rise. Some periods can partially be explained by meteorological influences. For example, at the beginning of the 20th century, up to 1.4 mm/yr of the observed MSL trend can be explained by the LRMs. From the second half of the 20th century to present, a nearly constant part of 1 mm/yr is traced to meteorological forcing, mainly occurring during winter season. However, even if some subperiods are driven by atmospheric trends or variability, the general shape of the curve remains unchanged. Hence, meteorological forcing plays an important role when explain-

ing MSL variability on intra-, inter-annual and decadal time scales in the German Bight, but long-term trends are less affected.

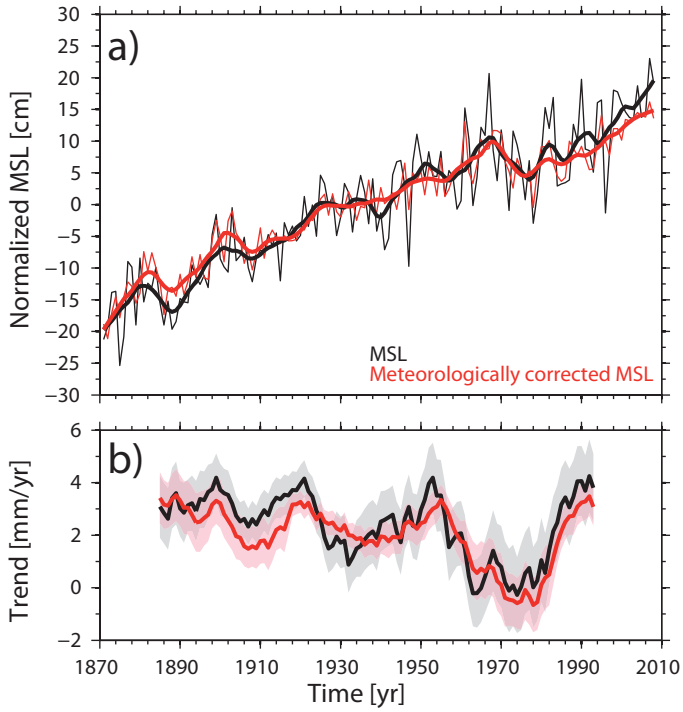

Figure 3-8: a) Observed (black) and meteorologically corrected (red) annual MSL at the Cuxhaven tide gauge over the period from 1871 to 2011. A ten year smoothed version is also shown (thick lines). b) The related 30yr moving trends for the time series shown in a).

In the residual annual MSL time series large parts of decadal variability remain unexplained by local meteorological forcing (Figure 3-8). Hence, the question arises, which other parameters or processes could explain these variations? There is a possibility that pressure differences over the subtropical gyre of the North Atlantic Ocean may lead to sea level variations at the coastlines through the propagation of oceanographic waves (Kolker and Hameed, 2007; Miller and Douglas, 2007). Miller and Douglas (2007) suggested that a spin down of the North Atlantic gyre could explain the higher SLR in the 20th century observed at tide gauges along North Atlantic coastlines. In contrast, more recent studies show that longshore components of wind stress and wave propagation along the boundary of the North Atlantic Ocean rather than changes in the North Atlantic gyre are the main contributors to decadal coastal sea level variability (Sturges and Douglas, 2011; Calafat et al., 2012). Calafat et al. (2012) found remarkable similarities between longshore wind stress integrated from the equator northwards and different tide gauges along the eastern North Atlantic and Mediterreanean and the outputs of a baroclinic model. Since this phenomenon shows an increasing influence at northwards latitudes, the influence on North Sea MSL should also be investigated in future.

3.4.4 The effect of SE reduction

An important question for the aspects of coastal planning is whether or not the models applied in this chapter may help to get more stable trend estimates for past MSL? The stability of the trend estimates is directly linked with the non-tidal variability and the length of the time series. Hence, especially in regions with large non-tidal variability, long and

high-quality measurements are needed. As mentioned before, in some areas the data availability is restricted to a few decades. For these areas it is of particular interest whether it is possible to accurately predict SLR. It is well known that large inter-annual variability influences the SE, which is related to the trend estimate. It has been demonstrated by several authors in different parts of the world that periods of 50 or 30 years are required to get a SE in the order of 0.5 and 0.3 mm/yr, respectively (Douglas, 1991; Tsimplis and Spencer, 1997; Woodworth, 1990; Woodworth et al., 1999; Haigh et al., 2009). For the German Bight, by contrast, longer periods are needed to get a comparable accuracy in estimating trends (Wahl et al., 2013). They explained that phenomenon with larger variability in this region. Hence, the SE of the meteorologically corrected time series should become smaller, i.e. shorter periods should be required to get a smaller SE.

A number of authors tried to reduce the variability (and therefore the SE of trend estimates) from atmospheric or oceanographic forcing by subtracting an index time series (a time series built on the basis of EOF or area weighted averages representing a larger geographical area; “master station” method) or a time series of a single station representing the typical variability in the study area (Woodworth, 1987; Woodworth et al., 1999; Haigh et al., 2009). This procedure works well in reducing the uncertainties related to trend estimates, but it does not help explaining the causes of the observed variability. The LRMs used in this chapter, aim to identify and explain the physical processes behind the atmospheric forcing. Understanding the processes driving regional sea level variability may help to identify the causes of differences between single tide gauge locations.

Following the method described in the above mentioned studies linear trends and their corresponding SEs are calculated with different time windows. Starting at the end of the Cuxhaven record linear trends and SEs are computed first for a period of 19 years, followed by a period of 20 years and so on. This procedure is done for the observed MSL time series as well as for the meteorologically corrected one and the residual time series after subtracting the detrended index time series from Wahl et al. (2011) from the Cuxhaven record. The results are shown in Figure 3-9. In contrast to other stations around the world a SE of 0.5 mm/yr requires a window size of at least 55 years. That is 25 years more compared to other tide gauges around the world (for example Newlyn, which is located at the southwestern boundary of the North Sea). After removing the influences of meteorological forcing this window can be reduced significantly. For the meteorologically corrected residuals, the SE is smaller than 0.5 mm/yr after 32 years. The effect is nearly the same when using the ‘master station’ method for reducing the regional variability. Hence, the multiple LRMs are able to explain the largest parts of the inter-annual variability. This is an important finding for two reasons. First, especially for tide gauges with shorter records in the area of the German Bight, data becomes comparable after reducing meteorologically induced variability. Second, the reduced variability enables for an earlier detection of acceleration or deceleration behavior of MSL rise, which is one of the most important questions in climate science and coastal planning requirements.

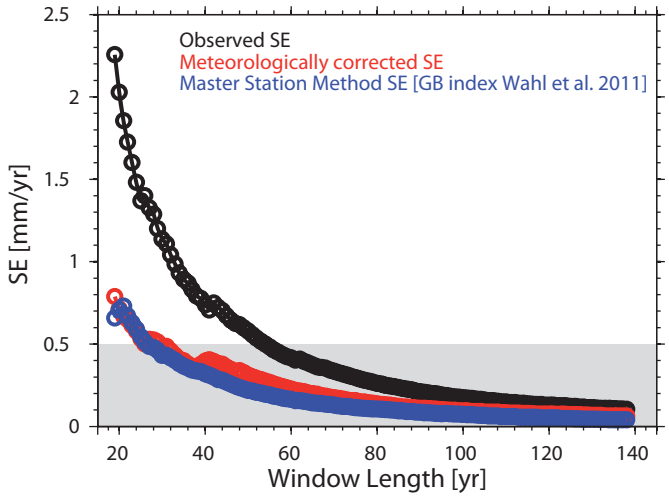

Figure 3-9: SE of observed (black), meteorologically corrected (red) and index corrected (blue) annual MSL trend calculated with changing numbers years at the tide gauge of Cuhaven. The grey shade marks the 0.5 SE area typically adopted as a moderate SE for tide gauges evaluations (Douglas, 1991).

3.5 Conclusions

This paper presents a case study of intra-, inter-annual and decadal variability and the role of meteorological forcing factors at the tide gauge record of Cuxhaven. It has been shown that there are considerable seasonal differences driven by meteorological forces. Stepwise regression has been applied to estimate the contribution of different meteorological forcing factors. Although there exist some barotropic models in the North Sea region (Tsimplis et al., 2005; Woodworth et al., 2007), that can be used for estimating the atmospheric contribution, these models are currently restricted to the period of available NCEP/NCAR (National Centre for Environmental Prediction/ National Centre for Atmospheric Research) data (i.e. from 1948 on) and only a constant bathymetry. Hence, statistical models are additionally important to study changes on longer time scales. Depending on the investigated season, the models explain between 54 (summer) and 90 % (winter) of the observed non-tidal variability during a period from 1871 to 2008. The variability is dominated by zonal wind stress through all seasons, while the contribution of precipitation, SLP and meridional wind stress is rather small but in some seasons still significant. The models are able to estimate the local atmospheric contribution to MSL variability timely independent, if 60 to 80 years of data or more are used to build up the LRMs. It is further supposed that major parts of the remaining variability should be related to transregional forcings, such as postulated by Sturges and Douglas (2011) and Calafat et al. (2012) for tide gauges located at the eastern boundary of the North Atlantic basin. Additionally, it has been shown that the large derivations of winter MSL in the second half of the 20th century are the result of changing pressure conditions over the North Atlantic, coming along with an increase in the local zonal wind conditions. However, even if meteorological forcing is partially able to explain considerable parts of the trend in some sub-periods, the long-term trend is less affected. This is consistent with the findings of Albrecht et al. (2012).

The dominant influence of zonal wind stress expresses itself in a clear pressure gradient between Scandinavia and the Iberian Peninsula. Although this pattern shows remarkable similarities to the NAO, it is able to explain a larger part of the non-tidal variability in the

German Bight. While the NAO explains between 30 and 35 % of the observed variability during winter season (Jevrejeva et al., 2005; Dangendorf et al., 2012, chapter 2 of this thesis), the more eastward gradient enables us to reconstruct between 70 and 80 % of the variability of monthly MSL anomalies. SLP is well reproduced by climate models (Weisse and von Storch, 2009). Hence, it can be suggested that the gradient between Scandinavia and the Iberian Peninsula indicates a larger potential for estimating future sea level variability and the related flood risk of near coastal areas. This is a scientific topic that has to be invetigated in the near future.

While studies related to GMSL are important to understand the climatic system of the Earth, for the aspects of coastal planning regional or local MSL studies are required (Nicholls and Cazenave, 2010). RMSL may differ significantly from the global mean (Wahl et al., 2010; Sallenger et al., 2012). Hence, the identification of forcing factors affecting regional MSL variability is a crucial step for estimating possible future states of SLR (Tsimplis et al., 200; Dangendorf et al., 2012, chapter 2 of this thesis). First steps in estimating future regional MSL are done (Katsman et al., 2010; Slangen et al., 2011), but these projections are restricted to the regional response of ice melting, ocean mass changes and GIA. The consequences of atmospheric forcings are not considered. With the knowledge of the link between atmospheric forcing and MSL, the additional effects could be integrated into these scenarios for the different regions. Hence, future studies should combine the results to establish scenarios including both possible trends (with considerable uncertainties) and variability.

Furthermore, some practical applications of the LRMs for the aspects of estimating SLR are shown. Due to the reduction of the non-tidal variability the related SE can be reduced significantly, which allows for a better evaluation of SLR patterns. With the application of the LRMs a similar variability reduction is reached as with the master station method used by Woodworth et al. (2009) and Haigh et al. (2009). This is important for the aspects of coastal planning. Haigh et al (2014) pointed to the uncertainties related to the search of acceleration patterns in SLR under the presence of larger inter-annual and decadal variability. Since the southeastern North Sea is an area of particular large variability it should be proved whether potential acceleration patterns can be better and earlier detected when removing meteorologically induced variability. The results presented in this study should be further applied to more tide gauges around the North Sea basin to analyze the regional differences in meteorological forcing. Additionally, future studies should address the comparison of the results of the LRMs with the output of barotropic models. All these points will be investigated in the following chapter.

4 MSL variability in the North Sea: processes and implications

4.1 Abstract

MSL variations across a range of timescales are examined for the North Sea under the consideration of different forcing factors since the late 19th century. Multiple linear regression models, which are validated for the second half of the 20th century against the output of a tide+surge model, are used to determine the barotropic response of the ocean to fluctuations in atmospheric forcing. It is found that local atmospheric forcing mainly initiates MSL variability on timescales up to a few years, with the IBE dominating the variability along the UK and Norwegian coastlines and wind controlling the MSL variability in the south from Belgium up to Denmark. On decadal timescales, MSL variability mainly reflects steric changes, which are largely forced remotely. A spatial correlation analysis of altimetry observations and gridded steric heights suggests evidence for a coherent signal extending from the Norwegian shelf down to the Canary Islands. This fits with the theory of longshore wind forcing along the eastern boundary of the North Atlantic causing coastally trapped waves to propagate over thousands of kilometers along the continental slope. Implications of these findings are assessed with statistical Monte-Carlo experiments. It is demonstrated that the removal of known variability increases the signal to noise ratio with the result that: (i) linear trends can be estimated more accurately; and (ii) possible accelerations (as expected e.g. due to anthropogenic climate change) can be detected much earlier. Such information is of crucial importance for anticipatory coastal management, engineering and planning.

4.2 Introduction

SLR is one of the most certain consequences of climate change. Due to this and its broad socio-economic and environmental impact on coastal zones, SLR has become a topic of major importance for scientists, governments and the general public. Hence, significant efforts have been devoted to better understand the processes driving SLR and variability with the aim of producing more accurate projections of future SLR, which can then serve as the basis for implementing appropriate adaptation measures. The challenge is to protect coastal zones against the impacts of SLR and assure high safety standards not only under present day but also future climate conditions. This complex task requires an ex-

tensive understanding of how sea level has changed in the past and might change in the future, on both regional and global scales.

There is observational evidence that global MSL (interpreted in terms of the volume of the global ocean) has risen at a mean rate of about 1.7 mm/yr during the 20th century (Church et al., 2013) and scientific consensus is that it will continue to rise through the 21st century: most likely at an accelerated rate, due to enhanced greenhouse gas emissions (e.g. Meehl et al., 2007; Rahmstorf and Vermeer, 2009; Church et al., 2013; Orlic and Psaric, 2013). Furthermore, it has been known for some time that the rate of SLR is not uniform but varies widely by region and over time, with some regions experiencing a much larger (or smaller) SLR than the global average (e.g. Douglas, 1991; Church et al., 2013). Additionally, some regions experience VLM which can further increase/decrease the risk of rising sea levels.

Some authors have claimed that the global MSL budget (interpreted in terms of the volume of the global ocean) can be reasonably closed within the observational errors by finding that the sum of its two major components (i.e., the mass and steric) agrees well with observations of total MSL for the past 50 years (Church et al., 2011). However, accurate local and regional budget analyses are still rare. The difficulty is related to the dynamic character of each component producing its individual regional pattern (Mitrovica et al., 2001; Levermann et al., 2005; Yin et al., 2009; Riva et al., 2010; Slangen et al., 2012). Additionally, each component is further characterized by its own temporal variability acting on timescales ranging from months to several decades (e.g. Sturges and Douglas, 2011; Calafat et al., 2012, 2013a, 2013b). Hence, understanding the regional dynamics of SLR and variability requires a careful assessment of each component separately before exploring the combined regional budget.

In this paper we investigate the mechanisms of intra-annual to decadal-scale MSL variability as measured by tide gauges (often referred to as local or relative sea level) in the North Sea basin with a particular focus on local and remote atmospheric forcing. Recently, an assessment of North Sea MSL changes from the early 19th century onwards was undertaken by Wahl et al. (2013). The authors focused on long-term changes in terms of geocentric (sometimes referred to as 'absolute') and relative MSL changes based on annually averaged time series. The study revealed that geocentric MSL rose by 1.6 mm/yr since 1900, a rate which is close to that of the global mean rate over the 20th Century (Church and White, 2011). The authors found an acceleration in geocentric MSL around the end of the 19th Century, prior to which geocentric MSL was relatively stable in the North Sea. Over the last few decades, an additional acceleration was found, but it was concluded that the recent high rates of SLR over the period were not unusual compared to the high rates observed at the end of the 19th century. In terms of variability, only fluctuations in the mean local SLP were compared to the MSL and it was found that, although they explain a significant fraction of the inter-annual variability in sea level, they fail to explain the major multi-decadal features.

Here, we extend the study of Wahl et al. (2013) by assessing the characteristics of intra-annual to decadal scale variability in more detail in order to better understand the pro-

cesses driving the observed sea level changes from the late 19th century onwards. Improving our understanding of such processes is essential to produce better regional projections of potential future sea level rise, and thus contribute to more effective coastal planning. In a recent paper, Haigh et al. (2014) highlighted that the presence of significant inter-annual to decadal variations linked to internal climate variability hampers the early detection of sea level accelerations linked to anthropogenic climate change and showed that removal of such variability will reduce the detection time. While reducing the noise is important, a careful assessment of processes contributing to SLR and variability is crucial to assess whether recent or possible future accelerations in sea level represent a temporal fluctuation relating to internal climate variability or are the response to anthropogenic forcing. From an engineering perspective it is further important to understand the sources of variability as elevated sea levels enhance the risk of coastal flooding.

Investigations of local MSL variability in the North Sea on intra- and inter-annual timescales have already been conducted by various authors (e.g. Plag and Tsimplis, 1999; Yan et al. 2003; Wakelin et al., 2003; Tsimplis et al., 2005; Jevrejeva et al., 2006; Albrecht and Weisse, 2012; Dangendorf et al., 2012, 2013a, 2013b, chapter 2, 3, 5 of this thesis; Richter et al., 2012). Plag and Tsimplis (1999) assessed the (non-stationary) seasonal cycle of MSL and found that, in the North Sea region, it is considerably affected by atmospherically induced variability. Yan et al. (2003) reported a strong link between local MSL variability and the NAO, a major mode of large-scale atmospheric variability in the North Atlantic region (Hurrel, 1995). This link is mainly related to the response of sea level to well understood wind and pressure forcing (Wakelin et al., 2003; Albrecht and Weisse, 2012; Dangendorf et al., 2012, chapter 2 of this thesis; Richter el al., 2012) and to changes in the position and intensity of the NAO's centers of action (Kolker and Hameed, 2007). However, the aforementioned studies are either based on numerical modeling studies limited to the second half of the 20th century and/or focused on specific seasons and coastline stretches (e.g. Richter et al., 2012; Dangendorf et al. 2013a, chapter 3 of this thesis). The role of atmospheric forcing on longer timescales and its contribution to acceleration/deceleration patterns in the entire region has not been explored. Furthermore, none of the above-mentioned studies investigated the nature of decadal variations, which are present in the records (Dangendorf et al., 2013a, b, chapter 3 and 5 of this thesis; Woodworth et al., 2009). Sturges and Douglas (2011) and Calafat et al. (2012) found that a significant fraction of the decadal-scale MSL variability along the eastern boundary of the North Atlantic can be explained as a response to changes in longshore winds, including the generation and propagation of coastally trapped waves. They also showed that such variability is part of a large coherent signal extending thousands of kilometers along the European Atlantic coast from the Canary Islands up to the coast of Ireland. Calafat et al. (2013a) furthermore showed that this coherent signal also propagates into large parts of the Nordic Seas and even into parts of the Arctic Ocean, while Marcos et al. (2013) demonstrated a similar response to the longshore wind in the tropical Atlantic at the Tenerife tide gauge. Whether this signal affects the North Sea, and if so, by how much, is a question yet to be answered.

Here we examine the nature of intra-annual to decadal scale MSL variability observed from a set of 22 long tide gauge records from the North Sea basin for the 140 year period from 1871 to 2011. This is done by consecutively investigating the variability in different frequency bands and exploring possible driving mechanisms. We start by assessing the temporal and spatial characteristic of high frequency variability in the basin before extending the study area to the Northeast Atlantic in order to examine its influence on the North Sea. To integrate spatial information into the analysis we use gridded satellite altimetry measurements and gridded temperature data. Plausible mechanisms are explored by combining atmospheric and oceanographic measurements, either local or remote, which are then used to reconstruct decadal scale fluctuations in the North Sea basin. Following that, we use statistical experiments to test whether the removal of known parts of the variability influences the: (i) robustness of linear trend estimations and (ii) the interpretation of acceleration and deceleration patterns as expected under different future greenhouse gas emission scenarios.

The paper is structured as follows. The data and methods used are described in Section 2. Results are presented and discussed in Section 3, and conclusions are given in Section 4.

4.3 Data and Methods

4.3.1 Data

A set of North Sea tide gauge records, similar to that used by Wahl et al. (2013) for the investigation of the inner North Sea, is examined. The region is shown in Figure 4-1 and spans from the eastern boundary of the English Channel along the southern coastlines and the Norwegian Trench to the eastern coastline of the UK. In contrast to Wahl et al. (2013) the records from the English Channel are not included in our analysis. A total of 22 tide gauge records at monthly resolution were selected, 18 of which were downloaded from the webpage of the Permanent Service for Mean Sea Level (PSMSL; Holgate et al., 2013), while the other four (from the German Bight) were reconstructed by Wahl et al. (2010, 2011). The records span different periods with some of them starting in the early 19th Century. Since we are interested in the link between atmospheric forcing and MSL variability, only the period for which both atmospheric and MSL data are available (i.e. from 1871 to 2011, see also below) is analyzed.

In addition to the individual stations, we compute and analyze five MSL index time series, representing the mean of four sub-regions (region 1, southwestern North Sea: stations 1 to 6; region 2, southeastern North Sea: stations 7 to 14; region 3, northeastern North Sea: stations 15 to 17; region 4, northwestern North Sea: stations 18 to 22) and the mean of all stations (North Sea). The indices are calculated following the method used by Haigh et al. (2009) and Wahl et al. (2011), which consists of differentiating the time series at each station (thereby removing the linear trend), averaging the residuals across stations, and then adding the averaged residuals cumulatively. The mean seasonal cycle (determined by the long-term average of each month) is removed from all time series prior to the anal-

yses. Decadal scale features are examined by applying a 48-month moving average filter to the de-seasonalized monthly records.

While the tide gauge records give unique insights into temporal variability of coastal sea level on long time scales, spatial dependencies between the open ocean and the coastal sea level are – due to the lack of information – much harder to assess. Therefore we complement our data set with satellite altimetry data for the northeast Atlantic. Although the records are limited in time, they provide near-global coverage making them a valuable source for the investigation of spatial characteristics. Here, we use monthly averaged SSH anomalies (corrected for the IBE) from TOPEX/Poseidon, ERS-1/2 and Envisat on a 1/3°×1/3° Mercartor grid spanning the period from January 1993 to December 2011 and obtained from AVISO (Ducet and Le Traon, 2001). The processing carried out on the altimetry dataset (i.e. the removal of the seasonal cycle and the smoothing) is identical to that undertaken for the tide gauge records.

We also analyze the output from a barotropic version (Tide+Surge Model, hereafter TSM) of the Hamburg Shelf Ocean Model (HAMSOM (Chen, 2014)). The TSM data are used to investigate the performance of the statistical-empirical LRMs described in the Methods section below. The model was run for the period 1952 to 2003. The TSM has a horizontal and temporal resolution of three kilometers and five minutes, respectively. It covers the entire North Sea region bounded by the Shetland Islands in the north, the Dover Strait in the south, the Orkney Islands in the west, and the Baltic Sea in the east. The TSM is nested into a larger Northwest European Shelf model (NWESM) also based on HAMSOM extending over the region from 47°N to 63°N and 15°W to 14°E. The NWESM is forced by the main tidal constituents at the model boundaries as well as gridded surface wind and pressure data from the NCEP/NCAR reanalysis (Kalnay et al., 2003). More information on the model is provided by Chen (2014).

To examine the contribution of atmospheric forcing, gridded data sets from 20CRv2 are evaluated. The 20CRv2 data represent the output of a global weather forecast model that assimilates six-hourly SLP observations, monthly sea surface temperature (SST) and sea ice extent observations (Compo et al., 2011). Time series of monthly mean SLP and zonal and meridional wind stress from the 20CRv2 are available on a 2°x 2° global grid and were downloaded from the webpage (http://www.esrl.noaa.gov/psd/data/20thC_Rean/) of the National Oceanic and Atmospheric Administration (NOAA). The time series of SLP and wind stress are processed similarly to the tide gauge records, that is: the mean seasonal cycle is removed; and for decadal scale investigations the time series are then smoothed with a 48-month moving average filter. Note that before 1900, the 20CRv2 data have been found to be affected by model internal inconsistencies (Dangendorf et al., 2014a, chapter 6 of this thesis), which are probably related to the lack of data available for assimilation in the early periods (Krüger et al., 2013), and thus results for this period should be interpreted with caution. Nevertheless, these inconsistencies were found to affect mostly extreme values whereas their impact on monthly means is suggested to be much smaller (Dangendorf et al., 2014a, chapter 6 of this thesis).

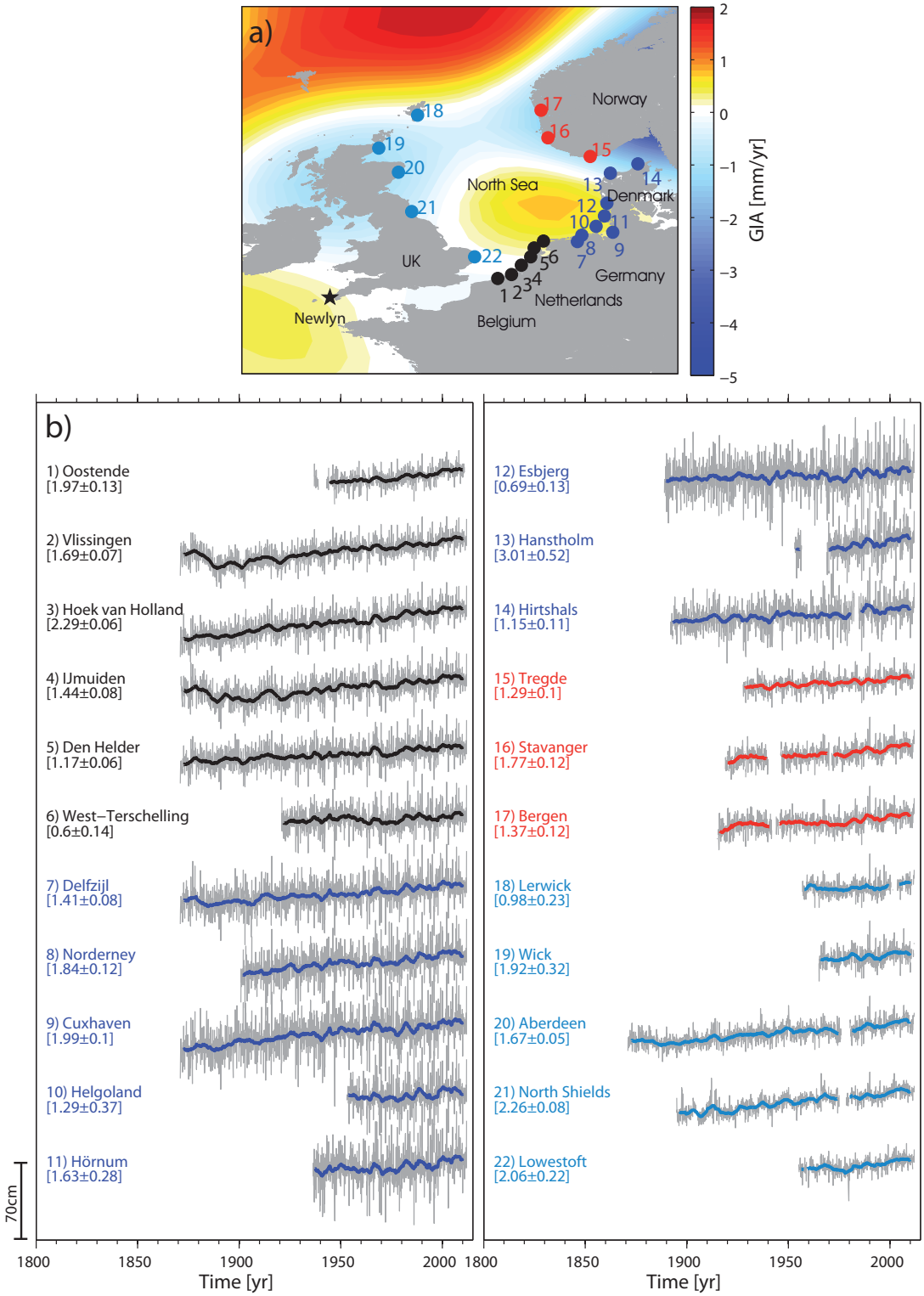

Figure 4-1: a) Investigation area and tide gauge locations with their station ID's. The GIA contribution as provided by Peltier (2004) is also shown. b) Monthly deseasonalized geocentric MSL (grey) and a 48 month low pass filtered version (black) for each tide gauge considered in the present chapter. Each station name together with its ID is shown beside the time series. The linear trend with its 2 SE for the full available period at each location is also given. The colors in a) and b) refer to the four sub-regions defined in the text.

Since the HAMSOM TSM run is forced by NCEP/NCAR reanalysis wind and SLP fields (Kalnay et al., 2003), we also use wind stress and SLP fields from the NCEP/NCAR reanalysis (available from the NOAA webpage) to further validate the LRMs (chapter 4.3.2).

Unlike the 20CRv2, the NCEP/NCAR reanalysis only covers the period from 1948 to present. This is sufficient for our purposes since we use the data to validate the LRMs by comparing their outputs with those of the TSM for the period from 1952 to 2003.

For the assessment of steric MSL changes (see the Methods section for details on their calculation) the global gridded temperature and salinity data set by Ishii and Kimoto (2009) is used. This data consists of monthly 1°x1° gridded fields covering the upper 1500 m of the water column with 24 unevenly distributed vertical levels and spanning the period 1945 to 2011. In addition to the gridded temperature and salinity fields, we examine in-situ measurements from a hydrographic station. Because of the special characteristics of the shallow shelf in the North Sea (with water depths mostly less than 100m), we restrict the examination of hydrographic data to the station of Sognesjoen. The station is located in the Norwegian Trench and provides temperature and salinity profiles covering the whole water column down to 300 m from 1950 to 2011 (http://www.imr.no/forskning/forskningsdata/stasjoner/).

4.3.2 Methods

The main focus of our study is on temporal variations of MSL as measured by tide gauges in the North Sea and their physical and geographical origin. It is important to note that tide gauges measure sea level relative to a benchmark on land (often referred to as local or relative sea level) or equivalently variations in the local distance from the sea surface to the sea floor. Local MSL variations can be viewed as the sum of three contributions: 1) changes in ocean bottom pressure (OBP); 2) changes in SLP; and 3) density changes due to temperature and salinity variations (the resulting sea level changes are often referred to as steric changes). Using this separation, local MSL changes can be described by:

$$\xi_{local} = \xi_{OBP} + \xi_{SLP} + \xi_{Steric} \,. \tag{4-1}$$

The first term, ξ_{OBP}, accounts for OBP changes resulting from both VLMs and any mass transport in the Earth system, including the effect of such mass transport on the gravity field as well as water mass transport and redistribution in the ocean induced by changes in atmospheric forcing. Note that, although changes in SLP cause water mass redistribution, they are not accompanied by OBP changes (departures from classical IB effect are usually small outside the tropics (Wunsch and Stammer, 1997)), and thus they are included in a different term (ξ_{SLP}). In general, the contribution of ξ_{OBP} can be directly measured by OBP recorders or satellite gravimetry. However, OBP recorders are absent in the region and gravimetry observations do not have sufficient spatial (and temporal) resolution for local studies. Hence, in practice, direct observations of ξ_{OBP} are not available in the region. The contribution of the SLP term, ξ_{SLP}, can be directly calculated by using SLP data and assuming that variations in SLP cause local MSL to change at a rate of -1cm/hPa, which is, in essence, the inverse barometer approximation.

The steric term, ξ_{steric}, can also be computed directly by vertically integrating the density anomalies (derived from the temperature and salinity data) at each grid point and for each time step, using the following equation:

$$\xi_{steric} = -\frac{1}{\rho_0} \int_{-H}^{0} (\rho - \bar{\rho}) dz \tag{4-2}$$

where ρ_0 is a reference density (1025 kg/m^3), H is the reference depth, ρ is the in situ density of sea water (calculated using the nonlinear equation of state for seawater), z denotes depth, and the overbar indicates time average taken over the entire investigation period from 1945 to 2011. Because temperature and salinity observations are usually scarce below 700 m, the steric height is referenced to two different levels: 200 m and 700 m. The steric height is deseasonalized prior to the analysis of the local MSL.

As mentioned previously, VLMs are reflected on OBP changes. VLMs generally stem from two different mechanisms: glacial isostatic adjustment (GIA), which is associated with the Earth's viscoelastic response to the last deglaciation, and tectonic effects coupled with local processes such as groundwater withdrawal, and earth quakes, or regional effects resulting from changes in land ice cover (e.g. Jiang et al., 2010) or changes in land water storage (e.g. Amos et al., 2014). The contribution of VLMs to ξ_{OBP} can be, in principle, obtained from Continuous Global Position System (CGPS), however, since such measurements are still uncertain in the region due to their shortness, limited availability, and noisy character (Wahl et al., 2011), we have decided not to use them (note, that the variability within the CGPS time series is usually less than 1-2 cm on a monthly scale, including the seasonal cycle). Instead, and following Wahl et al. (2013), we remove only GIA effects from the tide gauge records using the linear VLM trends as calculated by the ICE-5G model (Figure 4-1, Peltier, (2004)). Given the variety of available GIA models, which may differ significantly from each other at the local scale (Jevrejeva et al., 2014), this is a subjective choice. Nevertheless, since the GIA contribution is provided by all models as linear long-term rates of VLMs, using a different model will only affect the trends but not the temporal variability, which is the main focus of this study.

Because historic observations of ξ_{OBP} (let alone the contribution of the numerous processes affecting ξ_{OBP}) are not available in the region, here it will be assumed that, on interannual to decadal timescales, ξ_{OBP} is dominated by the response of the ocean to changes in atmospheric forcing, and thus its value can be estimated from atmospheric data. This, of course, assumes that the contribution of both VLMs and land-ocean mass exchange to ξ_{OBP} is small compared to that of atmospheric forcing, and thus can be neglected without introducing serious errors. The validity of this assumption is supported by the fact that 3D numerical ocean models forced only with wind and buoyancy fluxes can often capture the interannual and decadal sea level variability (corrected for the IBE) at tide gauge locations quite well (e.g., Carton et al., 2005; Stammer et al., 2013; Figure 2a in Calafat et al., 2014), despite missing the contribution of both VLMs and water mass exchange between land and the ocean (their contribution to the coastal MSL variability in the North Sea is suggested to be comparably small (roughly in a similar order as the variations of the glob-

al mean (Aimee Slangen pers. Comm., July 2014), which is less than one tenth of the variability of local MSL (Wahl et al., 2013)). It follows from these assumptions that ξ_{OBP} and ξ_{SLP} are then both a function only of atmospheric forcing, and thus it is convenient to combine them into a single term,

$$\xi_{atm} = \xi_{OBP} + \xi_{SLP}. \quad (4\text{-}3)$$

A simplified equation for the local MSL can then be written as

$$\xi_{local} = \xi_{atm} + \eta_{Steric}. \quad (4\text{-}4)$$

Therefore, here the focus is on the contributions of atmospherically induced MSL variations ξ_{atm} and steric variations ξ_{steric} (as determined by equation 2), which can be either locally or remotely driven. It is also important to note that strictly speaking variations in the SSH from altimetry only coincide with the MSL measured by the tide gauges if the sea floor has no vertical motion. However, since the contribution of VLMs on interannual to decadal timescales is relatively small, here we will assume that variations in altimetric SSH and local MSL are comparable.

To determine ξ_{atm}, a stepwise LRM as introduced by Dangendorf et al. (2013a, chapter 3 of this thesis) for the tide gauge in Cuxhaven is used. Detrended monthly local MSL anomalies are taken as a dependent variable, and detrended zonal/meridional wind stress and SLP anomalies as predictors. Time series of the atmospheric predictors are selected for each tide gauge among the grid points within an area of ± four degrees around the tide gauge as those with the highest linear correlation with the local MSL from the tide gauge record. Then a stepwise procedure with forward selection is applied, where one by one the predictors giving the highest linear correlation to the MSL record are included into the model until none of the remaining variables significantly improves the model performance (95 %-confidence level with f-statistics). The variance explained by ξ_{atm} (or each other contribution) at each tide gauge is measured by (von Storch and Zwiers, 1999):

$$VAR_{exp} = \left[1 - \frac{(var(\xi_{Geo} - \xi_{Atm}))}{var(\xi_{Geo})}\right]. \quad (4\text{-}5)$$

To estimate the contribution of ξ_{atm} to long-term trends we assume that the relationship found for detrended time series on inter-annual timescales also holds on longer timescales and apply the regression coefficients of the multiple LRM to the de-seasonalized but non-detrended windstress and SLP data.

The use of LRM's raises the question of whether they are able to give a realistic estimate of the atmospheric component, comparable to that provided by a barotropic TSM. The main reason for using LRMs is that none of the TSM runs available for the region cover the period prior to the mid-20th Century. Here the LRMs are validated for the second half of the 20th century by comparing them with a state of the art HAMSOM TSM (Chen, 2014) and later applied in a second step, together with 20CRv2 reanalysis data, to estimate the atmospheric component back to 1871.

The comparison between the LRMs and the TSM is shown in Figure 2. For each tide gauge record the atmospheric component is estimated using a stepwise LRM with atmospheric fields from the NCEP/NCAR as input data. The results are then compared with the output of the TSM at the nearest grid point to the tide gauge. The comparison is performed for the locations of Ijmuiden, Helgoland, Bergen and Aberdeen each of which is located in one of the four sub-regions (Figure 4-2a). The LRM and TSM time series agree well, with correlations above 0.92 for the four locations. Correlations for all other individual stations are similar to those found for the four selected stations (Figure 4-2b), with values that are mostly larger than 0.8. Maximum values exceed 0.9 along the coastlines from the Netherlands up to Norway, the Shetland Islands and northern Scotland. The only exceptions are Lowestoft and Hoek van Holland where correlation values of 0.49 and 0.62 are found. Since all surrounding stations compare well, local inaccuracies in the TSM may explain the discrepancies at these two sites. This suggestion is supported by the fact that in both cases the LRM estimates show significantly higher correlations (Hoek van Holland: 0.78, Lowestoft: 0.58) to the observed time series than the TSM estimates (Hoek van Holland: 0.63, Lowestoft: 0.41). Comparing the standard deviations of the time series from both models, we also find good agreement (Figure 4-2b). Slightly larger standard deviations originate for the LRM estimates at stations located in the German Bight. There are a number of reasons that may explain these discrepancies: (i) topographic model inaccuracies in the TSM; (ii) local wind variations which are often linked to changes in large-scale atmospheric circulation and included in the LRMs as remote effects (e.g., changes over the North Atlantic) but not captured by the TSM due to its regional boundary conditions; (iii) changes in atmospheric forcing causing not only barotropic effects but also density variations. Density-related MSL changes may of course be partly captured by the LRM but not by the barotropic TSM. It is difficult to determine which of these reasons is responsible for the differences between the LRMs and TSM. Nevertheless, overall the LRM's agree very well with the TSM, and so it is reasonable for our purposes. Moreover, the agreement is also good in terms of the linear trends (Figure 4-2c), which further demonstrates that the LRMs are well suited for a long-term assessment in the North Sea.

Linear trends in MSL are estimated using OLS regression. Since the residuals of the linear regression model usually contain positive serial correlation, the OLS SEs underestimate the true SE and thus need to be adjusted. The presence of serial correlation is mostly related to the inertia of the thermosteric component and does not affect the time series of the atmospheric component whose behavior is almost stochastic in nature without any significant correlation structure in the residuals. This is confirmed by an independent Durban-Watson-Test (Durbin and Watson, 1951) applied to the atmospheric component at each location (not shown). Hence, whenever the steric component is included in the model, it is assumed that the residuals follow an AR1 process and correct the SE for serial correlation by reducing the degrees of freedom as described by Santer et al. (1999). In cases where only the atmospheric component is analyzed the SEs directly estimated from OLS are used.

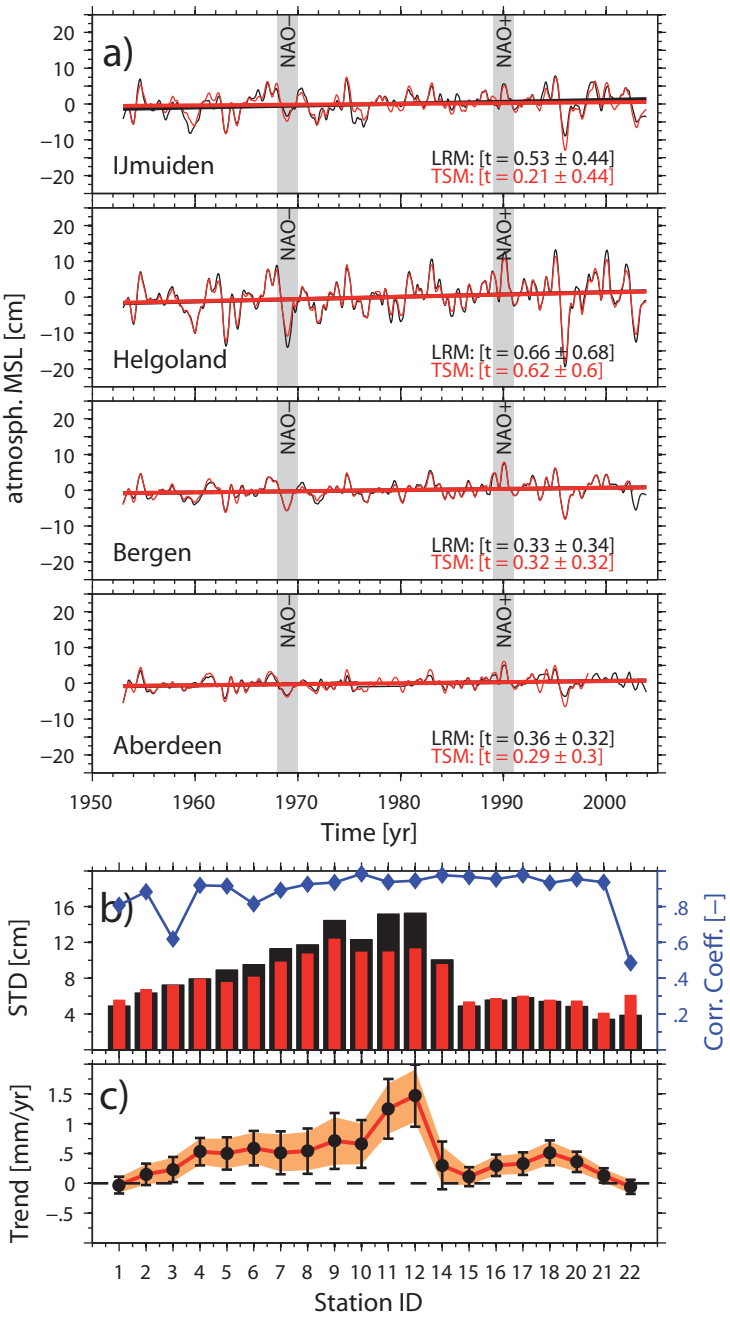

Figure 4-2: Comparison of the multiple LRM with a state of the art barotropic TSM (Chen, 2014) over the period from 1953 to 2003. a) Four examples for time series and their linear trends of the atmospheric contribution to MSL at the locations of Ijmuiden, Helgoland, Bergen and Aberdeen, respectively. For presentation purposes all time series have been low pass filtered with a 12 months moving average filter. The two years in which the NAO had its maximum and minimum are marked in grey. b) Comparison between standard deviations of the atmospheric contribution at different locations estimated with the multiple LRM and the TSM. The correlations between both estimates are shown by the blue diamonds. c) Comparison of linear trends, incuding their SEs shown as error bars and shading, respectively. In all subplots results of the multiple LRM are shown in black, while the results of the TSM are presented in red. Note that only those records have been regarded, where at least 75 % of data were available during the investigation period.

4.4 Results

4.4.1 The atmospheric contribution

The local MSL time series, after the removal of GIA effects estimated with the model of Peltier (2004), are characterized by large (up to ± 60 cm) intra-annual to decadal variability (Figure 4-1b). Comparing the different tide gauge records, the decadal scale variability is similar amongst sites, while the higher frequency fluctuations show considerable differences. Hence, this suggests that the driving factors for the decadal component have a common origin at all tide gauge sites, while different contributing factors influence the higher frequency fluctuations observed across the study area. In the high frequency bands

(i.e. intra- and inter-annual) the records along the Norwegian and UK coastline exhibit a slightly smaller variability, while along the southern coastlines the variability increases consistently moving eastwards, reaching a maximum in the German Bight, a finding consistent with that of Wahl et al. (2013).

To investigate these features in more detail, the local MSL variability is first compared to different contributions related to atmospheric forcing, i.e. SLP and wind stress. Figure 4-3 shows the anomalies of the four regional virtual station time series and the SLP and wind stress anomaly patterns related to phases of particular high (> two standard deviations) minus particular low (< two standard deviations) local MSL. Large local MSL values in the first two regions (i.e. the southwestern and the southeastern part of the North Sea) are characterized by a pronounced north-south pressure gradient with two anomaly centers of action over Scandinavia and the northeast Atlantic/Iberian Peninsula. This pressure gradient is consistent with a stronger than normal northwesterly flow, resulting in enhanced winds over the southeastern North Sea. The pattern resembles the Northern Scandinavian Iberian Peninsula Index (NSCI) as introduced by Dangendorf et al. (2013a, 2013b, chapter 3 and 5 of this thesis) and points to a dominant role of westerly winds in the region. The pattern shows similarities to the NAO, but its northern center of action is shifted from southern Iceland towards northern Scandinavia. The dominant zonal winds over the North Sea appear as westerly longshore winds along the southern coastlines. Because of the Ekman transport induced by the longshore winds towards the southern coasts and its resulting convergence of water mass on these coasts, the wind is likely to be more important in these two regions. This is consistent with recent investigations at the Cuxhaven tide gauge (Dangendorf et al., 2013a, chapter 3 of this thesis).

For regions three and four, i.e. the Norwegian and the UK coastlines (see also chapter 4.3.1), a pressure gradient is also obvious. However, compared to the first two regions, for the Norwegian tide gauge records a more meridional pressure gradient over the North Sea leads to a stronger westerly to southwesterly flow. Furthermore, the SLP anomalies in the region are more pronounced and the dominant winds appear cross-shore, suggesting that the IBE is little more important in this area in relation to the southern parts of the North Sea. For region 4 the SLP anomalies also show a strong north-south gradient but its northern center of action is more similar to that of the NAO. The lowest anomalies are found over southern Iceland and the wind pattern shows a stronger southwesterly direction, consistent with the imprint of strong NAO+ conditions. Similar to the Norwegian tide gauges the manifestation of SLP anomalies along the English coast are more pronounced and wind anomalies face away from the coast. Overall, the composites point to an important influence of local atmospheric forcing on the intra- and inter-annual local MSL variability; this is in agreement with earlier studies (e.g. Tsimplis et al., 2005).

The output of the LRMs allows a more detailed analysis of the processes described above and their contribution to the observed local MSL variability. Figure 4-4a shows the results expressed as explained variability at each individual location. Local atmospheric forcing accounts for most of the observed variability at virtually all stations. The largest contribution is found in the German Bight at the tide gauges of Hörnum and Esbjerg, where at-

mospheric forcing explains over 90 % of the variability. The amount of explained variability clearly follows the observed variability gradient along the coastline discussed above. It increases from values around 60 % near the English Channel to over 90 % in the German Bight and decreases along the Danish coastline to values around 60 % at the Norwegian sites. At the eastern coast of the UK values between 30 and 70 % are also observed, with lowest values at Lowestoft and North Shields.

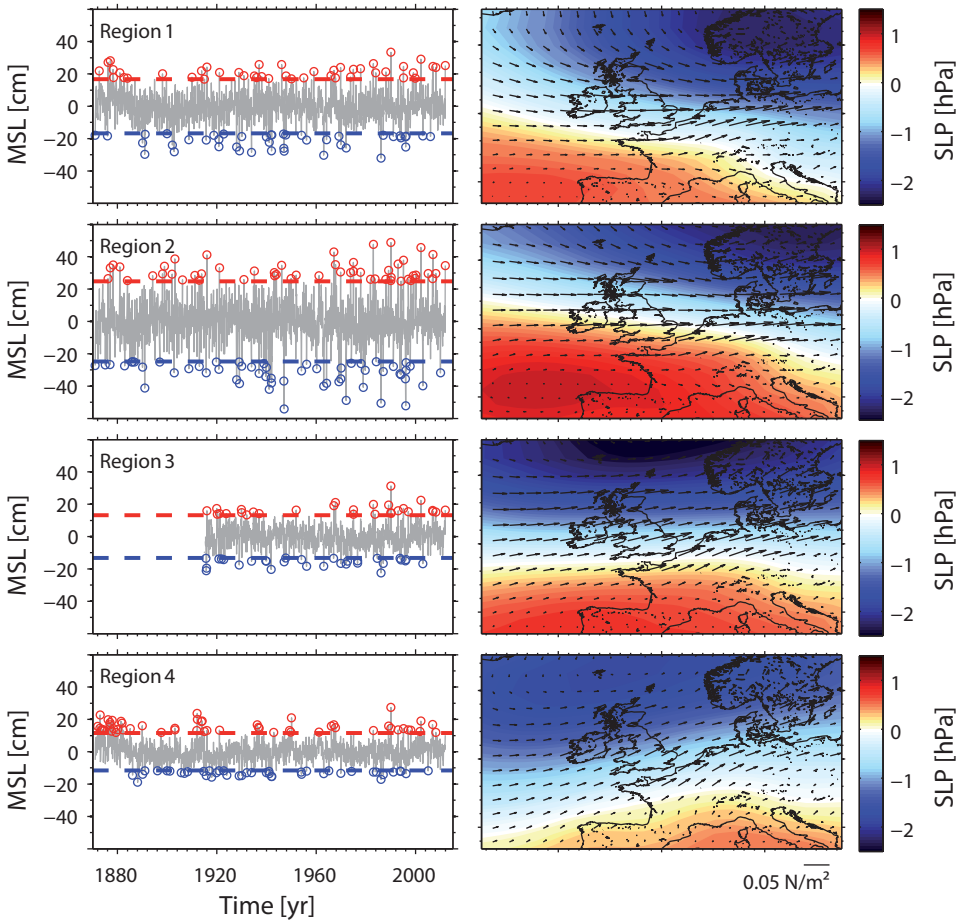

Figure 4-3: Composite plot for the mean SLP and wind stress (right) during times of particularly high (> two standard deviations, red circles) minus particularly low (< two standard deviations, blue circles) monthly MSL events (left). The plots are given for the virtual stations of four sub-regions as defined in section 2.

Comparing the individual contributions of SLP and zonal and meridional wind stress (Figure 4-4a) confirms the results presented as composite plots in Figure 4-3. While in the northern parts of the Norwegian coast and the eastern UK coastline SLP dominates the atmospherically induced local MSL variations, zonal winds are more dominant along the southern coastlines from Belgium up to Denmark. At some stations along the UK and Norwegian coastlines the meridional wind stress component gives a non-negligible contribution, which is consistent with the wind stress anomalies (and a resulting Ekman transport towards/away from the coast) shown in Figure 4-3. The results further confirm numerical modeling studies, also pointing to a two-tier system with an IBE dominated region spanning from the English Channel diagonal through the North Sea up to Norway (e.g. *Chen*, 2014).

Figure 4-4b shows the standard deviations of local MSL $\xi_{local}$and the atmospherically corrected time series ξ_{local} minus ξ_{atm}. Again, a pronounced variability gradient with up to three times larger standard deviations in the German Bight is visible. The mean standard deviation across all sites is ~9.5 cm with a deviation of ~3 cm between the individual stations. After removing the atmospheric component this variability gradient disappears. The mean standard deviation reduces to ~4.5 cm with an inter-station deviation of only ~0.5 cm, reflecting the fact that atmospheric forcing explains most of the variability gradient and accounts for a major part of the background noise in the local MSL time series. Removing the atmospheric component, therefore, will result in a more robust estimation of linear or non-linear trends (in the sense that the residual variance is reduced, which leads to smaller SEs, see also chapter 4.4.4).

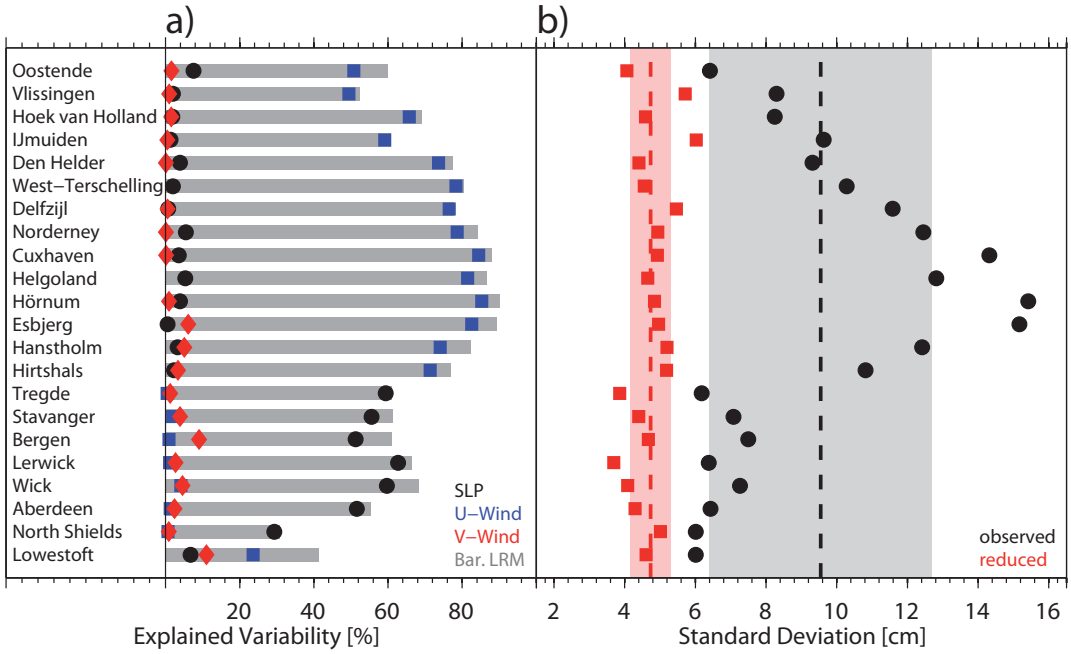

Figure 4-4: a) Explained variability by linear regressions between MSL at different tide gauges around the North Sea coastlines and different local atmospheric forcing factors as well as their combined contribution (barotropic LRM, grey bars). Only predictors explaining a significant fraction of variability are shown (95 % confidence level). b) Intra-annual de-seasonalized standard deviations of observed MSL and MSL corrected for local atmospheric effects. The means of intra-annual de-seasonalized standard deviations of all gauges are shown by the thick dotted lines together with their inter-station standard deviations.

It is clear from the results presented so far that the barotropic response of the ocean to local atmospheric forcing accounts for a considerable fraction of the observed intra-annual variability. Next we assess how it affects local MSL on longer timescales, including its contribution to accelerations. For this purpose, we compute moving trends for each component, i.e. for the local MSL, ξ_{local}, the atmospheric component, ξ_{atm}, and the atmospherically corrected time series (Figure 4-5). This was done for the virtual station time series for each region and using a window length of 37 years to account for the lunar nodal cycle which is superimposed on the trends (Baart et al., 2012).

Focusing first on the local MSL component ξ_{local} it is obvious that the moving trends alternate between higher and lower rates, with three major features common to all virtual station records: high rates in the early decades of the 20th century; a decrease towards al-

most zero in the 1960s; and a steady increase afterwards. These features were also found by Wahl et al. (2013). The atmospheric component ξ_{atm} is marked by a phase of relatively large trend rates in the early 20th Century and fluctuates around zero afterwards. Only in the southeastern North Sea (region 2) a considerable contribution of the atmospheric component to the acceleration in the rate of rise observed in recent decades can be found. This is due to an increase in the atmospheric contribution from the 1960s to the mid-1990s. Marcos and Tsimplis (2008) and Dangendorf et al. (2012, chapter 2 of this thesis) found that the increase mainly occurred during the winter season and they attributed it to particular strong NAO+ conditions with more frequent southwesterly winds (Siegismund and Schrum, 2001). Removing the atmospheric component from the observations reduces the 37-year trends by up to 1 mm/yr, but leaves the major longer-term features mostly unchanged. Hence, we conclude that local atmospheric forcing is a major contributor to sea level variability on intra- and inter-annual timescales but fails to explain longer-term variations.

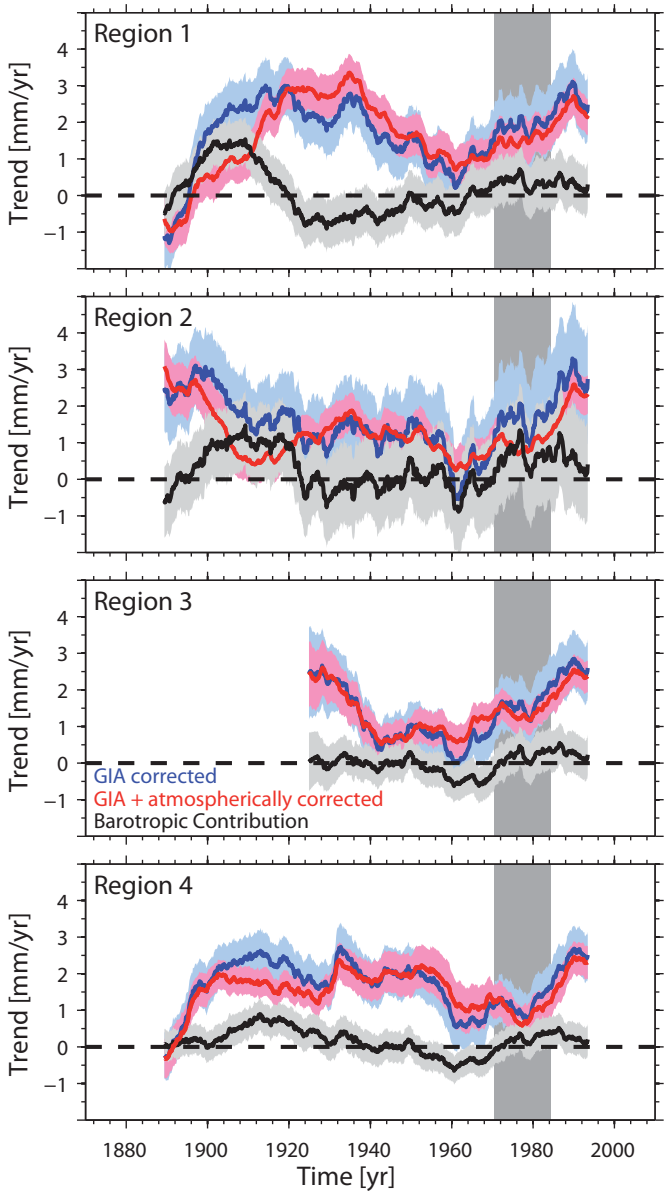

Figure 4-5: Moving linear trends (37 years) for the observed MSL (blue), the barotropic component of atmospheric MSL (black) and the atmospherically corrected MSL (red) for four different virtual stations corresponding to regions 1 to 4, respectively. The grey shaded vertical bar marks the period for which the barotropic component has been validated with the HAMSOM TSM.

4.4.2 Steric height

Following the assumptions made in chapter 4.3.2 and according to the separation in equation 4, the remaining signal of ξ_{local} after removing ξ_{atm} is to large extend determined by ξ_{steric}. The North Sea has – except in parts of the Norwegian Trench – water depths that are mostly less than 100 m. Along the coast, where most tide gauges are located, water depths are less than 10 m. Since the steric height is commonly computed as an integral over depth, its contribution is negligible if it is calculated in the shallow region over the continental shelf. This, however, does not imply that the variability measured by coastal tide gauges is unrelated to steric changes. In fact such variability is often produced by steric variations in the deep ocean external to the region. For instance, the isopycnals that intersect the continental slope may fluctuate vertically, which will be reflected as mass changes at the tide gauge. To get a measure of the steric contribution to coastal sea level, Bingham and Hughes (2012) demonstrated on the basis of an ocean model that for the European Atlantic coast the best results are obtained when the steric is computed in a depth range of 500 to 1000 m near the shore.

In the case of the North Sea one can either use the steric height inshore of the North Atlantic Current, near the northern entrance, or that obtained in the Norwegian Trench. The former is not possible due to the lack of data. However, the permanent station at Sognesjoen provides temperature and salinity data in the Norwegian Trench for the upper 300 m from which the steric component can be calculated. To demonstrate that – at least at longer time scales – the local MSL variability along the southwest coast of Norway near the Norwegian Trench is consistent with that in the North Sea, we have compared the the decadal component of local and atmospherically corrected MSL from the Stavanger tide gauge in Norway with that measured in the shallow parts of the North Sea as represented by four stations from the sub-regions (Ijmuiden, Delfzijl, Esbjerg, and Aberdeen) over the period from 1950 to 2011(see Figure 4-6a).

The time series of all five stations exhibit similar patterns of decadal variability with values ranging between ±5 cm (this is true for the local and the atmospherically corrected MSL). For example, all locations show a drop in the mid-1960s and a maximum at the end of the 1980s. Figure 4-6b compares the Stavanger local MSL with the steric height computed from temperature and salinity profiles at Sognesjoen in the Norwegian Trench. The decadal features fit reasonable well with the observed and atmospherically corrected decadal signals from the coastal sea level. This is expressed by high correlations between the steric height and both the observed local ($r = 0.66$) and the atmospherically corrected MSL ($r = 0.68$). The North Sea index is also significantly correlated with the steric height ($r = 0.57$).

Our results show that a considerable fraction of decadal scale variability of coastal MSL in the North Sea is – regardless of the question of its geographical origin – driven by steric sea level changes. Given the above mentioned spatial coherence of decadal local MSL variability in the region it can be assumed that temperature and salinity profiles from the Norwegian Trench can provide, at least to some extent, a good estimate of the steric component in the entire North Sea.

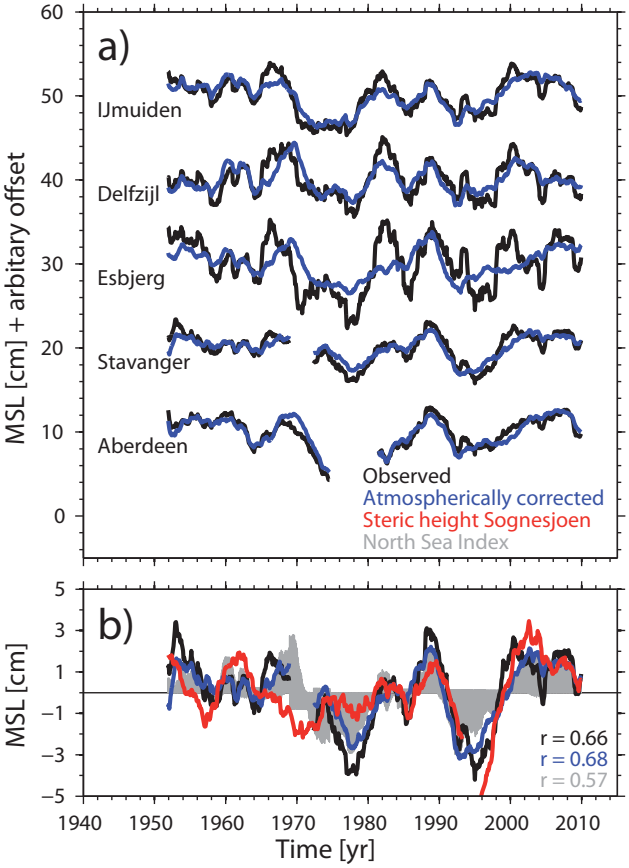

Figure 4-6: a) Low pass filtered MSL time series from five representative stations in the North Sea. The black lines represent the observed time series, while the time series corrected for atmospheric forcing are shown in blue. b) The observed and atmospherically corrected MSL record at Stavanger in comparison to the steric height calculated from temperature and salinity profiles at Sognesjoen. The North Sea index (atmospherically corrected; grey area) and linear correlations between all sea level time series and the steric height are also shown.

4.4.3 Remote forcing

The next question is concerned with the geographical and physical origin of the decadal fluctuations in the region. Sturges and Douglas (2011) explored the idea that the multi-decadal local MSL variability observed in the tide gauge record at Cascais, Portugal, may be related to changes in longshore winds. They argued that changes in the intensity or direction of the persistently southward blowing winds along the continental shelf produce an ocean response of both barotropic and baroclinic nature with a consequential change in sea level at the coast. Such response is not strictly local due to the possibility that coastally trapped waves may be excited and propagate northward along the coast, thus inducing sea level changes at all points northward of the region where the wind is blowing (Gill, 1982). In order to take the cumulative effect of the wind into account, Sturges and Douglas (2011) integrated the longshore wind from the equator up to Cascais. They found a good agreement between the integrated longshore wind and the local MSL at Cascais on decadal time scales, supporting their hypothesis. Calafat et al. (2012) expanded these investigations and demonstrated that the link with the longshore wind exists for a large portion of the eastern boundary of the North Atlantic and also for the Mediterranean Sea. With the help of an ocean model they also were able to show that the response of the ocean, responsible for this link, is of baroclinic rather than barotropic nature. In a subsequent study, Calafat et al. (2013a) used a proxy for the propagating signal of Atlantic origin in combination with local winds over the Norwegian continental shelf to show that

such signals can propagate further north into the Norwegian Sea and even in the western Siberian Seas. Using this reconstruction they were able to explain over 70 % of the observed local MSL variability along the Norwegian coast. Whether the signal affects also the North Sea, is still an open question which needs to be assessed.

To illustrate possible mechanisms of boundary wave generation in the northeast Atlantic Figure 4-7 (top) shows the average atmospheric conditions as estimated from the 20CRv2 wind and pressure fields over the period from 1950 to 2011. The region is characterized by a strong pressure gradient with a low-pressure center in the north and a high-pressure center over the Azores. The resulting wind stress patterns show a clockwise circulation centered on the Azores islands with prevailing (south-) westerlies from the Bay of Biscay northward. It is important to note that, in addition to the waves generated at distant locations (Calafat et al., 2012), the westerlies north of 45°N will generate new waves, and thus the associated sea level changes at higher latitudes can be considered as a superposition of continuously wind-forced coastally trapped waves (e.g. Gill, 1982). It is obvious that the westerlies will also intensify the North Atlantic Current and pile up the water on the North Sea coasts due to Ekman transport. The suggested coherence of decadal variability in the region is demonstrated by correlating the low pass filtered North Sea index derived from satellite altimetry (2°W to 10°E and 50°N to 62°N) with similarly filtered SSHs from satellite altimetry over the entire Northeast Atlantic area (Figure 4-7, middle). While the altimetry data is – due to the shortness of the observations – still limited for long-term variability investigations, it provides useful information on the spatial coherence of MSL in the region. The highest correlations are found over the continental shelf areas along the Norwegian coast and along the eastern boundary of the North Atlantic from western UK down to the Canary Islands. This suggests the existence of a coherent signal with a common origin in the North Atlantic and fits with the theory of wave propagation associated with longshore wind forcing. A similar correlation map is obtained when using steric height instead of altimetry data, for the longer period from 1945 to 2011 (Figure 4-7, bottom), reflecting a predominantly baroclinic behavior of the waves as found by Calafat et al. (2012). This further suggests that wind forcing over the region northward of the Gulf of Biscay is especially important for the generation of local MSL variability in the North Sea.

The link between decadal wind forcing and local MSL in the North Sea, which is suggested to be connected with the position and intensity of the NAO centers of action (e.g. Jevrejeva et al., 2006), is further investigated by comparing the longshore winds integrated from the equator up to higher latitudes. This is achieved (Figure 4-8) by comparing the time series via wavelet coherence plots (Grinsted et al., 2004). Significant coherence is found between the atmospherically corrected North Sea MSL and the integrated longshore winds in frequency bands of ~8 to 20 years, which is also supported by significant correlations between the time series itself ($r = 0.49$, the number of degrees of freedom was reduced with respect to the smoothing, Figure 4-8a). However, compared to the local MSL in Newlyn (Calafat et al., 2012) the coherence is lower, more confined to the decadal scales (note that inter-annual sea level variations in Newlyn are governed by local longshore winds, which are in turn also part of the integrated winds, while in the North Sea other factors are more important as discussed above) and also non-stationary in time

(Figure 4-8b). There are several possible causes for this. First, boundary waves may lose energy through radiation of westward-propagating Rossby waves as they propagate poleward along the coast. As an example, Marcos et al. (2013) provided evidence that local MSL at the Canary Islands is correlated with that along the continental boundary, reflecting the propagation of the signal from the coast to the offshore islands is in the form of Rossby waves. This implies that, for tide gauges located at high latitudes, it may be more appropriate to start the integration of the longshore wind from higher latitudes rather than from the equator. Second, coastally trapped waves can scatter strongly due to topographic variations (e.g., shelf width changes). Finally, inaccuracies in the wind data due to the lack of wind observations over the ocean may also contribute to the relatively low correlation between integrated longshore wind and steric MSL at high latitudes.

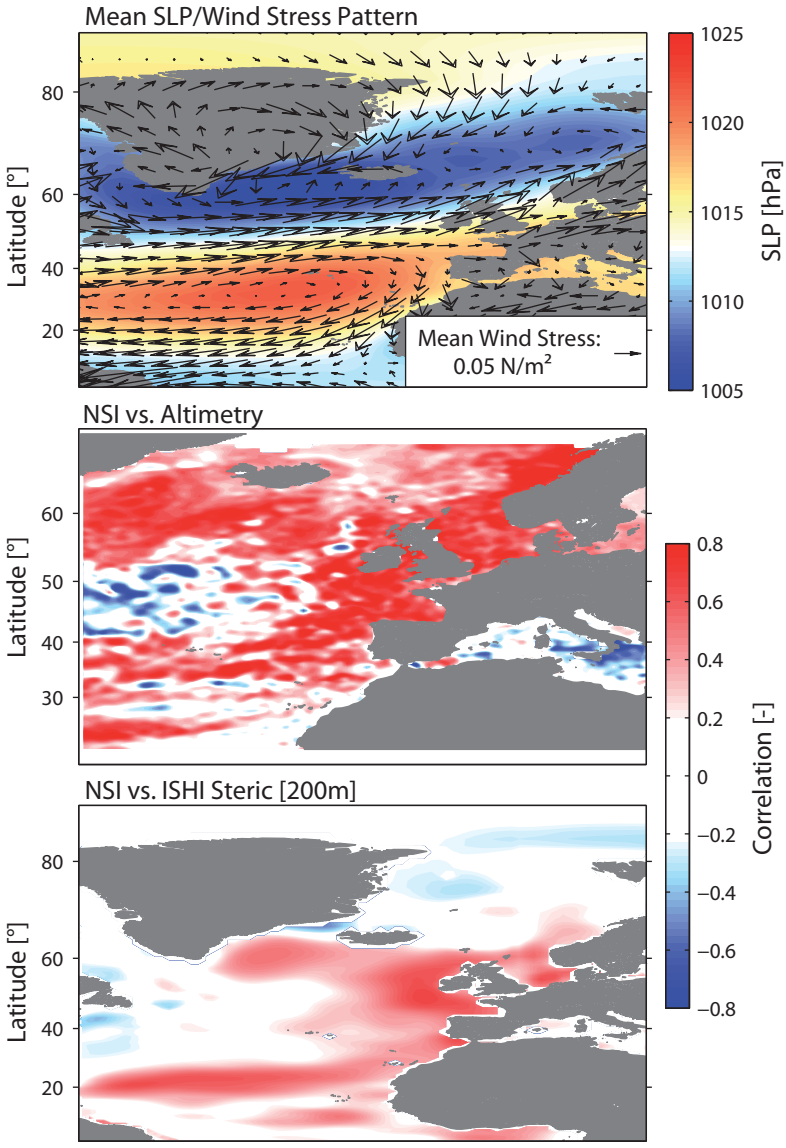

Figure 4-7: The average SLP and wind stress pattern over the period from 1945-2011 as estimated with 20CRv2 data (top). Linear correlations between the low-pass-filtered (48 months) mean North Sea MSL (2°W to 10°E and 50°N to 62°N) and each grid point time series of IBE corrected AVISO SSHs over the period 1993-2011 (middle), and between the atmospherically corrected North Sea index from tide gauges and the steric heights as provided by Ishii and Kimoto (2009) over the period 1945-2011 (bottom).

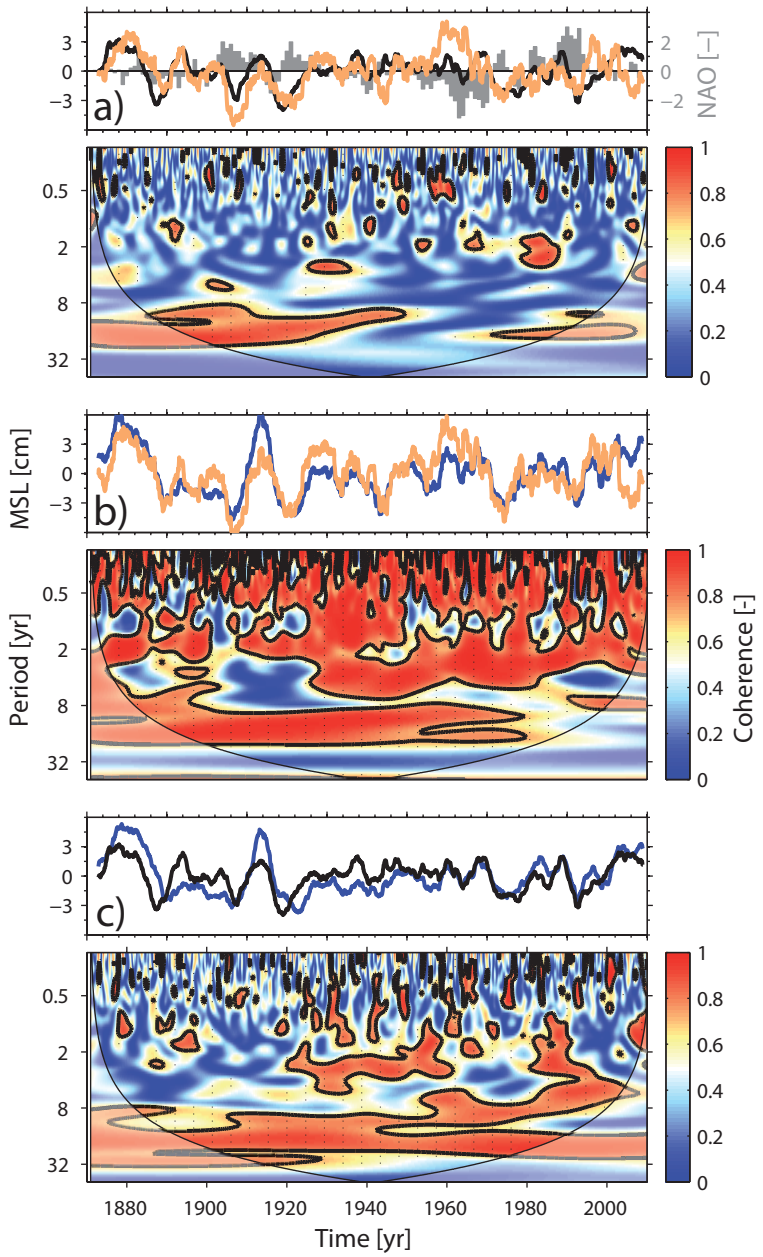

Figure 4-8: Wavelet coherence between a) the North Sea index of local atmospherically corrected MSL and longshore winds integrated from 6 to 55°N, b) local MSL at Newlyn and longshore winds integrated from 6 to 50°N, and c) the North Sea index of atmospherically corrected local MSL and the IBE corrected local MSL at Newlyn. Above each coherence plot also the corresponding low pass filtered time series (48 months moving average) are shown (North Sea index MSL: black, Newlyn MSL: blue, longshore winds: yellow). In a) also the winter NAO index (December to March) from Hurrel et al. (2003) is shown by the grey bars. The coherence has been calculated with the default version (Morlet wavelet) of the Grinsted et al. (2004) MATLAB wavelet toolbox. To extend the Newlyn record to the entire investigation period from 1871 to 2011, gaps have been filed via linear regression with the PSMSL Brest record, i.e. before 1916 all values are based on Brest data.

Hence, due to these limitations and following Calafat et al. (2013), it was decided to use local MSL data from the tide gauge record at Newlyn (UK, note that for the wavelet analysis gaps were filled using a linear regression to the Brest record (r = 0.94)) instead of winds themselves as a proxy for the propagating signal of Atlantic origin. The wavelet analysis of the IBE corrected Newlyn time series and the atmospherically corrected North Sea MSL index points to a more coherent and stationary relationship on decadal scales (Figure 4-8c), which is also supported by the low-pass filtered time series shown in Figure 4-9. Both time series show remarkable similarities with a correlation of ~0.84. In total ~70 % of the decadal-scale variability in the North Sea can be explained by the propagating signal of Atlantic origin alone. The correlation patterns with the steric height in Figure 4-7 further suggest that the regions north of Portugal and west of the UK are the most relevant to the generation of decadal MSL variability in the North Sea. As a complemen-

tary analysis, the tide gauge record at Newlyn is combined (in a multiple regression) with the steric height west of the UK (352°W: 52°N) and then again compared to the North Sea index (Figure 4-9). This further improves the model resulting in a linear correlation of 0.89 and an explained variability in the order of ~79 %. These results demonstrate that a significant fraction of the decadal variability is related to remote forcing over the North Atlantic.

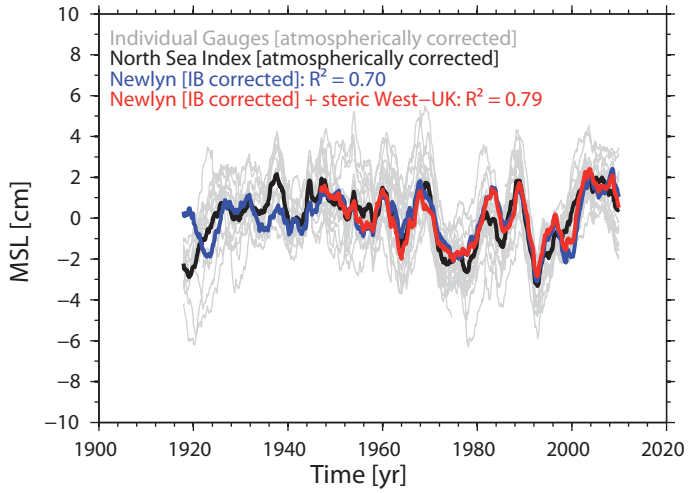

Figure 4-9: Comparison between the atmospherically corrected local MSL of the North Sea index (black), the IBE corrected MSL at Newlyn (NEWc, blue) and a reconstruction (multiple regression) based on the NEWc and the steric height observed west of the UK. The NEWc is used as a proxy for longshore wind forcing and the resulting wave propagation along the eastern boundary of the North Atlantic [*Calafat et al.*, 2012, see also Figure 8b]. Individual North Sea records are also shown (grey). All time series have been low pass filtered with a 48 month moving average filter.

4.4.4 Implications for the estimation of linear trends and acceleration patterns

The interest of this study is not only in understanding the different physical processes controlling local MSL variability in the North Sea but also in the influence of known variability to linear trends and acceleration/deceleration patterns. Dangendorf et al. (2013a, chapter 3 of this thesis) demonstrated (for the sea level record measured at the tide gauge of Cuxhaven) that the atmospheric contribution ξ_{atm} strongly influences its noise characteristics. Since the noise determines the SE of a linear trend, removal of known parts reduces the residual variance leading to smaller former trend uncertainty. Please note that this should ideally been done with the detrended atmospheric MSL, ξ_{atm}, unless one is also interested in trends of the internal variability. Dangendorf et al. (2013, chapter 3 of this thesis) showed that lengths of 50 to 60 years are required to obtain SEs in the order of 0.5 mm/yr, at Cuxhaven. After removing ξ_{atm} the required lengths reduced to ~30 years (a value comparable to those obtained at other tide gauges around the globe (Douglas, 1991)).

Here, a similar analysis is carried out for each of the tide gauge locations in the North Sea. In the procedure applied by Douglas (1991) and Dangendorf et al. (2013a, chapter 3 of this thesis), the observed records were used to estimate the SE in relation to the time series length by determining the linear trend and its SE for different window lengths starting with a window centered on the last 19 years and subsequently increasing the window length year by year back in time. This procedure is somewhat arbitrary since the SE strongly depends on the structure of the background noise in the respective time series

window (note that also the variance of the MSL time series is non-stationary). To get a more general expression of the dependence of the SE on the time series length, a Monte-Carlo experiment is conducted, in which an AR1 model is first estimated for each entire tide gauge record with the parameters a (noise variance) and g (lag-1 autocorrelation). These parameters are then used to simulate a set of 1000 artificial time series with noise typical for each of the considered tide gauge records by following the approach given by Allan and Smith (1994). The artificial time series are used to get a more robust estimate of the length required for the estimation of linear trends with a certain degree of accuracy, i.e. the SE is measured for different time series lengths 1000 times. This is done for 1000 time series containing noise typical for the local MSL, ξ_{local}, as well as 1000 time series with noise characteristics typical for the local MSL corrected for the atmospheric contribution ξ_{atm} (only the barotropic term).

Figure 4-10a exemplarily shows the results for the tide gauge record at Hörnum. For the local MSL ~52 ± 10 years (uncertainties estimated with the percentiles of the artificial time series) are required to estimate a linear trend with a SE in the order of 0.5 mm/yr. If the atmospheric contribution ,ξ_{atm}, is removed from the time series this value is reduced to ~33 ± 10 years (95 % confidence), highlighting the benefit of removing known variability from noisy time series before calculating trends.

Figure 4-10b shows the number of years required to obtain SEs in the order of 0.5 mm/year for both components, i.e. the local MSL and the atmospherically corrected MSL, for all study sites. As expected from the variability analyses described before, longer time series are required to achieve a moderate SE in the southeastern parts of the North Sea basin, compared to the other regions. When applying the atmospheric correction the number of years required to estimate the linear trend with the desired accuracy reduces to ~30 years, a number that is similar to the length reported by Douglas (1991) who analyzed selected records from tide gauges around the globe.

Finally, it is examined to what extent the atmospheric correction can improve the detection of acceleration/deceleration patterns, which is of particular relevance when searching for a possible increase in the rate of SLR of anthropogenic origin. To do this, methodology proposed by Haigh et al. (2014) is applied, i.e. tide gauge records are artificially extended to 2100, by combining future projections of SLR with realistic inter-annual variability. Then 37-year moving trends are calculated and the years in which a significant (95 % confidence) acceleration first becomes evident are detected. Four different projections are used (Figure 4-11a), two based on the IPCC's AR5 report (Church et al., 2013; hereafter P1 (0.50 m) and P2 (01.00 m), respectively; they correspond to the low and upper range of the Representative Concentration Pathway (RCP) 8.5, which correspond approximately to 0.5 and 1 m SLR by 2100, relative 1986-2005) and two accounting for higher values as estimated with semi-empirical models (e.g. Rahmstorf et al., 2007; Moore et al., 2013; hereafter P3 (1.5 m) and P4 (2.0 m), respectively). To all projections we add artificial noise (1000 time series, to account for uncertainty in future variability) from the AR1 model described above. Again, this is done for the local MSL and the atmospherically corrected MSL. For illustration we present results for three selected tide gauges (Delfzijl, Esbjerg,

Cuxhaven), which are: (i) long enough (i.e. covering the 20th Century) and (ii) contain a considerable fraction of atmospherically induced variability. We compute 37-year moving trends over the entire time series (observation + projection), identify the largest rate within the observations and search for the earliest period in the projections, in which five consecutive years exceed the maximum rate from the observations by taking into account their confidence intervals (Figure 4-11b). The last year of the 37-year period for which this criterion is fulfilled is assumed to be the 'detection point' at which we are able to tell that there is a significant acceleration. If no significant acceleration can be detected, the detection point is >2100.

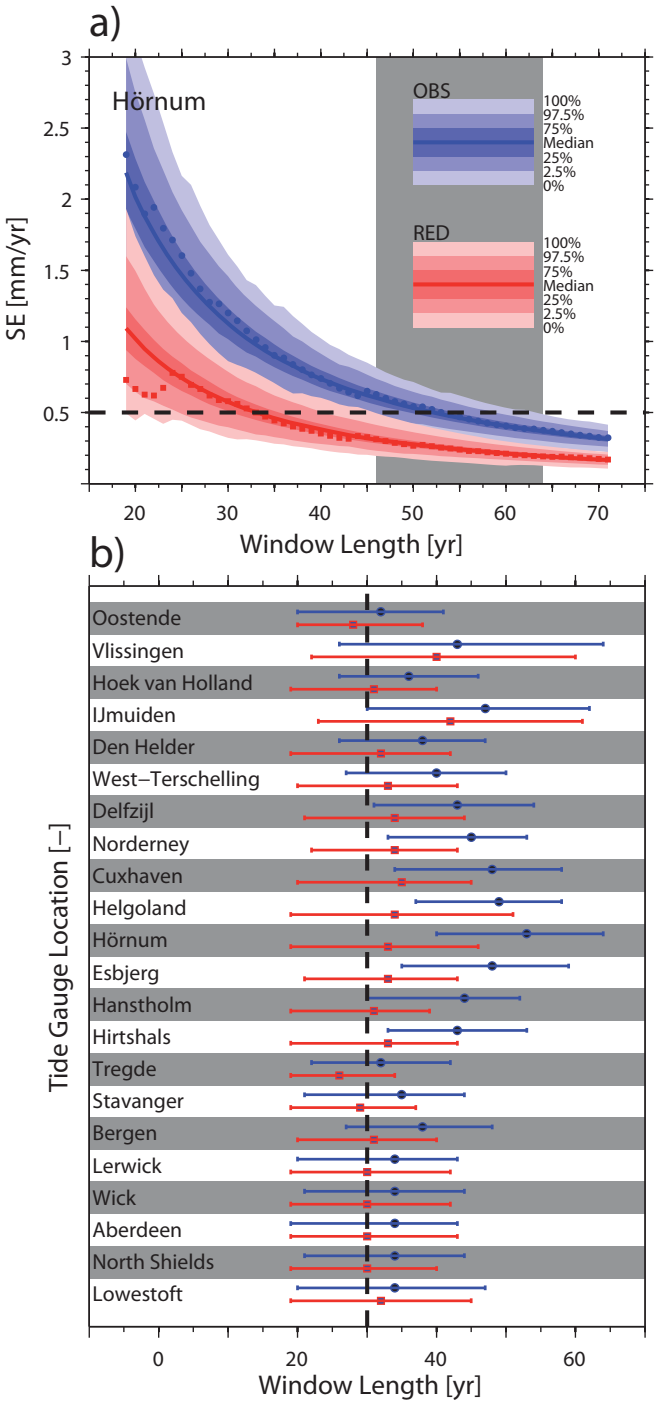

Figure 4-10: a) The SE as a function of time series length for observed (blue dots) and atmospherically corrected (red dots) MSL time series at the tide gauge of Hörnum. For both time series sets AR(1) models are used to simulate a set of 1000 artificial time series with realistic noise. The blue and red shaded areas represent the range of SEs estimated from the 1000 simulations. The black dotted line shows a SE of 0.5 mm/yr, a value that is typically as associated with 'robust' linear trend estimations. The grey shaded area marks the reduction that is reached through the atmospheric correction. b) Median (dots) and maximum/minimum range (lines) of SEs derived from the simulations used for (a) for observed (blue) and atmospherically corrected (red) time series at all stations. The black dotted line shows the 30 year window length, often needed to achieve a SE < 0.5 mm/yr (e.g. Douglas, 1991).

The results for each of the three tide gauge records are shown in the box plots of Figure 4-11c. According to Haigh et al. (2014) for the lowest scenario of 0.50 m SLR until 2100 the detection of a significant acceleration is a non-trivial task, as in a considerable number of simulations no significant acceleration can be detected before 2100. The median value of all simulations for P1 is 2061 (95 % percentiles: 2035->2100), >2100 (2075->2100) and >2100 (2054->2100) for the locations of Delfzijl, Esbjerg and Cuxhaven, respectively. The higher the SLR projection, the earlier a significant acceleration can be detected. With the exception of P2 at the locations of Esbjerg and Cuxhaven for all remaining projections a significant acceleration is detected at all sites. If noise typical for the atmospherically corrected MSL is applied the detection performance increases considerably, resulting in median values of 2050 (2029-2074) for Delfzijl, 2060 (2031->2100) for Esbjerg, and 2062 (2040->2100) for Cuxhaven. Under the assumption of the highest projection P4 median values of 2020 (2019-2026), 2025 (2019-2038) and 2022 (2019-2030) for time series with noise typical for local MSL and 2020 (2019-2025), 2021 (2017-2028), and 2022 (2019-2028) for time series with noise typical for atmospherically corrected MSL are calculated at the three stations. These results show that the detection of possible accelerations on a regional scale as considered here, strongly depends on the signal to noise ratio of the investigated time series. Atmospheric forcing might mask possible anthropogenic signals related to, for instance, global warming of the oceans or accelerated melt-water discharge. As an example, Calafat and Chambers (2013b) have recently shown that internal climate variability can contribute by up to 97 % (depending on the location) to local MSL accelerations at numerous tide gauges from around the world. By removing this contribution they were able to detect a statistically significant acceleration in coastal MSL between 1952 and 2011, which was related to external forcing (both anthropogenic and natural). Clearly, removing known patterns of variability from time series of local MSL enables earlier detection of possible underlying signals due to external forcing factors.

4.5 Conclusions

An assessment of MSL variability and its forcing across a range of different timescales has been undertaken for 22 tide gauge records in the North Sea; nine which extend back to the late 19th Century. The North Sea is one of the best instrumented regions worldwide and is therefore of particular importance for global MSL reconstructions (e.g. Jevrejeva et al., 2006; Church and White, 2011; Jevrejeva et al.; 2014). Our analysis suggests considerable intra-annual to decadal scale variability superimposed on well known long-term trends (Wahl et al., 2013). The largest intra- to inter-annual variability (up to ± 60 cm) is found in the southeastern part of the North Sea, which is up to three times larger than elsewhere in the region. On decadal timescales the variability is more coherent in magnitude throughout the region.

The variability on timescales ranging from months to a few years is dominated by atmospheric forcing and related barotropic adjustment processes in the ocean. However, the physical mechanisms driving the variability are different across the region. There is a

transverse line from the English Channel to Norway separating the North Sea into two distinct regions with different characteristics (Chen, 2014). In the northern parts the largest deviations around the mean are caused by the IBE. Here wind plays only a secondary role. In the southeastern parts the situation is reversed and the wind contributes to the majority of the variability. Generally, the North Sea region is characterized by a meridional pressure gradient leading to prevailing westerlies, acting as longshore winds along the southern coastline and piling up the water masses in the shallow southeastern parts of the basin (see also Wakelin et al., 2003).

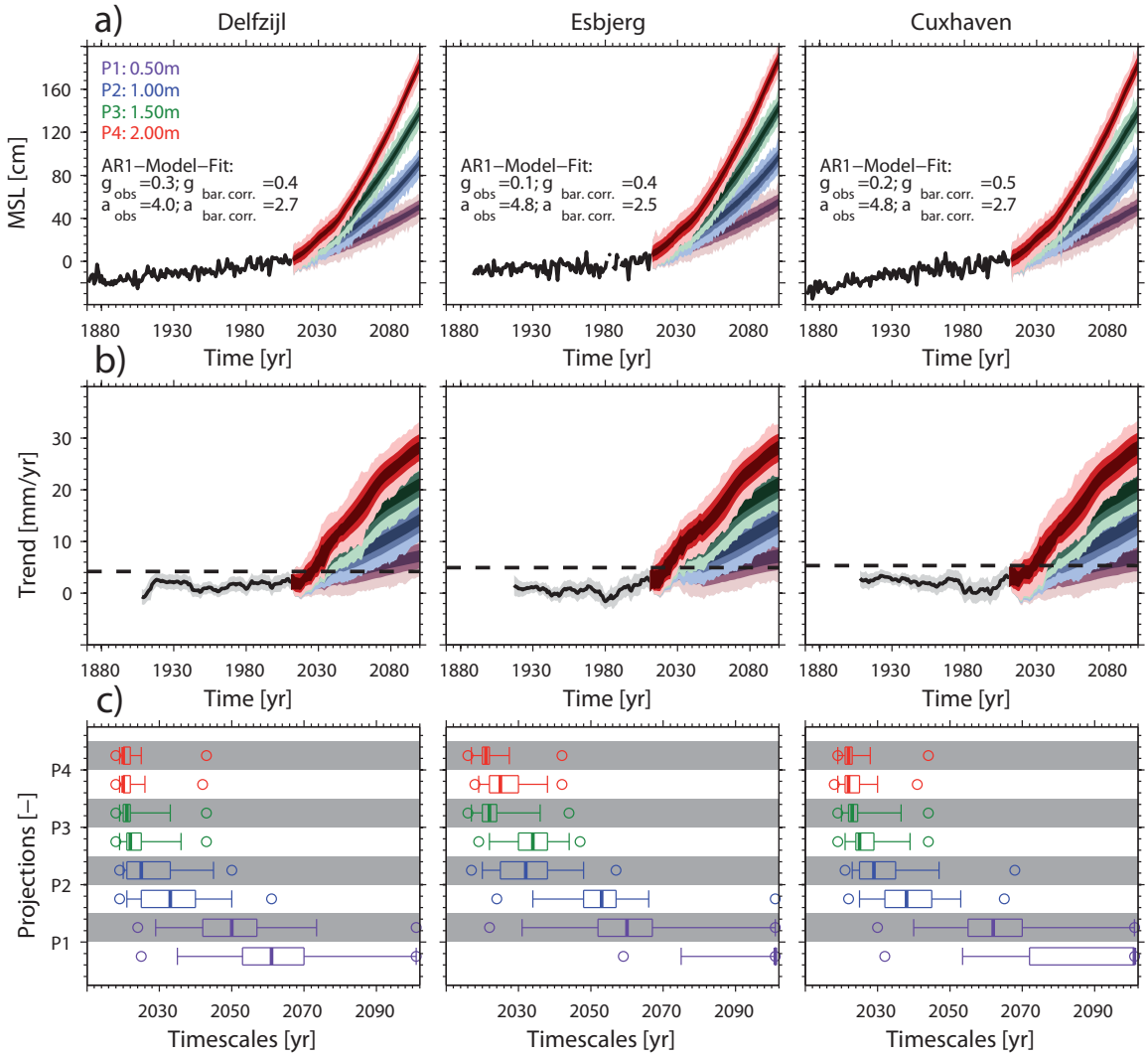

Figure 4-11: a) Observed annual MSL (black) for three different locations together with four artificial projections (P1, P2, P3, P4). Each projection is combined with 1000 time series of artificial noise, as simulated on the basis of an AR1 model. The different color shades contribute to different percentiles (100, 95 75, 50, 25 5, 0) of the 1000 artificial time series per projection. Estimates of the two AR1 parameters g (lag-1 autocorrelation) and a (noise variance) are also shown. b) 37 year moving trends for the observations (black and grey shading) and as estimated with the different artificial projections. Again the color shade is related to the percentiles of the full set of 1000 time series. c) Boxplots (100, 95 75, 50, 25 5, 0) of the years in which a significant acceleration can be detected for the four different projections relative to the historic observations. The white shading marks the results using realistic noise for the observed time series, while the grey shading represents the boxplots for realistic noise based on time series which have been corrected for local atmospheric forcing.

The large influence of atmospheric (barotropic) forcing on the shallow continental shelf area decouples the North Sea on intra- and inter-annual timescales from surrounding are-

as, resulting in low correlations for example with stations in the English Channel (Wahl et al., 2013). On decadal timescales, on the other hand, the coherence between the different stations in the basin is much higher (suggesting a common forcing mechanism) and the barotropic response of the ocean to local SLP and wind stress forcing becomes negligible. Since the North Sea is mostly shallow (with water depths below 100 m), the steric height calculated locally can also not account for the remaining fluctuations. Therefore we have estimated the steric component exemplary for the Norwegian Trench, where the water depth is large enough to give a significant steric signal. We found that the variations in the steric height agree well with the local MSL especially on longer time scales. Given the spatial coherence on these time scales we conclude that this result can be taken to be representative for the entire basin. The question that remains is where these steric MSL changes are triggered?

To answer this question, we have explored the coherence of North Sea MSL on decadal scales with the surrounding seas and found a band of coherent MSL variability extending from the Norwegian coastline along the eastern boundary down to the Canary Islands. This coherency suggests a common forcing and fits well with the theory of longshore winds as also proposed in recent studies by Sturges and Douglas (2011), Calafat et al. (2012, 2013a, b) and Marcos et al. (2013). These longshore winds cause a displacement of the thermocline leading to coastally trapped waves which propagate with the coast on the right (in the northern hemisphere) further northward. Complementary to the above-mentioned studies, we find evidence that the signal propagates on its way north into the North Sea region. Generally, the waves appear to be caused in the region south of 45 N by changes in the strengths of the prevailing anti-cyclonic circulation (around the Azores High) (e.g. Sturges and Douglas, 2011). Our results imply that the decadal local MSL variability in the North Sea represents a combination of propagating waves triggered at different latitudes. For instance, the highest dependencies are found between the atmospherically corrected North Sea MSL and the steric height in the Gulf of Biscay and especially the region west of the UK. As previously described e.g. by Orvik and Skageseth (2003) and Richter et al. (2009), the inflow of Atlantic waters into the Nordic Seas is strongly governed by low pressure systems with prevailing westerly to southwesterly winds and subsequent baroclinic adjustment processes in the ocean. If we combine the IBE corrected local MSL in Newlyn with the steric height west of the UK, we can explain ~79 % of the decadal variability demonstrating the dominance of the propagating signal on decadal and multi-decadal timescales.

The origin of this variability has important implications for developing future MSL projections in the region, since the signals described in the present study are superimposed onto the longer-term changes. Such decadal scale fluctuations can cause coastal MSL to exceed a certain threshold, even only for a few years, much earlier than the time expected for the global mean to cross the same threshold. Additionally, due to the coarse resolution of the ocean component, most global climate models in the AR5 are not able to resolve the described processes on the shallow continental shelf. Given the mostly baroclinic nature of the signal with a Rossby radius of about 20 km or less (Gill, 1982), it is clear that the zonal resolution of the most models (1° (~100 km) or larger) is too coarse. Hence,

statistical or dynamical downscaling techniques (e.g. von Storch et al., 1993; Dangendorf et al., 2013b, chapter 5 of this thesis) may represent a valuable tool to overcome these resolution problems. The finding that the decadal scale variability in the North Sea has its origin (at least partly) in baroclinic adjustment processes of the ocean in the North Atlantic further gives important information on the boundary conditions for the regional models generally used for dynamical downscaling.

Besides their influence on the temporal variability, it is also of interest to examine how much local atmospheric component contributes to 20th Century MSL trends at each site (Figure 4-12). The atmospheric component, ξ_{atm}, shows local differences up to 0.4 mm/yr between the individual sites (Figure 12). Wahl et al. (2013) also pointed to distinctive spatial differences in rates of SLR in the North Sea and suggested that these were mainly related to uncertainties in the estimates of VLMs. The results presented here show that local atmospheric forcing also affects the spatial trend patterns of local MSL and should therefore be removed before any VLM analysis in the region.

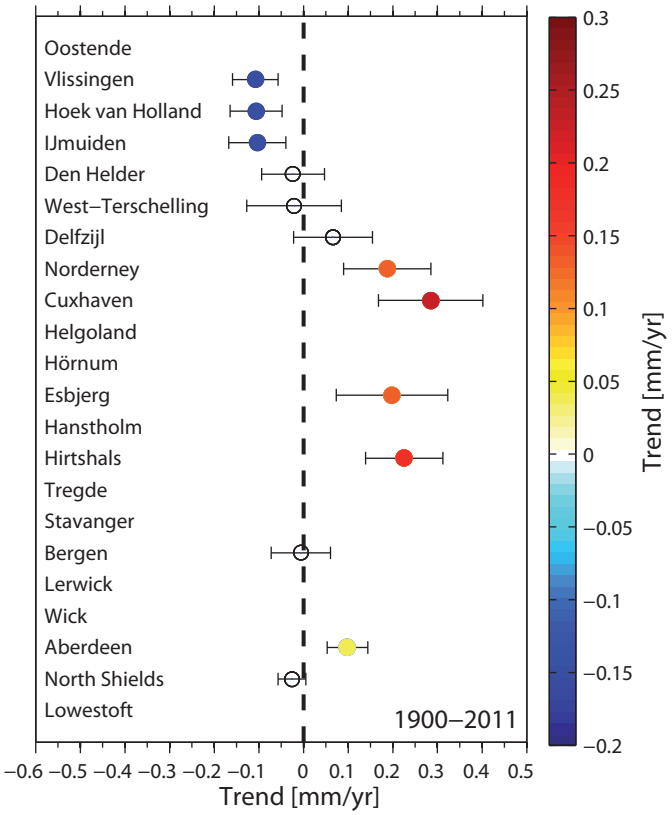

Figure 4-12: Linear trends ±2σ SE of the atmospheric contribution to MSL over the period 1900 to 2011. Only those trends are shown, where at least 75 % of the data was available. Statistically significant trends (95 % confidence level) are marked by a colored dot.

We further analyzed the role of local atmospheric forcing on the estimation of long-term trends and acceleration/deceleration patterns using a combination of observations and a set of artificially generated time series. The important finding from these analyses is that atmospheric forcing (dominating local MSL variability on intra- and inter-annual timescales) is the main factor controlling the signal to noise ratio in the time series. This has two significant implications:

The accuracy of the linear long-term trend strongly depends on whether the atmospheric correction has been applied or not. Removing known parts of variability leads to more robust trend estimates and hence shorter time series can be included in studies focusing on long-term trends. This finding is most relevant for areas where only short records exist (see also Dangendorf et al., 2013a, chapter 3 of this thesis). The effect of removing the known variability in the North Sea is largest in the wind-dominated areas, where the inter-annual variability is more pronounced.

The removal of atmospherically induced MSL variations increases the signal to noise ratio and therefore allows earlier detection of possible SLR accelerations (here up to 50 years depending on the location and the projection and compared to using uncorrected time series), as projected under a warming climate.

The later point is important for coastal planning and safety management. Today anthropogenic climate change represents one of the major global challenges and coastal societies are discussing major investments in order to adapt to climate change. Local authorities need to know as early as possible how much SLR is likely to be expected over the next decades in order to prevent coastal flooding. The earlier we identify which climate change pathway the Earth's climate system is following and how much SLR might be expected, the better we can adapt to it. Hence, we strongly recommend applying the atmospheric correction to the data in the region before estimating linear trends or possible accelerations.

5 A new atmospheric proxy for sea level variability in the southeastern North Sea: observations and future ensemble projections

5.1 Abstract

Atmosphere-ocean interactions are known to dominate seasonal to decadal sea level variability in the southeastern North Sea. In this chapter an atmospheric proxy for the observed sea level variability in the German Bight is introduced. Monthly MSL time series from 13 tide gauges located in the German Bight and one virtual station record are evaluated in comparison to SLP fields over the North Atlantic and Europe. A quasi-linear relationship between MSL in the German Bight and SLP over Scandinavia and the Iberian Peninsula is found. This relationship is used (i) to evaluate the atmospheric contribution to MSL variability in hindcast experiments over the period from 1871-2008 with data from the 20CRv2, (ii) to isolate the high frequency meteorological variability of MSL from longer-term changes, (iii) to derive ensemble projections of the atmospheric contribution to MSL until 2100 with eight different coupled global atmosphere-ocean models (AOGCM's) under the A1B emission scenario and (iv) two additional projections for one AOGCM (ECHAM5/MPI-OM) under the B1 and A2 emission scenarios. The hindcast produces a reasonable good reconstruction explaining approximately 80 % of the observed MSL variability over the period from 1871 to 2008. Observational features such as the divergent seasonal trend development in the second half of the twentieth century, i.e. larger trends from January to March compared to the rest of the year, and regional variations along the German North Sea coastline in trends and variability are well described. For the period from 1961 to 1990 the Kolmogorov-Smirnow test is used to evaluate the ability of the eight AOGCMs to reproduce the observed statistical properties of MSL variations. All models are able to reproduce the statistical distribution of atmospheric MSL. For the target year 2100 the models point to a slight increase in the atmospheric component of MSL with generally larger changes during winter months (October to March). Largest MSL changes in the order of ~5-6 cm are found for the high emission scenario A2, whereas the moderate B1 and intermediate A1B scenarios lead to moderate changes in the order of ~3 cm. All models point to an increasing atmospheric contribution to MSL in the German Bight, but the uncertainties are considerable, i.e. model and scenario uncertainties are in the same order of magnitude.

5.2 Introduction

MSL is an important environmental variable with considerable impact on coastal communities. Particularly in face of a warming climate, sea level is expected to rise throughout the 21st century, probably at accelerated rates. Hence, for coastal planners the knowledge about possible future SLR is of special importance, as it provides information for impacts and possible management strategies, including the upgrade of coastal structures. This is why in the recent past a growing number of scientists have tried to evaluate projections of SLR on regional (e.g. Lowe et al., 2009; Katsman et al., 2008, 2011; Slangen et al., 2012) and global scales (Meehl et al., 2007; Nicholls et al., 2011 and references therein) and under different climate change scenarios.

These projections are based on the present day knowledge about the different processes affecting sea level on various temporal and spatial scales. When assessing secular trends sea level may vary due to steric (i.e. the expansion/contraction of the ocean due to variations in temperature or salinity) or mass changes (i.e. melt water contributions from land ice or freshwater from land hydrology). However, superimposed on these secular changes on timescales up to a few decades internal climate variability may affect sea level due to changes in atmospheric forcing (e.g. Firing and Merrifield, 2004; Miller and Douglas, 2007; Nerem et al., 2010; Bromirski et al., 2011; Merrifield and Maltrud, 2011; Calafat et al., 2012; Calafat et al., 2013b) i.e. the redistribution of water masses due to wind forcing or associated upwelling/downwelling processes and the hydrostatic response of sea level to variations in regional SLP, widely known as the IBE. While the majority of recent sea level projections focused on the impacts of global warming (i.e. steric effects or added mass), Ponte (2006) and Stammer and Hüttemann (2008) have shown that especially on regional scales and time scales of several decades the IBE alone may contribute to sea level changes in the same order as land movements as result of GIA. Furthermore, a number of recent studies emphasized the importance of wind stress in forcing spatial and temporal differences in sea level trends and variability (Bromirski et al., 2011; Merrifield and Maltrud, 2011; Sturges and Douglas, 2011; Albrecht and Weisse, 2012; Dangendorf et al., 2012, 2013a, chapter 2 and 3 of this thesis).

There are some regions in the world that are particularly affected by changes in the atmosphere, for example the North and Baltic Sea region (Heyen et al., 1996; Hünicke et al., 2008; Albrecht and Weisse, 2012; Dangendorf et al., 2013a chapter 3 of this thesis), the Northeast Pacific coastlines (Merrifield and Maltrud, 2011), the Mediterranean Basin (Tsimplis and Josey, 2001; Marcos and Tsimplis, 2007), the eastern North Atlantic (Sturges and Douglas, 2011; Calafat et al., 2012), or the Arctic Ocean (Proshutinsky et al., 2007; Calafat et al. 2013). The focus of the present chapter is on the southeastern North Sea, more precisely on the German Bight. The North Sea is a shallow shelf sea at the eastern boundary of the North Atlantic. The dominant atmospheric mode in the region is the NAO influencing weather patterns especially during winter months (Hurrel, 1995). The NAO can be defined as the difference of pressure anomalies between southern Iceland and the Azores. In positive phases the NAO brings warm and wet air together with a strong westerly flow over Northern Europe, leading to positive MSL anomalies along

Northern European coastlines (Woolf et al., 2003). The NAO influences MSL through different coupled processes, such as the IBE, zonal wind stress forcing or precipitation (Suursaar and Sooäär, 2007). In the German Bight a positive NAO phase between the 1960s and mid-1990s lead to anomalous larger MSL trends during winter exceeding trends of the remaining seasons by up to 3 to 4 mm/yr (Dangendorf et al., 2012, chapter 2 of this thesis). The majority of MSL variability in the German Bight is related to zonal wind stress forcing. It explains up to ~90 % of the observed variability during winter season, whereby SLP and precipitation also contribute a statistically significant but even though smaller part (Dietrich, 1954; Dangendorf et al., 2013a, chapter 3 of this thesis).

Two different approaches are available for the estimation of the atmospheric contribution to SLR and variability. The most accurate way would be to analyze the outputs of two- or three dimensional (hereafter 2D and 3D) coupled barotropic or baroclinic ocean-atmosphere models (such as HAMSOM) for the separation of wind and pressure effects. The models are generally driven by oceanographic and meteorological forcing parameters (e.g. tides, temperature, salinity, wind and SLP) at the model boundaries. In Europe much effort in developing such models has gone into models of the Mediterranean (e.g. Somot et al., 2006; Gomis et al., 2008; Jorda et al., 2012) and the North Sea basin (e.g. Langenberg et al., 1999; Weisse and Pluess, 2008). However, these models are computationally very expensive (with computation times for century scale simulations depending on the region and the required accuracy of the bathymetry of several days/weeks for 2D barotropic and several months/years for 3D baroclinic models) making it difficult to perform analyses of a larger numbers of climate change scenarios, especially under the consideration of the outputs of different climate models. This disadvantage can be overcome by following the second approach, i.e. using statistical-empirical relationships between atmospheric and oceanographic variables for multiple LRMs (Heyen et al., 1996; Hünicke et al., 2008). These models are computationally considerably cheaper (with computation times for century scale simulations of several seconds or minutes) and therefore well placed for the evaluation of larger numbers of scenarios derived with different climate models.

In the present chapter a simple atmospheric proxy for MSL variability in the German Bight is introduced. The proxy is used (i) to examine the contribution of atmospheric forcing to MSL variability during the period from 1871 to 2008, (ii) to isolate the high frequency meteorologically induced variability of MSL from longer-term changes and (iii) to project the atmospheric contribution to MSL variability under three different climate change scenarios by statistically downscaling the output of eight different climate models. The paper is organized as follows. The considered data sets and applied methods are described in detail in the following Section 5.3. The results are presented and discussed in Section 5.4. This section is further split into four subsections discussing (i) the ability of the proxy to reconstruct typical features of atmospherically induced MSL changes as known from the literature, (ii) the timescales needed for adequately reproducing past MSL changes with the presented proxy, (iii) the ability of the AOGCM's in adequately simulating observed MSL changes, and (iv) changes in the atmospheric component of MSL under changing green-

house gas emissions until the target year 2100. The paper closes with concluding remarks given in Section 5.5.

5.3 Data and methods

5.3.1 Data

Monthly MSL time series from 13 tide gauges located in the German Bight are used (Figure 5-1). The time series were reconstructed as part of the AMSeL project (Wahl et al., 2010, 2011) and provide a spatially good coverage of the German Bight. The longest record covers a period of 166 years from 1843 to 2008. While Wahl et al. (2010, 2011) and Albrecht et al. (2011) focused on annual MSL time series, the monthly data sets were analyzed for the first time by Dangendorf et al. (2012, 2013a, chapter 2 and 3 of this thesis, 2013c). All records were extensively checked for systematic errors and local datum shifts. Additionally, a virtual station for the period from 1871 to 2008 that is representative of the entire German Bight is computed by following the approach used by Wahl et al. (2011). Rates of monthly MSL change rather than time series with different datum reference are averaged to form one common signal (Jevrejeva et al., 2006). This approach aims at solving the sampling problem of sea level time series from different tide gauges with varying reference levels.

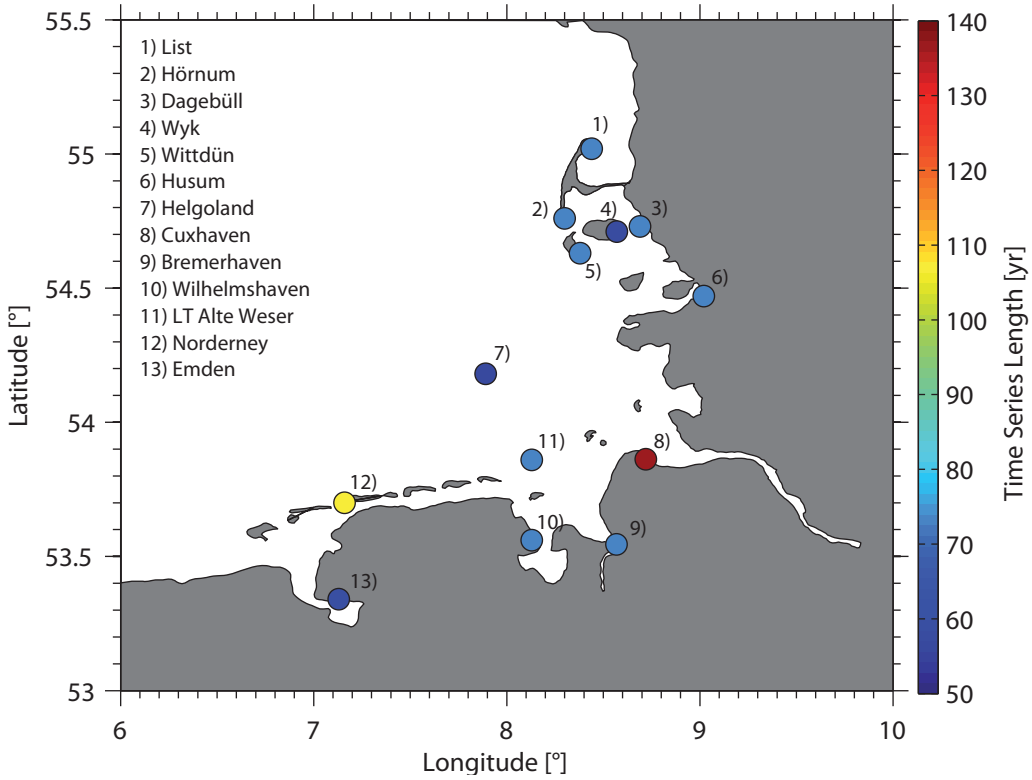

Figure 5-1: Investigation area of the German Bight and tide gauge locations. The names of the tide gauges are listed in the figure. The colorbar defines the availability of data in years until 2008.

A key issue of the present chapter is the presentation of an atmospheric proxy for MSL variability in the German Bight that is validated for the observation period of tide gauges. A common database for establishing links between atmospheric and oceanographic vari-

ables is to analyze atmospheric fields from reanalysis products over the past century. The newest available reanalysis product is the 20CRv2 provided by the National Oceanographic and Atmospheric Administration (NOAA) in Boulder, Colorado. The 20CRv2 extends earlier reanalysis products (Kalnay et al., 1996; Uppala et al., 2005) back into the 19th century and covers a period from 1871 to 2010 (Compo et al., 2011). Reanalysis fields are computed by assimilating observational data over a specified period. The 20CRv2 was generated by assimilating observations of SLP, sea surface temperature and sea ice as boundary conditions. Since the availability of assimilated data has improved over time, the homogeneity of the reanalysis data is suggested to be higher for the last decades compared to earlier periods before 1950. For example, Krüger et al. (2012) pointed to considerable differences between storminess trends from observational and reanalysis data over the North Sea. However, they have focused on trends of high percentiles and Dangendorf et al. (2013a, chapter 3 of this thesis) have shown that the mean monthly atmospheric variability over the southeastern North Sea is better represented back to the 19th century. Additionally, the present investigations focus on variability patterns. Hence, in the present case the trend bias in the 20CRv2 can be neglected.

Table 5-1: Climate models and available scenarios used in the present chapter.

Model	Institution, Country	Period	Forcings
BCM2	Bjerknes Centre for Climate Research, Norway (Furevik et al., 2003)	1950-2099	C20, AIB
CNCM3	Centre National de Recherches Meteorologiques, France (Salas-Melia et al., 2005)	1950-2100	C20, AIB
DMIEH5	Danish Meteorological Institute, Denmark (Junglcaus et al., 2006)	1950-2100	C20, AIB
EGMAM	Institute for Meteorology, FU Berlin, Germany (Huebener et al., 2007)	1950-2099	C20, AIB
HADGEM	Met Office, UK (Johns et al., 2006)	1950-2099	C20, AIB
HADCM3	Met Office, UK (Gordon et al., 2000)	1950-2100	C20, AIB
IPCM4	Institut Pierre Simon Laplace, France (Marti et al., 2005)	1950-2100	C20, AIB
MPEH5	Max-Planck-Institute for Meteorology, Germany (Junglcaus et al., 2006)	1950-2100	C20, B1, AIB, A2

For projecting the atmospheric component of MSL into the future, an assessment of monthly SLP fields from eight coupled Atmosphere-Ocean Global Circulations Models (AOGCM's) is carried out. The model data are available from the CERA database, maintained by the Model and Data group at the Max-Planck-Institute in Hamburg, Germany. Most models used in the present chapter are part of the ENSEMBLE project (Ensemble based predictions of climate change and their impacts, Niehörster et al., 2008 and Van der Linden and Mitchell, 2009). Additional runs were chosen, because they play an important role in climate impact research in Germany (e.g. Jacob et al., 2008; Nilson et al., 2010). Recently, these model runs were used for an assessment of climate change impacts in Germany within the KLIWAS program. For that purpose all models were transformed from different original global grids on a common regional rotated grid (Krahe et al.,

2011). For all models the first run of the 20th century (C20) experiments from 1950 to 2000 and one run for the 21st century from 2001 to 2100 (mostly using emission scenario A1B) are evaluated here. Background information on the models and their representation of different greenhouse gas emission scenarios is given in Table 5-1.

5.3.2 Methods

With respect to the first objective of the chapter, i.e. reconstructing observed changes in the atmospheric contribution to MSL over the period from 1871 to 2008, a link between large-scale atmospheric pressure and MSL anomalies in the German Bight is established. For that purpose, monthly MSL anomalies (i.e. linearly detrended and deseasonalized) from the virtual station time series of the German Bight are correlated with gridded SLP anomalies from the 20CRv2 data over the larger geographic area from 40W to 40E and 20N to 80N (Figure 5-2a). The correlations point to a strong negative relationship between MSL in the German Bight and SLP over Scandinavia and a significant positive connection to SLP over the Iberian Peninsula. This correlation pattern reflects the strong zonal flow over the North Sea leading to a dominant influence of zonal wind stress on sea level variability in the German Bight (Heyen et al., 1996; Dangendorf et al., 2013a, chapter 3 of this thesis), explaining a considerable fraction of the observed variability (Figure 5-2b).

The dominant influence on sea level variability can be related to persistent winds blowing over the North Sea basin, driving a counterclockwise circulation (e.g. Sündermann and Pohlmann, 2011) and piling up the water at the southeastern coastlines (Wakelin et al., 2003). This is demonstrated by the composite plot shown in Figure 5-3. During months of particular high MSL (> 2 standard deviations) negative SLP anomalies over Scandinavia together with prevailing westerly winds over the North Sea basin are observed. In phases of particular low MSL anomalies (< 2 standard deviations) the situation turns to the opposite with an increased easterly flow. Since the German Bight is a very shallow part of a shelf sea with water depths less than 10 m in near coastal areas and has a high tidal range between three to four meters and surges up to over four meters, this area is mostly well mixed without strong thermohaline stratification. Hence, upwelling processes and resulting changes in sea level are a transient phenomenon limited to a small area around Helgoland during the summer months (Becker et al., 1992). Also the IBE plays only a minor role for MSL variability in that region (Wakelin et al., 2003; Dangendorf et al., 2013a, chapter 3 of this thesis). Hence, the proxy mainly represents the effects of wind stress forcing and the resulting pile-up of water in the German Bight.

Here both centers of action in the SLP fields are used for introducing an atmospheric proxy for sea level variability in the German Bight. The atmospheric proxy consists of two time series; the first principal component (PC) of SLP anomalies over Scandinavia (14E to 22E, 60N to 66N) and the first PC of SLP anomalies over Iberian Peninsula (10W to 0E, 40N to 44N), both estimated over the entire period from 1871 to 2008. The first PC's account in both areas for more than 98 % of the observed variability and are therefore suitable for representing both SLP centers of action.

To assess the potential of the atmospheric proxy for the explanation of sea level variability in the German Bight the following multiple LRM is used:

$$\xi = a + b * SLP_{SC}(t) + c * SLP_{IB} + \varepsilon \quad (5\text{-}1)$$

where *a*, *b* and *c* are the regression coefficients and ε is an error term.

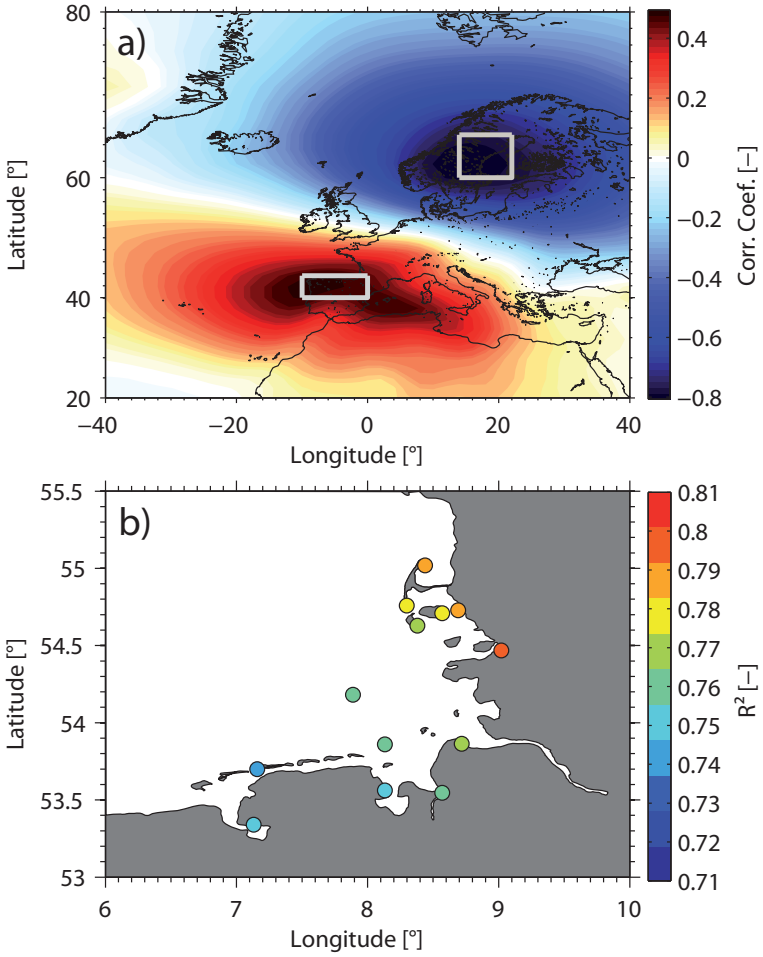

Figure 5-2: a) Correlation map between MSL from the virtual station German Bight and gridded SLP over the North Atlantic and European region. The two centers of action used for the proxy are shown with the two white squares b) Coefficient of determination for the reanalysis of monthly MSL at 13 stations in the German Bight.

While the MSL anomaly time series from each tide gauge (and the virtual station) is used as the dependent variable, time series of the first PC's of SLP anomalies (SLP_{SC} for Scandinavia and SLP_{IB} for the Iberian Peninsula) are employed as forcing parameters. The regression coefficients in equation 5-1 are estimated with detrended and deseasonalized time series. For assessing the influences of long-term changes due to atmospheric forcing, the estimated regression coefficients are later applied to non-detrended time series including also observed seasonal variations. All regression coefficients are estimated on the basis of the full available period of tide gauge data and the 20CRv2 SLP fields (see Table 5-2 and Figure 5-1 for the available periods). This implies the assumption of a stationary behavior of the centers of correlation. To test this assumption, the correlation analysis has been repeated decade by decade from 1871 to 2008 (Figure 5-4). The centers of high correlation remained relatively stationary, also during the 1980's and 1990's, a period which is known to be marked by an extraordinary high atmospheric variability in the region

(Hurrel, 2003). This analysis confirms the assumption of stationarity. Nevertheless, an extrapolation of this assumption onto climate change projections of two to four degrees temperature change can only be finally verified by numerical simulations, a step which should be further examined in future studies.

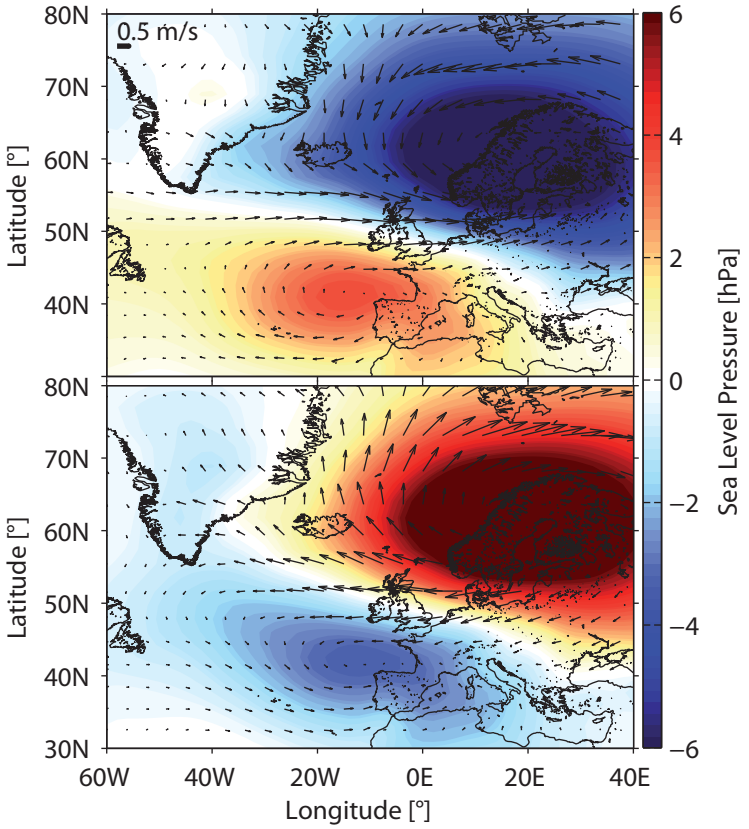

Figure 5-3: Composite plot showing the mean of SLP (contour) and wind (arrows) anomalies during periods of particular a) high (> 2 standard deviations) and b) particular low (< 2 standard deviations) (detrended) MSL at the virtual station of the German Bight.

First, the influence of atmospheric forcing on MSL variability over the period from 1871 to 2008 is investigated. It is analyzed (i) whether typical features of atmospherically induced MSL changes are adequately represented by the proxy and (ii) how many years of data are required for estimating the regression coefficients to a specified level of accuracy. After establishing the link between atmospheric forcing and sea level variability for the past, the ability of different climate models to reproduce MSL variability is tested for the climate period from 1961 to 1990. This is done by comparing modeled-MSL downscaled from the AOGCM's with the reference truth taken from the 20CRv2 reanalysis and tide gauge data for the hindcast period. To do so, the first PC's of SLP over Scandinavia and Iberian Peninsula are extracted from each AOGCM and used as forcing parameters for the regression model from equation 5-1. As a measure of the statistical significance, the Kolmogorov-Smirnow test (KS-test) is applied. The KS-test is a nonparametric test for the equality of continuous, one-dimensional probability distributions. It examines whether two samples are drawn from the same statistical population by measuring the distance between the empirical distributions of both samples:´

$$D_{KS} = \max_{x} \left| F_x(x) - F_y(x) \right| \qquad (5\text{-}2)$$

Large distances between both cumulative distributions *Fx (x)* and *Fy (x)*) indicate inconsistencies between the hindcasted (i.e. based on 20CRv2 data) and modeled data (i.e. based on AOGCM data) (von Storch and Zwiers, 1999).

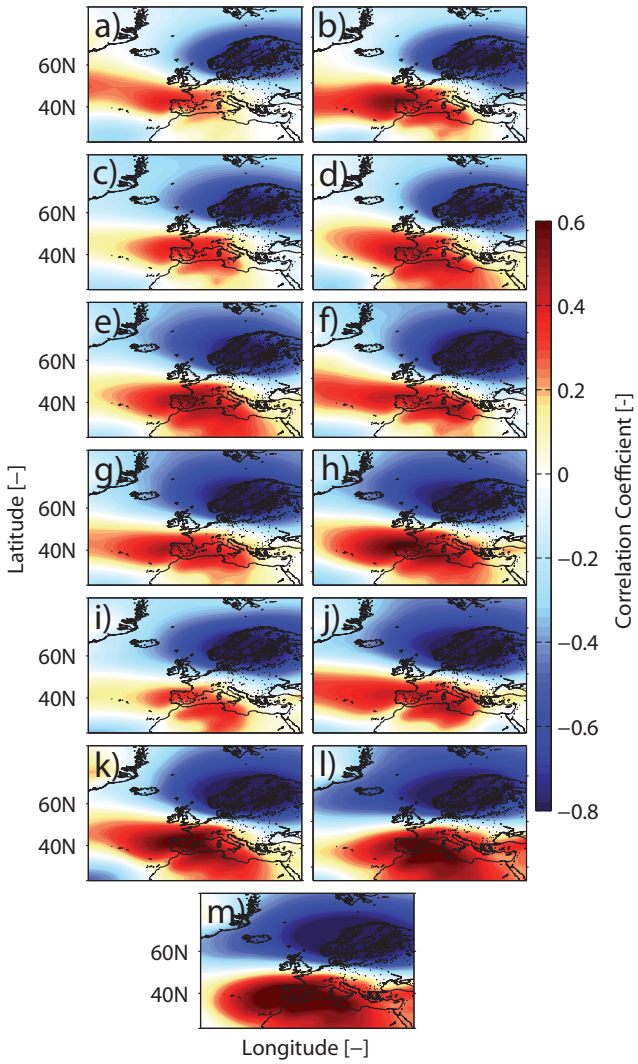

Figure 5-4: Decadal correlation maps between MSL in the German Bight (virtual station) for the periods from a) 1871 to 1980, b) 1881 to 1890, c) 1891 to 1900, d) 1901 to 1910, e) 1911 to 1920, f) 1921 to 1930, g) 1931 to 1940, h) 1941 to 1950, i) 1951 to 1960, j) 1961 to 1970, k) 1971 to 1980, l) 1981 to 1990 and m) 1991 to 2000.

The models are then used for projecting future changes in the MSL variability due to atmospheric forcing (i.e. the second objective of the chapter) by applying the regression coefficients from equation 5-1 to the outputs of the AOGCM's for the 21st century. The projected time series are investigated by estimating linear trends and moving averages for the modeled period from 2001-2100. Uncertainties related to the trend estimates are given as SEs considering that the residuals are serially correlated (Santer et al., 1999). This approach accounts for temporal correlation of the residuals by replacing the number of degrees of freedom by an effective sample size N_E based on the lag-1 autocorrelation coefficient r_1 and can be computed by using the formula:

$$N_E = N_t \frac{1 - r_1}{1 + r_1} \tag{5-3}$$

If not stated otherwise, the SEs are computed on the 95 % confidence level.

When investigating climate change projections different sources of uncertainty have to be discussed (Niehörster et al., 2008). Here, the focus is on the scenario (Nakicenovic et al., 2000) and model uncertainty (Palmer et al., 2005). Further uncertainties result from the internal climate variability within the models (Selten et al., 2006). This can be investigated by evaluating ensemble runs from each individual model. Imperfections in observation data can be evaluated using different observation data products. These are not further discussed in this paper.

1. The scenario uncertainty results from the assumption of a specified greenhouse gas emission scenario. Different emission scenarios for various time periods were defined in the Special Report on Emission Scenarios (SRES) (Nakicenovic et al., 2000). These scenarios are uncertain per definition, since they assume an unknown development of human society, economy and political decisions. To assess this uncertainty, model outputs from the ECHAM5/MPI-OM (MPEH5 hereafter, see alsoTable 5-1) are evaluated for the three SRES scenarios B1, A1B and A2, providing a wide range of possible pathways. SRES B1 assumes a “sustainable world” with rapid changes in economic structures, dematerialization and a global population reaching 7 billion people until 2100, i.e. B1 characterizes a low emission scenario. The A1B scenario supposes moderate greenhouse gas emissions and can be described by a “rich world” indicating a very rapid economic growth with new efficient technologies. As a high-end scenario the SRES A2, also denoted as “separated world”, is used. The A2 scenario is based on a more heterogeneous world with strong regional cultural differences.
2. Model uncertainties result from a limited theoretical understanding of underlying processes, uncertainties in model parameters and the inability to describe known processes accurately in the model (Knutti et al., 2011). These uncertainties are considered by investigating the outputs from eight different AOGCM’s under the SRES A1B.

5.4 Results and discussion

5.4.1 MSL hindcast (1871-2008)

An essential step of this chapter is to examine whether the atmospheric proxy represents a reliable measure of the atmospheric contribution to MSL variability over the period from 1871 to 2008. The regression coefficients and the coefficients of determination for the 13 tide gauge and the virtual station records are presented in Table 5-2 and Figure 5-2b. The explained variances (for the time series including the seasonal cycle) vary between a minimum value of 72 % (Norderney) in the southwestern part and a maximum value of 81 % (Husum) in the northeastern part of the German Bight. Hence, the majority of the observed variability is captured by the atmospheric proxy. The spectra of monthly MSL (Figure 5-5) shows, that the observed time series are dominated by the annual cycle with amplitudes between approximately 9 and 13 cm, increasing from the southwestern to the northeastern stations (Figure 5-5). This feature has recently been described by Dangen-

dorf et al. (2012 chapter 2 of this thesis) and has been attributed to the exposure of north-easterly located tide gauges against westerly winds, which are predominant in the region (Dangendorf et al. 2013a, chapter 3 of this thesis). The fact that the explained variances increase in a similar manner along the coastline show that the atmospheric proxy is able to picture this feature adequately. The spectra of the hindcasted MSL records follow the spectra of observed MSL time series closely up to periods of approximately 18 years (Figure 5-5). For longer periods the explanatory power of the atmospheric proxy is much smaller, indicating that on multi-decadal time scales other forcing factors such as integrated longshore winds over the North Atlantic Ocean (Calafat et al., 2012; Calafat et al., 2013; Dangendorf et al., 2014b, chapter 4 of this thesis) or westward propagating temperature anomalies (Francombe and Dijkstra, 2009) may become more influential.

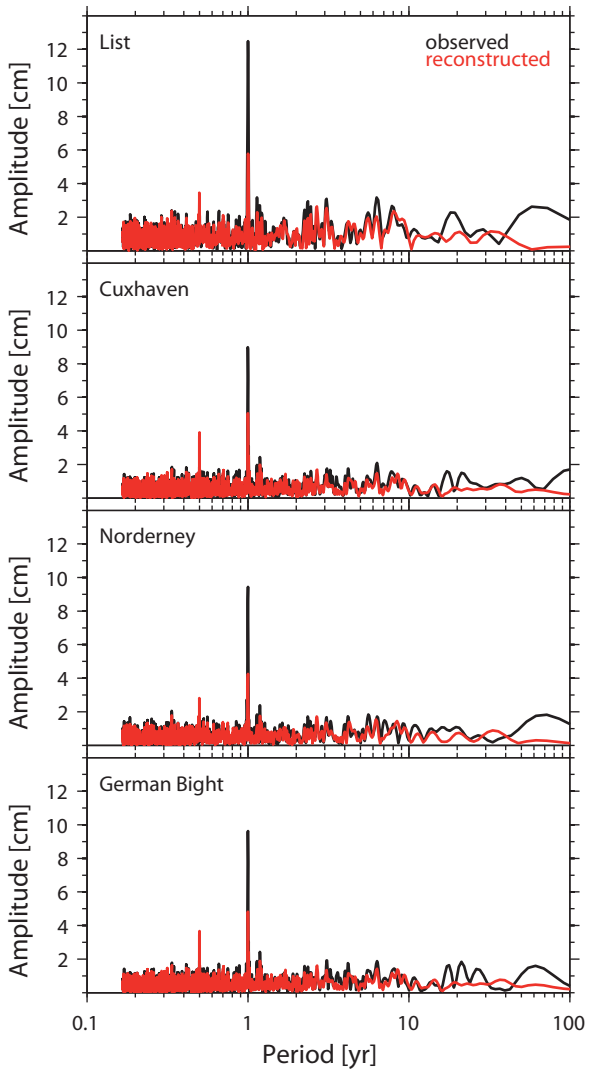

Figure 5-5: Spectra of monthly MSL for observed (black) and reconstructed (red) time series.

Figure 5-6 maps seasonal MSL trends for the original observations and the atmospherically corrected records (i.e. observations minus atmospherically induced MSL) in the German Bight from 1951 to 2008. It shows a divergent development of seasonal MSL through the second half of the 20th century, that also represents a known feature of monthly MSL time series in the German Bight (Langenberg et al., 1999; Marcos and Tsimplis,

2007; Dangendorf et al., 2012, chapter 2 of this thesis). Dangendorf et al. (2013a, chapter 3 of this thesis) has recently shown that this development can be attributed to a phase of particular high zonal flow over the North Atlantic European sector between the beginning of the 1960s and the mid-1990s. This resulted in more frequent and more intense south-westerly to westerly winds (see also Siegismund and Schrum, 2001) influencing amplitudes as well as phases of the seasonal MSL cycle in the region of interest. It is reflected by differing seasonal trends in the observed time series over the period from 1951 to 2008, as shown in Figure 6a. Boreal winter (January to March; JFM) trends are approximately double the annual trends at each station, while boreal summer (July to September; JAS) trends are approximately 1 mm/yr smaller than the annual mean. The SEs (here 1σSE), represented as error bars in Figure 5-6, are also considerably larger for winter compared to summer, the entire year, and the remaining seasons (not shown). When subtracting the atmospheric component -thus isolating the slow tectonic/climate component- from the observed MSL time series, the calculated seasonal trends become much more similar and the associated SEs are notably reduced.

Table 5-2: Results of the regression fits for tide gauge records in the German Bight and the atmospheric proxy for the full available time periods. All estimated regression coefficients are statistically significant on the 95 %-confidence level.

Tide gauge	Available period	Regression Coefficients			Coefficient of Determination
		a [-]	b [-]	c [-]	R^2 [-]
List	1937-2008	0.12	-0.49 (±0.02)	0.28 (±0.04)	0.76
Hörnum	1937-2008	0.12	-0.49 (±0.02)	0.28 (±0.04)	0.76
Dagebüll	1937-2008	0.23	-0.53 (±0.02)	0.33 (±0.04)	0.78
Wyk	1951-2008	-0.01	-0.51 (±0.03)	0.29 (±0.04)	0.78
Wittdün	1937-2008	0.2	-0.48 (±0.02)	0.27 (±0.04)	0.75
Husum	1937-2008	0.22	-0.52 (±0.02)	0.31 (±0.04)	0.81
Helgoland	1953-2008	0.11	-0.41 (±0.02)	0.21 (±0.04)	0.75
Cuxhaven	1871-2008	0	-0.46 (±0.02)	0.31 (±0.03)	0.75
Wilhelmshaven	1937-2008	0.2	-0.44 (±0.02)	0.32 (±0.04)	0.75
Bremerhaven	1937-2008	0.17	-0.40 (±0.02)	0.25 (±0.04)	0.74
LT Alte Weser	1935-2008	0.15	-0.41 (±0.02)	0.24 (±0.04)	0.74
Norderney	1900-2008	-0.04	-0.40 (±0.02)	0.22 (±0.04)	0.72
Emden	1949-2008	-0.07	-0.41 (±0.02)	0.25 (±0.04)	0.76
German Bight	1871-2008	0	-0.44 (±0.02)	0.28 (±0.04)	0.75

The remaining annual trends at the individual sites vary closely around a mean trend of about 2 mm/yr at the virtual station record. The only exceptions are the tide gauge records from Bremerhaven and Emden, which show considerably smaller trends. The tide gauges are located in the Weser and Ems estuaries, which were both subject to extensive coastal engineering works throughout the second half of the 20th century. As a result of man-made interventions, e.g. deepening of shipping channels, the tidal characteristics at these locations changed. Consequently, tidal low water levels decreased in relation to the tidal highs and also resulted in smaller MSL values (and trends) at these stations (Jensen et al., 2003). Hence, both sites are well suited for variability studies, but one has to be careful when analyzing their long-term trends. Overall, the reduction of the trends and SEs as

shown in Figure 5-6 is in a similar order as reported by Marcos and Tsimplis (2007), who used a hydrodynamic-numerical model for the estimation of atmospheric effects on MSL trends in the larger North Atlantic and Mediterranean region. Although Marcos and Tsimplis (2007) analyzed a different time period (i.e. 1960 to 2000), the magnitude of the trend reduction is quite similar. Marcos and Tsimplis (2007) provided a common estimate of the atmospheric contribution for the whole North Sea basin of 0.3 mm/yr for the annual time series, which is similar to the reduction of the observed trends for the virtual station time series of the German Bight. This supports the reliability of the present estimate by using a much simpler empirical-statistical LRM.

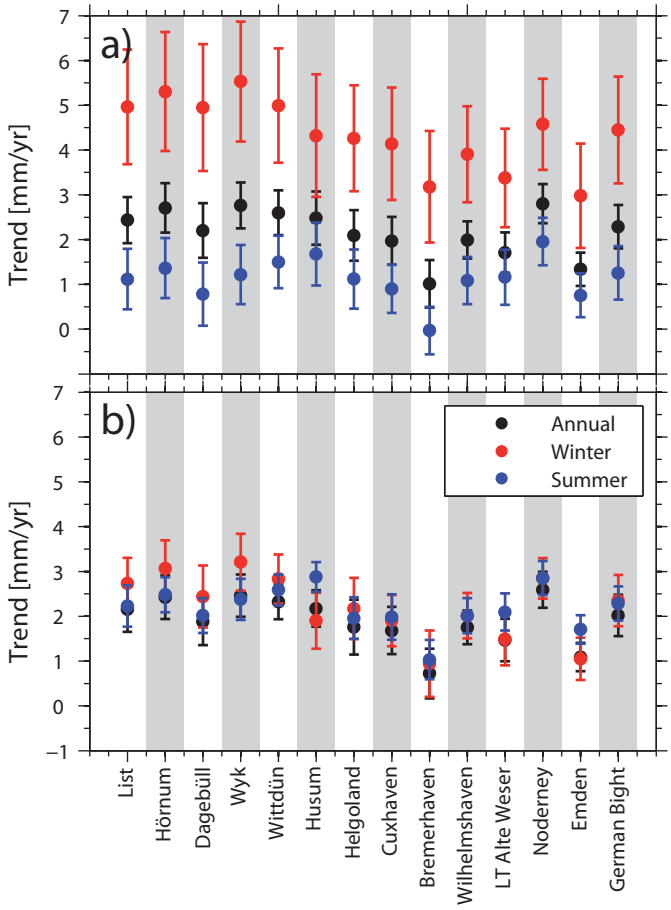

Figure 5-6: Seasonal and annual MSL trends for a) observations and b) atmospherically corrected records at stations in the German Bight from 1951 to 2008. Black dots correspond to annual MSL trends, red dots show boreal winter (JFM) MSL trends and blue dots indicate boreal summer (JAS) MSL trends.

Figure 5-7 shows the observed MSL time series from 1871 to 2008 in comparison to residual time series after applying the atmospheric correction. The effect of that process is self-evident. The subtraction of atmospherically induced MSL changes leads to a considerable lower inter-annual and decadal variability that often hampers the detection of acceleration/deceleration patterns in sea level time series (Rahmstorf et al., 2012). The residual time series contain a considerable lower fraction of background noise allowing more accurate trend analyses.

The spectra of observed and reconstructed MSL time series show that inter-annual fluctuations are well assessed by the atmospheric proxy. The multi-decadal features of annual MSL, however, remain more or less unexplained. Hence, the decadal trend rates obtained by Wahl et al. (2011) will not fundamentally change after subtracting the atmospheric

component. Amongst others, they found high rates of SLR at the end of the 19th century and for the period covering the last three decades. These temporal patterns are still evident in Figure 5-7 after correcting the observed time series for atmospheric influences captured by the proxy.

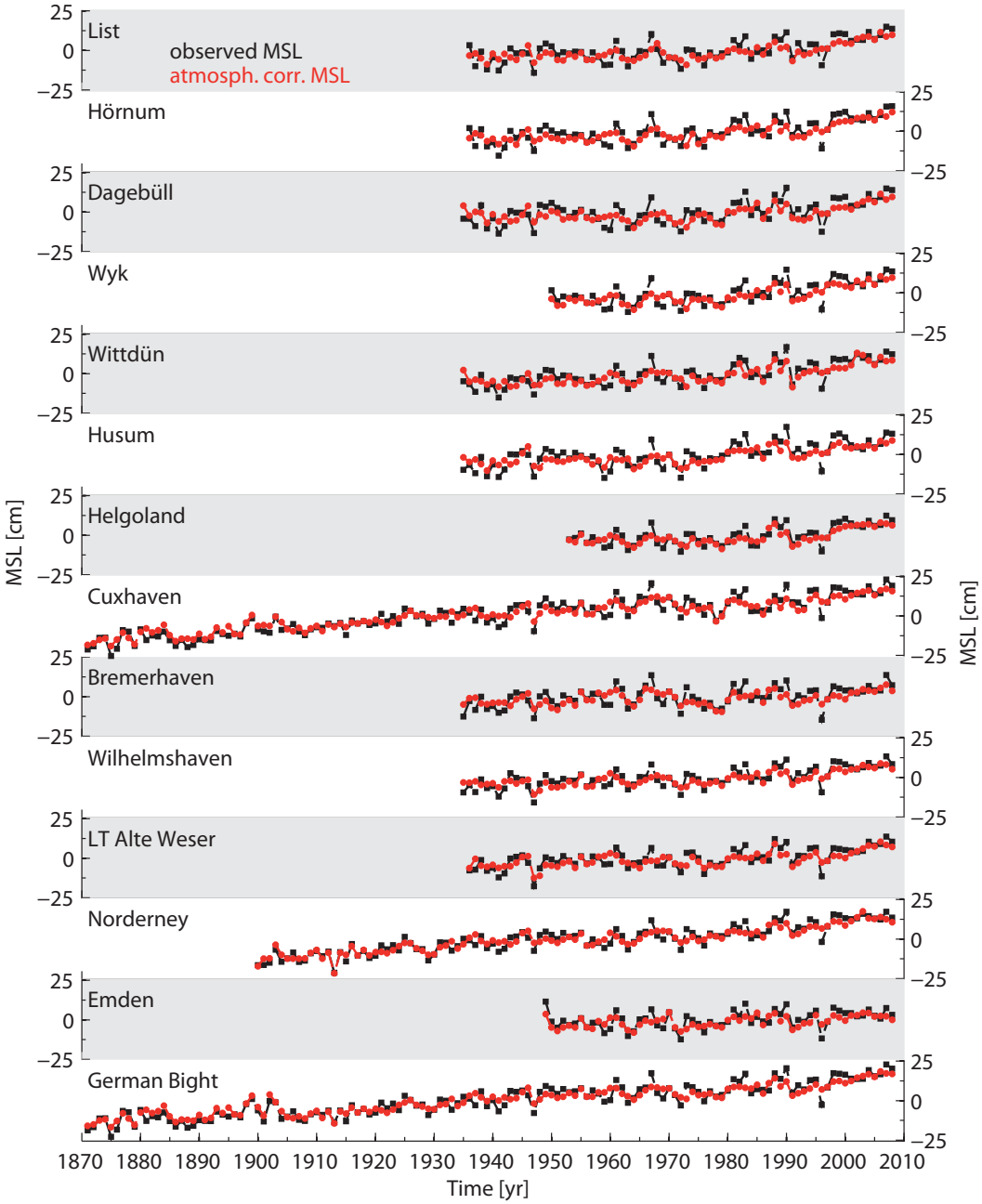

Figure 5-7: Normalized annual observed (black) and atmospherically corrected (red) MSL from 13 tide gauge records and the virtual station German Bight. The red numbers represent the variability explained by the atmospheric reconstruction on inter-annual time scales.

In summary, the atmospheric proxy introduced above is able to capture the main characteristics of atmospherically induced (from winds over the North Sea basin) MSL variations in the German Bight over the 1871 to 2008 period. The atmospheric contribution explains major parts of the observed variability up to ~18 years. It is well known that throughout the past century atmospheric forcing played an important role in the regional MSL develop-

ment along the North Sea coastlines (Tsimplis et al., 2005). Hence, the consideration of these effects is also important when assessing possible future sea level changes.

5.4.2 Model validation

When using empirical relationships between different climatic parameters for assessing greenhouse gas emission scenarios, a key issue is to assure that the observed links are stationary over time. In this context it is important (i) how many years of data are needed to estimate trustworthy regression coefficients and (ii) whether the regression coefficients depend on the considered time period. A common way to validate statistical models is to split the observational period in two sub-periods, in which one sub-period is predicted by the use of regression coefficients estimated within the other sub-period (the so called training period) (Hünicke et al., 2008; Albrecht and Weisse, 2012). However, this approach is somewhat arbitrary, since the two periods have to be selected with no a priori information about the required length of the training period. Hence, in the present chapter a more sophisticated approach is applied (see Dangendorf et al., 2013a, chapter 3 of this thesis) to the virtual station of the German Bight.

In this approach the observational data is first split into sub-samples considering all possible window sizes (here 1 to 137 years). Each sub-sample is used to estimate the regression coefficients of equation 5-1, which are then compared to the estimates derived from the full available period, i.e. the coefficients presented in Table 5-2. For testing the stationarity of the estimated regression coefficients, every window is moved by one year over the entire record. As result, an estimate of the regression coefficients for each window size is obtained. A challenge is now to get a realistic threshold, from which one can assume that the estimated regression coefficient lead to robust estimates for the atmospheric component of MSL. To compare the regression coefficients from the varying window sizes with the best estimate from Table 5-2 (b = -0.44 and c = 0.28), it is first assumed that a regression coefficient is adequately estimated, if the RMSE between the time series from the entire record and the time series predicted with a training period is below 1 cm. To obtain confidence bounds for the regression coefficients (related to RMSEs smaller than 1cm) estimated for the training periods, then different RMSEs from a possible range of regression coefficient combinations (-1 >= b <= 0 and -0.4 <= c <= 1) are estimated. The results of this computation are shown in Figure 5-8a. The RMSE varies within the simulations between values of 0 and 18 cm. A RMSE below 1 cm is reached if the regression coefficient b is between -0.47 and -0.40 and regression coefficient c is between 0.20 and 0.36. These values are used as best guess for the cross-validation.

The results of the cross-validation of regression coefficient b are presented in Figure 5-8b and Figure 5-8c. For small window sizes (<5 years) the estimated regression coefficient b varies considerably within a range of -0.1 and -0.8, but converges to the values estimated for the full period with increasing window sizes (Figure 5-8b). After approximately 40 to 60 years the regression coefficient estimated for the training periods are comparable to the best fit for the full period (i.e. the RMSE becomes smaller than 1 cm). Although the coefficient shows some time-dependent fluctuations, it remains within the confidence bounds

when the window is moved through the time series (Figure 5-8). Regression coefficient c shows a quite similar characteristic: stable regression coefficients are derived when using 40 years of data (Figure 5-8d and Figure 5-8e).

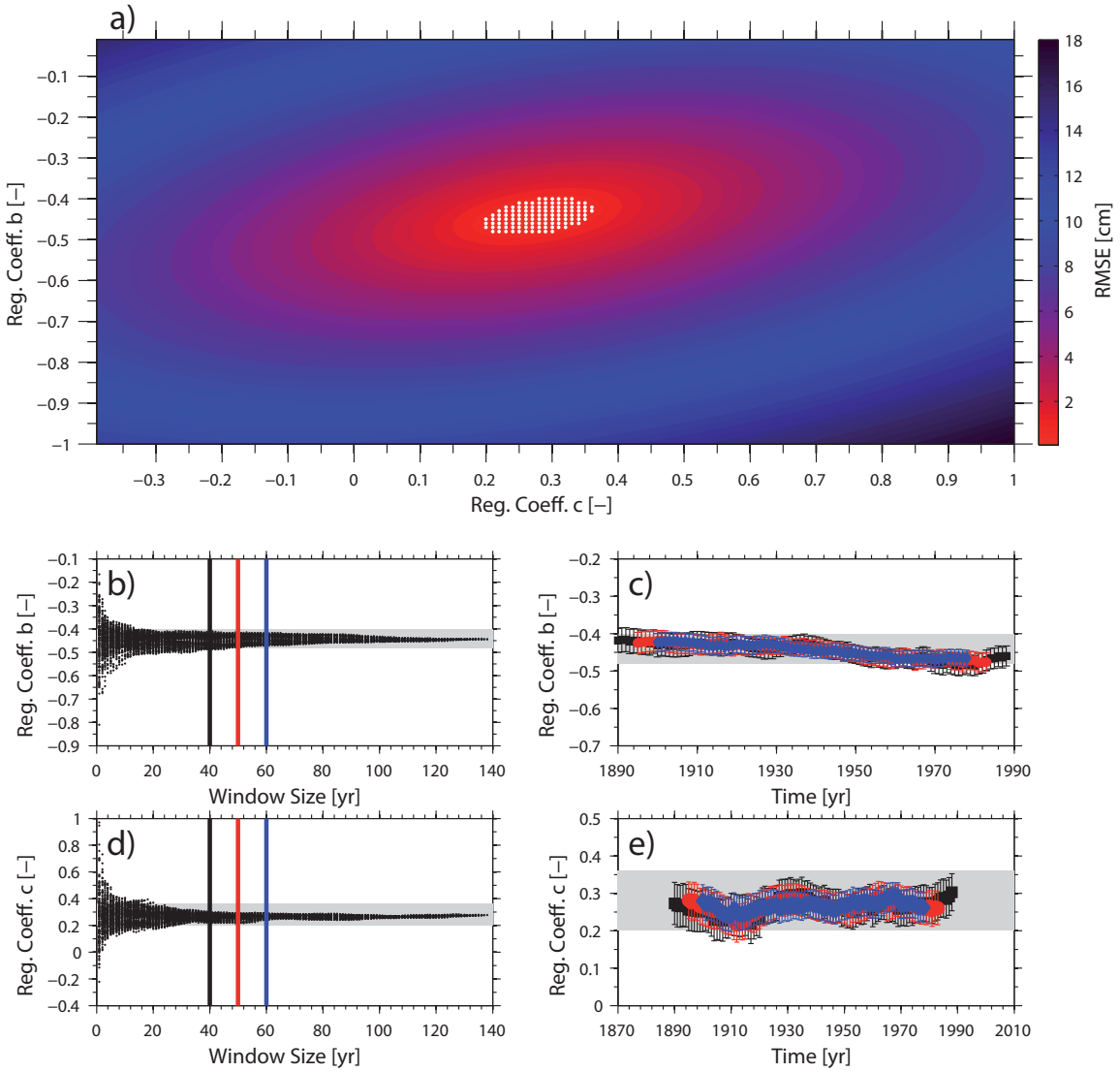

Figure 5-8: a) Root mean square error (RMSE) as a function of varying regression coefficients b and c (colored contours). Regression coefficient combinations resulting in RMSEs smaller than 1 cm (from a comparison with the best fit over the full period of 138 years) are marked with a white dot. b) Results of the model validations. Black dots show regression coefficients estimated within different sub-samples from varying window sizes. The grey area shows the confidence bounds for regression coefficient b estimated in a). The black, red and blue lines represent window sizes of 40, 50 and 60 years, respectively. c) Regression coefficient b estimated with a window size of 40 (black), 50 (red) and 60 (blue) years as a function of time. d) Same as b), but for regression coefficient c. e) Same as c), but for regression coefficient c.

The results presented in Figure 5-8 point to the stationarity of the estimated relationship, i.e. the regression coefficients have not fundamentally changed over time (note that the assumption that the RMSE is adequate if it is in the order 1 cm is somewhat arbitrary, but the value seems to be reasonable small compared to the standard deviations of ~14 cm in the atmospherically induced MSL. The value is further supported by the fact the water levels are generally measured with an accuracy of one centimeter. Smaller values were also tested, and it was found that while the required periods (as in Figure 5-8b and Figure 5-8d) increase the stationarity (as in Figure 5-8c and Figure 5-8e) remains unaffected).

Less than one third of the observational period is required to derive reliable regression coefficients and to accurately predict the time series for the entire period. This leads to the conclusion that the time periods considered here are long enough to derive valuable information on the atmospheric contribution to MSL until 2100.

5.4.3 Simulating the atmospheric contribution to MSL with AOGCMs for the control period (1961-1990)

Before applying the developed regression formulas to future projections of SLP, an essential step consists in the validation of the considered climate models. Currently, climate models cannot be expected to perfectly reproduce observed climate periods (Knutti et al., 2011). This is especially true if the AOGCM's are only forced by greenhouse gas and aerosol concentrations, and no observational data are assimilated. Nevertheless, the current AOGCM's are expected to produce time series with similar statistical characteristics but different temporal evolution. Hence, a commonly used method is to compare statistical distributions of observations and simulations rather than time series. For the present chapter the major question of interest is whether the climate model outputs can be used in combination with the estimated regression coefficients from the 20CRv2 to reproduce the distribution of the atmospheric component of MSLfor the control period from 1961 to 1990. The relationship between the hindcasted (20CRv2, i.e. the reference truth) and modeled time series is displayed by the quantile-quantile (Q-Q) plots shown in Figure 5-9. If the samples come from similar statistical populations the Q-Q plots follow a straight line with a slope of 45°.

The *p*-values (a *p*-value larger than 0.05 implies statistical significance on the 95 % confidence level) derived from a KS-test are also shown in Figure 5-9 for each of the eight climate models. For all AOGCMs the distributions derived from the model results fit well to the distributions derived from the hindcasted MSL. However, there are some differences in the performance of the individual models. The poorest but still statistical significant representation is given by the models IPCM4 and DMIEH5 with *p*-values of 0.22 and 0.25, respectively. Both models tend to continuously underestimate the extreme values of the MSL distribution, i.e. the highest monthly MSL values are generally higher in the 20CRv2 hindcast time series compared to the model time series. This is not the case for the models leading to the highest p-values, that are the BCM2 (p = 0.99) and HADCM3 (p = 0.81). The Q-Q plots show in both cases a more or less straight line leading to high p-values within the KS-test. For the extreme low monthly MSL values all models accurately match the 20CRv2 hindcast values. Hence, assuming that the performance of the models is stationary over time, it can be suggested that the simulated atmospheric fields until 2100 can be used for the purpose of this chapter. A bias correction is not necessary.

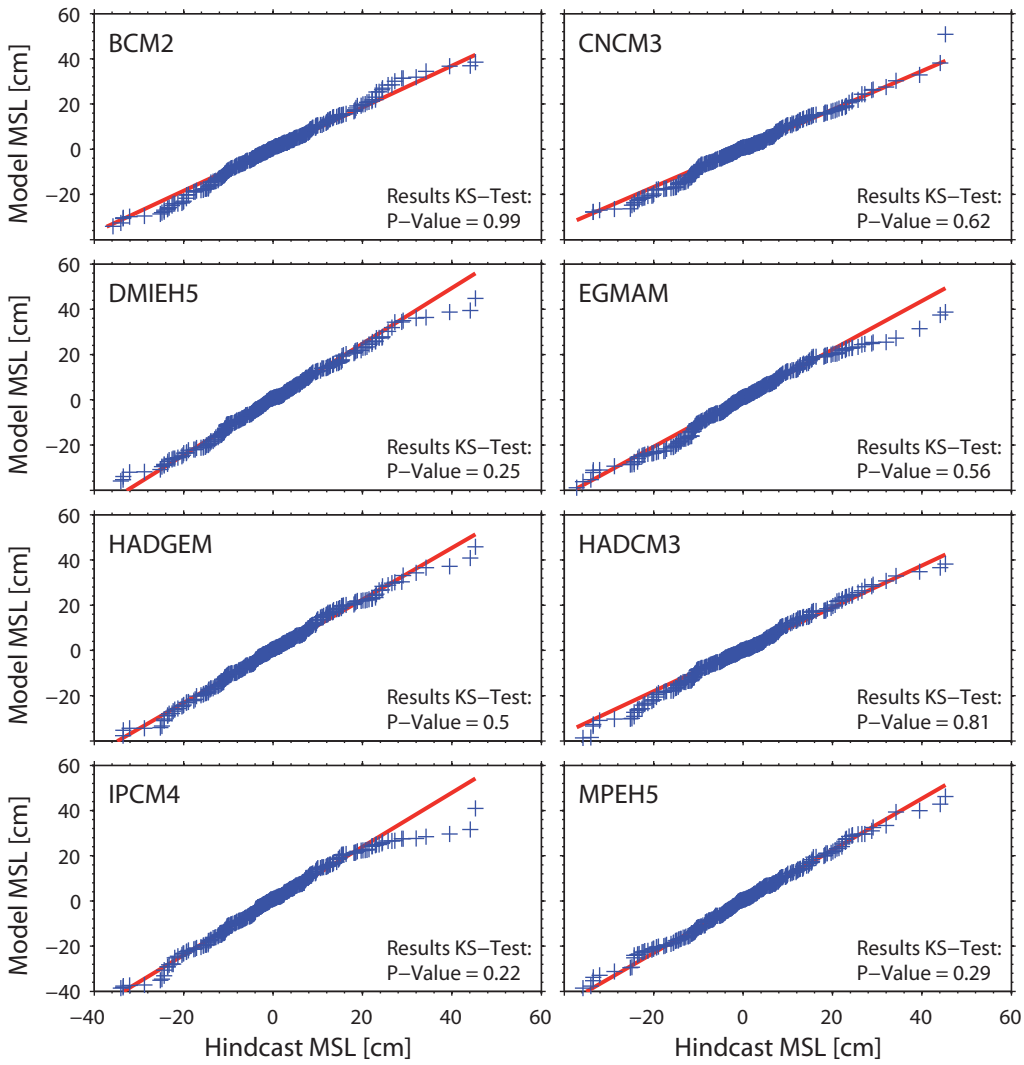

Figure 5-9: Quantile-quantile plots modeled and hindcasted atmospheric contribution to MSL for the validation period from 1961 to 1990. For each model the results of the Kolmogorov-Smirnow test are given.

5.4.4 Simulating the atmospheric contribution to MSL with AOGCMs for the 21st century

First, the projections of the atmospheric MSL proxy are evaluated on a seasonal and annual basis for each AOGCM and the multi-model-mean under the consideration of the A1B scenario. Linear trends are computed for each monthly subseries and the annual means over the common period from 2001-2100. For seasonal changes only the results for the virtual station time series are presented (Figure 5-10), whereas annual trends are presented for each tide gauge location in Figure 5-11 and the virtual station time series in Table 5-3. Additionally, moving averages are presented as time series from 1950 to 2100 for all models and scenarios (Figure 5-12) to identify inherent decadal variability in the projections.

The annual trends for the virtual station time series vary between the different models ranging from negative values in the order of -0.14 ± 0.34 mm/yr for IPCM4 to positive trends in the order of 0.60 ± 0.31 mm/y for BCM2 (Table 5-3, first column). The A1B multi-

model-mean trend is 0.30 ± 0.13 mm/yr (not listed in Table 5-3, but see Figure 5-11 for the ensemble mean at each individual station). With the exception of the IPCM4 all models show positive annual trends, whereas four models (BCM2, CNCM3, DMIEH5, EGMAM) exhibit statistically significant trends (95 %-confidence level).

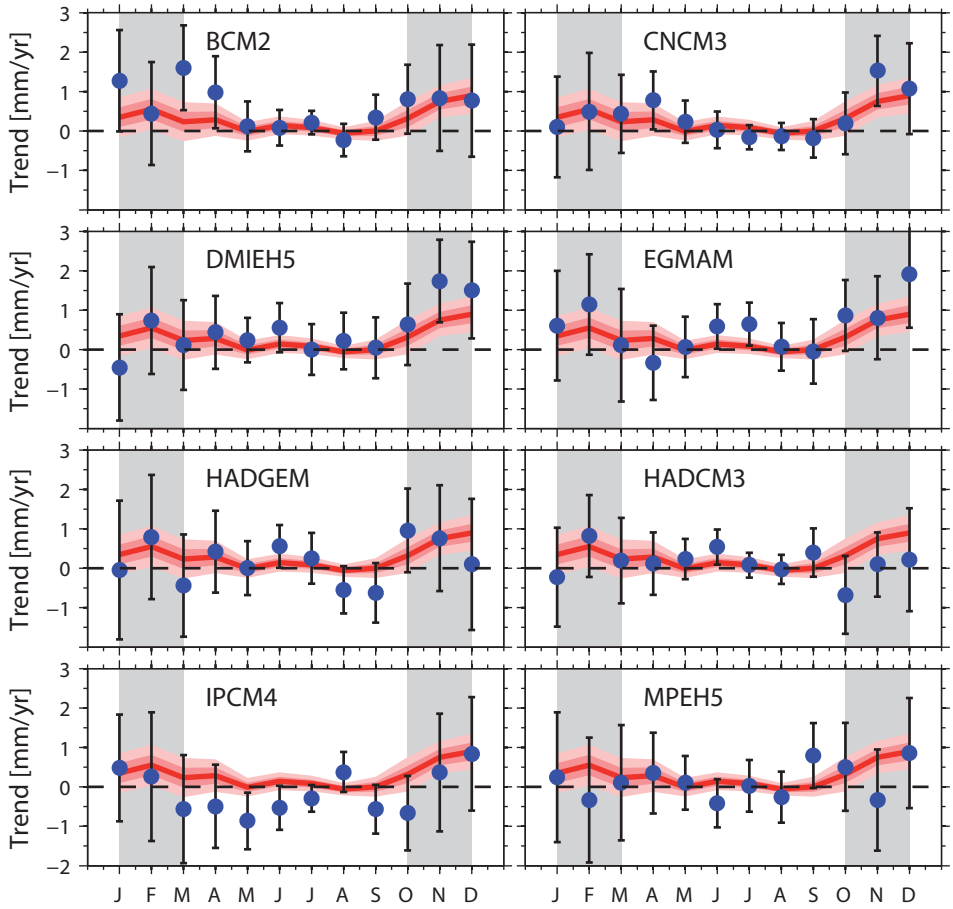

Figure 5-10: Linear Trends (blue dots) ± 2σSE (black bars) of monthly atmospherically contribution to MSL at the virtual station of the German Bight (i.e. the average series of all 13 tide gauge records) estimated from different climate models for the period 2001 to 2100 under the SRES A1B scenario. The linear trends of the multi model mean are shown by the red lines. 1 and 2σSEs of the multi-model mean are presented by the red shaded areas. The grey shaded areas mark the winter half year from October to March.

Most of the considered models point to slightly larger (although mostly insignificant) trends during the cold season from October to March compared to the warm season (i.e. April to September, Figure 5-10). The multi-model mean trend shown in Figure 5-10 implies largest trends during boreal autumn (OND; October to December). These findings indicate that changes in the amplitude and phase of the seasonal MSL cycle may occur. The trends of the monthly subseries vary between -0.74 and 1.5 mm/yr across all models and months. Exceptions are the MPEH5 and the HADCM3 models, which do not provide a significant seasonal pattern in the trends. Seasonal changes have already been found for the past century from evaluating the longest records in the German Bight (Dangendorf et al., 2013c). A further increase of monthly MSL during the cold season would lead to a further rise of annual amplitudes under higher greenhouse gas concentrations. Since MSL is the height upon which surges built, an increase in the amplitudes with higher values during the storm surge season from October to March exacerbates the flood risk for coastal

communities. Jorda et al. (2012) performed similar analysis for the Mediterranean region by using the barotropic version of the HAMSOM model. Considering the output from ensemble runs of another AOGCM (ARPEGE model) for the atmospheric forcing of the barotropic model they found a decrease of the annual amplitudes until 2100. This could be expected, as both regions, i.e. the North Sea and the Mediterranean, are atmospherically directly connected to the NAO with an inverse relationship (Tsimplis and Shaw, 2008). While stations along the North Sea coastlines exhibit a positive correlation to the NAO index, from the English Channel southwards the relationship reverses leading to strong negative correlations in the Mediterranean region (Tsimplis and Shaw, 2008). The fact that both studies show comparable results (under the consideration of regional differences) for the atmospheric contribution points first to a general consensus between the different models regarding the atmospheric development throughout the 21st century and second to a common large-scale driving mechanism behind the projections.

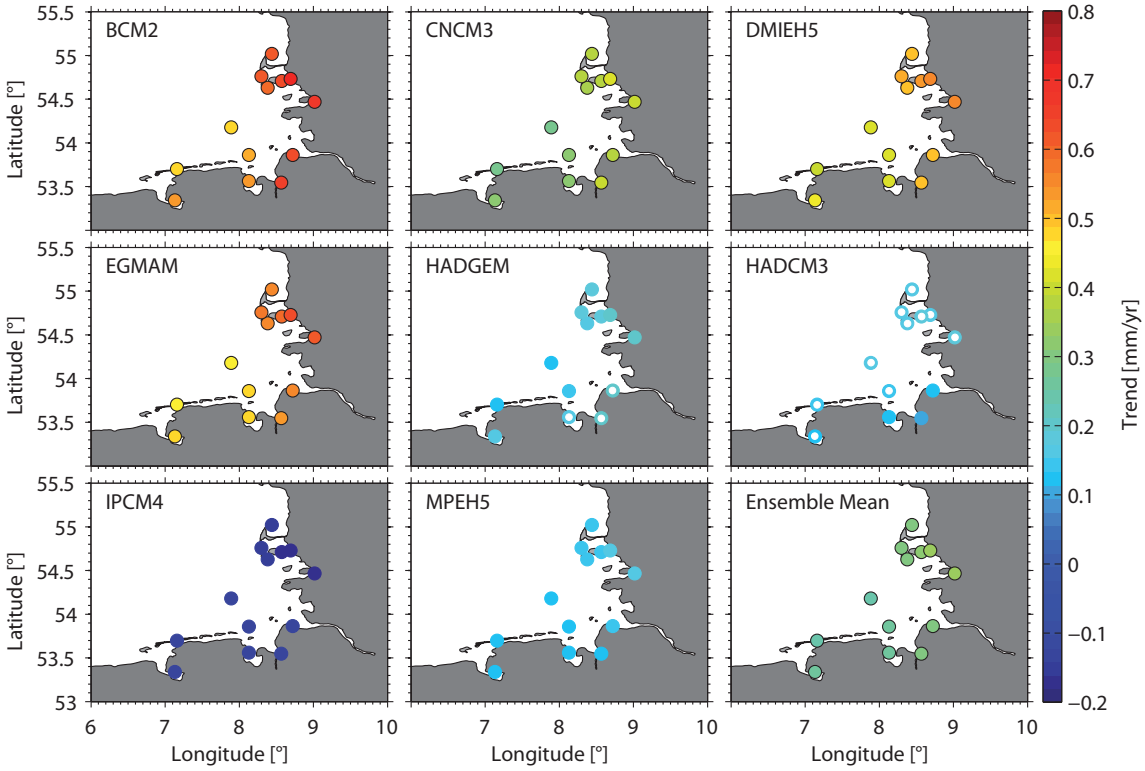

Figure 5-11: Linear Trends (annual means) for the time period 2001-2100 for all models at the tide gauge stations under the SRES A1B scenario. Trends, which are statistically significant on the 95 % confidence level, are marked by a black circle, while trends, which are statistically significant on the 68 % confidence level, are marked with a white dot.

For practical purposes (e.g. planning adaptation measures) the regional differences in future MSL development are of importance. Figure 5-11 and Figure 5-13 show the linear trends computed for the atmospheric contribution to annual MSL time series for each station and the projected period from 2001 to 2100 highlighting model differences in Figure 5-11 and differences between scenarios in Figure 5-13. Across all investigated models and scenarios there is a tendency towards larger trends along the northeastern stations compared to the stations along the southwestern coastline. However, this difference

strongly depends on the magnitude of the regional trends (i.e. the annual trend estimated for the projected virtual station time series) within the different models.

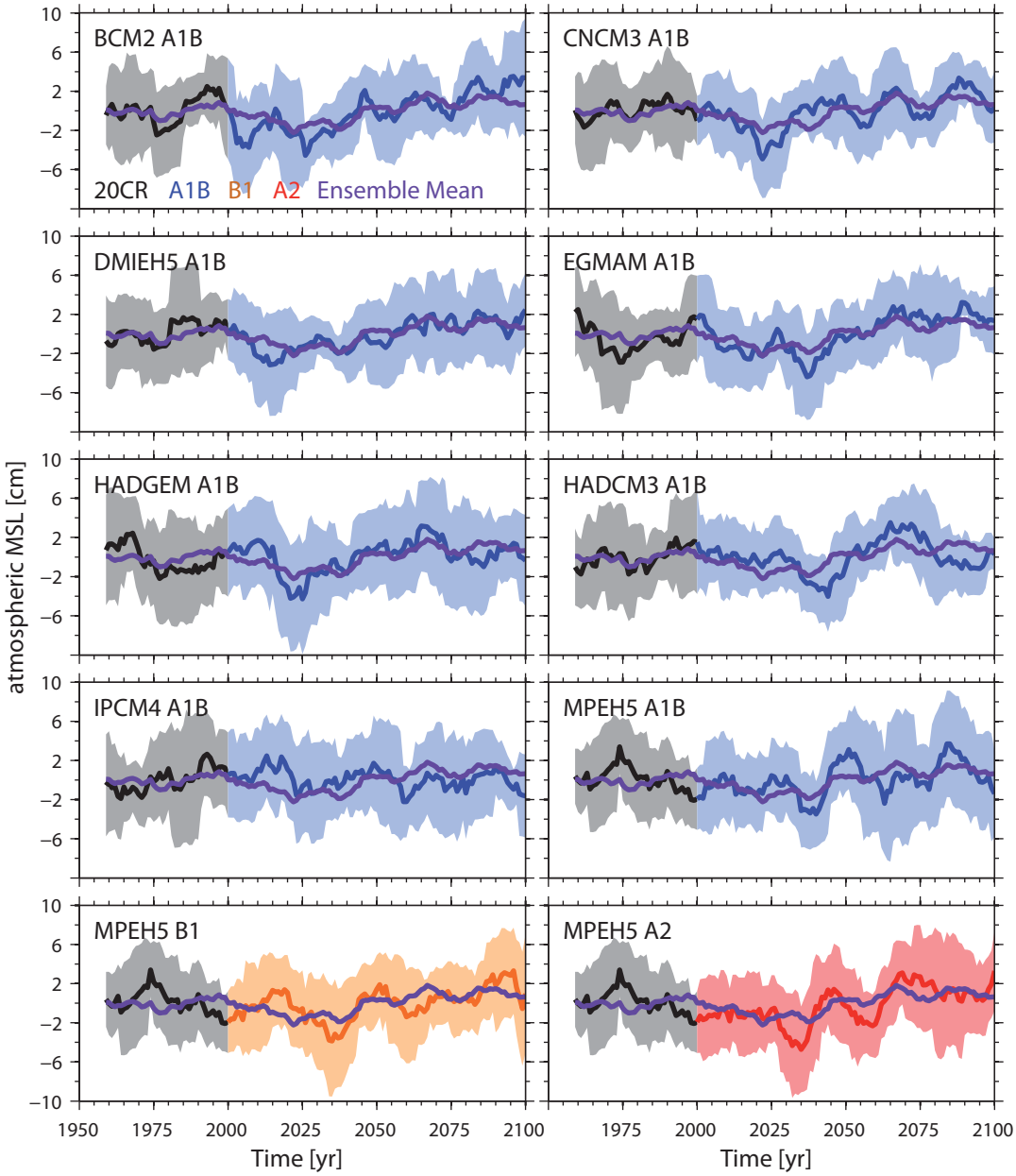

Figure 5-12: 10-year moving average (line) ± one standard deviation (shaded area) of the annual atmospheric contribution to MSL for the virtual station time series of the German Bight (i.e. the average series of all 13 tide gauge records) 1950 to 2100 simulated with different AOGCM's. The twentieth century run is shown in black, while the SRES run is presented in red. The 20CR/A1B multi-model-mean is shown in blue.

Figure 5-14 presents the relationship between the magnitude of the regional trend for the virtual station time series of the German Bight and the observed differences between stations located at the northeastern (List, Hörnum, Dagebüll, Wyk, Wittdün and Husum) and southwestern coastline (Cuxhaven, Bremerhaven, Wilhelmshaven, LT Alte Weser, Norderney and Emden). There is a clear tendency towards stronger differences in conjuncture with higher projections in the atmospheric component of MSL or higher trends for the virtual station, respectively. A similar development (i.e. larger trends in the atmospheric component along the northeastern coastline) has been observed in the recent past as a

consequence of more frequent and extensive southwesterly to westerly winds (Dangendorf et al., 2013a, chapter 3 of this thesis, Dangendorf et al. 2013c). Since the northeastern stations are more exposed to that wind direction, observed differences in the trend rates during the last three decades can be partially explained. The difference of trends found from the model simulations can be very likely explained through similar underlying processes.

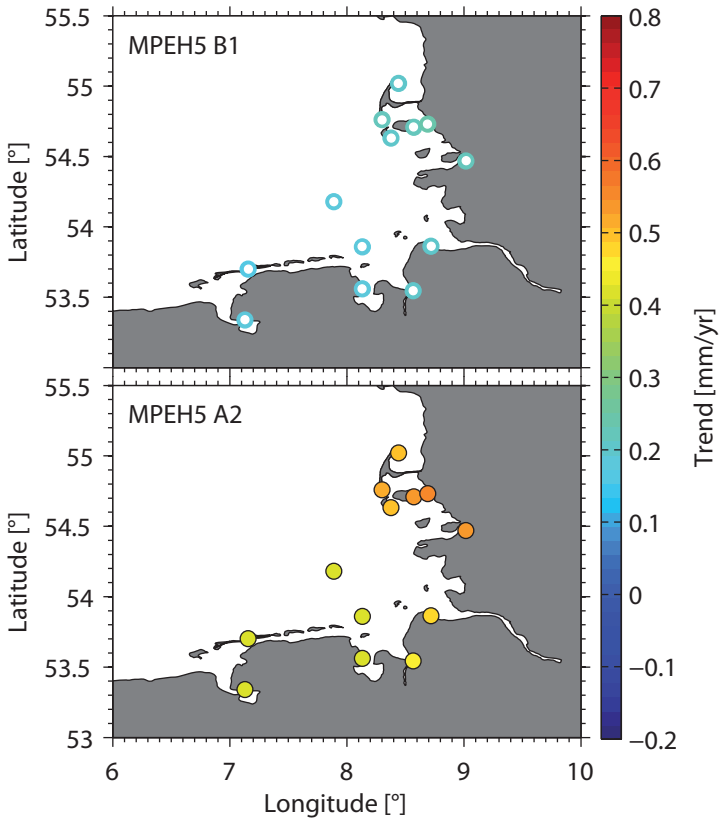

Figure 5-13: Linear trends (in mm/yr) of the atmospheric component of MSL from 2001 to 2100 for each tide gauge location in the German Bight estimated with the MPEH5 under the consideration of SRES B1 and SRES A2. Trends, which are statistically significant on the 95 % confidence level, are marked with a black circle. Trends, which are statistically significant on the 68 % confidence level, are shown with a white dot.

Several authors investigated possible changes in wind speeds and directions under changing greenhouse gas emissions until 2100 (Sterl et al., 2009; Donat et al., 2010; de Winter et al., 2012, 2013). Sterl et al. (2009) investigated the storm surge development along the Dutch coastline by driving a hydrodynamic model with 17 model members from the ESSENCE project. They found no evidence for long-term changes in the storm surge heights along the Dutch coast. The investigation of the regional wind field on the other hand pointed to an increase in extreme wind speed directions from southwesterly and westerly directions and this is more important for the storm surge climate along the exposed German North Sea coastlines. Donat et al. (2010) studied the relationship between large-scale atmospheric circulation patterns and storms over Europe using data from the same AOGCM's investigated here. They found a clear tendency to an increased westerly flow over Europe under future climate conditions, leading to both more days with westerly flow and more days with wind storms. They further pointed to an intensification of cyclones passing the North Sea region to southern Scandinavia in the order of 10 %. Hence, it is suggested that the observed changes in the atmospheric proxy partly represent such changes and therefore lead to increasing trends of regional MSL along the German North

Sea coastline. De Winter et al. (2012, 2013) used the newest generation of AOGCM from CMIP5 and reported similar results with slight increases in extreme westerly winds, which points first to the robustness of the presented results and second to the similarities between CMIP5 and CMIP3 simulations (Knutti and Sedlacek, 2012).

From various studies (Yan et al., 2004; Tsimplis et al., 2005; Jevrejeva et al., 2005; Woodworth et al., 2007; Tsimplis and Shaw, 2008; Dangendorf et al., 2012, chapter 2 of this thesis) it is known that the NAO is strongly connected to the atmospheric component of MSL in the German Bight for the observational record of the last two centuries. The 20th century AOGCM simulations (not shown) point also to a statistically significant relationship between the NAO and atmospherically induced MSL changes in the German Bight (note that the proxy represents a more regional pattern, i.e. the wind effects directly caused over the North Sea, which may not be necessarily linked to the NAO). Therefore, this relationship is analyzed also under varying future conditions to test whether the observed changes are a result of changes in the large-scale atmospheric circulation. Following the approach used by Jorda et al. (2012) and the development of the NAO index is compared with annual MSL trends and variability.

The NAO index was derived from the output of the same AOGCM's by computing the difference of normalized SLP between a northern (55°N-70°N and 0°W-40°W) and a southern zone (35°N-50°N and 0°W-40°W) over the North Atlantic area (Leckebusch et al., 2008). For all considered cases (different models and emission scenarios) statistically significant correlations are found between future NAO conditions and atmospherically induced MSL (Table 5-3). When regressing the atmospheric component of MSL against the NAO projections for each scenario of the different AOGCM's (Table 5-3) the variability and trends are largely explained. In all considered cases the trends are notably reduced. Only for the BCM2 and the DMIEH5 models considerable smaller but significant trends remain afterwards. The overall results suggest that it is likely that the NAO also contributes in future to the MSL development. A similar picture is given for the relationship between the observed trend difference along the coastline and the absolute atmospherically induced MSL changes (Figure 5-14b). Compared to Figure 5-14a the observed difference is notably reduced in most models and only remains in those models for which also positive MSL trends persist after the de-correlation process. Since the main driving factor of the regional differences in the recent past is related to changes in the prevailing wind directions due to a phase of particular strong positive decadal trends in the NAO, it is suggested that the major driving factor within the models is also due to large-scale atmospheric forcing. This is consistent with findings from Pinto et al. (2007), who found a shift towards more positive NAO values and an enhanced zonal flow within the MPEH5 simulations, leading to more frequently occurring westerly winds over the North Sea (Donat et al., 2010). The NAO is known to contribute to the genesis of extra-tropical cyclones and is therefore also linked to the frequency of extreme wind conditions over the North Sea (Pinto et al., 2009) leading to MSL changes in the German Bight. This large-scale connection between atmospherically induced MSL changes in the German Bight and SLP variations over the North Atlantic shows that the ability of robustly modeling MSL variations under the consideration of possible future emission scenarios is directly linked to the ability of modeling the NAO. This,

however, is until today a major challenge for the modeling community (Osborn, 2004). Even though most investigated models are able to simulate main features of inter-annual variability in the winter NAO, observed decadal trends are mostly underestimated (Stephenson et al., 2006).

Model	Annual Trend [mm/yr]	Trend after de-correlation [mm/yr]
BCM2	**0,60 ± 0,31**	**0,24 ± 0,23 (0.69)**
CNCM3	**0,37 ± 0,31**	-0,01 ± 0,21 (0.66)
DMIEH5	**0,48 ± 0,29**	0,33 ± 0,25 (0.53)
EGMAM	**0,54 ± 0,28**	0,13 ± 0,21 (0.59)
HADGEM	0,18 ± 0,36	-0,16 ± 0,29 (0.53)
HADCM3	0,15 ± 0,30	-0,08 ± 0,23 (0.59)
IPCM4	-0,14 ± 0,34	-0,03 ± 0,28 (0.49)
MPEH5	0,14 ± 0,36	-0,11 ± 0,26 (0.65)

Table 5-3: Linear trends of the annual atmospheric contribution to MSL for the virtual station time series German Bight (i.e. the average series of all 13 tide gauge records) before and after de-correlating the time series (2001 to 2100) with the NAO time series of each individual model under the consideration of SRES A1B. Statistically significant trends (95 % confidence level) are marked bold. The Correlation between atmospheric MSL and the NAO from each AOGCM are given in brackets behind the de-correlated trends

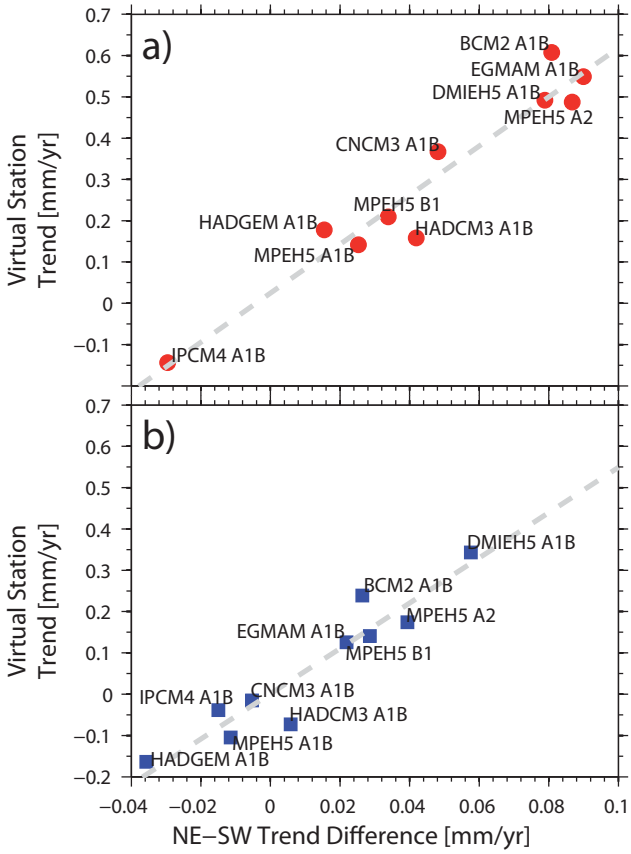

Figure 5-14: a) Estimated annual atmospheric MSL trend difference between north-eastern and southwestern stations (stations 1-6 minus stations 8-13) in relation to the absolute observed atmospheric MSL trend for the virtual station of the German Bight for all available models and model runs. b) Same as a) but the annual trends have been de-correlated with the NAO time series for each individual model.

Although there is statistical evidence for an increase of atmospherically induced MSL changes under possible future climate conditions the related uncertainties are considerable. The spread between the models is in the same order as the spread of the considered scenarios (B1, A1B, A2) for the MPEH5. Hence, the detection of a clear response of atmospherically forced MSL to greenhouse gas forcing is not yet possible, especially under the consideration of the strong inter-annual and decadal variability. Additionally, it should

be noted that the contribution of atmospheric forcing to MSL plays a secondary role when investigating long-term changes in MSL. The IPCC AR4 projected global MSL changes between 18 and 79 cm from 1990 to 2100 (Meehl et al., 2007). The investigations presented here would imply that the atmospheric contribution in the German Bight would only contribute approximately one tenth to the long-term trend. The majority of the models, however, pointed under the consideration of the A1B scenario to increasing seasonal MSL changes. Such changes are more important for coastal planning, since higher winter MSL would provide a higher baseline water level upon which surges can build.

5.5 Conclusions

In the present chapter an atmospheric proxy for MSL in the German Bight consisting of area weighted SLP fields over Scandinavia and Iberian Peninsula was introduced. The proxy represents the strong zonal flow over the North Sea area leading to anomalous high MSL in the German Bight. The proxy explains up to ~80 % of the observed variability and is able to reproduce major MSL fluctuations up to time scales of a few decades. Hence, the prediction potential of MSL using the new SLP proxy is considerably higher for tide gauges in the German Bight compared to the NAO, which explains only 30 to 35 % of the observed variability during winter (Jevrejeva et al., 2005; Dangendorf et al., 2012, chapter 2 of this thesis).

The atmospheric proxy has been extracted from 20CRv2 SLP fields and was used to hindcast MSL variations over the period from 1871 to 2008. The relationship was validated by comparing the results with known features of the atmospheric contribution to MSL variability in the study area, that is:

1. The proxy explains major parts of the divergent seasonal MSL development during the second half of the 20th century. This development has already been identified to be a result of strong changes in the regional wind field between the 1960s and mid-1990s (Marcos and Tsimplis, 2007; Dangendorf et al., 2013a). The fact that the proxy largely explains this feature points to its robustness in reconstructing MSL variability in the region.
2. Another feature of atmospherically induced changes in MSL is the north-south gradient in variability and trends of tide gauge records along the German North Sea coastline. The gradient is known to be mainly forced by a redistribution of predominant winds towards more frequent westerly directions (Dangendorf et al., 2012, chapter 2 of this thesis). This feature is clearly reproduced by the atmospheric proxy manifesting itself in larger explained variances at the northeastern stations.

Hence, it can be concluded that the atmospheric proxy represents a simple, computationally cheap possibility for reconstructing atmospherically induced MSL variability in the southeastern North Sea. The physical process behind the strong connection of MSL and both SLP fields is mainly caused by typical storm tracks passing the North Sea from the North Atlantic to southern Scandinavia (Heyen et al., 1996; Ullmann and Monbalio, 2010).

The fact, that the proxy adequately reproduces the observed changes between the 1960's and mid-1990's shows, that the proxy is able to display both MSL changes as a result of changes in wind speed as well as directions. This leaves potential for future studies. It would for example be interesting to test whether the proxy is able to adequately reconstruct extreme sea levels or wave heights in the region.

Another important finding was that the atmospheric proxy can be used to reduce major parts of the observed MSL variability (first of all on inter-annual time scales). This is important for two reasons. Firstly, inter-annual to multi-decadal variations in sea level hamper an early detection of trend or acceleration patterns (Haigh et al., 2014), which is, however, important for an anticipatory coastal risk management. With the proxy one major contributor to MSL variability can be eliminated from the time series in the southeastern North Sea. Secondly, regional basin-scale features of SLR and variability can be better explained as they are mainly caused by atmospheric forcing. This allows more accurate regional sea level reconstructions, as the resulting virtual station time series can be built based on homogenized individual records.

Based on the robust statistical relationship, the computationally cheap method was applied to a multi-model ensemble of climate models. First, the downscaling skills of eight different climate models for the control period from 1961 to 1990 were assessed. Although the performance varies across the models, they are all able to simulate the distribution of atmospherically induced MSL changes well. This is expressed in statistically significant relationships when applying the Kolmogorov-Smirnow test to hindcasted and simulated samples.

To display the range of different model responses to rising greenhouse gas emissions according to the SRES A1B scenario, an ensemble of eight different models was used. The projected changes generally point to an increase in the atmospherically induced sea level variability in the German Bight under enhanced greenhouse gas emissions, which reflects earlier findings for possible changes in the North Sea wind climate (Pinto et al., 2007; Donat et al., 2010). The changes are larger during winter months in most models. On annual scales the detected changes vary between ~-1 to ~7 cm until 2100 and the results are model and scenario dependent. On intra-annual time scales, the trends are larger in magnitude (although almost insignificant) leading to changes in the annual cycle (the latter is supported by the ensemble mean and six of nine models). The annual cycle dominates the monthly MSL spectra in the German Bight with mean amplitudes of ~9-13 cm (Dangendorf et al., 2013c). Hence, the annual cycle influences both the frequency and intensity of extreme events typically occurring during winter months. An increase in the annual amplitudes would therefore lead to an enhanced flood risk in the region and should be further considered in future studies.

For investigating the uncertainties from choosing certain greenhouse gas emission pathways three different scenarios were analyzed, namely the SRES B1, A1B and A2 each coupled to the AOGCM ECHAM5/MPI-OM (MPEH5). The scenarios characterize a low-, mid- and high-range emission pathway and therefore cover a wide range of possible future developments. Even for the moderate Scenario B1 an increase of annual MSL due to

atmospheric forcing is simulated. Interestingly, the spread caused by the three different emission scenarios (each coupled to MPEH5) approximately equals the spread between the different AOGCM's. This implies that model uncertainty is at least as high as the uncertainty associated with different emission scenarios.

Although the detected changes may contribute to larger MSL values in the German Bight, it should be noted that the magnitude of the detected changes is small when comparing to other forcing factors which are expected to drive MSL changes in the future. Especially, the changes related to global warming will be much larger in magnitude and therefore more important. Furthermore, the results clearly emphasize the large spread between the different models, which in turn is in the same order of magnitude than the spread derived from considering different emission scenarios. This clarifies the urgent need for further improvements of the AOGCM's in their ability of simulating regional climate change.

6 North Sea storminess from a novel storm surge record since AD 1843

6.1 Abstract

The detection of potential long-term changes in historical storm statistics and storm surges plays a vitally important role for protecting coastal communities. In the absence of long homogeneous wind records, a novel, independent and homogeneous storm surge record based on water level observations in the North Sea since AD 1843 is presented. Storm surges are characterized by considerable inter-annual to decadal variability linked to large-scale atmospheric circulation patterns. Time periods of increased storm surge levels prevailed in the late 19th and 20th centuries without any evidence for significant long-term trends. This contradicts with recent findings based on reanalysis data, which suggest increasing storminess in the region since the late 19th century. Wind and pressure fields from the 20CRv2 are compred with the storm surge record by applying state of the art empirical wind surge formulas. The comparison reveals that the reanalysis is a valuable tool which leads to good results over the past 100 years; previously the statistical relationship fails, leaving significantly lower values in the upper percentiles of the predicted surge time series. These low values lead to significant upward trends over the entire investigation period, which are in turn neither supported by the storm surge record nor by an independent circulation index based on homogeneous pressure readings. It is therefore suggested that these differences are related to higher uncertainties in the earlier years of the 20CRv2 over the North Sea region.

6.2 Introduction

Storm surges represent a serious hazard for coastal areas and are expected to become more severe in a warming climate (von Storch, 2012) due to the effects of rising MSL (Slangen et al., 2012) and potential changes in regional wind fields (Woth et al., 2006). Global MSL has risen through the last century (e.g. Church and White, 2011) and is expected to rise also through the 21st century, potentially at an accelerated rate (e.g. Slangen et al., 2012), shifting the entire distribution of extreme sea levels on a higher base level (Hunter, 2010). MSL changes in the North Sea region were recently reviewed by Wahl et al. (2013). While an ongoing sea-level rise is evident, changes in atmospheric circulation and storminess are presently more uncertain (Weisse and von Storch, 2010 and references therein). This is partly due to the fact that the detection of past changes in

storminess is often hampered by inhomogeneous or biased wind measurements (e.g. Lindenberg et al., 2012). Hence, the scientific community proceeded to the evaluation of more homogeneous storminess proxies, which have been observed over longer time periods. Typical examples for such proxies are storm indices calculated from single station pressure readings (e.g. Bärring and von Storch, 2004; Hanna et al., 2008), high annual percentiles of geostrophic winds derived through triangulation of pressure readings (Schmidt and von Storch, 1993; Alexandersson et al., 1998, 2000) or storm surge records from tide gauge measurements (von Storch and Reichhardt, 1997; Zhang et al., 2000).

The North Atlantic European sector is probably the most intensively studied and discussed region for that topic. From analyzing annual geostrophic wind statistics back to 1876, Schmidt and von Storch (1993) found pronounced decadal variability in the southern North Sea but no evidence for a significant long-term trend. These results were confirmed for the larger North Atlantic European region e.g. by Alexandersson et al. (1998, 2000) and Matulla et al. (2008) with the common finding that storminess was high at the end of the 19th century, subsequently declined until about 1960, followed by a strong upward trend until the mid-1990s. Since then, up until now, a return to average conditions is evident.

In contrast to annual storm statistics, Wang et al. (2009) pointed to differences in seasonal 99th geostrophic wind percentiles linking the high values at the end of the 19th century to a summer maximum and the high values in the 1990s to increasing storminess during winter. Apart from these seasonal differences over the Northeast Atlantic and North Sea region, Wang et al. (2009) confirmed the absence of any robust long-term trend for high annual percentiles of geostrophic wind speeds since 1874. The study showed in addition that the periods of high storm activity furthermore coincided with positive decadal trends in the NAO index (Hurrel, 2003). A similar NAO-link and strong decadal trends are also visible in extreme sea levels in the south-eastern North Sea (Dangendorf et al., 2013d; Mudersbach et al., 2013).

Using data from the 20CRv2 (Compo et al., 2011), Donat et al. (2011a) detected – contrary to observational analyses – significant upward long-term trends in the occurrence of extreme storms based on daily wind speeds since 1871 over Europe, and suggested that the increase could (at least partly) be a response to enhanced greenhouse gas emissions during the past decades. Brönnimann et al. (2012) showed that the variance of the 20CRv2 ensemble increases back in time, leading to a better representation of trends after 1950 than before. Krueger et al. (2013a) highlighted that the upward trends detected by Donat et al. (2011a) are inconsistent with observations and suggested this being mainly an artifact of assimilating less surface pressure data into 20CRv2 back in time leading to larger inconsistencies before 1940. This finding is currently controversially discussed (Krueger et al., 2013b; Wang et al., 2013) partly due to the usage of different storminess measures but also inhomogeneous observations, which were still present in the Krueger et al. (2013) study. By removing some potential inhomogeneitis in the pressure records Wang et al. (2013) were able to bring the storm indices from 20CRv2 and from observations closer together but fail to remove the major inconsistencies indicating that there still

might be severe homogeneity issues in the early years of the (i) 20CRv2 reanalysis, (ii) observations, or (iii) both.

In the light of these competing results, the aim of the present chapter is to analyze an independent and homogeneous storm surge record from the tide gauge of Cuxhaven located in the southeastern North Sea covering the period from 1843 to 2012. Since storm surges are generated by low atmospheric pressure and intense winds over the ocean, surges generally exhibit a comprehensive, independent and also more homogeneous archive (Zhang et al., 2000) of information about storminess. Although some tide gauge records reach back into the 17th and 18th century, storm surge records have been surprisingly rarely analyzed in the last decades and earlier assessments in the North Sea region just focused on the 20th century (Ullmann and Monbaliu, 2010). This is mainly attributed to the limited availability of continuous hourly measurements which are required for a harmonic analysis in order to remove the deterministic tidal water level components from the tide gauge data (Pawlowicz et al., 2002). In this chapter, a method first introduced by Horn (1948, 1960) is used that allows us to reconstruct a homogeneous storm surge record based on tidal high and low water levels only instead of hourly data, which is just available after 1918. This method allows extending the storm surge record in Cuxhaven back to 1843, enhancing information about storminess of conventional proxies in that region (Schmidt and von Storch, 1993) by more than 30 years. The method is globally applicable and will open potential for the assessment of storminess. Here, the (to my knowledge) contemporary longest storm surge record in the world is introduced. The record is (i) analyzed for long-term trends in the upper percentiles of storm surges, (ii) investigated for the relationship between storm surges and large-scale atmospheric patterns, and (iii) the empirical relationship between local winds and SLP is used to compare observations with the 20CRv2 data.

6.3 Data and methods

Tide gauges are well suited for the assessment of storminess as they measure beside tides and longer-term MSL changes the direct response of the ocean to the atmosphere. Especially in the North Atlantic region some gauges have measured sea level since hundreds of years (Amsterdam, the longest record, starts in 1682 (Woodworth et al., 2011)). Here, the focus is on a long sea level record observed at the tide gauge of Cuxhaven, which is located in the south-eastern North Sea. Sea levels have been observed in Cuxhaven since 1843. Until 1899 the measurements were taken as readings of high and low water levels four times per day. Since then continuous curves were registered on tidal charts and only the peaks were handwritten in logbooks. Digital recordings are available since the mid-1990s. To get the full information about the tidal curves before that time, extensive digitization works at the German Maritime and Hydrographic Agency made hourly data available back to 1918. In the present chapter both data types, i.e. tidal peaks and hourly observations, are combined to get insights into the history of all available measurements. The data sets were carefully checked for outliers, datum shifts, missing values and time drifts in earlier studies (Wahl et al., 2010, 2011). The overall quality was

found to be good. For example, Dangendorf et al. (2013d) demonstrated a high coherence of sea levels between the Cuxhaven record and 12 additional records all located in the German Bight.

Storm surges measured in the region can be decomposed into an external and a local/regional component; both caused by meteorological disturbances over the Northeast Atlantic and the entire North Sea basin, respectively (Müller-Navarra and Giese, 1999). Hence, it is reasonable to suggest that strong storms occurring over the Northeast Atlantic or North Sea region will leave a fingerprint in the surge record of Cuxhaven. To illustrate the genesis of such a storm event, Figure 6-1 shows the meteorological and oceanographic situation in the region during January 2007. In this month northern Europe was affected by a series of strong storms (Fink et al., 2009) leading also to a series of strong storm surge events (Figure 6-1). In total the long-term 95th percentile of daily surges was exceeded eight times in only 22 days. The genesis of storm surge events often starts with a low pressure system over the North Atlantic travelling westwards to the larger Baltic and Scandinavian area. On their way such pressure systems may trigger waves in the deep ocean northeast of Scotland, which then propagate into the North Sea elevating the water levels in the German Bight approximately 15 hours later (Rossiter 1958). Such external surges may increase a single high water event by up to one meter (Bruss et al., 2010). However, the most important factor for the surge generation is related to strong local winds from north-westerly directions blowing over the shallow shelf areas in the German Bight (depths <= 40m, along the coastlines <= 10m) occurring when the low pressure systems travel further eastwards into the Scandinavian/Baltic area. These winds cause an effect of water pile up with surges of up to more than four meters. In January 2007 the meteorological situation was characterized by a strong pressure gradient with pressure anomalies 16 hPa below the long-term mean over Scandinavia and exceeding it by 9 hPa west of the Iberian Peninsula (Fink et al., 2009). These conditions lead to the generation of a series of particular large surge events in the German Bight (Figure 6-1).

To study the long-term behavior of such storm events i.e. the first aim in the present chapter short-term periodic and long-term MSL changes have to be eliminated from the observational data first (Pugh, 2004). A common way of separating tides from surges is to apply a harmonic analysis to the raw data. However, this method has two general restrictions.

1. First, for a harmonic analysis at least hourly observations are needed. This restriction often hampers the evaluation of long tide gauge measurements back into the 18th and 19th century, since before 1900 most observations are limited to readings of tidal high and low water levels (and times).
2. Second, for tide gauges located in shallow continental shelf seas (such as Cuxhaven) non-linear shallow water effects often bias the harmonic representation of tides, leaving unwanted periodic constituents in values of non-tidal residuals (surges) (Pawlowicz et al., 2002).

To overcome these restrictions, Horn (1948, 1960) developed a more sophisticated technique that allows accurate predictions of the astronomical tides just on the basis of tidal

peaks. The approach is based on a harmonic representation of inequalities (see Müller-Navarra, 2013) for detailed information of different computation steps: http://www.bsh.de), usually resolving the decomposition of tides and surges more accurately in very shallow seas than the 'traditional' harmonic analysis (Pansch, 1989). The German Bight has distinct semidiurnal tides and under this assumption it is favorable to represent tidal high and low water heights and times as harmonic deviations of mean heights and intervals. This is also best practice in the operational service of the German Maritime and Hydrographic Agency since decades (Müller-Navarra, 2013). Additionally, as also mentioned above for the Cuxhaven record digitized hourly observations are limited to the period from 1918 onwards. Horn's method, however, allows extending the tidal analysis back to 1843 without being dependent on hourly data only available after 1918.

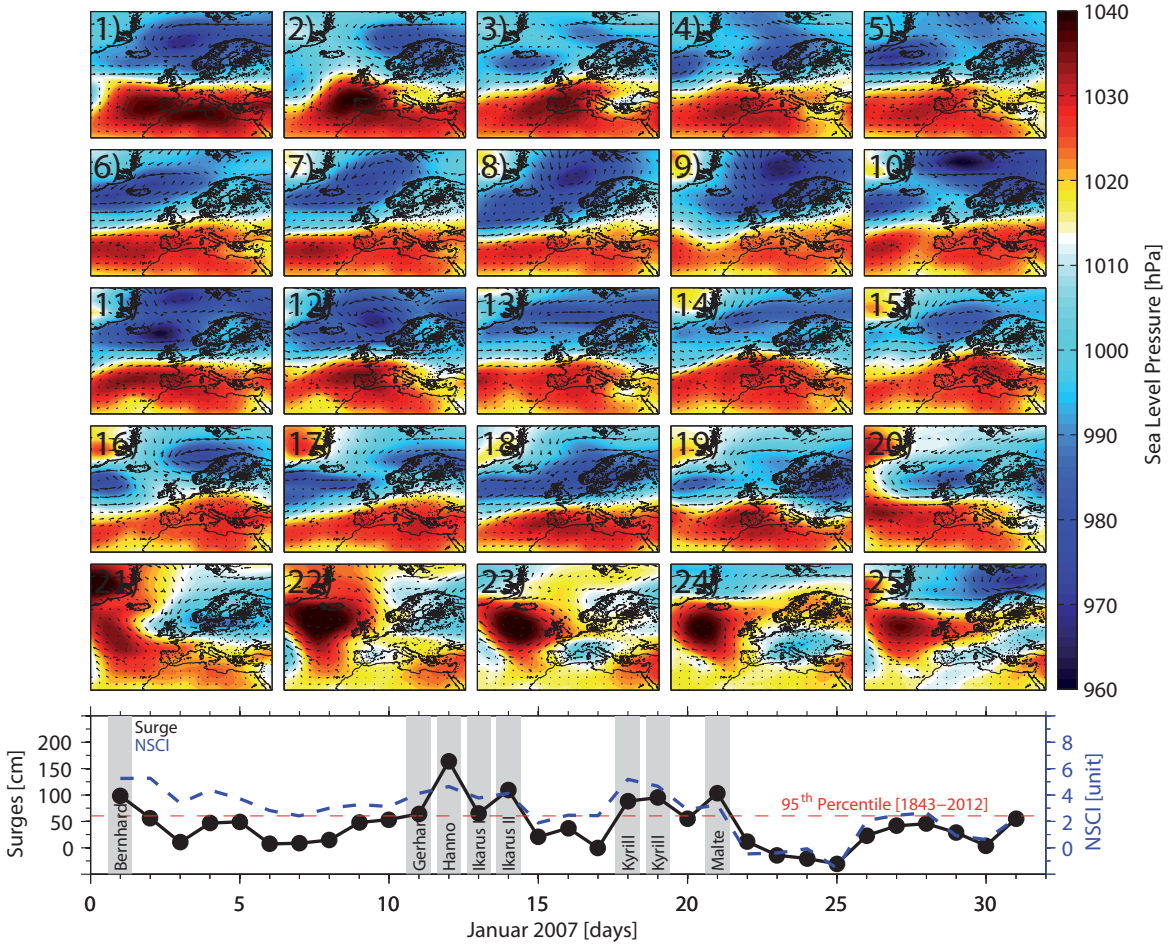

Figure 6-1: Visualization of the daily meteorological (top) situation during January 2007 and the related daily storm surges measured at the Cuxhaven tide gauge (bottom). (top) The colored contours represent areas of similar pressure, while the vectors show the wind speed and direction. For presentation purposes only the first 25 days are shown. (bottom) Daily surges (black) and daily NSCI index (blue; see also section 3; based on 20CRv2 data). The red line marks the long-term (1843-2012) 95th percentile of daily (skew) surges, while the grey areas represent single events exceeding this threshold.

After applying the tidal analysis to the raw data of observational peaks, a surge record is generated by subtracting the astronomical tides from the original signal. One should note that there is a difference between surges generated with hourly observations and tidal peaks. When using hourly values, astronomical tidal water levels are subtracted from contemporaneous observed water levels. When using only two tidal high and low water levels

per day, astronomical peaks are subtracted from the nearest observed peaks. The two may be up to a few hours apart from each other due to the wind influence, and therefore the resulting surges are known as 'skew surges'. Hence, it is first evaluated whether the skew surges (averaged to daily means) differ in the long-term from original surges (or non-tidal residuals) derived from hourly values for the overlapping period from 1918 to 2008 (Figure 6-2). For that purpose, different annual percentiles (0.1, 1, 2, 5, 10, 20, 30, 40, 50, 60, 70, 80, 90, 95, 98, 99, 99.9; Figure 6-2a) and the corresponding linear trends are computed (Figure 6-2b). The figure clearly demonstrates that the percentiles derived from both data sources show virtually the same characteristics in terms of both, variability (Figure 6-2a) and linear trends (Figure 6-2b). The highs and lows in the resulting time series are of similar characteristic, i.e. they show the same temporal development and also match in magnitude. This is further confirmed by the correlations in Table 6-1, which are all larger than 0.94 for the four upper percentiles (which are hereafter investigated in detail).

	Daily Skew Surges			
	95th	98th	99th	99.9th
Daily non-tidal residuals	0.96	0.96	0.94	0.98

Table 6-1: Pearson correlation coefficients between daily skew surges and daily non-tidal residuals (i.e. surges based on hourly measurements) over the period 1918 to 2008. They are all statistically significant (99 %).

Storminess is investigated by computing annual and seasonal (October to March for the cold season, hereafter winter; April to September for the warm season, hereafter summer) 95th, 98th, 99th and 99.9th percentiles of daily surges. Since no gaps are present in the record, there are no restrictions for the analysis of linear trends. Long-term changes are quantified by applying the ordinary least squares regression (OLS). The significance of linear trends is assessed using SEs considering serial correlation of the time series by reducing the number of degrees of freedom as suggested by Santer et al. (2000). It may happen in time series of extreme events that the trends are largely biased by outliers. In such cases robust regression methods such as the Theil-Sens Slope (Gilbert and Richard, 1987) are more appropriate. The results were therefore compared from a range of methods, but nor remarkable differences could be found in the trend estimates. This is mainly attributed to the fact that the time series considered here are long and that there are no obvious outliers in the record. Hence, it was decided to proceed the analysis with the common OLS method.

With respect to the second aim, i.e. comparing storm surges with the variability of large-scale atmospheric circulation patterns, three additional data sets were used:

1. The NAO index provided by Jones et al. (1997): The NAO index is a proxy describing large-scale atmospheric circulation over the North Atlantic region. It is calculated by the differences of pressure anomalies taken from stations in southern Iceland and Gibraltar, Spain. The updated index was downloaded from the webpage of the University of East Anglia, UK (http://www.cru.uea.ac.uk/cru/data/nao/).

2. 20CRv2 reanalysis wind and pressure fields (Compo et al., 2011): 20CRv2 is the newest generation of global reanalysis products covering a long period from 1871 to 2010. By assimilating daily SLP observations into a state-of-the-art climate model with monthly mean sea-surface temperatures and sea-ice as boundary conditions, 20CRv2 provides an ensemble of 56 equally likely best estimates of the atmospheric state at a given time step with a temporal resolution of 6 hours and on a global grid with a resolution of two degrees. For the present investigations daily data have been downloaded from the webpage of the National Oceanographic and Atmospheric Administration (NOAA), Boulder, Colorado (http://www.esrl.noaa.gov; http://portal.nersc.gov). Both, each individual ensemble member and the ensemble mean are analyzed.

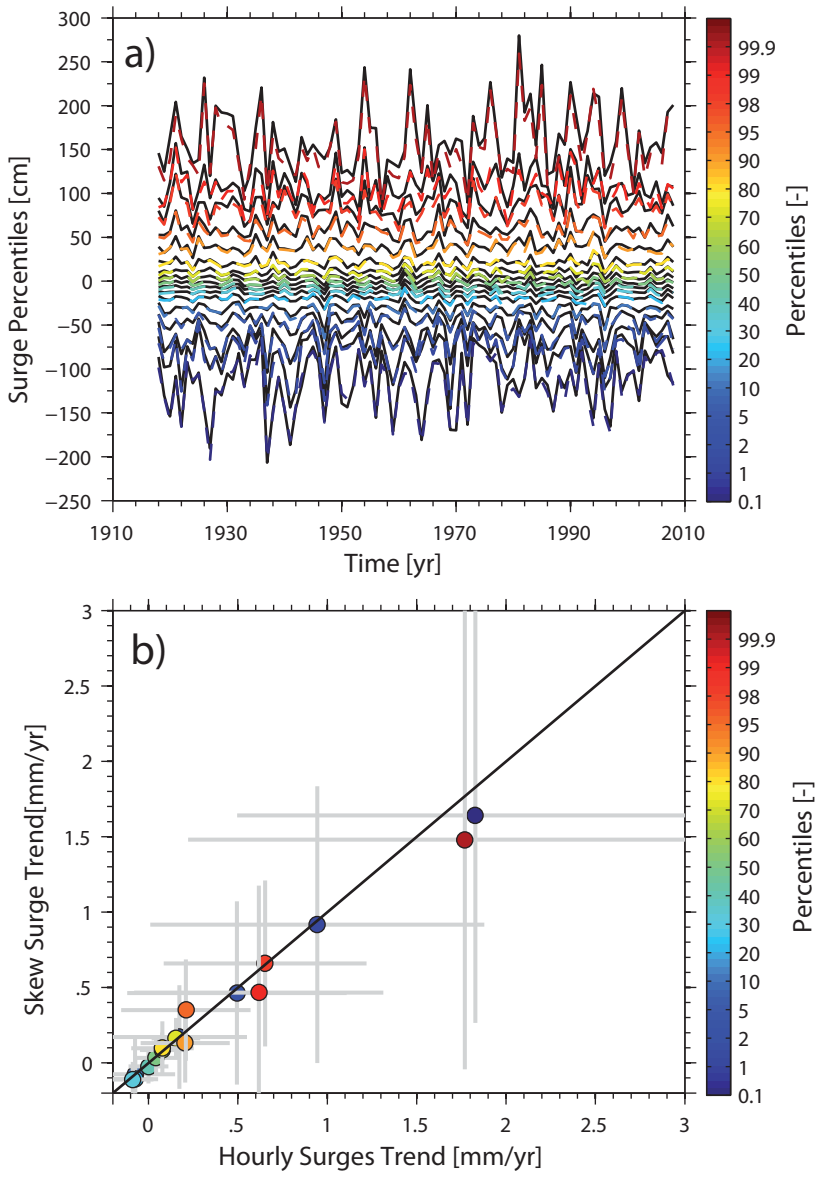

Figure 6-2: Comparison of the statistics of daily surges based on hourly observations (black) and the skew surge record (colored and dotted) over the common period from 1918 to 2008 at the tide gauge of Cuxhaven. a) Annual percentiles and b) linear trends of annual percentiles as a correlation plot. The grey lines mark the SEs of each trend.

The third objective of the chapter is to compare the long-term behavior of surges with that of reanalysis wind fields. In a shallow shelf sea such as the North Sea, the variability is clearly dominated by the wind stress, i.e. the downward transfer of the momentum from

the air into the water. Surges in the southeastern North Sea are caused by atmospheric disturbances over the ocean and can be accurately predicted in the region by the use of simplified statistical-empirical wind surge formulas (Müller-Navarra and Giese, 1999). The model used here describes surges *S(t)* by a number of functions g_j with coefficients a_j and residuals *ε(t)*

$$S(t) = \sum_{j=0}^{n} a_j g_j(t) + \varepsilon(t) \tag{6-1}$$

whereas here six functions g_j based on quadratic and cubic wind stress and SLP fluctuations are linearly fitted with the least squares method to the surges. The functions are given by:

$$g_0 = 1 \tag{6-2}$$

$$g_2 = f^2 cos(\beta) \tag{6-3}$$

$$g_3 = f^2 sin(\beta) \tag{6-4}$$

$$g_4 = f^3 cos(\beta) \tag{6-5}$$

$$g_5 = f^3 sin(\beta) \tag{6-6}$$

where g_0 is a constant term, g_1 and g_2 the quadratic wind stress, g_3 and g_4 the cubic wind stress and g_5 the static response of the water column to SLP changes. The abbreviations *f* and *ß* represent the wind speed and direction, respectively.

The empirical relationship is used to analyze whether the increasing trends in the 20CRv2 data, detected by Donat et al. (2011a), (i) are reflected in the statistical connection between winds, SLP and surges and (ii) whether the predicted surges differ (on decadal and longer time scales) from the observations. To do so, the wind-surge formulas are applied to daily wind and SLP data from the 20CRv2 (u-, v-winds and MSLP from the nearest grid point at 54°N and 8°E. Since surges measured in Cuxhaven are the cumulative response to changes in the wind field over the North Sea, it was also tested whether using additional grid point time series in the LRM (by using a stepwise regression) may improve the results. No grid point time series was able to increase the model performance significantly. Hence, it was decided to use only one grid point for the analysis. Regression coefficients are estimated for the period from 1950 to 2010, a period for which the 20CRv2 was proven to be of good quality (Compo et al., 2011; Krueger et al., 2013a).

Figure 6-3 shows the results of the cross validation between observed and predicted surges. The model is able to reproduce the observations during the validation period from 1950 to 2010, as demonstrated by a high correlation of 0.91 and a small RMSE of 13.9 cm for the ensemble mean (Figure 6-3a). The RMSE is close to those of hydrodynamic models applied in the region (e.g. Weisse and Pluess, 2006), which also confirms the skill of the model. While the performance is particularly high for moderate values, Fig-

ure 6-3a also suggests an underestimation of the most extreme events. This underestimation may be caused by different factors. First, the ensemble mean may potentially average a few single extreme events out. Second, due to the low temporal and spatial resolution of the model forcing (the reanalysis has a temporal and spatial resolution of 6 hours and 2 degrees, respectively) some extreme events which are present in the observations may be lost. Finally, model inaccuracies may be responsible for the underestimation of the most extreme events. To test whether the first reason mentioned above is responsible for the differences, the predictive skill was also tested for each ensemble member separately. While for some individual extreme events the model performance can be slightly improved (Figure 6-3a), the general performance cannot be increased significantly. Overall, the ensemble mean shows the highest skill (Figure 6-3b). It should be noted that the underestimation of some extreme events is not a unique shortcoming of the statistical model, but also present in numerical models (Weisse and Pluess, 2006; Arns et al., 2013). This is why it is suggested that the second reason discussed above, i.e. the temporal and spatial resolution of the model forcing, is most likely responsible for the deviations in the highest percentiles. Due to their stochastic occurrence, it is unlikely that these differences affect the long-term behavior which is further analyzed in the next sections.

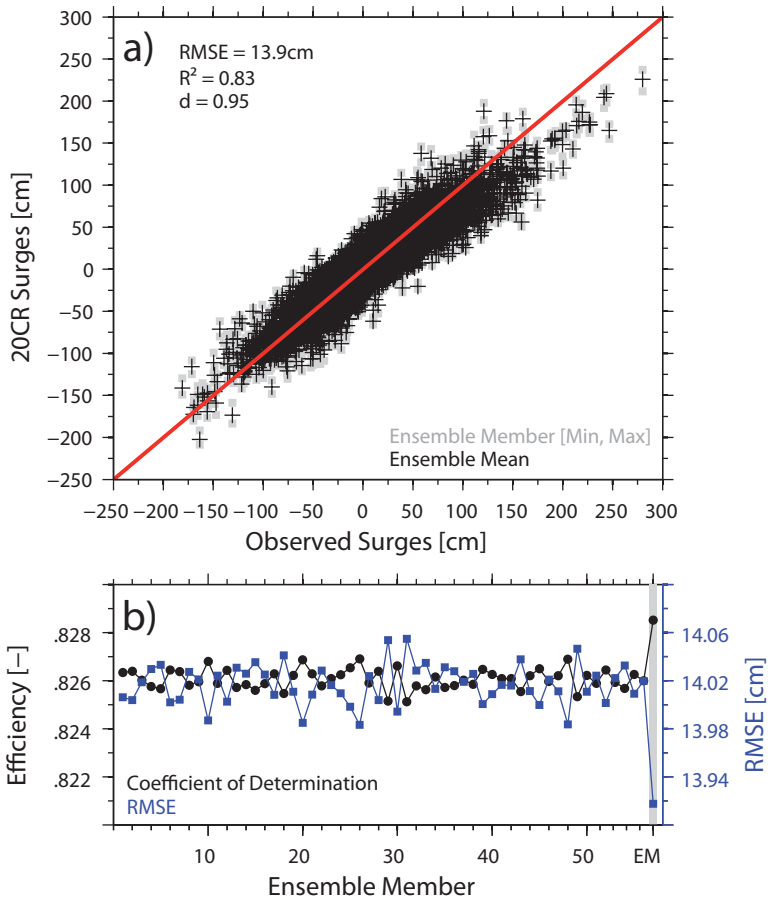

Figure 6-3: a) Correlation plot for observed and 20CRv2 derived surges at the tide gauge of Cuxhaven over the period from 1950 to 2010. The black crosses represent the result by using the Ensemble mean as input data, while the grey dots give the minimum and maximum range as a result of evaluating each Ensemble member separately. b) Coefficient of determination (i.e. squared correlation coefficient) and RMSE for each Ensemble member and the Ensemble mean (grey shaded).

As introduced the main aim is to determine whether the statistically significant relationship between surges and 20CRv2 wind and pressure fields remains stationary in time. Hence, the regression coefficients from equation 6-1 are applied to the entire reanalysis period

from 1871 to 2010. To test the stationarity of the relationship, different efficiency criteria, namely the coefficient of determination (R^2) and the RMSE, are calculated between observed and predicted surges for each year back to 1871.

6.4 Results

6.4.1 Storm surge trends and variability

The storm surge record is presented as a time series of normalized seasonal and annual 95th and 99.9th percentiles together with low pass filtered versions of the time series in Figure 6-4 and Figure 6-4b, respectively. Figure 6-4c shows linear trends for four upper seasonal and annual percentile (95th, 98th, 99th and 99.9th) time series. The time series are characterized by a considerable inter-annual to multi-decadal variability, while there is no evidence for any significant long-term trend: neither for the seasonal nor for the annual percentile time series. Generally, surge-levels are considerably higher and more variable during winter (both on intra-annual and inter-annual timescales) compared to the summer season. Periods of particular high surges are found at the end of the 19th and 20th centuries (note that the periods at the end of the 19th century are slightly different in timing between the 95th and 99th percentile). In both cases the high rates are dominated by the winter season. Between both peaks, especially the highest percentiles of surges are marked by a gradual decline until the mid-1960s as noted earlier for central European storminess (Matulla et al., 2008). After the mid-1990s maximum, surges returned to more moderate values.

The largest contribution to the observed variability in the storm surge record can be found on time scales up to a few decades. From a variety of studies it is well known that especially during the winter season a considerable fraction of sea level variability can be explained by the NAO (e.g. Yan et al., 2003; Dangendorf et al., 2012, chapter 2 of this thesis). It is also obvious that this relationship does not only exist for mean but also for extreme sea levels (Woodworth et al., 2007; Dangendorf et al., 2013d). Therefore, the relationship is examined for the winter season by comparing the updated station based NAO index from Jones et al. (1997) to the four upper percentiles of storm surges (Table 6-2). In all cases the comparison exhibits a weak but significant correlation (r = 0.37-0.45) between the time series, being slightly lower for the highest percentiles. This relationship is not stationary over time; it shows considerable fluctuations over the entire period (Figure 6-5b and d). In agreement to earlier studies between the NAO and MSL over the Northern European Shelf (Jevrejeva et al., 2005) the correlations are high during the mid-19th century decreasing to insignificant values until the 1960s and returning then back to particular high values at the end of the 20th century up to date. This suggests that (i) besides the NAO other factors play an important role for the variability of surges as found earlier also for storminess (Matulla et al., 2008), (ii) the statistical relationship stagnates in times of low large-scale atmospheric variability – i.e. bathymetric effects on the surge generation become more influential – and/or (iii) the influence of the NAO on surges depends on the position of the NAO centers of action (Kolker and Hameed, 2007).

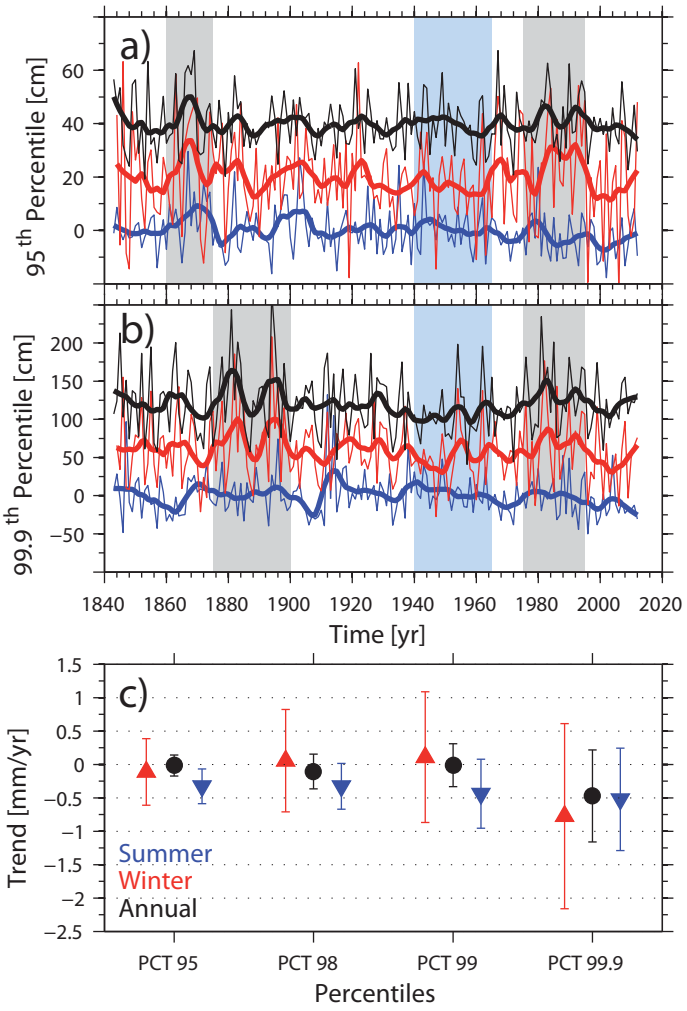

Figure 6-4: Normalized (i.e. the long-term average has been removed) annual (black) and seasonal (red = ONDJFM, blue = AMJJAS) time series of the a) 95th and b) 99.9th storm surge percentiles. Low-pass-filtered time series (LOWESS filter with a cut-off period of 10 years) are shown as thick lines. The grey and blue shaded areas represent periods of increased and decreased storminess, respectively. For presentation purposes the time series are shown with an arbitrary offset (0cm, 20cm, 40cm in a) and 0cm, 60cm, 120cm in b)). c) Linear trends ± 2σ SE of four upper percentile time series for the period 1843 to 2012.

Indices	Surge Percentiles			
	95th	98th	99th	99.9th
NAO	0.45	0.41	0.4	0.37
NSCI	0.66	0.57	0.51	0.44

Table 6-2: Pearson correlation coefficients between winter (ONDJFM) surge percentiles and winter (ONDJFM) SLP indices. All correlations are statistically significant on the 95 % confidence level.

To further examine the mechanisms behind this variability, the cross-correlations between daily surges in Cuxhaven and daily pressure fields from the 20CRv2 (Compo et al., 2011) over the larger geographic area from 60°W to 40°E and 20°N to 80°N wer calculated. To keep the results unbiased by the increasing uncertainties of reanalysis data in the early decades (Krueger et al., 2013), only the data over the period from 1950 to 2010 were evaluated. The correlation analysis suggests a dipole-like pattern between surges and SLP with significant negative correlations over Scandinavia and positive correlations over Iberian Peninsula (Figure 6-5a). This pattern is also known from MSL time series (Dangendorf et al., 2013b, chapter 5 of this thesis) in that region and represents the mean weather situation triggering strong storm surges (Heyen et al., 1996). Composite plots (not shown) suggest an increased westerly flow if surges deviate positively from the mean while the opposite is true for particular negative surges. The dipole-like pattern generally shows similarities to the NAO, but it has a more regional character with a more robust link to the local climate of the German Bight, that is also able to reproduce surges in response

to serial clustering of extra-tropical cyclones such as in January 2007 (Figure 6-1; Pinto et al. 2013).

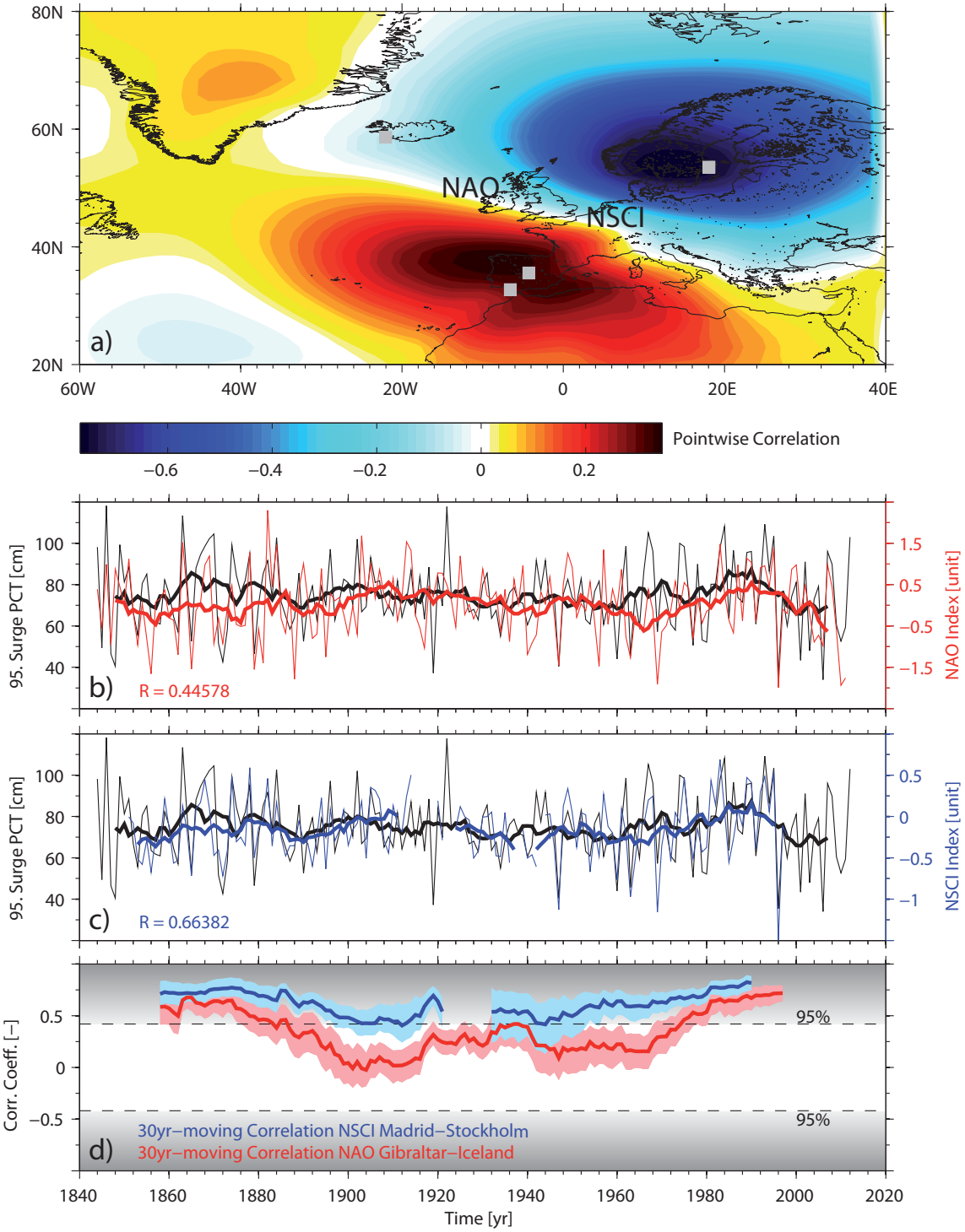

Figure 6-5: Point wise correlations between daily surges in Cuxhaven and gridded daily SLP fields from the 20CRv2 (1950-2010). b) 95th percentile time series of daily surges in Cuxhaven from 1843 to 2012 in comparison to the seasonal NAO index. A 10 year moving average is also shown by the thick line. c) Same as b) but in comparison to the seasonal NSCI index (SLP anomalies Madrid minus SLP anomalies Stockholm, shown as grey squares in a) together with the stations used for the NAO, i.e. Rejkjavik and Gibraltar). D) 30 year moving correlations between 95th percentile time series of daily surges in Cuxhaven and the seasonal NAO/NSCI index. The SEs of the correlation coefficients (blue and red shaded areas) have been computed using a bootstrap method with 500 simulations (Efron and Tibshirani, 1993). All time series from b) to d) are computed for the storm surge season from October to March (ONDJFM).

For taking this regionally more relevant large-scale feature of atmospheric variability into account, an additional index which is referred to as Northern Scandinavia Central Iberia index (NSCI) is defined. The index is computed in a similar manner as the station-based NAO-index (Jones et al., 1997) by using homogenized daily SLP records of Stockholm and Madrid since 1850 (EMULATE, (Ansell et al., 2006)). Both stations are located in the closest vicinity to the centers of the correlation pattern of surges at Cuxhaven with the pressure fields (Figure 6-5a).

As shown in Table 6-2, the correlations between the winter half year NSCI and high storm surge percentiles exceed those of the NAO. More importantly, the link of surges to the NSCI is temporally more stationary than to the NAO. This is indicated by the fact that the running 30 year correlations with the NSCI remain significant and relatively stable over the entire investigation period (Figure 6-5d). As a locally important circulation index like the NSCI can be defined for any location, the main advantage of such an index relates to the temporal long-term robustness of the link between a local variable and the dominating large-scale atmospheric variability. The robust link (in terms stationary running correlations) of high surges at Cuxhaven to the NSCI over time back to 1850 therefore suggests the homogeneity of the surge record, since both parameters (surge levels and SLP) are measured completely independently. Note that the high correlation between both can be taken as an independent measure of homogeneity in terms of low-frequency variability and long-term trends (e.g. Arns et al., 2010; Gouriou et al., 2013), while a partial disagreement could be explained either by inhomogeneities or changes in wind circulation (e.g. direction). Such periods of disagreement are, however, not detectable in the presented time series.

6.4.2 Differences between observations and reanalysis data

Since it was shown that the storm surge record has a stationary link to the NSCI back to 1850 and is also representative for North Sea storminess, the attention is now turned to the long-term comparison with reanalysis wind fields. For that purpose, the statistical relationship described in section 2 is used to test whether the significant trends in reanalysis wind fields, which were recently detected by Donat et al. (2011a), are consistent with the storm surge record. The evaluation of the reconstructed surge record (i.e. based on 20CRv2 wind/pressure time series from the ensemble mean) confirms a stationary and high predictive skill back until approximately 1910, which is indicated by the efficiency criteria shown in Figure 6-6. Before that time the efficiency criteria point to a decreasing predictive skill, i.e. the R^2 decreases and the RMSE increases significantly. While during the calibration period from 1951 to 2010 over 83 % of the observed variability can be explained by wind and pressure effects, before 1910 the performance gradually decreases to values between 70 and 80 % with an absolute minimum in 1871 of 60 %. Also for the RMSE the absolute minimum occurs in the early decades (RMSE = 20.64cm for the year 1883) exceeding the mean of the calibration period by approximately 150 %. As shown before with the stationary correlation of observed surge levels with the NSCI since 1850 (Figure 6-5b), the deviations of observed surge levels with those predicted through

20CRv2 are unlikely to be caused by the observational record (the NSCI and the storm surge record are measures independently).

A similar picture is retrieved by comparing the 10 year moving averages of the 99.9th percentile time series of observed and statistically reconstructed surges (Figure 6-6). Over the past 100 years the reconstruction fits well to the observations. The model predicts the known decline in storminess in the mid-20th century, the rapid increase until the mid-1990s and the downturn afterwards. Nevertheless, in the early 1910s, the prediction starts to decrease in a manner not visible in the observations (for both the ensemble mean as well as the ensemble spread). This decrease finally results in significant positive long-term trends over the entire reanalysis period from 1871 to 2010 if 20CRv2 is taken as predictor (note that a similar behavior was also observed for the 95th percentile (see Figure 9-1 in the Appendix)).

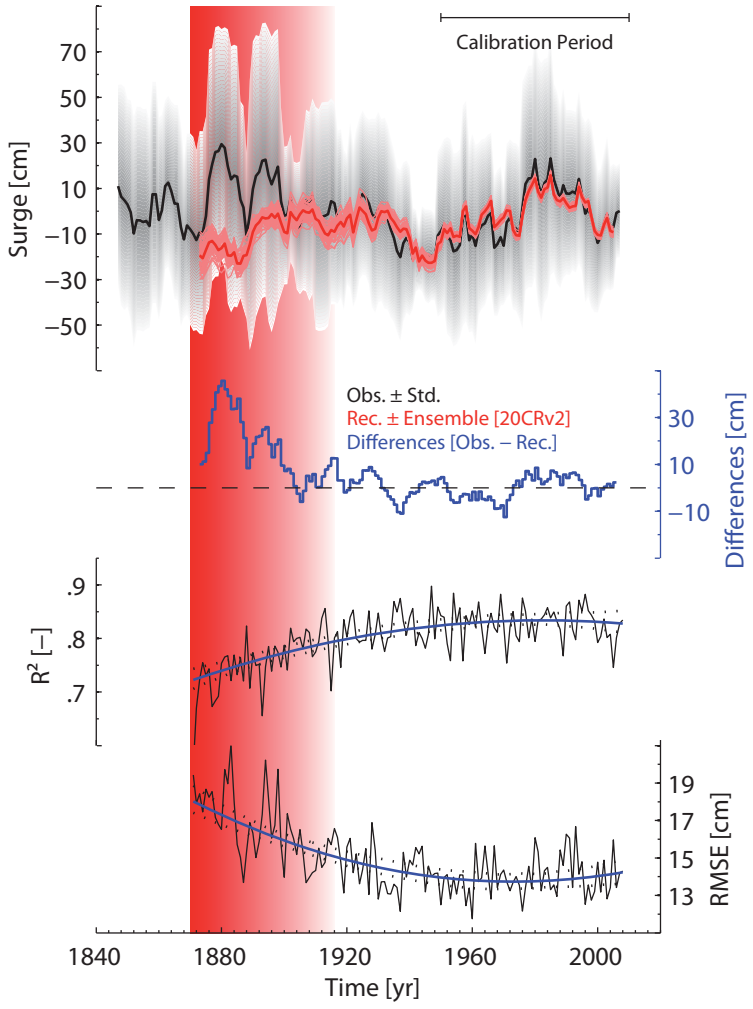

Figure 6-6: Reconstruction of surges based on 20CRv2 winds and SLP. 10 year moving averages of the 99.9th percentiles of observed surges ± standard deviations (black line with grey shaded area; the standard deviation has been computed as a measure of variability over each 10 year window) and their reconstructions based on 20CRv2 (light red: individual ensemble members, dark red: ensemble mean, both normalized to a common period from 1950-2011, i.e. the mean has been removed) are presented. Differences between both are shown in blue. Annual efficiency criteria between observed and reconstructed daily surges are presented in black. The red shaded area marks the period for which significant differences between observations and 20CRv2 are detected. The different shades demonstrate the gradual increase of inconsistencies before the 1910s.

Related to this, Brönnimann et al. (2012) demonstrated that the ensemble mean appears to be biased towards lower wind speeds during earlier decades. They recommended the use of single ensemble members rather than the ensemble mean when investigating long-term changes. To examine whether the results from Figure 6-6 are influenced by such biases, each ensemble member was additionally evaluated for long-term changes separately. First, the differences between the percentile time series from each 20CRv2 en-

semble member prediction and the observed time series were calculated. Then, in a second step, linear trends were computed for each of the residual time series. The results show that for each percentile all ensemble members point to significant positive long-term changes, which are further significantly different from the observations (Figure 6-7a). Additionally, it is found that the residual trends are generally increasing with the order of the percentiles, i.e. highest deviations are found within the highest percentiles.

In order to determine the exact timing from which the 20CRv2 generated surges start to deviate significantly from the observations, linear trends were further computed for the residual time series over 30 year moving windows. The results are shown in Figure 6-7b and Figure 6-7c for the 99^{th} and 99.9^{th} percentiles, respectively. While the trend estimates scatter around zero back to approximately 1910, before that time statistically significant differences are found for the ensemble mean as well as each individual ensemble member. While the bias of the ensemble mean reported by Brönnimann et al. (2012) (Figure 6-7b) can be confirmed, the results also illustrate that using individual members cannot improve the results significantly (when assessing the long-term behavior of storm surges in the German Bight). The reanalysis is significantly biased towards a lower occurrence of extreme values in the period prior to 1910 in both the ensemble mean as well as all members (in this region).

The decreasing coherence between reanalysis forcing and observed surges is generally in line with increasing uncertainties in the reanalysis due to less assimilated observational data in the earlier periods (Compo et al., 2011; Krueger et al. 2013a). The results therefore partly confirm the inconsistencies between storm observations and 20CRv2 found by Krueger et al. (2013a, b) over the North Atlantic region prior the 1940s. In contrast to this earlier study, the inconsistencies with surge levels at Cuxhaven are less pronounced and become clearly visible only for the period before the 1910s. It should be noted that the surges itself differ to the conventional storminess proxies insofar that they measure both changes in wind speed and direction. However, there are three reasons why this does not affect the main conclusion that the surge record is representative for storminess in the region:

1. The rank correlation (Spearman) between wind speeds and absolute surges is with a value of 0.53 statistically significant different from zero (see Figure 9-2 in the Appendix). Since during periods of low wind speeds the influence of bathymetric effects on the surge generation increases relative to the winds, the correlation between the extreme events which are analyzed here increases noticeably. For example, the correlation between the annual 95^{th} percentile time series of both factors increases to a value of 0.64 (not shown).
2. Dangendorf et al. (2013c) investigated changes in the frequency of different wind directions between January and March from 1871 to 2008 and could not find any evidence for significant changes during the period of interest.
3. The fact that Krüger et al. (2013a) previously detected similar differences in conventional proxies (although for a slightly different region and with larger differences

than detected here) and Donat et al. (2011a) pointed to significant trends in the wind speed further supports the reliability of the surge record as a measure of storminess.

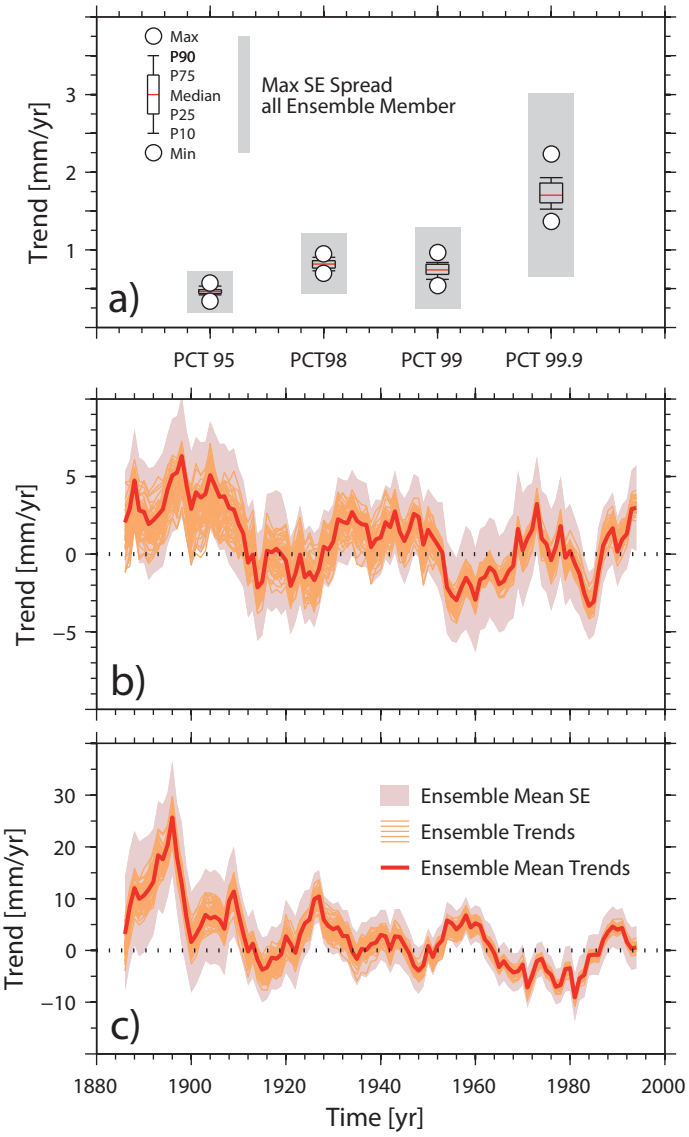

Figure 6-7: a) Box-Plot of residual percentile trends (20CRv2 generated surges minus observation) from all ensemble members over the period from 1871 to 2011. The grey shaded areas represent the maximal range of SEs (95 % confidence level), i.e. residual trends are significant for all ensemble members and percentiles. b) 30 year moving trends for the 99th percentile residuals (20CRv2 generated surges minus observation). All 56 Ensemble members are shown in orange. The ensemble mean together with the related SEs is given by the red line and the red shaded area, respectively. c) Same as b), but for the 99.9th percentile residuals.

Additionally, one could argue that the use of a single grid point time series rather than the entire wind field over the North Sea as input for the empirical wind surge model could bias the results. When looking at Figure 3 in the Donat et al. (2011a) paper it can clearly be seen that the linear trends are evident over the entire North Sea area. In fact, strongest trends in wind speeds have been found for the grid points not used as input data in the present chapter. Therefore, using other additional grid points as input parameters for the wind surge formulas would lead to even larger inconsistencies between 20CRv2 and surge observations.

On this basis it is concluded that the significant trend detected by Donat et al. (2011a) was less a result of the large decadal trends in storminess in the last decades but rather reflects lower occurrence of extreme values in the early decades of the reanalysis. The lat-

ter are neither supported by pressure-based storm indices (Krueger et al., 2013a, b) nor by the surge observations at Cuxhaven since AD 1843.

6.5 Discussion and conclusions

A new storm surge record for the tide gauge of Cuxhaven has been established, extending conventional records back to AD 1843. This could be achieved by using a generally known but in the last decades less considered method (Horn, 1948, 1960) that enables decomposing measurements of tidal high and low water levels into tides, MSL and (skew) surges. The method can open a worldwide available but in terms of surges unappreciated data source for investigating surges and hence storminess. For Europe, tide gauges located in Liverpool, Amsterdam and Brest provide readings of tidal high and/or low water levels back into the 17th century. Additionally, Talke and Jay (2013) recently pointed to the availability of records in the Pacific and western Atlantic region going back to the mid-19th century with more than 50 records available from 1900 onwards. The analysis of these valuable and more or less robust oceanographic measurements could be of high importance for the analysis of storms going into times for which only a few conventional proxies for storminess exist.

Despite the fact that surges measure changes in wind speed and direction, the analysis of high annual percentiles of surges at Cuxhaven confirms earlier observational studies on storminess over the European-Atlantic region with conventional proxies (Schmidt and von Storch, 1993; Alexandersson et al., 1998, 2000; Bärring and von Storch, 2004; Matulla et al., 2008; Hanna et al., 2008; Wang et al., 2009) in terms of both variability and trends. Consistent with the different pressure based storm indices of the last up to 150 years, periods of increased storminess with higher occurrence of extreme storm surges prevailed at the end of the 19th and 20th century with very low levels in the 1970s. While a considerable inter-annual to multi-decadal variability, which is significantly correlated to large-scale atmospheric variability over the North Atlantic and European region, could be identified, no robust long-term trend could be detected in surges since AD 1843 at the tide gauge of Cuxhaven. The absence of any robust long-term trends in annual storminess in observations of the last up to 170 years over the Euro-Atlantic region seems to support global modeling results of externally forced coupled atmosphere-ocean general circulation models (AOGCM). They indicate no long-term changes in storminess (Fischer-Bruns et al., 2005) or cyclone characteristics (Xia et al., 2012) for the northern hemisphere through the last millennium, although most AOGCM's point to an increase in storminess under enhanced greenhouse gas emission in a future climate (e.g. Gastineau and Soden, 2009; Pinto et al., 2007; Donat et al., 2011b).

By applying a simple statistical model to reanalysis (20CRv2) winds and SLP over the North Sea, storm surges in the German Bight were further reconstructed over the entire reanalysis period since 1871. Based on the ensemble mean as well as the ensemble spread it was demonstrated that the reanalysis data has a high predictive skill back to the 1910s, while previously the model skill decreases considerably leading to lower occurrence of extreme storm surges in the first four to five decades of the reanalysis. This de-

crease in storminess is neither visible in surge observations at Cuxhaven nor in different pressure based storm indices (Krueger et al., 2013a, b) over the European-Atlantic region. Hence, the significant positive trends detected in 20CRv2 storminess by Donat et al. (2011a) appears to be less a result of the large decadal trends in storminess in the last decades but rather reflects the lower occurrences of extreme winds in the early decades of the reanalysis. In contrast to the results from Krueger et al. (2013a) which are partly from a different region this chapter points to increasing inconsistencies between reanalysis and observation data before the 1910s. The inconsistencies and their dating are supported by each ensemble member as well as the ensemble mean. As the link of surge levels at Cuxhaven with the fully independent NSCI remains stationary back to 1850, the discrepancies with 20CRv2 are unlikely to be explained with inconsistencies in the surge record. Thus, it is concluded that the 20CRv2 represents a useful database for the North Sea region from the beginning of the 20th century, but one has to be careful by computing linear trends in particular when periods before 1910 are included in the analysis.

It is further recommended that the presented methods can be used as an independent quality check of reanalysis and tide gauge data in other regions of the world. Especially in regions where meteorological observations are sparse, the cross validation with homogeneous tide gauge data might provide information on the consistency of reanalysis data on longer time scales. In turn, in regions where the tide gauge network is sparse, homogenous reanalysis data may provide information on the homogeneity of sea level measurements. In case of inconsistencies in the long-term variations between reanalysis and sea level observations, an independent pressure index like the NSCI for the German Bight can be established from observations to study the robustness of the local observations or reanalysis data relative to this index. Whether a similar link between large-scale forcing (pressure and wind) and local surges can be also established e.g. in tropical regions needs to be evaluated. The homogeneity of observations and reanalysis data is indispensable for oceanographers and meteorologists to study multi-decadal variations or trends in storminess or exchange processes between the atmosphere and the ocean, which is in turn an important step in understanding the predictability of the system.

7 Summary and conclusions

The research in this thesis was concentrated on the characterization and the understanding of regional sea level variability in the North Sea (with a particular focus on the German Bight) on different temporal and spatial scales and under the consideration of various forcing factors. Changes in coastal sea level were analysed by incorporating oceanographic, hydrographic and atmospheric data, various statistical and numerical models and physical theory. The major focus was on different components: the slowly varying MSL (averaged over at least one month) and the high frequency fluctuations (storm surges). All investigations were performed with the overall aim of improving our (i) knowledge about local and remote oceanographic processes leading to enhanced coastal flood risk and (ii) the reduction of uncertainties related to the estimation of long-term changes in regional sea level, which is in turn crucial for deriving future states in the region.

In chapter 2 and 3 particular attention was given to the seasonal MSL cycle and its inter-annual to multidecadal variations. The seasonal cycle was described in chapter 2 for a data set of 13 tide gauge records all located in the German Bight. It was found that MSL varied by about 20 to 30 cm on average with generally larger variability during the cold season from October to March. Larger amplitudes and variability were found along the northeastern coastline (Schleswig-Holstein) compared to the southwestern part (Lower Saxony). These differences along the coastline are suggested to be caused by the more exposed position of the northeastern stations against the prevailing westerlies over the North Sea. The phase was found to be more coherent in the region peaking in November and reaching a minimum during April and May at all stations. It was further illustrated that the seasonal cycle is not stationary showing distinctive variability on inter-annual to multi-decadal timescales with annual amplitudes in some years exceeding 100 cm. Although no significant long-term trend was detected over the period from 1937 to 2008, a remarkable multi-decadal amplification was found between the 1960s and the mid-1990s. This amplification was accompanied by a phase shift with peaks moving from November/December towards January/February. The reason for these multi-decadal modifications was found in up to three times larger trends during winter from January to March compared to the rest of the year. A comparison to the NAO index revealed that the majority of the observed amplification was coherent with anomalous large decadal trends in the large-scale atmospheric circulation over the North Atlantic. These findings confirm earlier assessments conducted by Plag and Tsimplis (1999) for the larger North Sea and Baltic Sea region, Barbosa et al. (2006) for the entire North Atlantic basin and Hünicke et al. (2008) for the Baltic

catchment. Up to now such fluctuations in the seasonal cycle were widely ignored when analyzing the flood risk in coastal areas. However, the presented results demonstrate that variations in the amplitudes or shifts of the phase towards or away from the storm surge season may increase (or decrease) the risk of coastal flooding.

The NAO, which was used to study variations in seasonal MSL in chapter 2, does not influence sea level directly: it rather appears as a proxy for different coinciding physical processes such as wind, SLP and precipitation. Therefore, in chapter 3 the influence of these parameters was investigated in more detail in a multiple regression framework. First, each parameter was analysed regarding its spatial relationship to seasonal MSL in Cuxhaven. This was done by applying a spatial correlation analysis to MSL in comparison to the different parameters derived from the 20CRv2 data set over the period from 1871 to 2008. The analysis revealed a dominant impact of wind stress forcing and smaller but significant contributions by SLP and precipitation. By applying multiple stepwise LRMs (which account for the co-variability between the different predictor variables) to seasonal averages, the quantitative contribution of each factor was assessed. It was found that zonal wind stress plays the most important role throughout all seasons while the other forcing factors vary seasonally. For instance, the role of precipitation (affecting the small hydrological cycle; e.g. Dietrich, 1954) is only significant during spring when the atmospheric influence on the North Sea circulation decreases and density related processes become more pronounced (Sündermann and Pohlmann, 2011).

Overall the models are able to capture up to 90 % (winter: January to March) of the observed variability. During spring and summer, when the atmospheric variability is much smaller in the region, the performance decreases to values in the order of approximately 50 %. In an attempt to identify the reason for the divergent seasonal trend development during the second half of the 20th century, the meteorologically modelled contribution was removed from the original data. A comprehensive trend analysis demonstrated that the meteorologically induced sea level variations primarily drive the seasonal differences in the time series. It was also shown that the intensification of the NAO during the months from January to March between the 1960s and mid-1990s led to a significant increase in the zonal winds over the Northeast Altlantic region piling up more water in the German Bight. In spite of this tremendous influence of meteorological forcing on inter-annual to decadal changes in seasonal sea level, the corrected annual time series still show an unaltered behavior on decadal time scales. It follows that the main characteristics of acceleration and deceleration patterns during the past 138 years, which were already identified by Wahl et al. (2010, 2011), remained unchanged. However, the SE, which determines the accuracy and therefore also the significance of such patterns, was shown to be largely reduced. Consequently, the removal of the meteorologically driven component in MSL has specified the identification of decadal to centennial features of SLR in the region. It was concluded that the different phases of acceleration and deceleration (i.e. the high rates at the end of the 19th and 20th century and the downturn in between) were likely driven by external processes acting outside the German Bight and/or North Sea.

These features were analysed in more detail in chapter 4 where the investigation area was extended to the entire North Sea basin, and selected measurements from the North-east Atlantic were also included. In contrast to the chapters before, the focus was on inter-annual to decadal scale processes and spatial dependencies. Addtionally, the processes affecting MSL were distinguished differently into density (baroclinic) and mechanically (barotropic) driven components. The LRMs, as also introduced in chapter 3, were applied to estimate the barotropic response of the ocean to atmospheric forcing (wind and SLP) at each considered location. For the first time this component was assessed over long time scales covering the period from 1871 to 2011. Hence, estimates available from numerical models in the region after 1948 could be enlarged by approximately 80 years. To verify the validity of the LRMs their estimates were compared to those derived from a state of the art numerical model based on HAMSOM (Chen, 2014) for the second half of the 20th century. The performance was found to be reasonable well, suggesting sufficient evidence for the application to the longer period from 1871 to 2011. The implementation of the LRMs to each tide gauge location in the North Sea confirms the conclusion from chapter 3 that atmosperic forcing dominates the sea level spectra on time scales up to a few years, but fails in explaining the decadal scale fluctuations, which determine periods of acceleration and deceleration in SLR. The predominant westerly winds appear as longshore winds along the southern North Sea coastlines from Belgium up to Denmark and off- and onshore for the coastlines of the UK and Norway. This leads to a two-tier system in the basin with larger variability in the southeast and less variability along the UK and Norwegian coastlines. The sea levels along the southern coastlines are consequently controlled by the rise and fall in response to Ekman transport towards or away from the coast, while along the coasts of the UK and Norway the IBE (i.e. the hydrostatic response of the ocean to SLP variations) is more important.

The investigation of the decadal scale features highlights a more coherent picture in the region mostly governed by fluctuations in the steric height (here approximated by temperature and salinity profiles in the deep parts of the Norwegian Trench). Given the low water depths on the continental shelf it is further clear that the origin of the steric variations must be external to the region. The evaluation of gridded sea level anomalies derived from satellite altimetry and steric sea level fields from Ishii and Kimoto (2009) revealed a coherent signal extending from the Norwegian coastline along the continental slope down to the Canary Islands. The long-distance correlations suggest that boundary waves triggered by longshore winds along the eastern coast of the North Atlantic are a possible driver of sea level variability in the North Sea. This complements earlier findings by Sturges and Douglas (2011), Calafat et al. (2012) and Calafat et al. (2013), who showed that longshore winds control decadal sea level variability in the Mediterranean, the eastern North Atlantic and possibly also parts of the Arctic Ocean. The correlation maps derived from the gridded steric heights and satellite altimetry further point out that for the North Sea the region north of the Gulf of Biscay is most important for the wave generation. This indicates that the signal propagating into the North Sea represents a hybrid of waves triggered at different latitudes. The fact that the signal is similarly visible in the steric height further confirms

the baroclinic character of the waves (i.e. baroclinic Kelvin waves with a speed of 1 to 3 m/s).

After analyzing the variability of sea level and the contribution of different processes, the improved knowledge was transferred into a statistical investigation of linear long-term trends and acceleration and deceleration patterns. With the help of Monte-Carlo simulations a surrogate ensemble of MSL time series consisting of 1000 series with characteristics typical for the observed records and 1000 series representative for time series corrected for atmospheric forcing were generated. In a first experiment it was tested whether atmospheric forcing influences the accuracy of linear trends, i.e the SE was computed for both ensembles as a function of time series length. The experiment showed that removing atmospheric forcing greatly increases the signal to noise ratio and therefore the accuracy of a linear trend. This in turn allows the estimation of linear trends from much shorter time series with a similar accuracy as derived from longer records. The effect is, not surprisingly, greatest in regions with larger non-tidal variability related to atmospheric forcing. Consequently in the North Sea basin the largest SE reduction is reached for records in the German Bight. In the second experiment the surrogate ensembles were combined with global projections of 21st century SLR. Following a recent analysis of Haigh et al. (2014) three representative long tide gauge records were artificially extended until 2100 and then analysed for prospective accelerations. In accordance to Haigh et al. (2014) it was found that due to the presence of large inter-annual variability the detection of projected accelerations becomes first evident in the second half of the 20th century or later for the moderate projections (in the order of approximately 0.54 m of SLR until 2100) and in the early 2020s when following high end scenarios (up to 2 m SLR until 2100). When using the surrogate ensemble with noise typical for time series corrected for atmospheric forcing the detection time can be shifted by up to 60 years depending on the underlying scenario and location. The results of these experiments have profound implications for the purposes of coastal planning and management. Improving our knowledge of processes affecting sea level regionally clearly supports timely adaption. The earlier we know which climate change pathway the Earth's climate system is following, the earlier appropriate adaption measures can be initiated.

The characterization of past North Sea/German Bight sea level variability illustrated its importance for the regional flood risk in coastal areas. Beside the projected increase in ocean heat content and mass loss from ice sheets and glaciers, such variability may represent another source of climate change impact. However, the processes involved in the generation of variability act on much smaller spatial scales than resolved by global climate models. Therefore, in chater 6 an atmospheric proxy for the barotropic component of sea level variability was introduced. The proxy is based on SLP fields over the larger European and North Atlantic region and resambles the predominant wind conditions. Since SLP is generally well represented by the climate models with course resolution, such a proxy indicates the potential for statistical downscaling. First, the validity of the proxy in estimating atmospherically induced sea level variability in the German Bight was proved. The main observational features, such as the divergent seasonal trend development elaborated in chapters 2 and 3 and the variability gradient along the coastline described in chap-

ters 2 and 4, were well captured by the proxy. Additionally, a simple but effective method was introduced, which allows for testing the stationarity of the statistical relationship on which the models are based that are subsequently used for the downscaling. It was found that when using at least 40 to 60 years of monthly data for the derivation of regression coefficients, the atmospheric component can be estimated with a sufficient degree of accuracy at least for the 138 years of available observations. Based on this finding SLP fields from eight AOGCMs were used to approximate the atmospheric contribution to sea level variability at 13 stations in the German Bight. For all models first a control run from 1961 to 1990 was carried out to compare the statistical distribution of AOGCM derived estimates with those approximated from observations (reanalysis).

Then, after demonstrating their validity, projections were calculated following three different climate change scenarios (B1, A1B, and A2 representing a low, moderate and high emission scenario). For the A1B scenario a multi model ensemble was evaluated, while for one model (MPEH5) also the scenario uncertainty was explored. The projections point to a moderate increase in the atmospheric component in the order of up to five to six centimeters until 2100. The increase is model and scenario dependent, whereby the model and scenario uncertainties were of similar magnitude. In all models and scenarios larger trends are found for the northeastern coastline of Schlewig-Holstein. Consistent with past observations this feature seems to depend on the state of the NAO and the related wind conditions over the North Sea. Some models further point to seasonal differences and therefore contain the potential for an amplification of the seasonal cycle, a finding that needs deeper investigations. In terms of long-term changes, i.e. linear trends, the projections point to a minor contribution of atmospheric forcing on future states of SLR in the region when compared to steric or mass changes. However, atmospheric forcing may lead to decades of above average conditions with the result that a certain threshold might be exceeded much earlier/later than expected from linear projections alone. Hence, it is important to incorporate such fluctuations as an additional uncertainty into the projections of furture states of SLR. It is further important to notice that the decadal fluctuations of baroclinic origin as described in chapter 5 are still not included in the proxy presented here.

In chapter 7, observational evidence for changes in high frequency sea level changes, i.e. storm surges which are directly related to changes in regional storminess, were investigated. As introduced, changes in regional storminess/storm surges represent another source of change in regional flood risk and they act upon the previously discussed MSL component. Information about storm surges was limited to hourly records so far, since their reconstruction requires a harmonic analysis of hourly values to remove tidal signals (e.g. Pawlowicz et al., 2004). As hourly records are mostly limited to the 20th century (in Cuxhaven from 1918 onwards), storm surge evaluations were restricted to these periods as well (e.g. Ullmann et al., 2009). However, Horn (1948, 1960) developed a technique which also allows for the separation of tidal cycles from surges just on the basis of tidal high and low water levels. Here, the technique was applied to the long record of Cuxhaven, enhancing information about storm surges by 76 years. Trends in extreme storm surges were assessed by applying percentile analysis to daily averages of surges. This

was done seasonally as well as annually over the entire investigation period from 1843 to 2012. While the record is characterized by a considerable inter-annual to decadal scale variability, no evidence for any significant long-term trend was detected: neither annually nor seasonally. This finding confirms studies of conventional storminess proxies such as pressure based indices (e.g. Schmidt and von Storch, 1993; Matulla et al., 2008). In agreement to these studies the storm surge record is marked by enhanced storm surge values at the end of the 19th and 20th century and a downturn in between. Hence, an increase, which could be possibly expected due to anthropogenic climate change (e.g. Woth et al., 2006, 2008; von Storch, 2009) is not yet detectable. This contradicts with recent storminess evaluations based on the 20CRv2 wind fields in the North Sea region (Donat et al., 2011). Krüger et al. (2013) already argued that this mismatch could be related to increasing uncertainties in the renanalyis when going back in time, which could be associated with less assimilated data in the earlier decades. This argumentation was recently controversially discussed (Wang et al., 2014; Krüger et al., 2014), whereby considerable debate remains about the timing when the 20CRv2 data starts to be biased significantly.

Therefore, the storm surge record was raised as an independent measure of storminess. First, the record was compared to an alternative index the NSCI as also introduced in chapter 6 of independently measured pressure readings in close vicinity to the centres of high correlation derived from SLP fields over the entire European and North Atlantic region. The index points to a stationary significant link between surges measured in Cuxhaven and large-scale atmospheric circulation over Northern Europe. Then, in a second step, it was tested whether the relationship between North Sea winds and SLP from the 20CRv2 data base changes back in time. This was achieved by applying state of the art wind-surge formulas (Müller-Navarra and Giese, 1999; Jensen et al., 2014) to the wind and pressure fields from the 20CRv2 data set. By doing so, it was found that the 20CRv2 input data reveals a stationary link to the surges back to approximately 1910, while previously the relationship gets significantly weaker. This indicates artificial low values in the 20CRv2 wind and pressure fields which are neither supported by the surges, nor the SLP based NSCI index, nor the conventional proxies analyzed so far (e.g. Schmidt and von Storch 1993). This evaluation implies that (i) until now there is no evidence for any significant increase in regional storminess, (ii) the 20CRv2 represents a useful data base for evaluating climate variability in the region over long time scales, but one has to be careful when estimating linear trends before approximately 1910, and (iii) a novel methodological framework was introduced for the validation of reanalysis products.

To conclude, the five major research objectives formulated in chapter 1 were mostly accomplished:

1. The characteristics of North Sea MSL (with a particular focus on the German Bight) were described for different frequency bands from months to several decades.

2. Different contributing factors were explored by combining tide gauge measurements with gridded atmospheric and oceanographic data sets, various statistical techniques and physical theory.
3. The knowledge about the composition of MSL in the North Sea was transferred into the issue of temporal characteristics of SLR over the past 140 years. By simulating a surrogate ensemble of sea level records it was demonstrated (i) how atmospheric forcing affects the accuracy and timing of linear trends and acceleration/deceleration patterns of SLR, and (ii) by how far the removal of known parts of variability can improve the estimates.
4. By combining a novel atmospheric proxy based on SLP fields and statistical downscaling techniques future states of variability were assessed for a set of 13 tide gauge records in the German Bight.
5. A novel storm surge record was established over the period 1843 to 2012. It was proven that the record contains valuable information about storminess in the region and was compared to the 20CRv2 reanalysis data set. A new methodological framework for testing the homogeneity of observational and reanalysis data was presented.

8 Recommendations for further research

The present thesis has provided new insights into past changes of SLR and storm surges in the North Sea region. However, each new piece of knowledge generates new and deeper questions and new theoretical and experimental challenges. In the following, major research questions and challenges resulting from the conducted research are listed step by step. These research questions can in my personal opinion contribute to a better understanding of ocean physics and dynamics and their relevance for coastal flood risk.

- **Digitize analogue (historic) sea level data**

As already mentioned by my colleague Dr. Thomas Wahl, hundreds of years of data are stored in the basements of water and shipping departements and other authorities since decades (Wahl, 2012). These data sets provide vitally important insights into past changes of sea level and storm surges. This is not only valid for the North Sea region, but also globally (Talke and Jay, 2013). For instance, in the Pacific region alone more than 50 tide gauges provide non-digitized data going back into the 19th century. These data sets improve the confidence in temporal variations of sea level especially before 1900 where up to date only a few tide gauge records are available. Although the observational network has improved allowing the monitoring of each component seperatly (satellites measure sea level relative to the Earth; ARGO profiles give measurement of the heat and salt content of the ocean; GRACE determines changes in ocean mass, ice melt, and changes in hydrology; CGPS provides rates of VLM), tide gauges connect with pre-industrial periods, where the human influence on climate change was less distinct. Hence, they are still indispensable especially in the light of detecting deterministic (i.e. externally forced changes) trends in sea level.

- **Enhance the analysis of seasonal MSL changes to larger regions**

As demonstrated in chapters 2 and 3 of the thesis seasonal fluctuations in MSL play an important role for the timing and magnitude of extreme events along the coast and the ecological health of the ocean. Regional studies on changes in the seasonal cycle have been conducted for some marginal seas of the global ocean, e.g. the Mediterranean (Marcos and Tsimplis, 2007), the Baltic Sea (Hünicke et al., 2008), the Caribbean (Torres and Tsimplis, 2011) and the Gulf of Mexico (Wahl et al., 2014). However, the last assessment for the entire North and Baltic Sea region has been conducted by Plag and Tsimplis (1999). Today, more than 20 years of satellite altimetry data provide information on spatial characteristics and historic reanalysis data sets give different forcing variables. Hence, an assessment of all available data sets could provide new insights into the spatial

characteristics of the seasonal cycle and its temporal behavior. Furthermore, the quasi-global PSMSL data set has only been analysed for the characteristics of the mean seasonal cycle (Tsimplis and Woodworth, 1994), but not for temporal changes in amplitudes of phases of the seasonal cycle. The analysis of these data sets could help understanding nonstationarities in coastal flood risk.

- **Clarify the role of the NAO on the combined risk of storm surges and extreme precipitation**

Beside its link to SSHs in the North Sea the NAO also influences precipitation patterns and therefore the river flooding (Martin et al., 2011) in Northern Europe. This combined forcing might comprise the situation that during anomalous strong NAO+ conditions enhanced westerly winds coincide with heavy rainfall in the upland watershed. Especially in the case of Schleswig-Holstein such events represent a serious hazard, since they bring higher than normal loading from both directions: the seaside and the inland. The region lies mostly below sea level and is passed by big rivers such as the Eider. The inland drainage becomes increasingly complicated when sea levels are rising, requiring, for instance, the support of pumping stations. Hence, it will be important to investigate in future studies the multivariate risk of storm surges and heavy rainfall (and/or rainfall).

- **Combine the information given by tide gauges, satellite altimetry and numerical models to reconstruct spatial fields of sea level for the North and Baltic Sea back into the 19th century**

As shown in chapter 4, satellite altimetry provides valuable information about the spatial variability in sea level, while temporal variations are due to the shortness of the record still less well resolved. Recently, various authors combined the information given by tide gauges and remote sensing to reconstruct century long sea level fields on a global grid (e.g. Church and White, 2011; Wenzel and Schröter, 2011; Meyssignac et al., 2012; Calafat et al., 2014). However, in some of these reconstructions marginal seas such as the North Sea and Baltic Sea have been disregarded, because they produce -due to their low water depths and the increasing continental influences- their own temporal variability, which is in turn not connected to the variations of the global mean. Hence, it will be crucial to establish regional reconstructions. Since the North Sea and Baltic Sea are equipped with a huge number of century long tide gauges, these would provide complementary information to the existing global reconstructions. When further combined with the outputs of state of the art dynamical models (e.g. Chen, 2014), also multidecadal spatial and temporal features could be well described and exchange processes via the Skagerrak and Kasttegat region could be better resolved.

- **Clarify the role of ocean dynamics on the low frequency variability of sea level in the North Sea with numerical models and GRACE measurements**

As outlined in chapter 4 decadal sea level variability in the North Sea has due to the shallow water depths its origin external to the region. Such changes -even steric in nature- appear as mass changes along the coast. Hence, they become visible when analyzing ocean bottom pressure. Nowadays, more than 10 years of GRACE measurements

provide information of changes in ocean mass. Furthermore, near-global baroclinic high resolution ocean models are available to analyze the mechanisms of decadal sea level change and its spatial origin (Carton and Giese, 2008). The combined assessment of these new data sources is indespensible for improving our knowledge about exchange processes between the deep ocean in the North Atlantic, the Nordic Seas and the North Sea. This will further help us to refine the accuracy of regional SLR scenarios for the North Sea and Nordic Seas. As a first step the Bjerkness Centre for Climate Research in Bergen, Norway, has funded a visiting fellowship for 2014. During September and October 2014 I will work together with my colleagues Dr. Jan Øie Even Nielsen and Dr. Kristin Richter to analyze both above mentioned data sets.

- **Integrate the knowledge about decadal sea level variability into future states of sea level along the coast**

The decadal fluctuations in sea level have been demonstrated to reach ±8 cm at some locations in the North Sea. This is approximately one half of the totally observed SLR during the 20th century (Wahl et al., 2013). Considering this and the fact that these fluctuations may persist over periods of at least 10 years, it becomes obvious that they must also be considered for future SLR projections and coastal adaption strategies. However, even today global climate models have a horizontal resolution which exceeds the spatial scales of the underlying oceanographic adjustment processes. Hence, statistical or dynamical downscaling should be applied to derive more accurate sea level projections for the North Sea. There are two different ways how this can be achieved. Since the decadal fluctuations are mainly forced by changes in large-scale wind and pressure fields, one could search for a proxy similar to that presented in chapter 5 to downscale these processes along the coasts over the continental shelf. Another possibility would be to extend the existing dynamical models to a larger region covering the continental shelf down to the strait of Gribraltar. This is important to make sure that the processes envolved into the generation of decadal sea level variability are adequately resolved by the numerical models.

- **Integrate historical storm surge reconstructions into the validation process of reanalysis assessments**

In chapter 6, it has been demonstrated how storm surge records can be used as an independent measure of storminess. Since sea level is directly affected by atmospheric disturbances over the ocean, any change in the intensity or direction of prevailing winds should be also visible in tide gauge observations. Therefore, sea level measurements represent a complementary archive for long-term changes in storminess. Such records, however, are not yet used for the validation of historic atmospheric reanalyses. The methodological framework introduced in chapter 6 could be easily extended into other areas worldwide. Especially in regions where up to date less atmospheric data for the assimilation into the weather models exists, sea levels might provide an indespensible measure for the correctness of the reanalyses.

References

Albrecht, F., Wahl, T., Jensen, J., Weisse, R. (2011): Determining sea level change in the German Bight, *Ocean. Dyn.*, 61, 2037-2050, doi:10.1007/s10236-011-0462-z.

Albrecht, F., Weisse, R. (2012): Pressure effects on past regional sea level trends and variability in the German Bight, *Ocean. Dyn.,* 62, 1169-1186, doi:10.1007/s10236-012-0557-1.

Alexandersson, H., Schmith, T., Iden, K., Tuomenvirta, H. (1998): Long-term variations of the storm climate over NW Europe, *Global Atmos. Ocean Syst.*, 6(2), 97-120, ISSN 1023-6732.

Alexandersson, H., Tuomenvirta, H., Schmith, T., Iden, K. (2000): Trends of storms in NW Europe derived from an updated pressure data set, *Clim. Res.*, 14, 71–73. doi:10.3354/cr014071.

Allan, M.R., and L.A. Smith (1994): Investigating the origins and significance of low-frequency modes of climate variability, *Geophys. Res. Lett.*, 21, 883-886, doi:10.1029/94GL00978.

Ambaum, M.H.P., Hoskins, B.J., Stephenson, D.B. (2001): Arctic Oscillation or North Atlantic Oscillation?, *J. Clim.*, 14, 3496-3507.

Ansell, T. J., Jones, P.D., Allan, R.J., et al. (2006): Daily mean sea level pressure reconstructions for the European - North Atlantic region for the period 1850-2003, *J. Climate*, 19, 2717-2742, doi:10.1175/JCLI3775.1.

Arns, A., Jensen, J. (2010): Developing sustainable coastal protection- and management strategies for Schleswig-Holstein's Halligen considering climate change (ZukunftHallig) - Subproject A: Hydrodynamic analyses in the region of the Halligen, Proceedings of the 1. CoastDoc-Workshop, *Mitteilungen des Forschungsinstituts Wasser und Umwelt*, Heft 2, ISSN 1868-6613.

Arns, A., van Eynatten, H., Häußling, R., van Riesen, D., Schüttrumpf, H., Jensen, J. (2011): Developing sustainable coastal protection- and management strategies for Schleswig-Holstein's Halligen Considering Climate Change (ZukunftHallig), 5th International Short Conference on Applied Coastal Research, Aachen, 2011.

Arguez, A., Yu, P., O'Brien, J.J. (2008): A new method for time series filtering near endpoints, *J. Atmos. Ocean. Technol.,* 25, 534-546, doi:10.1175/2007JTECHA924.1.

Baart, F., van Gelder P.H.A.J.M., de Ronde J., van Koningsveld M., Wouters, B. (2012): The effect oft he 18.6-year lunar nodal cycle on regional sea level rise estimation, *J. Coast. Res.,* 28, 511-516, doi:10.2112/JCOASTRES-D-11-00169.1.

Baerring, L., von Storch, H. (2004): Scandinavian storminess since about 1800, *Geophys. Res. Lett.*, 31, L20202, doi:10.1029/2004GL020441.

Barbosa, S.M., Fernandes M.J., Silva, M.E. (2004): Nonlinear sea level trends from European tide gauge records, *Ann. Geoph.,* 22, 1465-1472, doi:10.5194/angeo-22-1465-2004.

Barbosa, S.M., Silva, M.E. (2009): Low-frequency sea-level change in Chesapeake Bay: Changing seasonality and long.term trends, *Estuar. Coast. Shelf. Sci.*, 83, 30-38, doi:10.1016/j.ecss.2009.03.014.

Barbosa, S.M., Silva, M.E., Fernandes M.J. (2008): Changing seasonality in North Atlantic coastal sea level from the analysis of long tide gauge records, *Tellus,* 60A, 165-177, doi:10.1111/j.1600-0870.2007.00280.x.

Becker, G.A., Dick, S., Dippner, J.W. (1992): Hydrography of the German Bight, *Mar. Ecol. Prog. Ser.*, 91, 9-18.

Bindoff, N.L., Willebrand, J., Artale, V., Cazenave, A., Gregory, J., Gulev, S., Hanawa, K., Le Quéré, C., Levitus, S., Nojiri, Y., et al. (2007): Observations: Oceanic climate Change and sea level, *Climate Change 2007: The Physical Science Basis. Contribution of Working Group I to the Fourth Assessment Report of the Intergovernmental Panel on Climate Change*, Solomon, S., Qin, D., Manning, M., Chen, Z.,Marquis, M., Averyt, K.B., Tignor, M., Miller, H.L., Eds., Cambridge University Press: Cambridge, UK, New York, NY, USA, 385-428, ISBN 0521705967.

Bingham, R.J., Hughes, C.W. (2012): Local diagnostics to estimate density-induced sea level variations over topography and along coastlines, *J. Geophys. Res.*, 117, C01013, doi:10.1029/2011JC007276.

Boening, C., Willis, J.K., Landerer, F.W., Nerem, R.S., Fasullo, J. (2012): The 2011 La Nina: So strong, the ocean fell, *Geophys. Res. Lett.*, 39, L19602, doi:10.1029/2012GL053055.

Broennimann, S., Martius, O., Von Waldow, H., Welker, C., Luterbacher, J., Compo, G. P., Sardeshmukh, P. D., Usbeck, T. (2012): Extreme winds at northern mid-latitudes since 1871. *Meteorologische Zeitschrift*, 21, 13-27, doi:10.1127/0941-2948/2012/0337.

Bromirski, P.D., Miller, A.J., Flick, R.E., Auad, G. (2011): Dynamical suppression of sea level rise along the Pacific coast of North America: indications for imminent acceleration, *J. Geophys. Res.*, 116, C07005, doi:10.1029/2010JC006759.

Bruss, G., Gönnert, G., Mayerle, R. (2010): Extreme scenarios at the German North Sea coast: a numerical modeling study. *Coastal Engineeering*, Shanghai, China.

Calafat, F.M., Chambers, D.P., Tsimplis, M.N. (2012): Mechanisms of decadal sea level variability in the eastern North Atlantic and Mediterranean Sea. *J. Geophys. Res.*, 117, C09022, doi:10.1029/2012JC008285.

Calafat, F.M., Chambers, D.P., Tsimplis, M.N. (2013a): Inter-annual to decadal sea level variability in the coastal zones of the Norwegian and Siberian Seas: the role of atmospheric forcing, *J. Geophys. Res.*, 118, 1287-1301, doi:10.1002/jgrc.20106.

Calafat, F.M., Chambers, D.P. (2013b): Quantifying recent acceleration in sea level unrelated to internal climate variability, *Geophys. Res. Lett.,* 40, 3661-3666, doi:10.1002/grl.50731.

Calafat, F.M., Chambers, D.P., Tsimplis, M.N. (2014): On the ability of global sea level reconstructions to determine trends and variability, *J. Geophys. Res*., 119, 3, 1572-1592, doi:10.1002/2013JC009298.

Cazenave, A., Nerem, R.S. (2004): Present-day sea level change: observations and causes, *Rev. Geophys.*, 42, RG3001, doi:10.1029/2003RG000139.

Cazenave, A., Henry, O., Munier, S., Delcroix, T., Gordon, A., et al. (2012): Estimating ENSO influence on the global mean sea level, *Mar. Geod.*, in press, doi:10.1080/01490419.2012.718209.

Chambers, D.P., Merrifield, M.A., Nerem, R.S. (2012): Is there a 60-year oscillation in global mean sea level? *Geophys. Res. Lett.* 39(18), L18607, doi:10.1029/2012GL052885.

Chao, B.F., Wu, Y.H., Li, Y.S. (2008), Impact of artificial reservoir water impoundment on global sea level, *Science*, 320, 212-124, doi:10.1126/science.1154580.

Chen, X. (2014): Investigation of temperature and sea level changes in the North Sea for the period 1948-2010, *PhD thesis*, Hamburg, Germany, urn:nbn:de:gbv:18-66524.

Church, J.A., White, N.J., Coleman, R., Lambeck, K., Mitrovica, J.X. (2004): Estimates of the regional distribution of sea-level rise over the 1950 to 2000 period, *J. Clim.*, 17, 2609-2625, doi:10.1175/1520-0442(2004)017<2609:EOTRDO>2.0.CO;2.

Church, J.A., White, N.J. (2006): A 20th century acceleration in global sea-level rise, *Geophys. Res. Lett.*, 33, L10602, doi:10.1029/2005GL024826.

Church, J.A., White, N.J., Aarup, T., Wilson, W.S., Woodworth, P.L., Domingues, C.M., Hunter, J.R., Lambeck, K. (2008): Understanding global sea levels: Past, present and future, *Sustain. Sci.*, 3, 9-22, doi:10.1007/s11625-008-0042-4.

Church, J.A., Woodworth, P.L., Arup, T., Wilson, W.S. (2010): Understanding Sea-Level Rise and Variability, *Wiley-Blackwell: Chichester*, UK, 1 st ed., 402-419, doi: 10.1002/9781444323276.

Church, J.A., White, N.J. (2011): Sea-level rise from the late 19th to the early 21st century, *Surv. Geophys.,* doi:10.1007/s10712-011-9119-1.

Church, J.A., White, N.J., Konikow, L.F., Domingues, C.M., Cogley, J.G., Rignot, E., Gregory, J.M., van den Broeke, M.R., Monaghan, A.J., Velcogna, I. (2011): Revisiting the Earth's sea level and energy budgets from 1961 to 2008, *Geophys. Res. Lett.*, 38, L18601, doi:10.1029/2011GL048794.

Church, J.A., Clark, P.U., Cazenave, A., Gregory, J.M., Jevrejeva, S., Merrifield, M.A., Milne, G.A., Nerem, R.S., Nunn, P.D., Payne, A.J., Pfeffer, W.T., Stammer, D., Unnikrishnan, A.S. (2013): Sea level change, *Climate Change 2013: The Physical Science Basis. Contribution of Working Group I to the Fifths Assessment Report of the Intergovernmental*

Panel on Climate Change [Stocker et al. (eds.)], Cambridge University Press, Cambridge, United Kingdom and New York, NY, USA.

Christiansen, B., Schmith, T., Theijl, P. (2010): A surrogate ensemble study of sea level reconstructions, *J. Climate*, 23, 4306-4326, doi:10.1175/2010JCLI3014.1.

Cleveland, W.S. (1979): Robust locally weighted regression and smoothing scatterplots, *J. Am. Stat. Assoc.*, 74, 829-836, doi:10.1080/01621459.1979.10481038.

Cleveland, W.S., Devlin, S.J. (1988): Locally weighted regression and smoothing scatterplots, *J. Am. Stat. Assoc.,* 83, 596-610, doi:10.1080/01621459.1988.10478639.

Compo, G.P., Whitaker, J.S., Sardeshmukh, P.D., et al. (2011): The twentieth sentury reanalysis project, *Quarter Journal of the Royal Meteorological Society*, 137, 1-28, doi:10.1002/qj.776.

Dangendorf, S., Wahl, T., Hein, H., Jensen, J., Mai, S., Mudersbach, C. (2012): Mean sea level variability and influence oft he North Atlantic oscillation on long-term trends in the German Bight, *Water,* 4(1), 170-195, doi:10.3390/w4010170, ISSN 2073-4441.

Dangendorf, S., Mudersbach, C., Wahl, T., Jensen, J. (2013a): Characteristics of intra-, inter-annual and decadal sea-level variability and the role of meteorological forcing: the long record of Cuxhaven, *Ocean. Dyn.*, 63(2-3), 209-224, doi:10.1007/s10236-013-0598-0.

Dangendorf, S., Wahl, T., Nilson, E., Klein, B., Jensen, J. (2013b): A new atmospheric proxy for sea level variability in the south-eastern North Sea: Observations and future ensemble predictions, *Climate Dynamics*, online first, doi:10.1007/00382-013-1932-4.

Dangendorf, S., Mudersbach, C., Wahl, T., Jensen, J. (2013c): The seasonal mean sea level cycle in the southeastern North Sea, Conley, D.C., Masselink, G., Russell, P.E., O'Hare, T.J., eds., Proceedings 12th international coastal symposium (Plymouth, England)*, J. Coastal Res.*, Special Issue 65, 1915-1920, ISSN 0749-0208.

Dangendorf, S., Mudersbach, C., Jensen, J., Ganske, A., Heinrich, H. (2013d): Seasonal to decadal forcing of high water level percentiles in the German Bight throughout the past century, *Ocean Dyn.*, 63, 533-548, doi:10.1007/s10236-013-0614-4.

Dangendorf, S., Müller-Navarra, S., Jensen J., Schenk F., Wahl, T., Weisse, R. (2014a): North Sea storminess from a novel storm surge record since AD 1843, *Journal of Climate*, 27, 3582-3595, doi:10.1175/JCLI-D-13-00427.1.

Dangendorf, S., Calafat, C.M., Arns, A., Wahl, T., Haigh, I.D., Jensen, J. (2014b), Mean sea level variability in the North Sea: processes and implications, *J. Geophys. Res.*, 119, 6820-6841, doi:10.1002/2014JC009901

De Winter, R.C., Sterl, A., de Vries, J.W., Weber, S.L., Ruessink, G. (2012): The effect of climate change on extreme wave heights in front of the Dutch coast, *Ocean. Dyn.,* 62(8), 1139-1152, doi:10.1007/s10236-012-0551-7.

De Winter, R.C., Sterl, A., Ruessink, B.G. (2013): Wind extremes in the North Sea basin under climate change: an ensemble study of 12 CMIP5 GCMs, *J. Geophys. Res.,* 118, 1-12, doi:10.1002/jgrd.50147.

Dietrich, G. (1954): Ozeanographisch-meteorologische Einflüsse auf Wasserstandsänderungen des Meeres am Fallbeispiel der Pegelbeobachtungen von Esbjerg, *Die Küste,* 2, 130-156.

Donat, M.G., Leckebusch, G.C., Pinto, J.G., Ulbrich, U. (2010): European storminess and associated circulation weather types: future changes deduced from a multi-model ensemble of GCM simulations, *Clim. Res.*, 42, 24-43, doi:10.3354/cr00853.

Donat, M., Renggli, D., Wild, S., Alexander, L., Leckebusch, G.C., Ulbrich, U. (2011a): Reanalysis suggests long-term upward trends in European storminess since 1871, *Geophys. Res. Lett.*, 38(14), L14703, doi:10.1029/2011GL047995.

Donat, M. G., Leckebusch, G.C., Wild, S., Ulbrich, U. (2011b): Future changes in European winter storm losses and extreme wind speeds inferred from GCM and RCM multi model simulations, *Nat. Hazards Earth Syst. Sci.*, 11, 1351-1370, doi:10.5194/nhess-11-1351-2011.

Douglas, B.C. (1991): Global sea level rise, *J.Geophys. Res.*, 96(C4), 6981-6992, doi:10.1029/91JC00064.

Douglas, B.C. (2001): Sea level change in the era of the recording tide gauge, in *Sea Level Rise: History and Consequences*, *Int. Geophys. Ser.*, vol. 75, edited by Douglas, B.C., Kearney M.S., and Leatherman, S.P., chapter 3, pp. 37-64, Elsevier, New York, ISBN 9780080516790.

Ducet, N., Le Traon, P.Y. (2001): A comparison of surface eddy kinetic energy and Reynolds stresses in the Guld Stream and the Kuroshio current systems from merged TOPEX/Poseidon and ERS-1/2 altimetric data, *J. Geophys. Res.*, 106(16), 2671-2688, doi:10.1029/2000JC000205.

Efron, B., Tibshirani, J.R. (1993): An Introduction to the Bootstrap, *Monographs on Statistics and Applied Probability*, 57, Chapman & Hall, ISBN 9780412042317.

Ekman, M. (1999): Climate changes detected through the world's longest sea level series. *Global. Planet. Change*, 21, 215-224, doi:10.1016/S0921-8181(99)00045-4.

Fasullo, J.T., Boening, C., Landerer, F.W., Nerem, R.S. (2013): Australia's unique influence on global sea level in 2010-2011, *Geophys. Res. Lett.*, 40, 4368-4373, doi:10.1002/grl.50834.

Fink, A.H., Brücher, T., Ermert, V., Krüger, A., Pinto, J.G. (2009): The European storm Kyrill in January 2007: synoptic evolution, meteorological impacts and some considerations with respect to climate change, *Nat. Hazards Earth Syst. Sci.*, 9, 405-423, doi:10.5194/nhess-9-405-2009.

Firing, Y.L., Merrifield, M.A. (2004): Extreme sea level events at Hawaii: influences of mesoscale eddies, *Geophys. Res. Lett.*, 31, L24306, doi:10.1029/2004GL021539.

Fischer-Bruns, I., von Storch, H., González-Rouco, J. F., Zorita, E. (2005): Modelling the variability of mid-latitude storm activity on decadal to century time scales. *Climate Dynamics*, 25, 461-476, doi:10.1007/s00382-005-0036-1.

Francombe, L.M., Dijkstra, H.M. (2009): Coherent multi-decadal variability in North Atlantic sea level, *Geophys. Res. Lett.*, 26, L15604, doi:10.1029/2009GL039455.

Führböter, A., Jensen, J. (1985): Sekularänderungen der mitleren Tidewasserstände in der Deutschen Bucht, *Die Küste,* 42, 78-100.

Furevic, T., Bentsen, M., Drange, H., Kindem, I.K.T., Kvamtso, N.G., Sorteberg, A. (2003): Description and evaluation of the Bergen climate model: arpege coupled with MICOM, *Clim. Dyn.*, 21, 27-51, doi:10.1007/s00382-003-0317-5.

Gastineau, G., Soden, B.J. (2009): Model projected changes of extreme wind events in response to global warming, *Geophys. Res. Lett.*, 36, L10810, doi:10.1029/2009GL037500.

Gill, A.E. (1982): *Atmosphere-Ocean Dynamics*, 662 pp., Academic, London, ISBN 9780080570525.

Gomis, D., Ruiz, S., Sotillo, M.G., Alvarez-Fanjul, E., Terradas, J. (2008): Low frequency Mediterranean sea level variability: the contribution of atmospheric pressure and wind, *Global Planet Change*, 63(2-3), 215-229, doi:10.1016/j.gloplacha.2008.06.005.

Gordon, C., Cooper, C., Senior, C.A., Banks, H., et al. (2000): The simulation of SST, sea ice extents and ocean heat transports in a version of the Hadley Centre coupled model without flux adjustments, *Clim. Dyn.,* 16, 147-168, doi:10.1007/s003820050010.

Gouriou, G., Miguez, M.B., Wöppelmann, G. (2013): Reconstruction of a two-century long sea level record for the Pertuis d'Antioche (France), *Cont. Shelf Res.*, 61-62, 31-40, doi:10.1016/j.csr.2013.04.028.

Haenngi, P., Jetel, M.M., Küttel, M., Wanner, H., Weingartner, R. (2011): Wetterlagebezogene Trendanalyse der Niederschläge in der Schweiz, *Hydrologie und Wasserbewirtschaftung,* 55, 3, 140-154.

Haigh, I.D., Nicholls, R.J., Wells, N.C. (2009): Mean sea-level trends around the English Channel over the 20th century and their wider context, *Cont. Shelf. Res.*, 29(17), 2083-2098, doi:10.1016/j.csr.2009.07.013.

Haigh, I.D., Nicholls, R.J., Wells, N.C. (2010): Assessing changes in extreme sea levels: application to the English Channel, 1900-2006, *Cont. Shelf. Res.*, 9, 1042-1055, doi:10.1016/j.csr.2010.02002.

Haigh, I.D., Elliot, M., Pattiaratchi, C. (2011): Global influences of the 18.61 year nodal cycle of lunar perigee on high tidal levels, *J. Geophys. Res.*, 116, C06025, doi:10.1029/2010JC006645.

Haigh, I.D., Wahl, T., Price, R.M., Pattiariatchi, C., Calafat, C.M., Dangendorf, S. (2014): Timescales for detecting a significant acceleration in sea level rise, *Nature Communications*, 5, 3635, doi:10.1038/ncomms4635.

Hanna, E., Cappelen, J., Allan, R., Jónsson, T., le Blancq, F., Lillington, T., Hickey, K. (2008): New insights into north European and North Atlantic surface pressure variability, storminess and related climatic change since 1830, J. Clim., 21(24), 6739-6766, doi:10.1175/2008JCLI2296.1.

Heyen, H., Zorita, E., von Storch, H. (1996): Statistical downscaling of monthly mean North Atlantic air-pressure to sea level anomalies in the Baltic Sea, *Tellus*, 48A, 312-323, doi:10.1034/j.1600-0870.1996.t01-1-00008.x.

Hilmer, M., Jung, T. (2000): Evidence of a recent change in the link between the North Atlantic Oscillation and Arctic ice transport, *Geophys. Res. Lett.*, 7, 989-992, doi:10.1029/1999GL010944.

Holgate, S.J. (2007): On the decadal rates of sea level change during the twentieth century, *Geophys. Res. Lett*., 34, L01602, doi:10.1029/2006GL028492.

Holgate, S.J., Matthews, A., Woodworth, P.L., Rickards, L.J., Tamisiea, M.E., Bradshaw, E., Foden, P.R., Gordon, K.M., Jevrejeva, S., Pugh, J. (2013): New data systems and products at the Permanent Servise for Mean Sea Level, *J. Coast. Res.*, 29, 493-504, doi:10.2112/JCOASTRES-D-12-00175.1.

Horn, W. (1948): Über die Darstellung der Gezeiten als Funktion der Zeit, *Dt. hydrogr. Z.*, 1, 124-140, doi:10.1007/BF02226142.

Horn, W. (1960): Some recent approaches to tidal problems, *Int. Hydrogr. Rev.*, 37(2), 65-84.

Huebener, H., Cubasch, U., Langematz, U., Spangehl, T., Niehörster, F., Fats, I., Kunze, M. (2007): Ensemble climate simulations using a fully coupled ocean-troposphere-stratosphere GCM, *Phil. Trans. R. Soc. A.,* 365, 2089-2101, doi:10.1098/rsta.2007.2078.

Huenicke, B., Luterbacher, J., Pauling, A., Zorita, E. (2008): Regional differences in winter sea level variations in the Baltic Sea for the past 200 yr, *Tellus*, 60A, 384-393, doi:10.1111/j.1600-0870.2007.00298.x.

Hunter, J. (2010): Estimating sea-level extremes under conditions of uncertain sea-level rise, *Climatic Change*, 99, 331-350. doi:10.1007/s10584-009-9671-6.

Hurrell, J.W. (1995): Decadal trends in the North Atlantic Oscillation: Regional temperatures and precipitation, *Science,* 269, 676-679, doi:10.1126/science.269.5224.676.

Hurrell, J.W., Kushnir, Y., Visbeck, M., Ottersen, G. (2003): An overview of the North Atlantic Oscilliation, *Proceedings of the EGS-AGU-EUG Joint Assembly*, Hurrell, J.W., Kushnir, Y., Visbeck, M., Ottersen, G., Eds., Nice, France, 6-11 April 2003, 134, 1-35.

Hurrell, J.W., Deser, C. (2009): North Atlantic climate variability: The role of the North Atlantic Oscillation, *J. Mar. Syst.*, 78, 28-41, doi:10.1016/j.jmarsys.2009.11.002.

IKÜS (2008): Aufbau eines intergrierten Höhenüberwachungssystems in Küstenregionen durch Kombination höhenrelevanter Sensorik (final report). Online available from: http://tu-dresden.de.

IPCC (2007), *Climate Change 2007: The Physical Science Basis. Contribution of the Working Group I to the Fourth Assessment Report of the Intergovernmental Panel on Climate Change*, Solomon, S., Qin, D., Manning, M., Chen, Z., Marquis, M., Averyt, K.B., Tignor, M., Miller, H.L., Eds., Cambridge University Press, Cambridge, UK, and New York, NY, USA, 2007, 996.

Ishii, M., Kimoto, M. (2009): Reevaluation of historical ocean heat content variations with varying XBT and MBT depths bias corrections, *J. Oceanogr.*, 65, 287-299, doi:10.1007/s10872-009-0027-7.

Jacob, D., Göttel, H., Kotlarski, S., Lorenz, P., Sieck, K. (2008): Klimaauswirkungen und Anpassung in Deutschland, Phase 1: Erstellen regionaler Klimaszenarien für Deutschland, *UBA Forschungsbericht,* 204, 41-138, Online available from: http://www.umweltbundesamt.de/publikationen/fpdf-1/3513.pdf

Jensen, J. (1985): Über instationäre Entwicklungen der Wasserstände an der deutschen Nordseeküste, *Mitteilungen Leichtweiß-Institut der TU Braunschweig*, 88, 151-319.

Jensen, J., Mügge, H.E., Schönfeld, W. (1992): Analyse der Wasserstandsentwicklung und Tidedynamik in der Deutschen Bucht, *Die Küste*, 53, 212-275.

Jensen, J., Hofstede, J., Kunz, H., De Ronde, J., Heinen, P., Siefert, W. (1993): Long term water level observations and variations, *Coastal Zone '93, spezial volume "Coastlines of the Southern North Sea".*

Jensen, J., Mudersbach, C., Blasi, C. (2005): Hydrological changes in in tidal estuaries due to natural and atmospheric circulation on European sea level results based on the wavelet transform method, *Özhan (ed) Proceedings of the sixth intenational conference on the Mediterranean coastal environment,* MEDCOAST 03, 2257-2266.

Jensen, J., Mudersbach, C., (2007): Zeitliche Änderungen in den Wasserstandszeitreihen an den deutschen Küsten, *Berichte zu Deutschen Landeskunde, Themenheft: Küstenszenarien*, Glaser, R., Schenk. W., Voigt, J., Wießner, R., Zepp, H., Wardenga, U., Eds., Selbstverlag Deutsche Akademie für Landeskunde E.V., Leipzig, Germany, Band 81, Heft 2, 99-112.

Jensen, J., Wahl, T., Frank, T., Dangendorf, S. (2011): Ermittlung des MSL (Mean Sea Level) und Analyse von hochaufgelösten Tidewasserständen an der deutschen Nordseeküste, Abschlussbericht AMSeL, online available under: http://vzb.baw.de/publikationen.php?file=kfki_projekte/0/097_2_1_e35918.pdf.

Jevrejeva, S., Moore, J.C., Woodworth, P.L., Grinsted, A. (2005): Influence of large-scale atmospheric circulation on European sea level: Results based on the wavelet transform method, *Tellus,* 57A, 183-193, doi:10.1111/j.1600-0870.2005.00090.x.

Jevrejeva, S., Grinsted, A., Moore, J.C., Holgate, S. (2006): Nonlinear trends and multi-year cycles in sea level records, *J. Geophys. Res.*, 111, C09012, doi:10.1029/2005JC003229.

Jevrejeva, S., Moore, J.C., Grinsted, A., Woodworth, P.L. (2008): Recent global sea level acceleration started over 200 years ago? *Geophys. Res. Lett.,* 35, L08715, doi: 10.1029/2008GL033611.

Jevrejeva, S., Moore, J.C., Grinsted, A., Matthews, A., Spada, G. (2014): Trends and acceleration in global and regional sea level since 1807, *Global and Planetary Change*, 113, 11-22, doi:10.1016/j.gloplacha.2013.12.004.

Johansson, M., Boman, H., Kahma, K.K., Launiainen, J. (2001): Trends in sea level variability in the Baltic Sea, *Boreal Environ. Res.*, 6, 159-179, ISSN 1239-6095.

Johns, T.C., Durmann, C.F., Banks, H.T., Roberts, M.J., et al. (2006): The new Hadley Centre climate model (HadGEM1): evaluation and coupled simulations, *J. Clim.,* 19, 1327-1353, ISSN 0894-8755.

Jones, P.D., Jonsson, T., Wheeler, D. (1997): Extension to the North Atlantic Oscillation using early instrumental pressure observations from Gibraltar and south-west Iceland, *Int. J. Climatol,* 17, 1433-1450, doi:10.1002/(SICI)1097-0088(19971115)17:13<1433::AID-JOC203>3.0.CO;2-P.

Jorda, G., Gomis, D., Alvarez-Fanjul, E., Somot, S. (2012): Atmospheric contribution to Mediterranean and nearby Atlantic sea level variability under different climate change scenarios, *Global Planet Change*, 80-81, 198-214, doi:10.1016/j.gloplacha.2011.10.013.

Jorda, G., Gomis, D. (2013): On the interpretation of the steric and mass components of sea level variability; The case of the Mediterranean basin, *J. Geophys. Res.*, 118, 953-963, doi:10.1002/jgrc.20060.

Jungclaus, J.H., Keenlyside, H., Botzet, M., Haak, H., et al. (2006): Ocean circulation and tropical variability in the coupled model ECHAM5/MPI-OM, *J. Clim.,* 19, 3952-3972, doi:10.1175/JCLI3827.1.

Kalnay E., Kanamitsu, M., Kistler, W., et al. (1996): The NCEP/NCAR 40-year reanalysis project, *Bull. Amer. Meteor. Soc.,* 77, 437-471, doi:10.1175/1520-0477(1996)077<0437:TNYRP>2.0.CO;2.

Katsman C.A., Hazeleger, W., Drijfhout, S.S., van Oldenborgh, G.J., Burger, G.J.H. (2008): Climate scenarios for sea level rise for the northeast Atlantic Ocean: a study including the effects of ocean dynamics and gravity changes induced by ice melt, *Climate Change,* 91, 351-374, doi:10.1007/s10584-008-9442-9.

Katsman C.A., Sterl, A., Beersma, J.J., et al. (2011): Exploring high-end scenarios for local sealevel rise to develop flood protection strategies for a low-lying delta-The Netherlands as an example, *Clim. Chang.*, doi: 10.1007/s10584-011-0037-5.

Knutti, R., Furrer, R., Tebaldi, C., Cermak, J., Meehl, G.A. (2010): Challenges in combining projections from multiple models, *J. Clim.*, 23, 2739-2758, doi:10.1175/2009JCLI3361.1.

Knutti, R., Sedlacek, J. (2012): Robustness and uncertainties in the new CMIP5 climate model projections, *Nat. Clim. Chang.,* doi:10.1038/nclimate1716.

Kolker, A.S., Hameed, S. (2007): Meteorogically driven trends in sea level rise, *Geophys. Res. Lett.*, 34, doi:10.1029/2007GL031814.

Krahe, P., Nilson, E., Gelhardt, U., Lang, J. (2011): Auswertungen ausgewählter globaler Klimamodelle hinsichtlich atmosphärischer Zirkulationsbedingungen im nordatlantisch-mitteleuropäischen Sektor, *BfG-1682.*

Krueger, O., Schenk, F., Feser, F., Weisse, R. (2012): Inconsistencies between long-term trends in storminess derived from the 20CR reanalysis and observations, *J. Clim.*, doi:10.1175/JCLI-D-12-00309.1.

Krueger, O., Feser, F., Baerring, L., Kaas, E., Schmith, T., Tuomenvirta, H., von Storch, H. (2013b): Comment on Trends and low frequency variability of extra-tropical cyclone activity in the ensemble of Twentieth Century Reanalysis. *Clim. Dyn.*, doi:10.1007/s00382-013-1814-9.

Kuzmina, S.I., Bengtsson, L., Johannessen, O.M., Drange, H., Bobylev, L.P., Miles, M.W. (2005): The North Atlantic Oscillation and greenhouse-gas forcing, *Geophys. Res. Lett.*, 32, doi:10.1029/2004GL021064.

Langenberg, H., Pfizenmayer, A., von Storch, H., Sündermann, J. (1999): Storm-related sea level variations along the North Sea coast: natural variability and anthropogenic change, *Cont. Shelf. Res.,* 19(6), 821-842, doi:10.1016/S0278-4343(98)00113-7.

Leckebusch, G.C., Kapala, A., Mächel, H., Pinto, J.G., Reyers, M. (2006): Indizes der Nordatlantischen und Arktischen Oszillation, *Promet,* 34(3-4), 95-100.

Lehmann, A., Getzlaff, K., Harlaß, J. (2011): Detailed assessment of climate variability in the Baltic Sea area fort he period 1958 to 2009, *Clim. Res.,* 46, 185-196 doi:10.3354/cr00876.

Levermann, A., Griesel, A., Hofmann, M., Montoya, M., Rahmstorf, S. (2005): Dynamic sea level changes following changes in the thermohaline circulation, *Clim. Dyn.*, 24(4), 347-354, doi:10.1007/s00382-004-0505-y.

Lindenberg, J., Mengelkamp, H., Rosenhagen, G. (2012): Representativity of near surface wind measurements from coastal stations at the German Bight, Meteorologische Zeitschrift, 21(1), 99-106, doi:10.1127/0941-2948/2012/0131.

Lohrbacher, K., Marsland, S.J., Church, J.A., Griffies, S.M., Stammer, D. (2012): Rapid barotropic sea level rise from ice sheet melting, *J. Geophys. Res.*, 117, C06003, doi:10.1029/2011JC007733.

Lowe, J.A., Howard, T.P., Pardaens, A., Tinker, J., Holt, J., Wakelin, S., Milne, G., Leake, J., Wolf, J., Horsburgh, K., Reeder, T., Jenkins, G., Ridley, J., Dye, S., Bradley, S. (2009): UK Climate Projections science report: Marine and coastal projections. *Met. Office Hadley Centre,* Exeter.

Lüders, K. (1936): Über das Ansteigen der Wasserstände an der deutschen Nordseeküste, *Jahresbericht 1969*, Band XXI, Forschungsstelle für Insel- und Küstenschutz Norderney.

Mai, S., Zimermann, C. (2005): Risk Analysis A Tool for Coastal Hazard Mitigation, *Proceedings of the Solutions to Coastal Disasters 2005,* 1st ed., Wallendorf, L., Ewing, L., Rogers, S., Jones, C., Eds., American Society of Civil Engineers, Charleston, SC, USA, 2005, 649-659, doi:10.1061/40774(176)65.

Mann, M.E. (2004): On smoothing potentially non-stationary climate time series, *Geophys. Res. Lett.*, 31, doi:101029/2004GL019569.

Mann, M.E. (2008): Smoothing of climate time series revisited, *Geophys. Res. Lett.*, 31, doi:101029/2008GL019569.

Marcos, M., Tsimplis, M.N. (2007): Forcing of coastal sea level rise patterns in the North Atlantic and the Mediterranean Sea, *Geophys. Res. Lett.,* 34, doi:10.1029/2007GL030641.

Marcos, M., Puyol, B., Calafat, F.M., Wöppelmann, G. (2013): Sea level changes at Tenerife Island (NE Tropical Atlantic) since 1927, *J. Geophys. Res.*, 118, 4899-4910, doi: 10.1002/jgrc.20377.

Marti, O., Braconnot, P., Bellier, J., Benshila, R. (2005): The new IPSL climate system model: IPSL-CM4, *Note du Pol de Modelisation,* 26.

Martin, M.L., Valero, F., Pascual, A., Morata, A. Luna, M.Y. (2001): Springtime connections between the large-scale sea-level pressure fields and gust wind speed over Iberia and the Balearics, *Nat. Hazards Earth Syst. Sci.*, 11, 191-203, doi:10.5194/nhess-11-191-2011.

Matulla, C., Schöner, W., Alexandersson, H., von Storch, H., Wang, X.L. (2008): European storminess: late nineteenth century to present, *Climate Dynamics*, 31(2-3), 125-130, doi:10.1007/s00382-007-0333-y.

Meehl, G.A., et al. (2007): Global Climate projections. Solomon S., Qin, D., Manning, M., Chen, Z., Marquis, M., Averyt, K.B., Tignor, M., Miller, H.L., eds., *Climate Change 2007: The Physical Science Basis. Contribution of Working Group I to the Fourth Assessment Report of the Intergovernmental Panel on Climate Change*, Cambridge University Press: Cambridge, 433-497.

Merrifield, M.A., Merrifield S.A., Mitchum G.T. (2009): An anomalous recent acceleration of global sea level rise, *J. Clim.,* 22, 5772-5781, doi:10.1175/2009JCLI2985.1.

Merrifield, M.A. (2011): A shift in western tropical sea level trends during the 1990s, *J. Climate, 24*, 4126-4138, doi:10.1175/2011JCLI3932.1.

Merrifield, M.A., Maltrude, M.E. (2011): Regional sea level trends due to a Pacific trade wind intensification, *Geophys. Res. Lett.,* 38, L21605, doi:10.1029/2011GL049576.

Merrifield, M.A., Thompson, P.R., Lander, M. (2012): Multidecadal sea level anomalies and trends in the western tropical Pacific, *Geophys. Res. Lett*., 39, 13, L13602, doi:10.1029/2012GL052032.

Meyssignac, B., Salas y Melia, D., Becker, M., Llovel, W., Cazenave, A. (2012): Tropical Pacific spatial trend patterns in observed sea level: Internal variability and/or anthropogenic signature, *Clim. Past. Disuss*., 8, 349-389, doi:10.5194/cp-8-787-2012.

Miller, L., Douglas, B.C. (2007): Gyre-scale atmospheric pressure variations and their relation to the 19th and 20th century sea level rise, *Geophys. Res. Lett.*, 34, L16602, doi:10.1029/2007GL030862.

Milne, G.A., Gehrels, W.R., Hughes C.W., Tamisiea, M.E. (2009): Identifying the causes of sea-level change, *Nat. Geosci.*, 2, 471-478, doi: 10.1038/ngeo544.

Mitrovica, J.X., Tamisiea, M.E., Davis, J.L., Milne, G.A. (2001): Recent mass balance of polar ice-sheets inferred from patterns of global sea-level change, *Nature*, 409, 1026-1029, doi:10.1038/35059054.

Moore, J.C., Grinsted, A., Zwinger, T., Jevrejeva, S. (2013): Semiempirical and process-based global sea level rise projections, *Rev. Geophys.*, 51, 484-522, doi:10.1002/rog.20015.

Mudersbach, C., Jensen, J. (2010): Nonstationary extreme value analysis of annual maximum water levels for designing coastal structures on the German North Sea coastline, *Journal of Floodrisk Management*, 3(1), 52-62, doi:10.1111/j.1753-318X.2009.01054.x.

Mudersbach, C., Wahl, T., Haigh, I.D., Jensen, J. (2013): Trends in high sea levels along the German North Sea coastline compared to regional mean sea level changes, *Cont. Shelf Res.*, 65, 111-120, doi:10.1016/j.csr.2013.06.016.

Müller-Navarra, S. H., Giese, H. (1999): Improvements of an empirical model to forecast wind surge in the German Bight, Ocean Dynamics, 51, 385-405, doi:10.1007/BF02764162.

Müller-Navarra, S. H. (2013): On tidal predictions by means of harmonic representation of inequalities, *Reports by the Federal Maritime and Hydrographic Agency*, 50, Hamburg, Germany.

Nakicenovic, R.J., Alcamo, J., Davis, G., et al. (2000): Emission Scenarios, *A special report of Working Group III of the Intergovernmental Panel on Climate Change,* Cambridge University Press: Cambridge.

Nerem, R.S., Chambers, D.P., Choe, C., Mitchum, G.T. (2010): Estimating mean sea level change from TOPEX and Jason altimeter missions, *Mar. Geol.,* 33, 435-446.

Nicholls, R.J., Cazenave, A. (2010): Sea-level rise and its impact on coastal zones, *Science*, 328, 1517-1520, doi:10.1126/science.1185782.

Nicholls, R.J., Marinova, N., Lowe, J.A., Brown, S., Vellinga, P., de Gusmao, D., Hinkel, J., Tol, R.S.J. (2011): Sea level rise and its possible impacts given a 'beyond 4°C world' in the twenty-first century, *Phil. Trans. R. Soc. A.,* 369, 161-181, doi:10.1098/rsta.2010.0291.

Niehörster, F., Fats, I., Huebener, H., Cubasch, U. (2008): The steam one ENSEMBLE projections of future climate change, *ENSEMBLES Technical Report,* 3, Available online: http://ensembles-eu.metoffice.com/tech_reports/ETR_3_vn0.pdf.

Nilson, E., Perrin, C., Beersma, J., Carambia, M., Krahe, P., de Keizer, O., Görgen, K. (2010): Evaluation of data and processing procedures, Görgen, K., Beersma, J., Brahmer, G., Buiteveld, R., Carambia, M., de Keizer, O., Krahe, P., Nilson, E., Lammersen, R., Perrin, C., Volken, D. Assessment of climate-change impacts on discharge in the Rhine, River Basin: results of the RheinBlick2050 Project, *CHR Report,* I-23, 51-95, download at: http://chr-khr.org/files/CHR_I-23.pdf.

Orlic, M., Pasaric, Z. (2013): Semi-empirical versus process-based sea-level projections for the twenty-first century, *Nature Climate Change*, 3(5), doi:10.1038/NCLIMATE1877.

Orvik, K.A., Skageseth, Ø. (2003): The impact of wind stress curl in the North Atlantic on the Atlantic inflow to the Nowegian Sea toward the Arctic, *Geophys. Res. Lett.*, 30, 1884, doi:10.1029/2003GL017932.

Osborn, T.J. (2004): Simulating the winter North Atlantic Oscillation: The roles of internal variability and greenhouse forcing, *Clim. Dyn.*, 22, 605-623, doi:10.1007/s00382-004-0405-1.

OSPAR (2000): Quality Status Report 2000: Region II: Greater North Sea. OSPAR Comission for the protection of the Marine Environment of the North-East Atlantic, ISBN 0-946956-48-0.

Otto, L., Zimmermann, J.T.F., Furnes, G.K., Mork, M., Saetre, R., Becker, G. (1990): Review of the physical oceanography of the North Sea, *Neth. J. Sea Res*., 26(2-4), 161-238, doi:10.1016/077-7579(90)90091-T.

Palmer, T., Shutts G., Hagedorn, R., Doblas-Reyes, F., Jung, T., Leutbecher, M. (2005): Representing model uncertainty in weather and climate prediction. *Annu. Rev. Earth. Plent. Sci.,* 33, 163-193, doi:10.1146/annurev.earth.33.092203.122552.

Pawlowicz, R., Beardsley, B., Lentz, S. (2002): Classical tidal harmonic analysis including error estimates in MATLAB using T_TIDE, *Computers and Geosciences*, 28(8), 929-937, doi: 10.1016/S0098-3004(02)00013-4.

Peltier, W.R. (2004): Global glacial isostacy and the surface of the Ice-Age earth: The ICE-5G(VM2) model and GRACE, *Ann. Rev. Earth. Planet. Sci.,* 32, 111-149, doi:10.1146/annurev.earth.32.082503.144359.

Petrow, T., Zimmer, J., Merz, B. (2009): Changes in the flood hazard in Germany through changing frequency and persistence of circulation patterns, *Nat. Hazards Earth Syst. Sci.*, 9, 1409-1423.

Pezzulli, S., Stephenson, D.B., Hannachi, A. (2005): The variability of seasonality, *J. Clim.,* 18, 71-88, doi:10.1175/JCLI-3256.1.

Pinto, J.G., Ulbrich, U., Leckebusch, G.C., Spangehl, T., Reyears, M., Zacharias, S. (2007): Changes in storm track and cyclone activity in three SRES ensemble experiments with the ECHAM5/MPI-OM1 GCM, *Clim. Dyn.,* 29, 195-210, doi:10.1007/s00382-007-0230-4.

Pinto, J.G., Zacharias, S., Fink, A.H., Leckebusch, G.C., Ulbrich, U. (2009): Factors contributing to the development of extreme North Atlantic cyclones and their relationship with the NAO, *Clim. Dyn.,* 32, 711-737, doi:10.1007/s00382-008-0396-4.

Pinto, J.G., Bellenbaum, N., Karremann, M.K., Della-Marta, P.M. (2013): Serial clustering of extratropical cyclones over the North Atlantic and Europe under recent and future climate conditions. *J. Geophys. Res.*, 118(12), 476-485, doi:10.1002/2013JD020564.

Plag, H.P., Tsimplis, M.N. (1999): Temporal variability of the seasonal sea-level cycle in the North Sea and Baltic Sea in relation to climate variability, *Glob. Planet. Change.,* 20, 173-203, doi:10.1016/S0921-8181(98)00069-1.

Ponte, R.M. (2006): Low-frequency sea level variability and the inverted barometer effect. *J. Atmos. Oceanic. Technol.,* 23, 619-629, doi:10.1175/JTECH1864.1.

Proshutinsky, A., Ashik, I., Häkkinen, S., Hunke, E., Krishfield, R., Maltrud, M., Maslowski, W., Zhang, J. (2007): Sea level variability in the Arctic Ocean from AOMIP models, *J. Geophys. Res.,* 112, C04S08, doi: 10.1029/2006JC003916.

Pugh, D. (2004): *Changing Sea Levels, Effects of Tides, Weather and Climate*, 1st ed., Cambridge University Press, Cambridge, UK, 1-48, ISBN 9780521532181.

Rahmstorf, S., Perrette, M., Vermeer, M. (2012): Testing the robustness of semi-empirical sea level projections, *Clim. Dyn.*, 39, 861-875, doi:10.1007/s00382-011-1226-7.

Richter, K., Furevik, T., Orvik, K.A. (2009): Effect of wintertime low-pressure systems on the Atlantic inflow to the Nordic seas, *J. Geophys. Res.*, 114, C09006, doi:10.1029/2009JC005392.

Richter, K., Nilsen, J.E.Ø., Drange, H. (2012): Contributions to sea level variability along the Norwegian coast for 1960-2010, *J. Geophys. Res.*, 117, C05038, doi:10.1029/2011JC007826

Rietschel, E. (1933): Neuere Untersuchungen zur Frage der Küstensenkung, *Dt. Wasserwirtschaft*, 5, Berlin.

Riva, R.E.M., Bamber, J.L., Lavallee, D.A., Wouters, B. (2010): Sea-level fingerprint of continental water and ice mass change from GRACE, *Geophys. Res. Lett.*, 19, L19605, doi:10.1029/2010GL044770.

Rodhe, J. (1998): The Baltic and North Seas: a process-oriented review of the physical oceanography, *The Sea*, 11, 699-732.

Rossiter, J.R. (1958): Storm Surges in the North Sea, 11 to 30 December 1954, *Phil. Trans. R. Soc. Lond. A*, 251, 139-160, doi:10.1098/rsta.1958.0012.

Salas-Melia, D., Chauvin, F., Deque, M., Douville, H., Gueremy, J., Marquet, P., Planton, S., Roger, J., Tyteca, S. (2005): Decription and validation on the CNRM-CM3 global coupled model. *CNRM working note 103*.

Sallenger, A.H., Doran, K.S., Howd, P.A. (2012): Hotspot of accelerated sea-level rise on the Atlantic coast of North America, *Nature. Clim. Change*, doi:10.1038/ncclimate1597.

Santer, B.D., Wigley, T.M.L., Boyle, J.S., Gaffen, D.J., Hnilo, J.J., Nychka, D., Parker, D.E., Taylor, K.E. (2000): Statistical significance of trends and trend differences in layer-average atmospheric temperature time series, *J. Geophys. Res.,* 105, 7337-7356, doi:10.1029/1999JD901105.

Schmidt, H., von Storch, H. (1993): German Bight storm analysed, *Nature*, 365, 791, doi: 10.1038/365791a0.

Small, C., Nicholls, R.J. (2003): A global analysis of human settlement in coastal zones, *Journal of Coastal Research*, 19(3), 584-599.

Schott, F. (1966): Der Oberflächensalzgehalt in der Nordsee, *Dt. Hydrogr. Zt.*, A9, 1-58.

Schuchardt, B., Schirmer, M., Bakkenist, S., Eppel, D.P., Elsner, A., Elsner, W., Grabemann, I., Grabemann, H.-J., Haarmann, M., Hahn, B., et al. KRIM (2005): Climate Change, coastal protection and risk management in North-West Germany, *Proceedings of the Final Symposium on DEKLIM*, Leipzig, Germany, 10-12 May 2005, 133-141.

Schütte, H. (1908): Neuzeitliche Senkungserscheinungen an unserer Nordseeküste, *Jahrbuch Oldenburg*, Ver. Altertumskunde, Landesgesch. 16, Oldenburg.

Selten, F.M., Branstator, G.W., Dijkstra, H.A., Kliphuis, M. (2004): Tropical originals for recent and future northern hemisphere climate change, *Geophys. Res. Lett.,* 31, L21205, doi: 101019/2004GL020739.

Siegismund, F., Schrum, C. (2001): Decadal changes in the wind forcing over the North Sea, *Clim. Res.,* 18,39-45.

Slangen A.B.A., Katsman, C.A., van de Wal R.S.M., Vermeersen L.L.A., Riva R.E.M. (2011): Towards regional projections of twenty-first century sea-level change based on IPCC SRES scenarios, *Clim. Dyn.,* 38,1191-1209, doi:10.1007/s00382-011-1057-6.

Somot, S., Sevault, F., Dequet, M. (2006): Transient climate change scenario simulation of the Mediterranean Sea for the twenty-first century using a high-resolution ocean circulation model, *Clim. Dyn.,* 27, 851-879, doi:10.1007/s00382-006-0167-z.

Stammer, D. (2008): Response of the global ocean to Greenland and Antarctica melting, *J. Geophys. Res*., 116, C02020, doi:10.1029/2006JC004079.

Stammer, D., Hütteman, S. (2008): Response of regional sea level to atmospheric pressure loading in a climate change scenario, *J. Climate.,* 21, 2093-2101, doi:10.1175/2007JCLI1803.1.

Stammer, D., Cazenave, A., Ponte, R.M., Tamisiea, M.E. (2013): Causes of contemporary regional sea level changes, *Annu. Rev. Mar. Sci*., 5, 21-46, doi:10.1146/annurev-marine-121211-172406.

Steffen, H., Wu, P. (2011): Glacial isostatic adjustment in Fennoscandia – a review of data and modeling, *J. Geodyn.*, 52, 169-204, doi:10.1016/j.jog.2011.03.002.

Stephenson, D.B., Pavan, V., Collins. M., Junge, M.M., Quadrelli, R. (2006): North Atlantic Oscillation response to transient greenhouse gas forcing and the impact on European winter climate: a CMIP2 multi-model assessment, *Clim.Dyn.,* 27, 401-420, doi:10.1007/s00382-006-0140-x.

Sterl, A., van den Brink, H., de Vries, H., Haarsma, R., van Meijgaard, E. (2009): An ensemble study of extreme North Sea storm surges in a changing climate, *Ocean. Sci.,* 5, 369-378.

Stine, A.R., Huybers, P., Fung, I.Y. (2009): Changes in the phase of the annual cycle of surface temperature, *Nature*, 457, 435-439, doi:10.1038/nature07675.

Sturges, W., Douglas, B.C. (2011): Wind effects on estimates of sea level rise, *j. Geophys. Res.,* 116, C06008, doi:10.1029/2010JC006492.

Suendermann, J., Pohlmann, T. (2011): A brief analysis of North Sea physics, *Oceanologica*, 53(3), 663-689, doi:10.5697/oc.53-3.663.

Suursaar, Ü., Sooäär, J. (2007): Decadal variations in mean and extreme sea level values along the Estonian coast of the Baltic Sea, *Tellus*, 59A, 249-260, doi:10.1111/j.1600-0870.2006.00220.x.

Talke, S.A., Jay, D.A. (2013): Nineteenth Century North American and Pacific Tidal Data: Lost or Just Forgotten? *Journal of Coastal Research*, doi:10.2112/JCOASTRES651D-12-00181.1 (in press: http://www.jcronline.org/doi/pdf/10.2112/JCOASTRES-D-12-00181.1).

Tamisiea, M.E., Hill, E.M., Ponte, R.M., Davis, J.L., Velicogna, I., Vinogradova, N.T. (2010): Impact of self-attraction and loading on the annual cycle in sea level, *J. Geophys. Res.*, 115, C07004, doi:10.1029/2009JC005687.

Thompson, D.W.J., Wallace, J.M. (1998): The Arctic Oscillation signature in the wintertime geopotential height and temperature fields, *Geophys. Res. Lett.*, 9, 1297-1300, doi:10.1029/98GL00950.

Timmermann, A., McGregor, S., Jin, F.F. (2010), Wind effects on past and future regional sea level trends in the southern Indo-Pacific, *J. Climate*, 24, 267-285, doi:10.1175/2010JCLI3519.1.

Tsimplis, M.N., Woodworth, P.L. (1994): The global distribution of the seasonal sea level cycle calculated from coastal tide gauge data, *J. Geophys. Res.*, 99(C8), 16,031-16,039, doi:10.1029/94JC01115.

Tsimplis, M.N., Spencer, N.E. (1997): Collection and analysis of monthliy mean sea level data in the Mediterranean and Black Sea, *J. Coast. Res.*, 13,534-544.

Tsimplis, M.N., Josey, S.A. (2001): Forcing of the Mediterranean Sea by atmospheric oscillations over the North Atlantic, *Geophys. Res. Lett.*, 28,803-806, doi:10.1029/2000GL012098.

Tsimplis, M.N., Woolf, D.K., Osborn, T.J., Wakelin, S., Wolf, J., Flather, R., Shaw, A.G.P., Woodworth, P.L., Challenor, P., Blackmen, D., et al. (2005): Towards a vulnerability assessment of the UK and Northern European coasts: the role of regional climate variability, *Phillos. Trans. R. Soc. A.,* 363, 1329-1358, doi: 10.1098/rsta.2005.1571.

Tsimplis, M.N., Shaw, A.G.P., Flather, R., Woolf, D.K. (2006): The influence of the North Atlantic Oscillation on sea level around the northern European coasts reconsidered: the thermosteric effects, *Philos. Trans. R. Soc. A.*, 364, 845-856, doi:10.1098/rsta.2006.1740.

Tsimplis, M.N., Shaw, A.G.P. (2008): The forcing of mean sea level variability around Europe, *Glob. Planet. Change,* 63(2-3), 196-202, doi:10.1016/j.gloplacha.2007.08.018.

Turrel, W., Henderson, E., Payne, R., Adams, R. (1992): Seasonal changes in the circulation of the northern North Sea, *Cont. Shelf Res.*, 12 (2-3), 257-286, doi:10.1016/0278-4343(92)90032-F.

Ullmann, A., Monbauliu, J. (2010): Changes in atmospheric circulation over the North Atlantic and sea surge variations along the Belgian coast during the twentieth century, *Int. J. Clim.*, 30, 558-568, doi: 10.1002/joc.1904.

Uppala, S.M., Kallberg, P.W., Simmons, A.J., et al. (2005): The ERA-40 reanalysis, *Q. J. R. Meteorl. Soc.,* 131, 2961-3012, doi:10.1256/qj.04.176.

Van der Linden, P., Mitchell, J.F.B. (2009): *ENSEMBLES-climate-change and its impacts: summary of research and results from the ENSEMBLES project*, Met. Office. Hadley. Centre., FitzRoy Road, Exeter EX1 3 PB, UK, 160 p.

Von Storch, H., Zorita, E., Cubasch, U. (1993): Downscaling of global climate change estimates to regional scales: An application to Iberian rainfall in wintertime, *J. Clim.*, 6, 1161-1171, doi:10.1175/1520-0442(1993)006<1161:DOGCCE>2.0.CO;2.

Von Storch, H., Reichardt, H. (1997): A scenario of storm surge statistics for the German Bight at the expected time of doubled atmospheric carbon dioxide concentration, *Journal of Climate*, 10, 2653-2662, doi:10.1175/1520-0442(1997)010<2653:ASOSSS>2.0CO;2.

Von Storch, H.V., Zwiers, F.W. (1999): *Statistical Analysis in Climate Research,* 1st ed., Cambridge University Press: Cambridge, UK, ISBN 9780521012300.

Von Storch, H. (2012): Storm Surges: Phenomena, Forecasting and Scenarios of Change, *Procedia IUTAM*, 00(2012) 000-000, doi:10.1016/j.piutam.2014.01.030.

Von Storch, H. (2013): Regional Sea Level along the North Sea coasts, Presentation, *High End Sea Level Rise Workshop*, Hamburg.

Wahl, T., Jensen, J., Frank, T. (2010): On analysing sea level rise in the German Bight since 1844, *Nat. Hazards Earth Syst. Sci.*, 10, 171-179, doi:10.5194/nhess-10-171-2010.

Wahl, T., Jensen, J., Haigh, I.D., Frank, T. (2011): Improved estimates of mean sea level changes in the German Bight over the past 166 years, *Ocean Dynamics*, 5, 701-715, doi:10.1007/s10236-011-0383-x.

Wahl, T. (2012): Statistical methods to assess the hydrodynamic boundary conditions for risk based design methods approaches in coastal engineering – methods and application to the German North Sea coastline, *PhD Thesis*, University of Siegen, Siegen.

Wahl, T., Haigh, I.D., Woodworth, P.L., Albrecht, F., Dillingh, D., Jensen, J., Nicholls, R.J., Weisse, R., Woeppelmann, G. (2013): Observed mean sea level changes around the North Sea coastlines from 1800 to present, *Earth Science Reviews,* 124, 51-67, doi:10.1016/j.earscirev.2013.05.003.

Wakelin, S.L., Woodworth, P.L., Flather, R.A., Williams, J.A. (2003): Sea-level dependence on the NAO over the NW European continental shelf, *Geophys. Res. Lett.*, 7, 56:1-56:4, doi:1029/2003GL017041.

Wang, X. L., Zwiers, F. W., Swail, V.R., Feng, Y. (2009): Trends and variability of storminess in the Northeast Atlantic region, 1874–2007. *Clim. Dyn.*, 33, 1179–1195, doi:10.1007/s00382-008-0504-5.

Wang, X.L., Feng, Y., Compo, G.P., Zwiers, F.W., Allan, R.J., Swail, V.R., Sardeshmukh, P.D. (2013): Is the storminess in the twentieth century reanalysis really inconsistent with observations? – A reply to the comment by Krüger et al. (2013), *Geophys. Res. Abstr.*, 15, EGU2013-1937, doi:10.1007/s00382-013-1828-3.

Weisse, R., Pluess, A. (2006): Storm-related sea level variation along the North Sea coast as simulated by a high-resolution model 1958-2002, *Ocean. Dyn.*, 56(1), 16-25, doi:10.1007/s10236-005-0037-y.

Weisse, R., von Storch, H. (2009): *Marine climate and climate change: Storms, wind waves and storm surges*, 1st edn Springer, Heidelberg, Germany, ISBN 9783540684916.

Wenzel, M., Schröter, J. (2010): Reconstruction of mean sea level anomalies from tide gauges using neuronal networks, *J. Geophys. Res.*, 115, C08013, doi:10.1029/2009JC005630.

Woodworth, P.L. (1987): Trends in U.K. mean sea level, *Mar. Geod.,* 11, 57-87, doi:10.1080/15210608709379549.

Woodworth, P.L. (1990): A search for acceleration in records of European mean sea level, *Int. J. Clim.*, 7(3), 699-710, doi:10.1002/joc.3370100203.

Woodworth, P.L., Flather, R.A., Williams, J.A, Wakelin, S.L., Jevrejeva, S. (2007): The dependence of UK extreme sea levels and storm surges on the North Atlantic Oscillation, *Cont. Shelf. Res.*, 27(1), 935-946, doi:10.1016/j.csr.2006.12.007.

Woodworth, P.L., White, N.J., Jevrejeva, S., Holgate, S.J., Gehrels, W.R. (2009): Evidence for the accerations of sea level on multidecade and century time scales, *Int. J. Climatol.*, 29(6), 777-789, doi:10.1002/joc.1771.

Woodworth, P.L., Pouvreau, N., Woeppelmann, G. (2010): The gyre-scale circulation of the North Atlantic and sea level at Brest, *Ocean. Sci.*, 6, 185-190, doi:10.5194/os-6-185-2010.

Woodworth, P.L., Menéndez, M., Gehrels, W.R. (2011): Evidence for century-timescale acceleration in mean sea levels and for recent changes in extreme sea levels, *Surv. Geophy.*, 32, 602-618, doi:10.1007/s10712-011-9112-8.

Woolf, D.K., Tsimplis, M. (2002): The influence of the North Atlantic Oscilliation on sea level in the Mediterranean and the Black Sea derived from satellite altimetry, *Proceedings of the Second International Conference on Oceanography of the Eastern Mediterranean and Black Sea: Similarities and Differences of Two Inter-connected Basins*, Ankara, Turkey, 14-18, 145-150.

Woolf, D.K., Shaw, A.G.P., Tsimplis, M.N. (2003): The influence of the North Atlantic Oscillation on sea level variability in the North Atlantic region, *The Global Atmosphere and Ocean System*, 9, 145-167, doi:10.1080/10236730310001633803.

Wöppelmann, G., Letetrel, C., Santamaria, A., Bouin, M.N., Collilieux, X., Altamimi, Z., Williams, S.D.P., Miguez, M.B. (2009): Rates of sea level change over the past century in a geocentric reference frame, *Geophys. Res. Lett.*, 36, 12, L12607, doi:10.1029/2009GL038720.

Wöppelmann, G., Marcos, M., Santamaria-Gomez, A., Martin-Miguez, B., Bouin, M.N., Gravelle, M. (2014): Evidence for a differential sea level rise between hemispheres over the twentieth century, *Geophys. Res. Lett.*, 41, 5, 1639-1643, doi:10.1002/2013GL059039.

Woth, K., Weisse, R., von Storch, H. (2006): Dynamical modeling of North Sea storm surge extremes under climate change conditions – an ensemble study, *Ocean Dynamics*, 56, 3-15, doi:10.1007/s10236-005-0024-3.

Xia, L., von Storch, H., Feser, F. (2012): Quasi-stationarity of centennial Northern Hemisphere mid-latitude winter storm tracks, *Climate Dynamics*, online first, doi:10.1007/s00382-012-1543-5

Yan, Z., Tsimplis, M.N., Woolf, D. (2004): Analysis of the relationship between the North Atlantic Oscillation and sea level changes in Northwest Europe, *Int. J. Climatol.,* 24, 743-758, doi:10.1002/joc.1035.

Yin, J., Schlesinger, M.E., Stouffer, R.J. (2009): Model projections of rapid sea-level rise on the northeast coast of the United States, *Nat. Geosci.*, 2, 262-266, doi:10.1038/NGEO4062.

Zhang, K., Douglas, B.C., Leatherman, S.P. (2000): Twentieth century storm activity along the U.S. east coast, *J. Clim.*, 13, 1748-1761, doi:10.1175/1520-0442(2000)013<1748:TCSAAT>2.0.CO;2.

9 Appendix

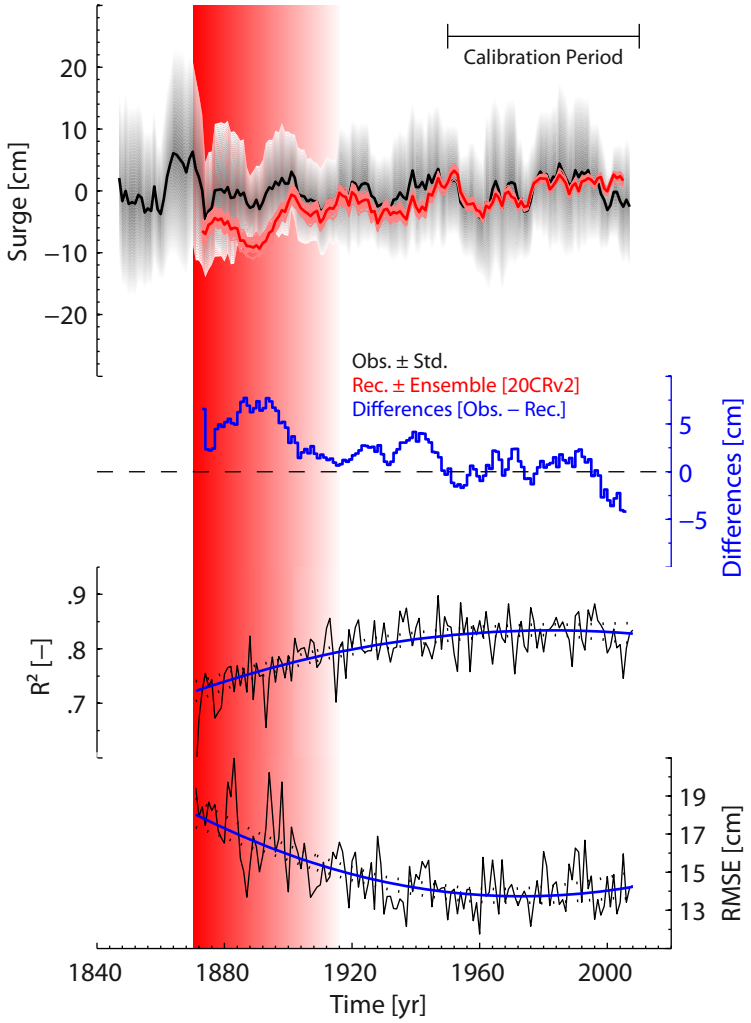

Figure 9-1: Reconstruction of surges based on 20CRv2 winds and SLP. 10 year moving averages of the 95th percentiles of observed surges ± standard deviations (black line with grey shaded area; the standard deviation has been computed as a measure of variability over each 10 year window) and their reconstructions based on 20CRv2 (light red: individual ensemble members, dark red: ensemble mean, both normalized to a common period from 1950-2011, i.e. the mean has been removed) are presented. Differences between both are shown in blue. Annual efficiency criteria between observed and reconstructed daily surges are presented in black. The red shaded area marks the period for which significant differences between observations and 20CRv2 are detected. The different shades demonstrate the gradual increase of inconsistencies before the 1910s.

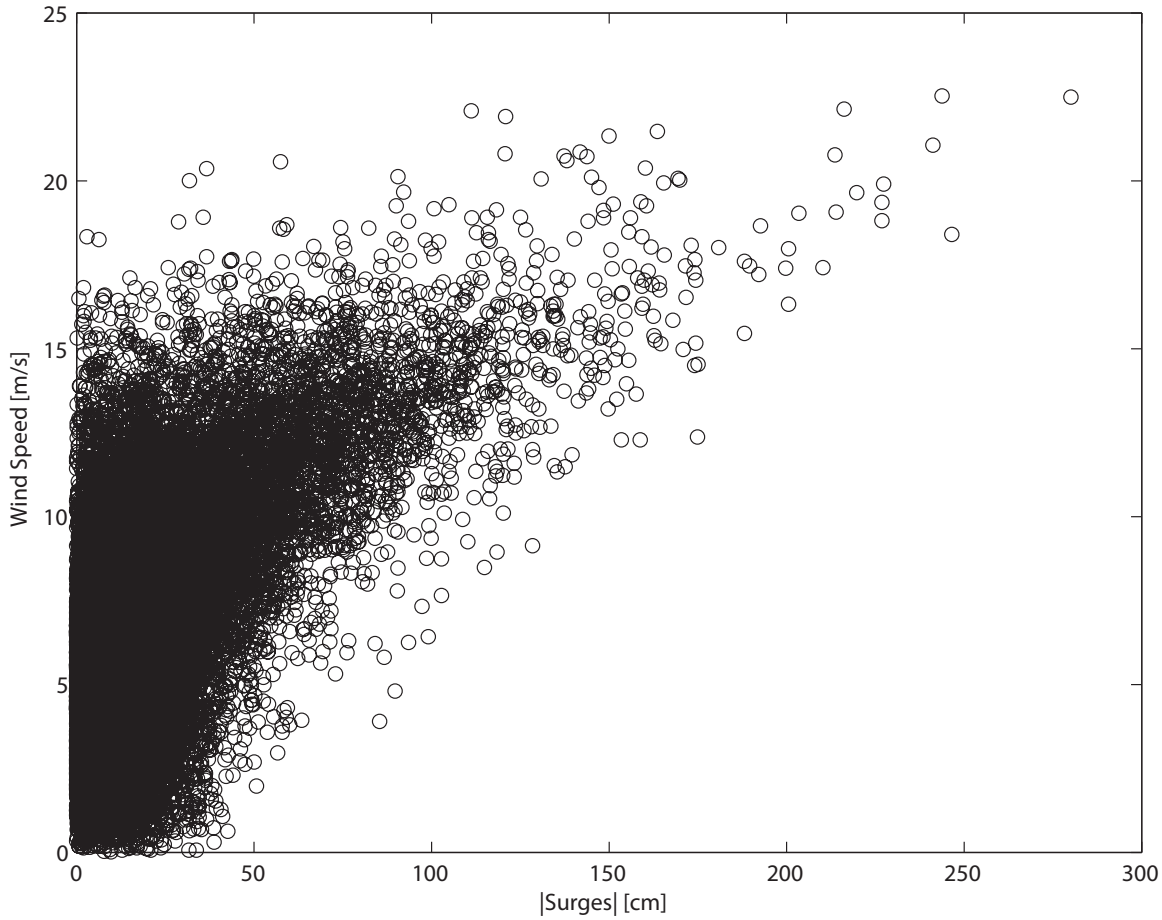

Figure 9-2: Correlation plot between absolute daily skew surges and daily 20CRv2 wind speeds over the period 1950-2010.

Herausgeber:
Forschungsinstitut Wasser und
Umwelt (fwu) der Universität Siegen
Paul-Bonatz-Straße 9-11
57076 Siegen